CIRCULATING FLUIDIZED BED BOILER MODEL FOR PREDICTING EMISSION LEVELS OF TIRE FUEL USING BASE CASE OF LIGNITE FUEL

A Thesis

by

AUBREY ALVIN SPEAR, IV

Submitted to the Office of Graduate and Professional Studies of
Texas A&M University
in partial fulfillment of the requirements for the degree of

MASTER OF SCIENCE

Chair of Committee,	Kalyan Annamalai
Committee Members,	Eric L. Peterson
	Yassin A. Hassan
Head of Department,	Andreas A. Polycarpou

August 2015

Major Subject: Mechanical Engineering

ABSTRACT

Government regulations on emission standards and constantly fluctuating fuel availability and prices have led to the need of more readily usable and available models for power generating combustors. A common, versatile, power generating combustor is the circulating fluidized bed (CFB) boiler. Waste tire is viewed as a potential fuel in a CFB boiler. Extensive literature review is used to create a model of a CFB boiler.

The model is programmed using Microsoft Excel software. The program consists of four major tabs being the 'Input', 'Bed', 'Riser', and 'Output' tabs. The 'Input' tab consists of appropriate and minimal input parameters to allow for enough variability while not over burdening the user with acquiring large amounts of data. The 'Bed' tab describes the instantaneous chemical reactions assumed to take place in the dense bed region of the combustor. The 'Riser' tab tracks the time dependent chemical kinetics through a predetermined number of time steps divided evenly throughout the lean riser region of the combustor. The 'Output' tab calculates the concentration at the exit of the combustor riser for ten different species important to both combustion and government regulations being CO, H_2O, O_2, N_2, NH_3, HCN, SO_2, CO_2, H_2, and NO. With 5,000 chemical kinetics calculation rows, the computation time for varying an input is approximately ten seconds.

The model has been validated against an anonymous industrial CFB boiler firing lignite coal fuel resulting in emission concentrations being 22% different or less between the model predictions and the actual emissions when kinetics are slightly modified. The

model was also validated against a Babcock and Wilcox pilot/laboratory scale bubbling fluidized bed (BFB) boiler firing subbituminous coal fuel resulting in emission concentrations being 10% different at most between the model predictions and the actual emissions without kinetics modification except for the O_2 concentration being off by about 74% due to differences with CFB.

The anonymous CFB boiler had fuel switched to waste tire fuel, and 24 inputs were varied as part of a parametric analysis of the fuel to discover emission trends.

DEDICATION

I dedicate this thesis to all students of integrity that have struggled to get to higher levels of education and achieved what others, and maybe even they, have thought that they couldn’t.

ACKNOWLEDGEMENTS

I give thanks to Heavenly Father for his willingness to guide me through difficulties, pour out knowledge, and provide all of His creations for my use through His son Jesus Christ. I also am appreciative of the marital companion I have chosen for eternity, Corrinas, for her support and encouragement while she worked and attended school.

I thank Dr. Kalyan Annamalai for his concern for me both as a student and a person as well as his depth of knowledge that he readily shared. I also thank Dr. Eric L. Peterson and Dr. Yassin A. Hassan for the use of their valuable time to further my education.

I would also like to thank the students who received their doctorates in my Coal and Biomass Energy Laboratory (CABEL) at Texas A&M University. Thanks go to Benjamin D. Lawrence for his wealth of knowledge and teaching expertise. Dustin Eseltine was a fellow companion as we took course work and wrote our theses together. Wei Chen was a great friend to laugh with. Siva Sankar Thanapal was always willing to help even when it wasn't convenient.

I also thank other family members and friends for helping to lighten the everyday burdens.

NOMENCLATURE

a	area, m^2
a’	area per particle, $\frac{m^2}{particle}$ or acceleration of particle, $\frac{m}{S^2 * particle}$
C_{Drag}	drag coefficient, dimensionless
CSR	Calcium-Sulfur Ratio, $\frac{kmol\ limestone\ CaCO_3}{kmol\ volatile\ SO_2}$
d	Sauter Mean Diameter of particle, m
d_{cp}	average/center-point particle diameter between two sieve sizes, m
D	diffusivity of species through mixture, $\frac{m}{s}$
F’	force on particle, $\frac{N}{particle}$
FCR	Fixed Carbon Ratio, $\frac{kg\ fixed\ Nitrogen}{kg\ fixed\ Carbon}$
h	height, m
$h_{avg,conv,m}$	average convection mass transfer coefficient, $\frac{m}{s}$
hhv	higher heating value, $\frac{kJ}{kg}$
m	mass of species, kg
m’	mass per particle, $\frac{kg}{particle}$
m’’’	mass per unit volume, $\frac{kg}{m^3}$
$\dot{m}$	mass flow rate, $\frac{kg}{s}$
$\dot{m}$’	reaction rate of mass per particle, $\frac{kg}{s * particle}$

$\overline{m}$	molecular weight, $\frac{kg}{kmol}$
Δm_F	mass fraction for certain particle d_{cp}, kg
n’’’	particles per unit volume, $\frac{particles}{m^3}$
N	moles of species, kmol
N’’’	moles per unit volume, $\frac{kmol}{m^3}$
$\dot{N}$’	reaction rate of mole per particle, $\frac{kmol}{s*particle}$
$\dot{N}$’’’	reaction rate of mole concentration of species, $\frac{kmol}{m^3*s}$
P	pressure, bara
Re	Reynolds number, dimensionless
Sc	Schmidt number, dimensionless
Sh	Sherwood number, dimensionless
SR	Stoichiometric Ratio, dimensionless
t	time, s
T	temperature, K
v	volume, m^3
V	velocity, $\frac{m}{s}$
V’	average volume of molecule, $\frac{m^3}{molecule}$
X	mole fraction of species in mixture, $\frac{kmol\ species}{kmol\ mixture}$
Y	mass fraction of species in mixture, $\frac{kg\ species}{kg\ mixture}$
λ	mean free path between molecules, m

μ	dynamic/absolute viscosity, $\frac{kg}{m*s}$
ρ	density, $\frac{kg}{m^3}$
σ'	effective diameter of molecule, $\frac{m}{molecule}$
ϕ	equivalence ratio, dimensionless
$\phi_{species\ 1\|species\ 2}$	correction factor for mole fraction of species 2 in mixture of gases with respect to dynamic/absolute viscosity of species 1, dimensionless

TABLE OF CONTENTS

LIST OF FIGURES

LIST OF TABLES

1. INTRODUCTION

There is constant search for the best fuels for given circumstances and the efficient extraction of useful energy derived from them. Especially in light of government regulation and abundance of certain fuels in specific areas of the earth, the search for the optimal fuel and energy derivation combination can be highly important.

1.1 Waste Tire

Of the many manifestations of fuel known, common municipal solid waste (MSW) has been found to contain the potential to be a fuel source. A specific component of interest in this waste is vehicle tires. The potential energy of tires may be released through burning rather than just buried in public landfills [1-3]. In fact, tires have a higher heating value of 27,000 to 39,000 kilojoules per kilogram which is greater than most coals [1,4,5].

It has been estimated that $1.5x10^6$ tons per year in the European Community, $2.5x10^6$ tons per year in North America, $0.5x10^6$ tons per year in Japan, and $1.0x10^6$ tons per year in China of waste tires is available [3]. This means there are about 250 million tires (one passenger car tire weighs about 20 pounds) on average disposed of in the United States (US) per year (about one tire per person per year). Only about 50 million of these US tires are being recycled or further used in some way while the other 200 million tires are sent to landfills. An estimated 3 billion tires are currently accumulated in landfills in the US, and tires are non-biodegradable. However, boilers dedicated to burning this material may have problems in ensuring long term supplies of

tires and in that case fluidized bed combustion (FBC) fuel flexibility may offer a significant advantage in allowing the boiler to be operated with other fuels such as lignite coal in the event that tire-derived fuel becomes unavailable. Economics begin to play more of a factor as available landfill sites are decreasing and tipping money for disposal is increasing as well as fossil fuels being expensive. Several processing routes have been proposed for converting waste tires into useful products, namely, devulcanization to produce elastomers, pyrolysis, gasification, and combustion. Of these, the combustion route may be an especially attractive solution. Several types of combustors (grate-fired, rotary-kiln and fluidized-bed) have been developed to incinerate waste tires. Fluidized bed combustion is considered to be an attractive procedure for the combustion of waste tires largely due to fuel flexibility, the possibility to handle other wastes simultaneously, high thermal efficiency, and low emission levels of pollutants. Burning/energy recovery will decrease the volume of the final tire disposal in landfills by about 90% with the other 10% being unburnable constituents such as wiring and some ash [1,4-6].

1.2 Fluidized Bed Combustion

Table 1 below by Koornneef et al. displays important events in the history of FBC beginning with the Winkler patent of a gasifier in 1922 which was the first time fuel conversion took place in a fluidized bed [7,17].

Table 1

Timeline of fluidized bed combustion [7].

Year	Event
1922	Winkler patent
1965	Start of the Atmospheric Fluidized Bed Combustion Program (between 1965 and 1992) [23]
1965	First BFB test facility commissioned [2]
1972	First contract awarded for Rivesville
1973	EPI provided the first fluidized bed combustion (FBC) system in the US capable of converting waste biomass into usable energy
1976	BFB Rivesville industrial scale demonstration project
1976	Start of large scale R&D program by ERDA (USA)
1978	European Commission starts supporting FBC technology with demonstration projects until 1990 [3]
1979	First CFB industrial scale power plant by Foster Wheeler
1981	First coal fired commercial CFB boiler supplied by Alstrom (now Foster Wheeler)
1981	First commercial BFB fired with biomass as main fuel type supplied by EPI
Mid 1980s	First HYBEX (BFB), Kvaerner
1982	First Lurgi Lentjes CFB is commissioned
1983	First commercial CFB fired with biomass as main fuel type by Foster Wheeler
1986	The Clean Coal Technology (CCT) Demonstration Program started (USA). Ended in 1993.
1988	Large scale (142 MWe net) BFB demonstration project in the USA.
1988	First commercial CIRCOFLUID by Babcock
1990	EU THERMIE (RD&D) programme includes 3 CFB projects, ends 1996
1992	First commercial operation INTREX by Foster Wheeler (CFB)
1994	Model project on CFB implemented in 1994 under Green Aid Programme for Asia-Pacific countries
1994	First CYMIC® Kvaerner (CFB)
1996	First IR-CFB B&W (CFB)
1999	International Energy Agency (IEA) FBC implementing agreement started, now 12 countries are member
2003	First supercritical CFB boiler Lagisza Poland Foster Wheeler with Siemens OTU (once through unit) design. Start-up is planned in 2009

The combustion processes are similar in a circulating, turbulent, or bubbling fluidized bed, but the burning rates of char are different in these beds [24]. Furthermore, fluidized-bed incinerators/combustors can be operated in two modes, bubbling or circulating, depending upon the air velocities. As the velocity of air that is passed through the bed is increased, the bed becomes fluidized and assumes fluid-like characteristics with typically small inter-particle friction. On further increase in gas velocity, the bed expands to allow most of the excess air to pass through it in the bubble phase. This bubbling or boiling action thoroughly mixes the particles and quickly establishes thermal equilibrium between gases and the particles. In the circulating bed

design, air velocities are much greater so that the well-defined surface of the bed begins to disappear, and the solids are blown overhead, separated in a cyclone, and returned to the combustion chamber. Typical air velocities in bubbling beds are usually in the range of 3 to 10 feet per second (0.9-3.1 meters per second) and for circulating beds, air velocities are around 15 to 30 feet per second (4.6-9.1 meters per second). Also, circulating beds usually operate with larger bubbles when compared to the equivalent bubbling ones. In most of the cases, circulating fluidization leads to slugging flow or bubble taking the entire cross-sectional area of the bed or dense region. This greatly decreases the mass or solids held in that region, thus most of the particles are found in the lean region. This implies that a considerable fraction of transformations or gas-solid reactions take place in the lean region as well. Due to the fluidized bed combustors having no moving parts, a compact furnace, and large heat content of the fluidized material, starting and stopping becomes very easy so they may be used for either continuous or semi-continuous operation [13,15,19,23,25,26].

1.3 Circulating Fluidized Bed

A table of thermal efficiencies for some typical FBC technologies is shown in Table 2 below by J. Koornneef et al.

Table 2

Thermal efficiency of FBC technologies [7].

Technology	Size (in MWe)	Fuel	Thermal efficiency (in %)	HHV or LHV[a]	Source
CFB	20	Biomass	33	Unknown	[83]
	150	Coal and biomass	37	LHV	[61]
	160	Lignite	41	LHV	[61]
	250	Coal	39	HHV	[84]
	297.5	Coal	36	HHV	[47]
	2 × 233	Coal	37	LHV	[61]
	460 supercritical[b]	Coal	>43	Unknown	[51]
	600 supercritical	Coal	46	LHV	[61]
BFB	25	Biomass	30	LHV	[85]

[a]HHV = higher heating value. LHV = lower heating value. The latter does not account for the enthalpy in water vapour remaining in flue gas, as this is often not converted into useful energy. HHV does account for this enthalpy and efficiencies are subsequently lower when HHV of fuel is used.

[b]To be build by Foster Wheeler in Poland, expected start-up in 2009 [51].

As can be seen by the thermal efficiencies in Table 2, (external) circulating fluidized bed (CFB) boilers are typically utilized to efficiently extract the potential energy within a fuel such as tire. "The circulating fluidized bed (CFB) is a technology for the combustion of solid fuels. It was first used for combustion of coal because of its unique ability to handle low-quality, high-sulfur coals." [8,9] In a typical CFB combustor used for coal combustion, crushed coal together with limestone or dolomite and ash particles are fluidized by the combustion air entering at the bottom of the bed (evenly distributed over the furnace cross-section) and at one or several secondary air injection points (mounted in the walls above the bottom where primary air enters) [10-18]. A large portion of the bed particles exits the riser of the CFB combustor with the

flue gas due to the high superficial gas velocities utilized. The particles are then separated from the exhaust gas in a gas/solid separator (often a cyclone) and recycled into the riser to promote complete combustion of the coal. There is perfect mixing of solids (individual ash, char particles and sorbents) in the lower region and in each zone of the upper region [10,11,19,20]. This assumption is justified by the high internal and external recirculation of solids in the bed [21]. The contribution of the cyclone and the circulation loop on the overall combustion process is often neglected [10-12,21].

A unique feature of a CFB combustor is the recirculation of solids, captured by the cyclone at the top of the riser and recycled back to the base of the riser [10,16,22]. Particles below the cut-size of the cyclone are carried forward to the boiler and de-dusting part of the plant [23]. Fig. 1 below by Basu discloses the schematic of a CFB boiler furnace showing the lower dense zone and the core and annular regions in the upper fast fluidized bed zone.

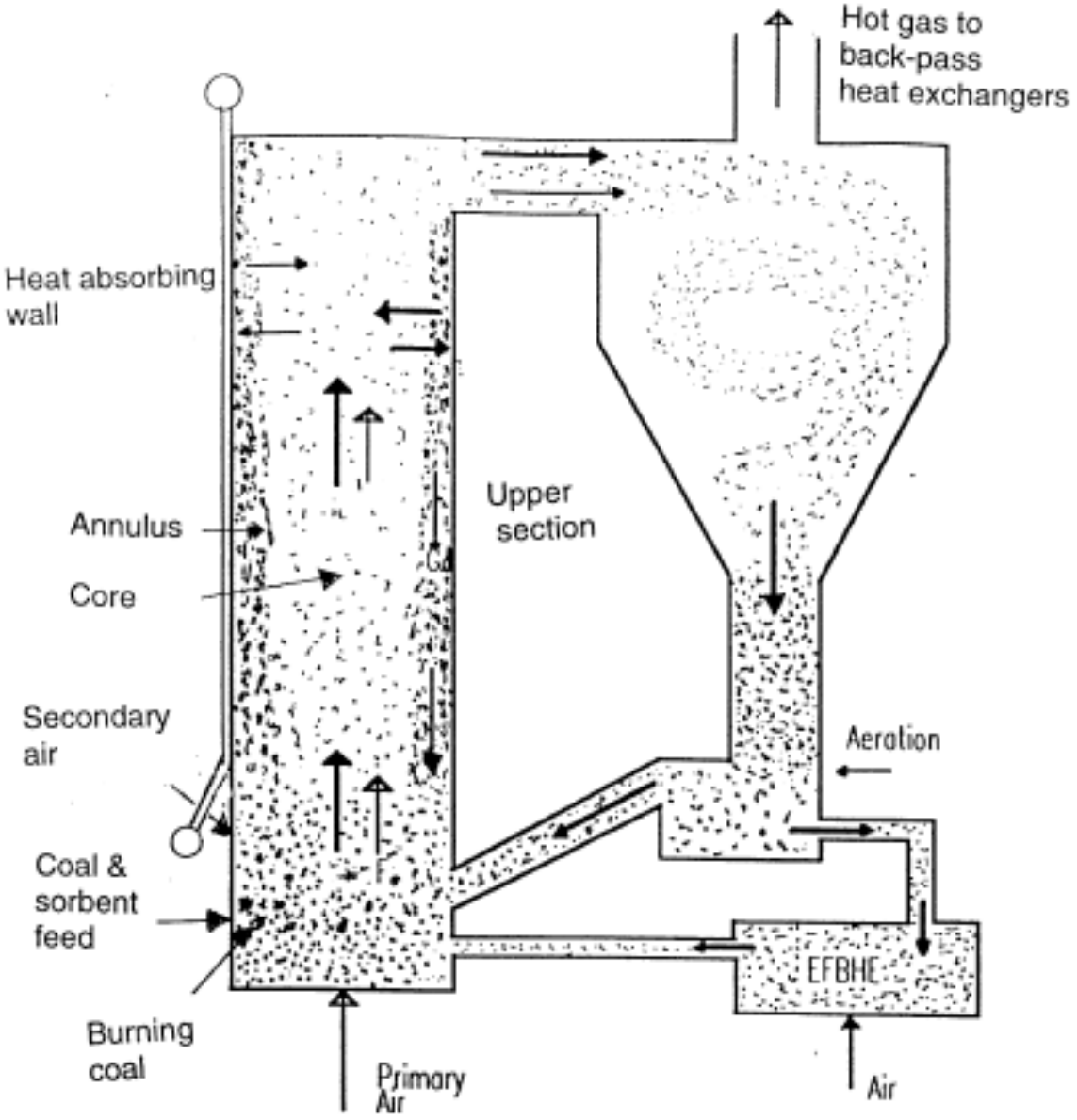

Fig. 1. Schematic of CFB boiler [24].

Both capacity and number of CFB boilers in use are increasing as exhibited in Fig. 2 below by Basu. At the time of writing, more than 500 CFB boilers were either in operation or under construction [24].

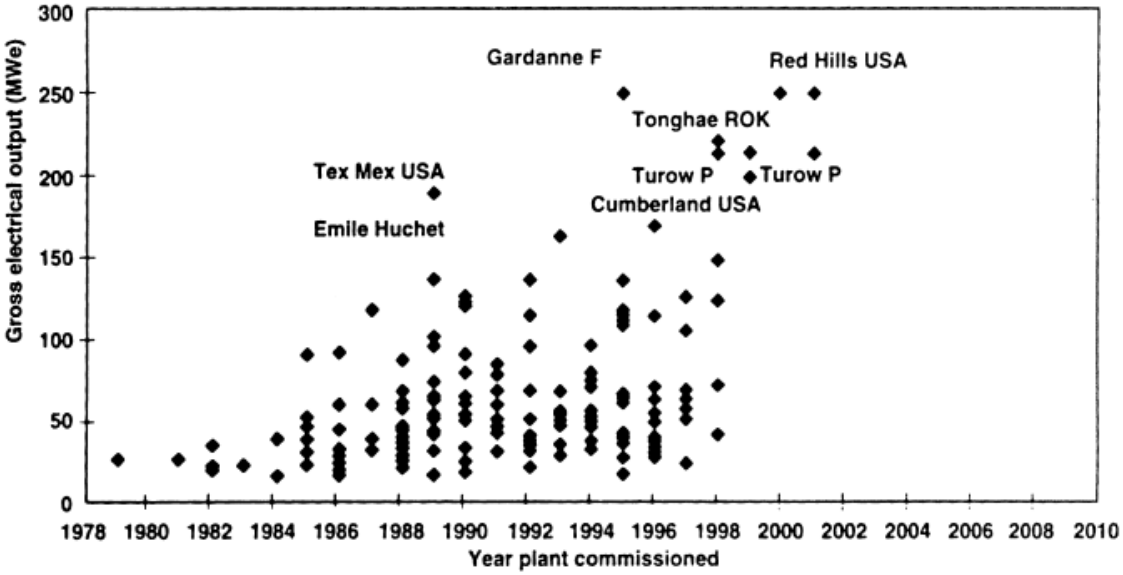

Fig. 2. Growth of CFB boilers constructed and electric output [24].

The present thesis is concerned with modeling combustion of waste tire via similarities with lignite coal combustion in the CFB boiler as well as developing and presenting a Microsoft Excel based program which can be used to predict emissions from the CFB boiler.

2. LITERATURE REVIEW

A list of CFB (as well as other fluidized beds highlighted in yellow) experiments and models that have information regarding emission concentrations at the top of the riser (entrance to cyclone) are listed in Table 3 below. Key species and parameters that were mentioned have been marked with an 'X'. If certain items had to be indirectly found through calculation, were not mentioned, or were not applicable, then the corresponding cells were left blank (without an 'X').

The chosen experiments and models cover a wide range of fuels including biomass, coal, tire, and waste (but only one type of fuel is fired at once so no co-firing of fuels). There is also a wide range of fluidized beds performing combustion with air as the oxidizer, but not gasification nor stationary or fluidized beds with little entrainment of fuel particles in the freeboard because these are not accurately depicted by the proposed model due to fuel particles shrinking in the bed instead of moving along with the gaseous mixture into the freeboard/riser. While this is not a comprehensive listing of all known fluidized bed experiments and models, this is a good sample of what is readily available from 1974 to 2013.

Table 3

CFB and other fluidized bed (yellow) models and experiments.

Authors (Year)	Computer Program	Model Validation	CO	H2O	O2	N2	NH3	HCN	SO2	CO2	H2	NO	Species Concentration Basis	Fuel
MODELS														
Overturf & Reklaitis (1983) [39]		X	X		X					X				Coal
de Souza-Santos (1989) [40]		X	X	X	X	X	X		X	X	X	X	Dry, Wet	Coal
Das & Bhattacharya (1990) [22]	FORTRAN	X	X		X					X				Coal
Oymak et al. (1993) [41]	FORTRAN	X	X		X					X				Coal
Wang et al. (1994) [35]		X	X		X									Coal
Arena et al. (1995) [11]					X									Coal
Goel et al. (1996) [42]		X	X		X		X	X		X		X		Biomass, Coal
Desroches-Ducarne et al. (1998) [31]		X	X		X		X	X		X		X		Waste
Huilin et al. (1998) [21]			X	X	X				X	X			Wet	Coal
Sotudeh-Gharebaagh et al. (1998) [10]	ASPEN PLUS	X	X						X			X		Coal
Huilin et al. (1999) [12]		X	X	X	X				X	X			Wet	Coal
Knoebig et al. (1999) [38]		X	X		X								Dry	Coal
Lee & Kim (1999) [18]			X		X				X	X		X		Coal
Wang et al. (1999) [14]		X			X				X			X		Coal
Huilin et al. (2000) [13]		X	X	X	X				X	X			Wet	Coal
Adanez et al. (2003) [8]		X	X	X	X					X	X		Wet	Biomass
Lee et al. (2003) [43]		X	X	X	X				X	X			Wet	Coal
Gungor & Eskin (2006) [32]	FORTRAN	X			X				X			X		Coal
de Souza-Santos (2007) [36]		X	X		X	X	X	X	X	X	X	X	Dry	Coal
Gungor (2007) [44]	FORTRAN	X	X		X		X					X		Biomass
Gungor & Eskin (2007) [45]	FORTRAN	X	X		X				X			X		Coal
Alagoz et al. (2008) [30]		X	X		X					X			Dry	Coal
Gungor (2008) [16]	FORTRAN	X							X			X		Coal
Gungor (2010) [46]	FORTRAN	X	X									X		Biomass
Lee et al. (2013) [9]		X							X			X		Coal
EXPERIMENTS														
Pereira et al. (1974) [47]												X		Coal
Chang et al. (1991) [25]			X						X			X		Waste
Dam-Johansen & Ostergaard (1991) [48]									X	X				Coal
Kim et al. (1994) [4]			X									X		Coal, Tire
Ogada & Werther (1996) [49]			X		X					X				Waste
Knobig et al. (1998) [50]			X		X		X					X	Dry	Biomass, Coal
Lyngfelt & Leckner (1999) [51]			X									X	Dry	Biomass
Topal et al. (2003) [52]			X		X				X	X		X		Biomass, Coal
Fang et al. (2004) [53]			X		X				X	X		X		Biomass

Table 3

Continued.

Authors (Year)	Fuel Feed Rate	Fuel Particle Density	Fuel Sauter Mean Diameter	Fuel Higher Heating Value	Proximate Fuel Analysis	Ultimate Fuel Analysis	N Released as Volatiles	Volatile N Released as N2	Volatile N Released as NH3	Volatile N Released as HCN	Excess Air	Limestone	Ca/S Ratio	Limestone Diameter	Limestone Moisture	Limestone Sulphation	Pressure	Temperature	Riser Cross-Sectional Area	Riser Height
MODELS																				
Overturf & Reklaitis (1983) [39]	X				X	X					X		X		X		X	X	X	X
de Souza-Santos (1989) [40]	X				X	X					X		X			X			X	X
Das & Bhattacharya (1990) [22]	X				X						X							X	X	X
Oymak et al. (1993) [41]	X	X	X	X	X	X					X						X		X	X
Wang et al. (1994) [35]				X	X	X					X							X	X	X
Arena et al. (1995) [11]											X						X	X	X	X
Goel et al. (1996) [42]	X						X	X	X	X	X						X	X	X	X
Desroches-Ducarne et al. (1998) [31]							X	X	X	X	X							X	X	X
Huilin et al. (1998) [21]	X	X			X	X					X		X	X			X	X	X	X
Sotudeh-Gharebaagh et al. (1998) [10]	X										X		X					X	X	X
Huilin et al. (1999) [12]	X					X					X		X	X				X	X	X
Knoebig et al. (1999) [38]																		X	X	X
Lee & Kim (1999) [18]	X				X						X		X					X	X	X
Wang et al. (1999) [14]	X			X	X	X					X								X	X
Huilin et al. (2000) [13]	X					X							X	X				X		X
Adanez et al. (2003) [8]						X					X							X	X	X
Lee et al. (2003) [43]	X	X			X	X					X		X					X	X	X
Gungor & Eskin (2006) [32]			X			X					X			X					X	X
de Souza-Santos (2007) [36]	X	X			X	X					X		X		X	X	X	X	X	X
Gungor (2007) [44]			X		X	X					X						X	X	X	X
Gungor & Eskin (2007) [45]	X		X		X	X					X		X	X			X	X	X	X
Alagoz et al. (2008) [30]	X	X		X	X	X					X						X	X	X	X
Gungor (2008) [16]	X		X		X	X					X		X	X			X	X	X	X
Gungor (2010) [46]	X				X	X					X						X	X	X	X
Lee et al. (2013) [9]	X	X			X	X					X		X						X	X
EXPERIMENTS																				
Pereira et al. (1974) [47]					X	X					X							X	X	X
Chang et al. (1991) [25]	X			X	X	X							X	X				X	X	X
Dam-Johansen & Ostergaard (1991) [48]	X																X		X	X
Kim et al. (1994) [4]				X	X	X					X							X	X	X
Ogada & Werther (1996) [49]					X	X			X									X	X	X
Knobig et al. (1998) [50]					X	X					X							X	X	X
Lyngfelt & Leckner (1999) [51]					X	X					X							X	X	X
Topal et al. (2003) [52]	X	X		X	X	X					X							X	X	X
Fang et al. (2004) [53]		X		X	X	X												X	X	X

There are some important trends seen in Table 3. Almost all software noted for model calculations was FORTRAN except for one that used ASPEN PLUS [10]. To the

author's knowledge, there have been no CFB models that have used Microsoft Excel for calculations. However, almost all models were validated with experimental data.

None of the models or experiments investigated in Table 3 showed concentrations for all ten key species (CO, H_2O, O_2, N_2, NH_3, HCN, SO_2, CO_2, H_2, and NO) at the exit of the CFB riser. In fact, most models and experiments only focused on a few of the key species (with CO, O_2, SO_2, CO_2, and NO being the most common probably due to regulation specific to these species) except for de Souza-Santos who had nine of the ten key species modeled [36,40]. Surprisingly, the form in which the species' concentration was reported is also rarely clear whether it is on a dry or wet basis and if it was corrected/normalized to a standard percent O_2 or not.

The fuel feed rate, proximate fuel analysis, ultimate fuel analysis, excess air, Calcium to Sulfur ratio when applicable, temperature, riser cross-sectional area, and riser height were almost always provided by the models and experiments reviewed as seen in Table 3.

2.1 Modeling

Few papers existed on modeling CFB combustors in 1993 [22,35]. However, CFB combustion was receiving wide research attention in 2003 in view of its potential as an economic and environmentally acceptable technology for burning low-grade coals along with biomass and organic wastes and their mixtures. There was also a focus in 2003 on developing models of CFB for burning biomass and waste material [27].

Mathematical modeling allows the testing of many variable combustion parameters in a much shorter time period and at lower costs. Therefore, mathematical

modeling application in the CFB combustion process to enhance combustion performance and reduce pollutants is seen as an attractive solution [16].

Of course, mathematical models can only represent approximations of reality. Nonetheless, the degree of deviation between real operational data and simulation results can be decreased. In addition, the range of applicability of a model may also be extended. It is important to have in mind that detailed data concerning geometry and operational conditions of units are not easily available. In addition, reliable operational data collected during real steady-state operations are also rare [9,36]. Also, incompleteness of the published data required to fix the initial conditions for the prediction procedures, or to compare with the predictions of the models so that a test of the model can be performed is evident [37].

Still, much is to be done in the field of mathematical modeling and simulation of combustion in CFB combustors. One problem is that surprisingly little is known about the processes in large combustion chambers. The cost and time of investigations on commercial-size boilers and the inaccessibility of boiler furnaces are probably the reasons why only a few publications are available in the open literature describing in-furnace processes. This might be attributed to the fact that the combustion process occurring in CFB combustors involves complex phenomena including chemical reactions, heat and mass transfer, particle size reduction due to combustion, attrition, fragmentation, and other mechanisms, gas and solid flow structure, etc. [10,12,13,16-18,29]

Furthermore, the numerous homogeneous and heterogeneous catalytic gas-phase reactions and their kinetics for the description of the combustion phenomena, and the pollutant formation and destruction are not completely known. Therefore, it is necessary to develop simplified modeling approaches, which can describe both, the gas-solid flow structure and the combustion process with sufficient accuracy [16,38].

2.1.1 One-dimensional

A few models assume the gaseous phase in a CFB riser to be one-dimensional plug flow [10,11,14,16,22,24,27,35,36,42,43] consistent with experimental evidence based on gas-backmixing tests which gives an overall picture of combustion, but this does not take into account the denser down-flowing annular or wall region of the furnace [10,16,21,24,27,35,75]. However, it has been argued that the 'core-annulus' flow structure in CFB risers is not well understood, that the use of 'block' and 'annulus-core' structures in modelling CFB combustion is not necessarily better than simply assuming that solids are dispersed evenly in the riser, and that the radial solids flux profile is uniform [6,35].

These models also assume particles are spherical [8,10,21,22,24,27,31,35,45,60] and characterized by an equivalent particle diameter, the fluidized bed is isothermal, and devolatilization and volatile combustion processes take place exclusively in the lower region of the CFB reactor [10,12,13,21,54,62] so that only char combustion, NO_x formation, and SO_2 capture are considered to occur in the upper region [10,24,27,35].

Fig. 3 below by Lee and Kim gives an idea of the similar solid fraction in each part of the combustor even during different loads.

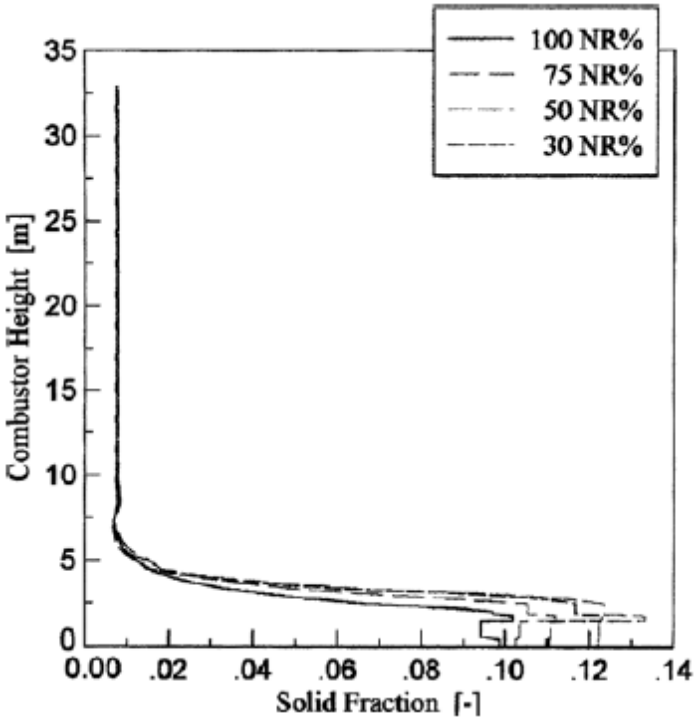

Fig. 3. Solid fraction versus combustor height at various loads [18].

However, each particle size in the solid fraction is moving at differing speeds. As seen in Fig. 4 below by Huilin et al., particle velocity sharply increases at the entrance of the combustor for all sizes and quickly levels out indicating that the particles quickly reach terminal velocity in the lower portion of the combustor to a velocity appropriate to the size of the particle. On the other hand, the velocity of the gas mixture is fairly constant with slight changes as it flows up the combustor due to less particles blocking the gas flow so that the effective cross-sectional area increases causing the velocity to slightly decrease. This decrease in gas velocity is reflected in a similar slight decrease in particle velocity in the upper portion of the combustor [21].

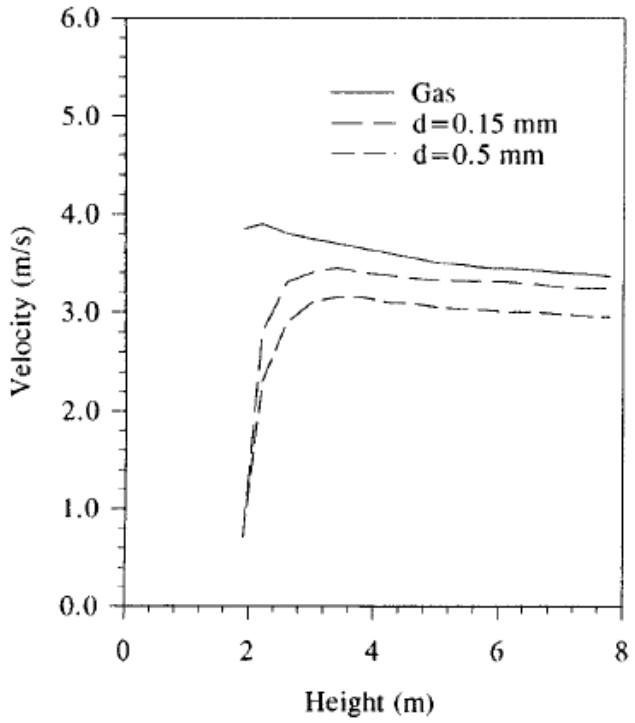

Fig. 4. Gas and different size particles' velocities along the combustor [21].

2.1.2 Three-dimensional

The semi-empirical description of the flow structure for three dimensions is still at the beginning of its development and such models are therefore relatively scarce in literature. Three-dimensional models describing the flow behavior of gas and solids in CFB riser are usually either empirical or based on the fundamental equations of fluid dynamics. Computational fluid dynamic (CFD) models employ the full set of partial differential equations that describe the conservation of mass, momentum, energy and chemical species. However, these models are at present just too complex to serve as a basis for reactor modeling. Furthermore, their computational times are very long due to the unsteady character of the numerous partial differential equations, which restricts

their application to pure fluid dynamical simulations at present. A semi-empirical model approach, which is based on experimental findings and empirical correlations obtained from measurements, provides the possibility to account for the complex flow patterns inside CFB combustors with comparatively low computational error. This allows an application of this type of model to the complex reaction schemes typical for the combustion process. In order to be able to account for the complex kinetics of pollutants formation and destruction, the fluid dynamic part of the model is kept comparatively simple [38,43].

2.1.3 Computer computational time

Some program/computer combinations of combustion models are the IBM 370 Model 145 computer with typical running times of 16 minutes for no recycle of elutriated char particles [37], the Burroughs 6900 computer with a program running time of about 2 minutes [73], and the HP Exemplar S Class (SPP-2000) computer with one solution of the balances in the combustion chamber requiring a computational time of approximately 2.5 hours. Since the simulations of the HP Exemplar S Class contain an iterative determination of the mass flux of recycled char the total calculation time for one operating condition may exceed 12 hours [38].

2.2 Fuels

CFB boilers have been installed worldwide to burn a wide variety of biomass and biomass wastes along with other opportunity fuels and coals due to expansion of Renewable Portfolio Standards by utilities and power generation companies through biomass fuels [10,24,27,28]. However, “A number of technical problems are inherent in

biomass combustion that limit the increasing utilization of biomass. Alkali-ash deposition and emissions, fairly high NOx emissions in potential violation of future strict legislation, and high costs of construction, operation, and maintenance of biofuel plants due to size limitations are the most severe issues with respect to boilers." [8]

Lignite is estimated to comprise approximately 29% of the solid fuel reserves of the US. Also, there are considerable reserves of lignite in Turkey. Most of the Turkish lignite reserves are of low-grade lignites with a calorific value of about 12,000 kilojoules per kilogram, ash content of about 25–30% and average sulfur content of typically less than 4%. As can be seen, the lignite is characterized by its high ash and VM/FC ratio. Lignite is a particularly attractive fuel for FBC applications for at least two reasons. First, lignite is highly reactive, largely due to its very porous nature; and second, it contains significant quantities of alkali mineral matter relative to sulfur content. As a result, high carbon conversion can be achieved in a once-through fluidized bed system, while retention of sulfur dioxide by the coal mineral matter may significantly reduce the quantity of limestone or other sorbent material which must be used [16,29-31].

Nonetheless, CFB technology fires many different types of fuels such as MSW and lignite, and has demonstrated ability to fire fuels with heating values ranging from 9,300 to 32,500 kilojoules per kilogram as well as high sulfur content fuels by primarily using limestone sorbent for sulfur capture. Some CFB combustion advantages are high combustion efficiency, larger fuel particles may be used due to longer residence times when compared to a typical pulverized coal boiler (reduces auxiliary power consumption for grinding), adding limestone with fuel in the CFB to capture sulfur which may

eliminate a downstream scrubber, and flue gas NO_x emission levels are inherently low due to a relatively low combustor temperature [6,8,10,13,16,21,24,25,27,28,32,33].

Some down sides to combusting scrap tires is its containing wire which can form 'bird-nest' in the bed material. These must be removed by properly designed extraction systems to avoid plugging of the bed drains and subsequent de-fluidization. Tires can also contain fiberglass which can form clinkers or lead to agglomeration. In addition, the ash can contain elevated zinc oxide levels which make ash disposal more problematic [5].

Also, tire must be ground to less than 2.5 centimeters (25,000 microns) via cryogenic grinding which is costly at 3-5 times more than normal coal grinding in order to achieve complete combustion in a coal-fired boiler. In one instance, waste tires were crushed in a shredder to remove steel cords and textiles in order to obtain granule sizes of 1.4-2.3 mm. Bituminous coal particles were also prepared for combustion at the same size as the crushed waste tires [1,4].

It has been shown for ground tire particles of 75 to 90 microns that diffusion-controlled combustion predicted to burn the particles in 8.5-12.5 milliseconds (same size coal predicted in 25 to 36 milliseconds), but observed 30-60 milliseconds (coal 20-37 milliseconds) when actually burned. For ground tire particles of 180-212 microns, diffusion-controlled combustion predicted 50-70 milliseconds (coal 144-200 milliseconds), but observed 43-85 milliseconds (coal 150-170 milliseconds) [1]. Although literature seems sparse on the comparison between coal and tire combustion as well as tire combustion in general, these experiments revealed similarities between the burning of coal and tire [4,34].

2.2.1 Fuel density

The fuel particle density (ρ_{Fuel}) was only provided by a few in the literature. Therefore, Annamalai and Puri [54] can be used to find the density of various grades of coal while Table 4 below by Van Caneghem et al. can be used to find the density of several biomass and waste materials.

Table 4

Density and moisture content for domestic, commercial, and industrial solid waste [23].

Item	Density (kg/m^3)		Moisture content (% by mass)	
	Range	Typical	Range	Typical
Loose residential waste				
Food waste (mixed)	130–480	290	50–80	70
Paper	40–130	85	4–10	6
Cardboard	40–80	50	4–8	6
Plastics	40–130	65	1–4	2
Rubber	100–200	130	1–4	2
Garden trimmings	60–225	100	30–80	60
Wood	130–320	240	15–40	20
Dirt, ashes, etc.	320–1000	450	6–12	8
Ashes	650–830	745	6–12	6
MSW (mixed)	90–180	130	5–20	15
Wastewater treatment sludge	1000–1050	1030	50–75	35
Commercial waste				
Food wastes (wet)	475–950	535	5–85	75
Wooden crates	110–160	110	10–30	20
Tree trimmings	100–180	150	20–80	30
Industrial waste				
Chemical sludge (wet)	800–1100	1000	75–99	80
Fly ash	700–900	800	2–10	4
Oils, tars, asphalts	800–1000	950	0–5	2
Sawdust	100–350	290	10–40	15
Textile wastes	100–220	180	6–15	10
Wood (mixed)	400–675	500	10–40	20
Agricultural waste				
Agricultural (mixed)	400–750	360	40–80	50
Fruit wastes (mixed)	250–750	360	60–90	75
Manure (wet)	900–1050	1000	75–96	94
Vegetable wastes (mixed)	200–700	360	50–80	65

2.2.2 Fuel higher heating value

The fuel higher heating value (hhv_{Fuel}) also was only provided by a few in the literature. The hhv_{Fuel} of fuels can be estimated from the Boie equation. "The Boie equation is an empirical relation that can be used to determine the HHV of many CHNOS fuels, including solid and liquid fuels. The relation is HHV kJ kg^-1 = 35,160 x Y_C + 116,225 x Y_H - 11,090 x Y_O + 6,280 x Y_N + 10,465 x Y_S where Y_C, Y_H, Y_O, Y_N, and Y_S denote the mass fractions of carbon, hydrogen, oxygen, nitrogen, and sulfur in the fuel (as received)." [54]

2.2.3 Fuel Nitrogen

In only a couple instances was it found that $Y_{VN,N}x100$, $Y_{N_2,N}x100$, $Y_{NH_3,N}x100$, and $Y_{HCN,N}x100$ for fuels used in experimentation was given in the literature. However, Kambara et al. show several coals that have been tested for these values at certain temperatures [57]. The high pyrolysis rate is typical of CFB combustion applications [19]. Also, these values can be extended to other fuel types of similar proximate and ultimate analyses. "The temperature increase results in increased NH_3 formation until most of the volatile matter has been released but after about 1000 K, the effect of temperature is the reverse. In high temperature pyrolysis, HCN becomes the dominating nitrogen compound...In all the gasifiers examined so far, more NH_3 than other compounds is formed irrespective of the fuel which is gasified. The content of NH_3 in the fuel gas depends most of all on the fuel nitrogen content…quaternary nitrogen in fuel produces NH_3 while pyrrole and pyridine nitrogen in fuel produces HCN." [57,58]

Therefore, the Nitrogen volatiles partitioning depends on fuel type, pyrolysis temperature, and heating rate. Higher heating rates appear to increase the HCN/NH_3 ratio for both coal and biomass fuels. At low heating rates, NH_3 is generally the dominant product, both for coals and biomass [59].

Nelson et al. also found HCN to be the dominant gaseous Nitrogen compound at temperatures greater than 1,000 K, independent of coal type for seven coals tested (brown coal to bituminous coal). It was concluded that cracking reactions of the tars are a probable source of HCN and NH_3, but release of Nitrogen from structures which are not volatilized as tar occurs also. It is obvious from the results that tar cracking or pyrolysis is important, because the tar yield decreases simultaneously with the increases in HCN and NH_3 yields at approximately 900 K [6].“The origin of nitrogen in coal is the plant materials of the geological period at which the coal originated…the nitrogen present in coal is virtually exclusively organic nitrogen and is principally in the form of pyridinic, pyrrolic and quaternary functional groups in polycyclic aromatic compounds which are part of the macromolecular structure.” [62] In order to utilize the appropriate $Y_{VN,N}x100$, $Y_{N_2,N}x100$, $Y_{NH_3,N}x100$, and $Y_{HCN,N}x100$, Table 5 below by Kambara et al. should be used to compare the fuel’s proximate and ultimate analyses to that of Kambara’s coals to find the closest match. Once the best coal type fit is chosen, then Fig. 5 below by Kambara et al. is used to find $Y_{VN,N}x100$ at a certain temperature [62,63], Fig. 6 below by Kambara et al. is used to find $Y_{N_2,N}x100$ and $Y_{NH_3,N}x100$ at a certain temperature, and Fig. 7 below by Kambara et al. is used to find $Y_{HCN,N}x100$ at a certain temperature. For lower grade fuels such as biomass, waste, etc., the lowest rank

coal (Coal T in Table 5) can be used to give estimates of $Y_{VN,N}x100$, $Y_{N_2,N}x100$, $Y_{NH_3,N}x100$, and $Y_{HCN,N}x100$. Also, Wendt has derived a purely empirical correlation for twenty coals and two coal chars of weight percent Nitrogen loss dependent upon temperature which seems to be in line with much of Kambara's results [64]. In addition, Fig. 8 below by Kambara et al. verifies that tar yields are negligible [6,15,36,40,57,65].

Table 5

Proximate and ultimate fuel analyses of several coals [57].

		proximate analysis [wt %, db]			ultimate analysis [wt %, daf]				
coal	source	ash	volatile matter	fixed carbon	C	H	N	O[a]	S
A	Canada	10.0	20.8	69.2	88.1	4.5	1.20	5.8	0.37
B	Australia	12.4	26.3	61.4	85.1	4.8	1.70	8.0	0.40
C	Australia	16.2	29.6	54.2	84.9	5.0	1.92	7.6	0.61
D	Australia	8.0	30.3	61.7	84.6	5.1	2.25	7.1	0.94
E	Australia	12.6	26.6	60.8	83.9	4.7	1.74	9.3	0.36
F	Australia	12.4	31.9	55.7	82.6	5.2	1.40	10.5	0.32
G	Australia	7.4	29.0	63.7	82.5	4.6	1.90	10.5	0.51
H	Australia	8.3	31.8	60.0	81.9	5.2	1.84	10.3	0.74
I	China	5.8	31.4	62.9	81.9	4.8	1.01	11.8	0.50
J	Australia	8.8	39.1	52.1	81.8	5.6	1.82	10.0	0.78
K	Australia	13.2	32.8	54.0	81.5	5.4	1.88	10.7	0.51
L	Australia	9.7	33.8	56.5	81.1	5.3	1.76	11.3	0.49
M	Australia	11.1	30.7	58.1	80.8	5.1	1.35	12.3	0.39
N	Australia	7.3	30.6	62.1	80.8	4.5	1.82	12.7	0.25
O	Australia	9.6	41.8	48.6	80.1	5.9	1.40	12.0	0.55
P	Canada	7.7	38.3	54.0	78.0	5.3	1.03	15.6	0.14
Q	Japan	11.8	44.8	43.4	76.2	6.1	1.20	16.5	0.07
R	U.S.A.	5.1	43.5	51.4	72.8	4.6	1.08	21.3	0.16
S	U.S.A.	8.1	48.8	43.0	69.2	4.9	0.90	25.0	0.04
T	Australia	1.5	47.1	51.4	65.4	4.4	0.56	29.4	0.28

[a] O = 100 − (C + H + N + S).

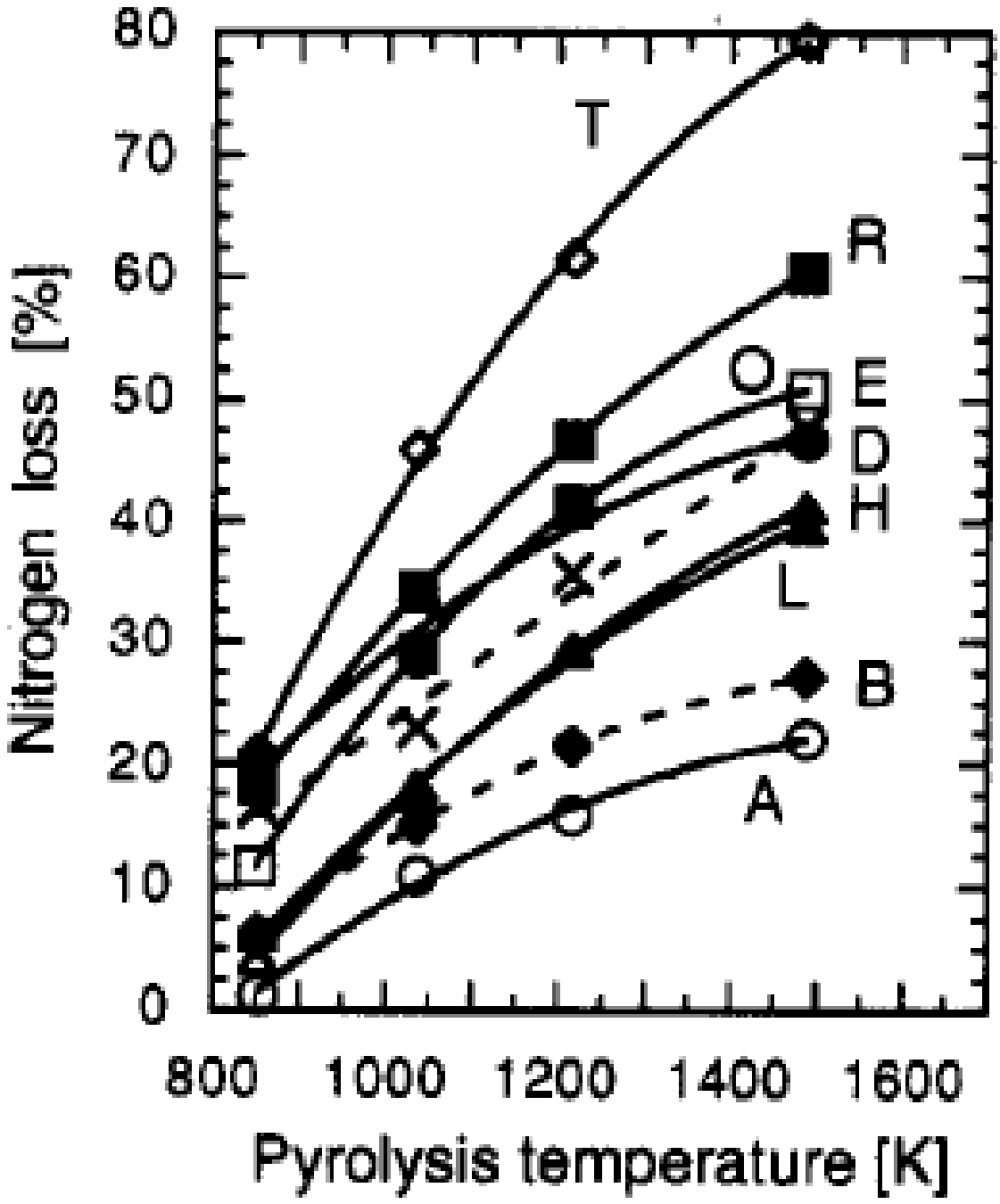

Fig. 5. Nitrogen loss versus pyrolysis temperature for several coals [57].

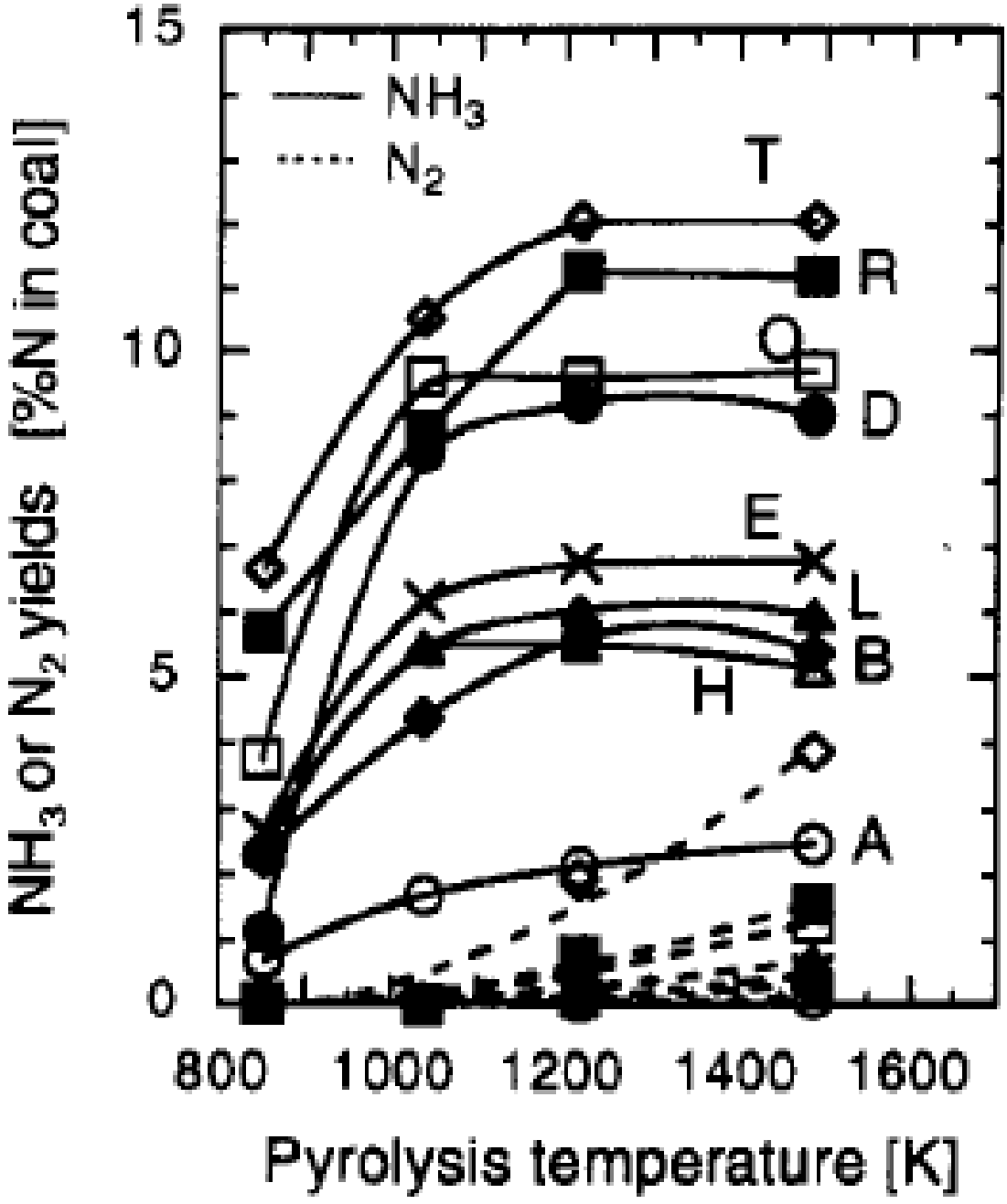

Fig. 6. NH_3 and N_2 yield versus pyrolysis temperature for several coals [57].

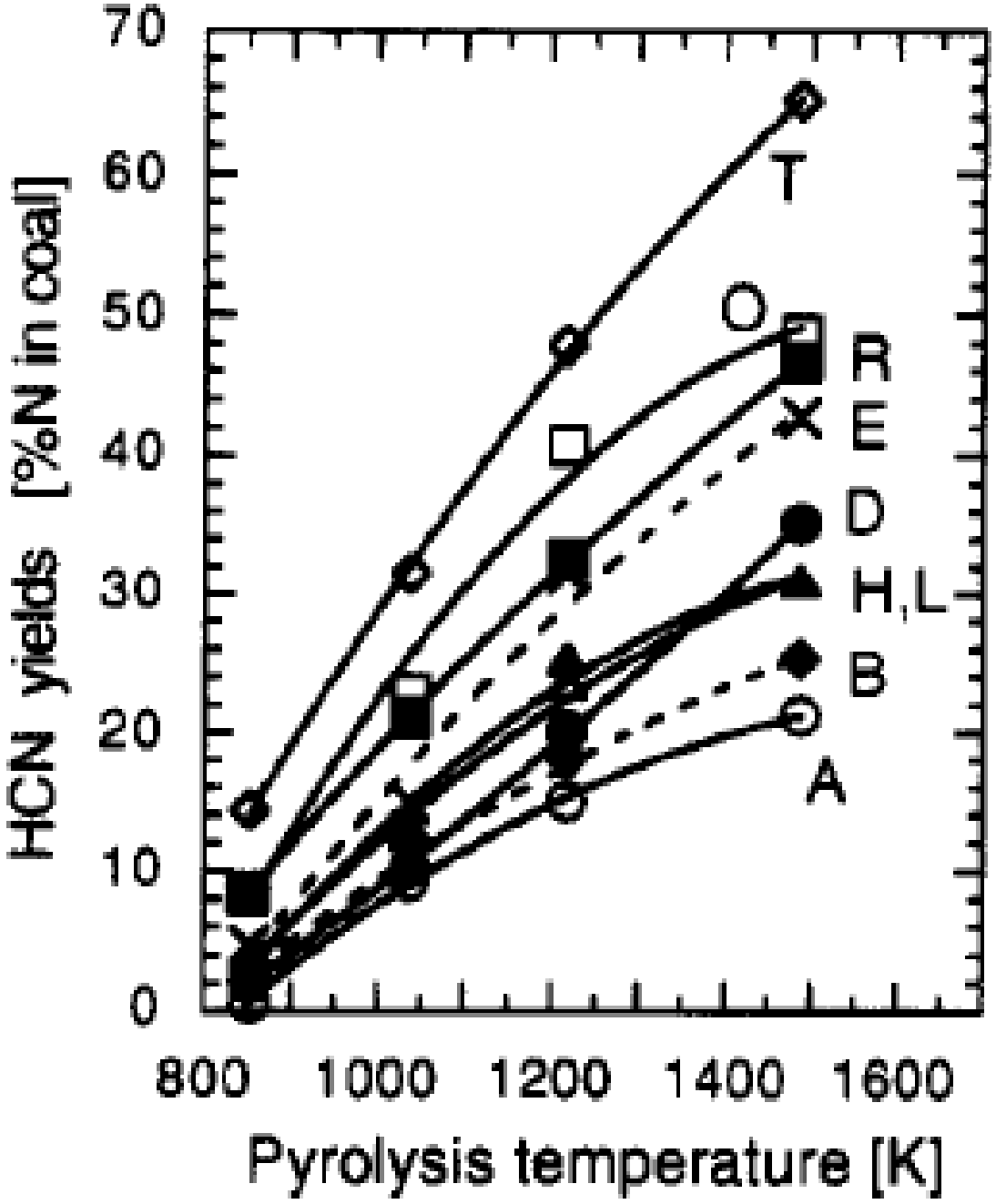

Fig. 7. HCN yield versus pyrolysis temperature for several coals [57].

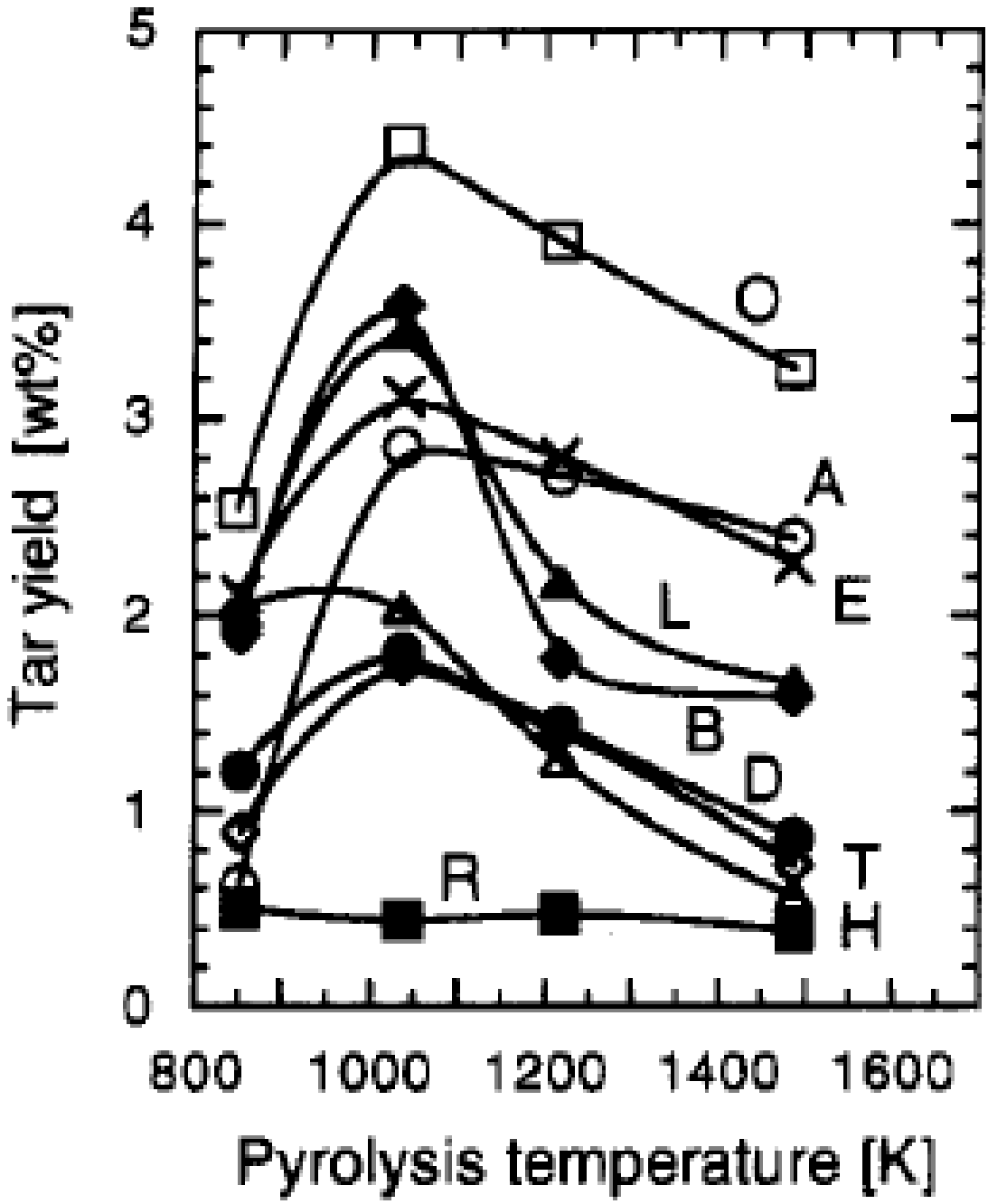

Fig. 8. Tar yield versus pyrolysis temperature for several coals [57].

HCN and NH_3 can react homogeneously with both O_2 and NO (NH_3 oxidation can be faster yet it is highly temperature sensitive due to higher activation energy) to

form mostly NO and N_2, respectively [6,16,17,31,58,60]. Fig. 9 below by Johnsson and Glarborg gives a snapshot of relative reaction rates of several Nitrogen species reactions.

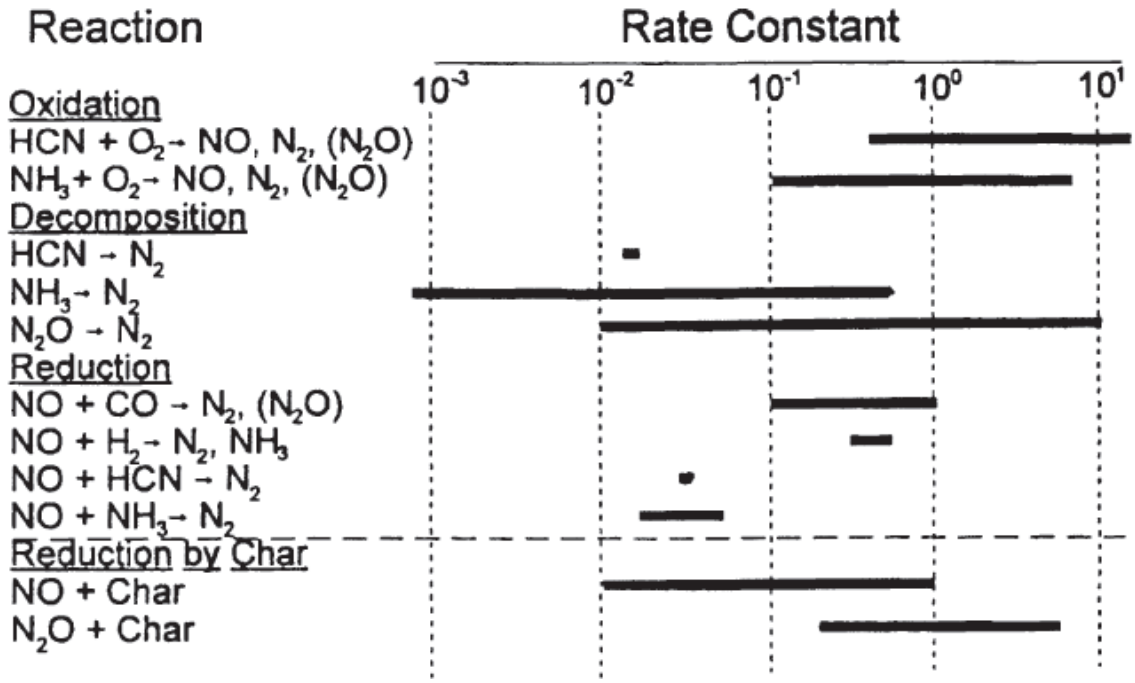

Fig. 9. Reaction rates of key Nitrogen species' reactions [61].

A chart showing the theoretical path of the fuel Nitrogen is given in Fig. 10 below by Desroches-Ducarne et al.

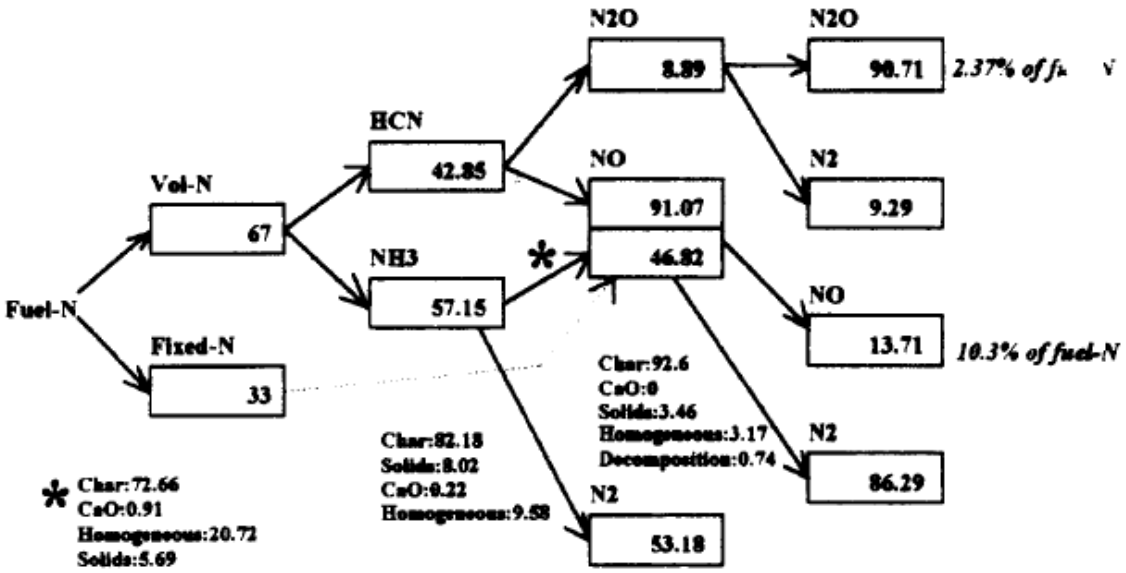

Fig. 10. Path of fuel Nitrogen in a CFB combustor [31].

2.3 Combustion

In general, a fresh coal particle, dropped into the bed, undergoes the following sequence of events: 1.) heating and drying, 2.) devolatilization and volatile combustion, 3.) swelling and primary fragmentation (for some types of coal), 4.) burning of char [12,24,63,71]. Graphical overviews can be seen in Fig. 11 below by Thomas and Fig. 12 below by Annamalai and Ryan.

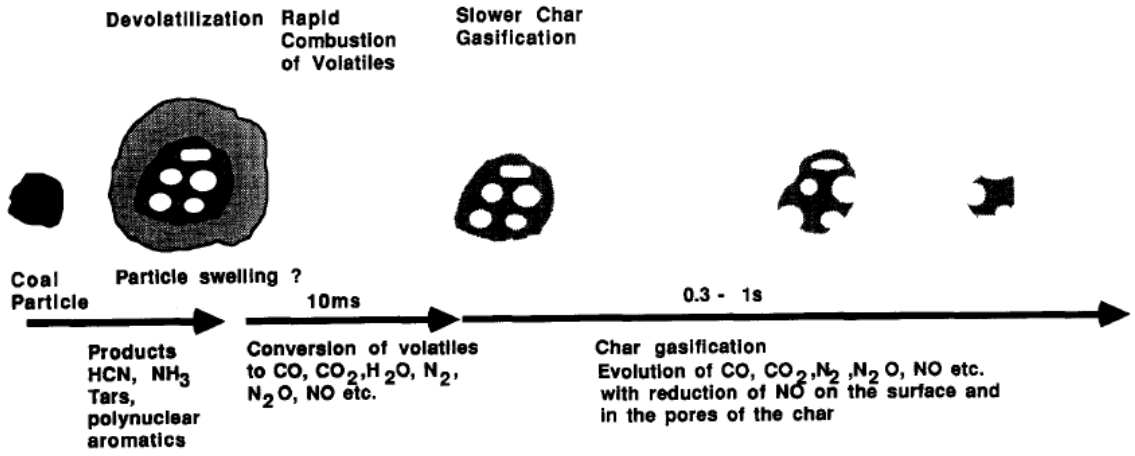

Fig. 11. Horizontal overview of coal combustion [62].

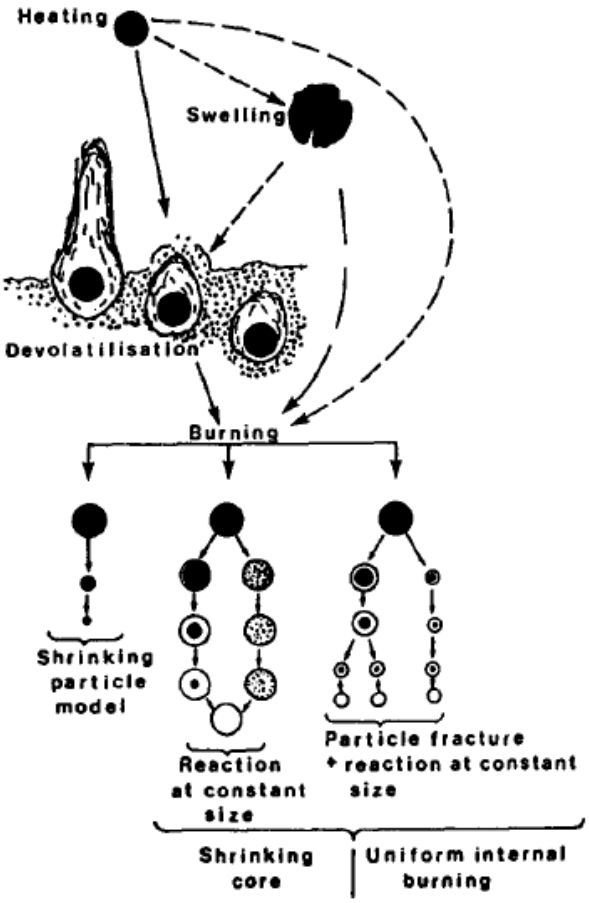

Fig. 12. Vertical overview of coal combustion [71].

2.3.1 Devolatilization

Some models have volatile matter assumed to be released immediately from coal upon entry into the furnace [10,13-15,24,29,31,35,38,42,49,72-74] and coal burned uniformly throughout the riser. This seems to be a good assumption since release of vapor from the waste particle core cools the particle's surface and keeps its temperature low, so that it can be assumed that char combustion starts only after devolatilization is completed [10,23,65].

Non-swelling particles do not become liquid during heating, but rather crack and allow pores or fissures to open up, allowing volatiles to escape through them. These particles, somewhat more typical of the Western low-rank coals, do not change their size appreciably during devolatilization even though they lose mass. Wendt depicts both melting and non-melting solid fuel volatile release in Fig. 13 below.

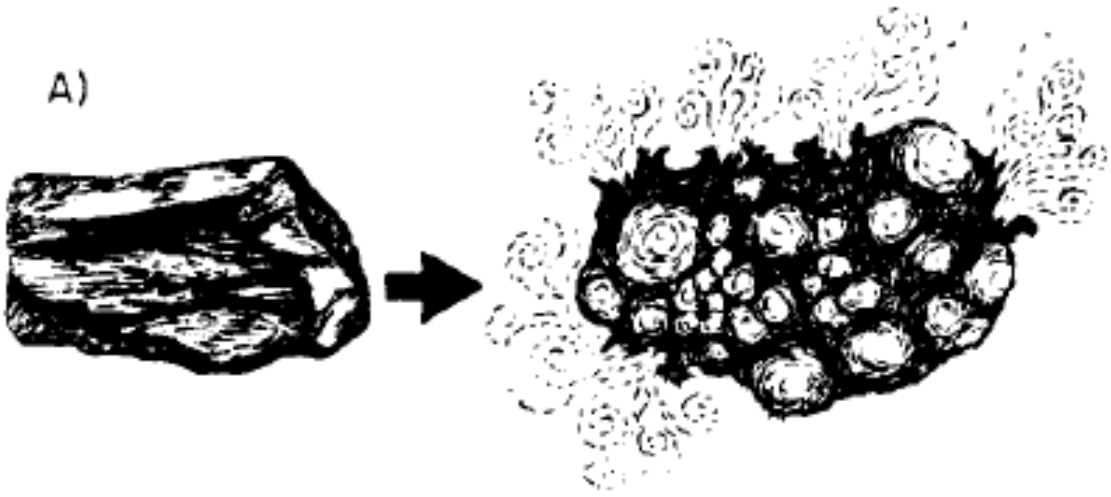

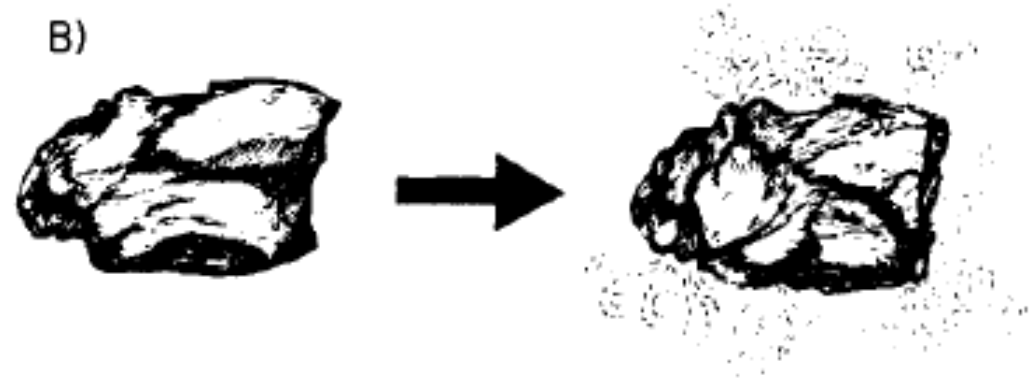

Fig. 13. Volatile release via melting and non-melting fuels [64].

2.3.2 Char burning

The combustion rate of char which is left after devolatilization is an order of magnitude less than the devolatilization rate, and the degree of devolatilization and its rate increase with increasing temperature [16,24,32,57]. Combustion of residual char particles is presumed to begin with oxygen diffusion to the burning char particle as depicted in Fig. 14 below by Annamalai and Ryan, but chemical reaction rate at the surface/pores of the particle is also important as seen in Fig. 15 below also by Annamalai and Ryan.

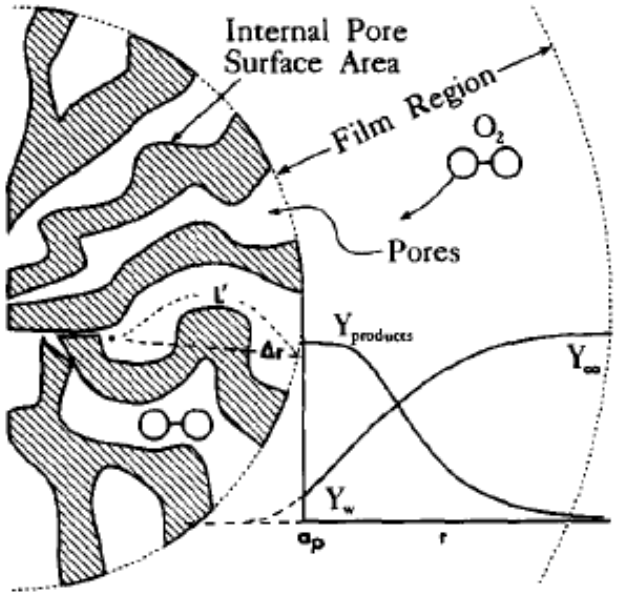

Step 1: O_2 diffuses through the film region to the particle surface.
Step 2: O_2 diffuses into the pores.
Step 3: O_2 undergoes heterogeneous reactions
Step 4: Products diffuse out of the pores toward the particle surface.
Step 5: Products diffuse outward toward the free stream through the film region.

Fig. 14. Porous char combustion [71].

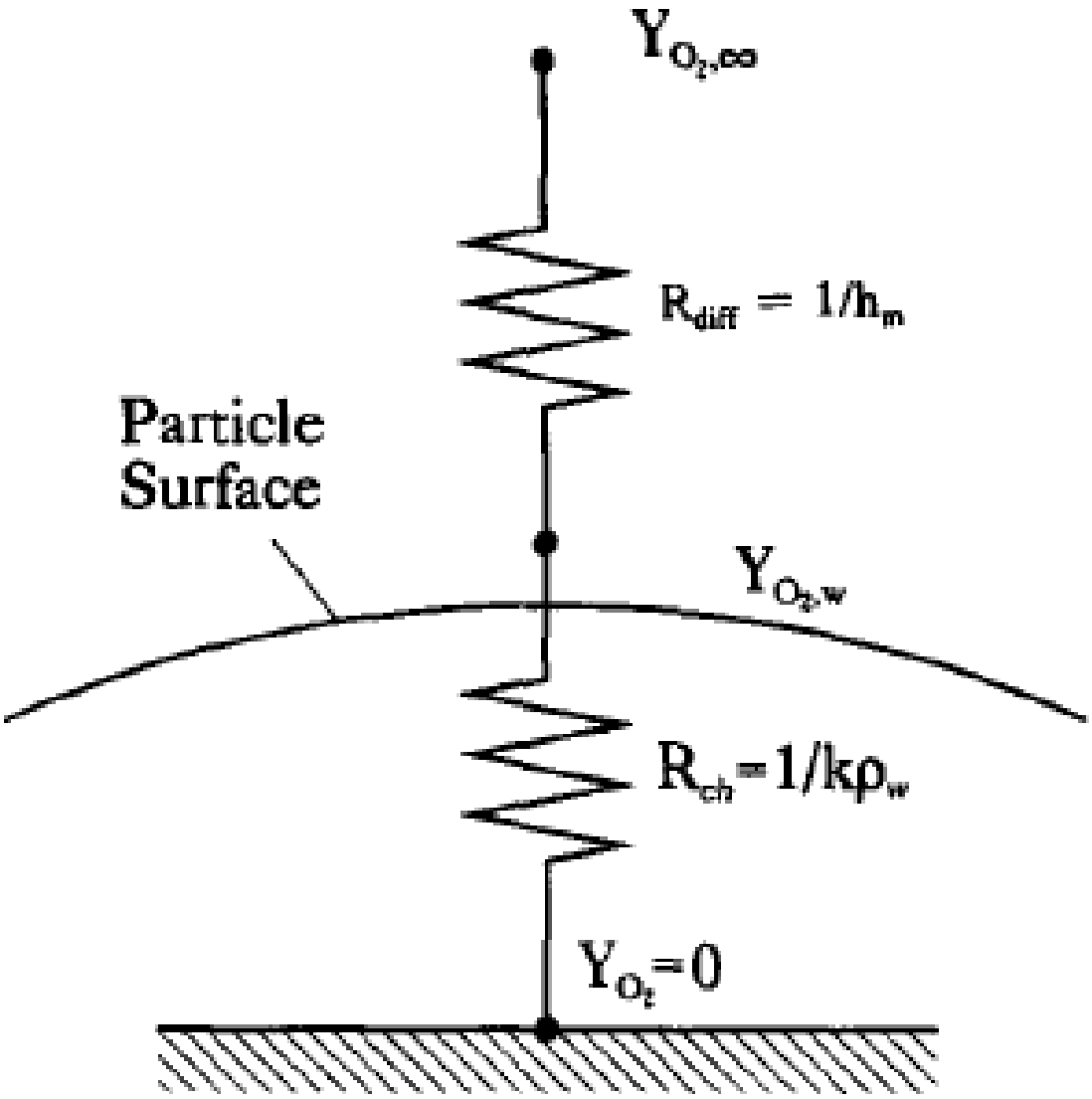

Fig. 15. Oxygen diffusion and chemical reaction resistances for carbon combustion [71].

Shrinkage of char particles is assumed to be the result of the combined effects of combustion and combustion-assisted attrition. CO is produced from volatile matter released from fresh coal [31,35] and char combustion while CO is depleted by CO

oxidation to form CO_2 [38]. A uniform gas temperature is also expected throughout the riser [3,8,11-13,15,17,21,22,27,31,35].

The models thus far encountered are based on the assumption that particles are sufficiently separated from each other that the single-particle combustion analysis is valid for each [12,13,21]. One model presents two different modes of char combustion as seen in Fig. 16 below by Desroches-Ducarne et al. The first mode ('shrinking core' model) shown on top in Fig. 16 proposes when Carbon burns that ashes are released and the particle diameter decreases to zero when combustion is over while the second mode on bottom suggests the particle density is decreasing while the diameter is held constant [31,71].

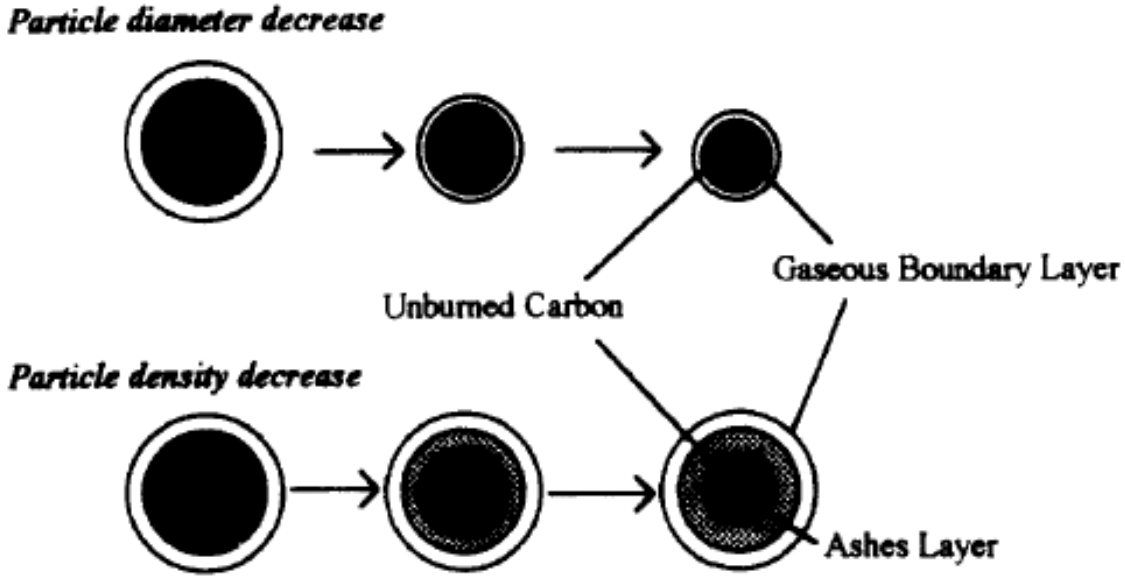

Fig. 16. Two differing char combustion modes [31].

However, the differences between the two modes seem to be minimal as seen in Fig. 17 and Fig. 18 below also by Desroches-Ducarne et al.

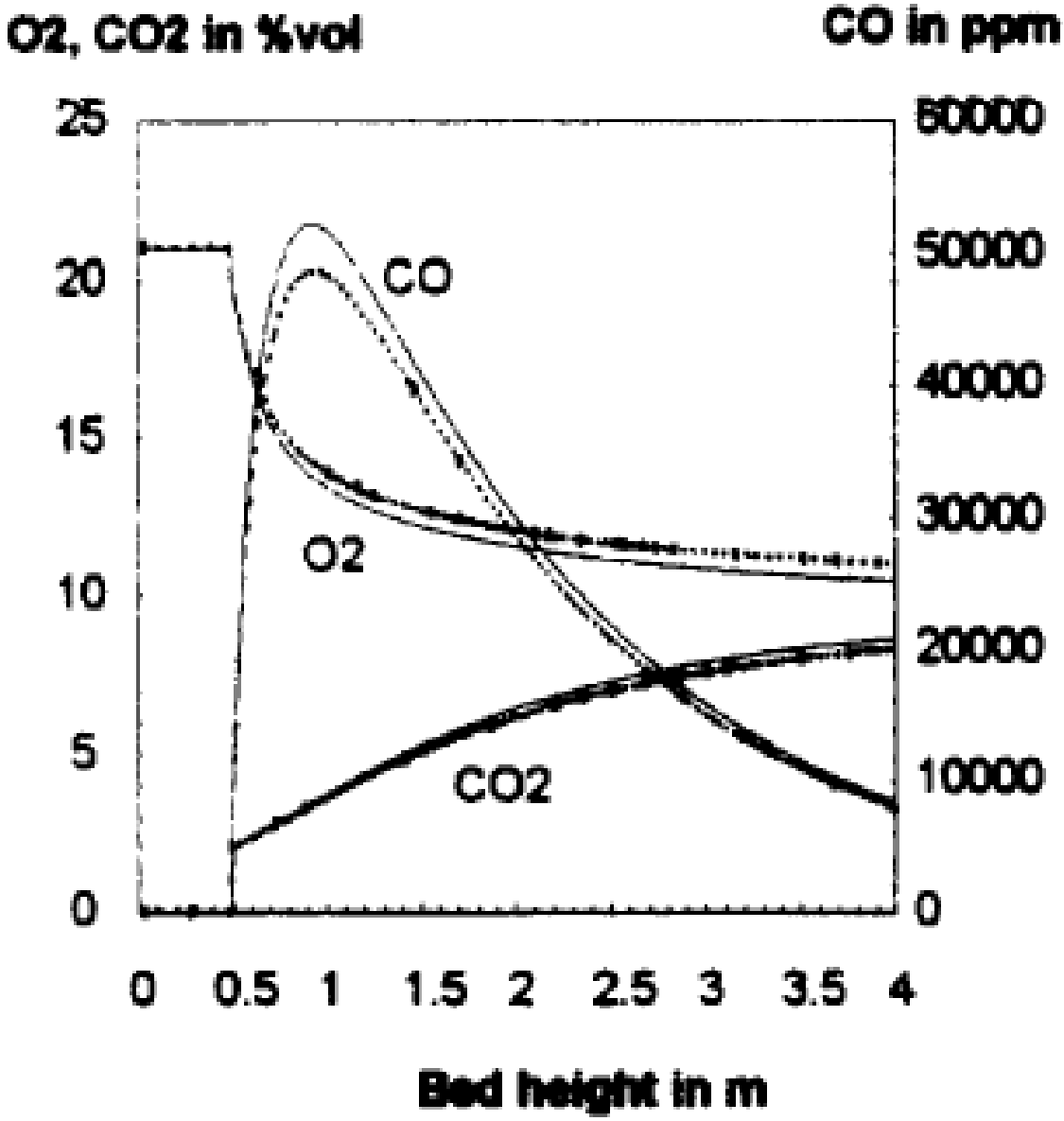

Fig. 17. Concentrations comparison of two differing char combustion modes [31].

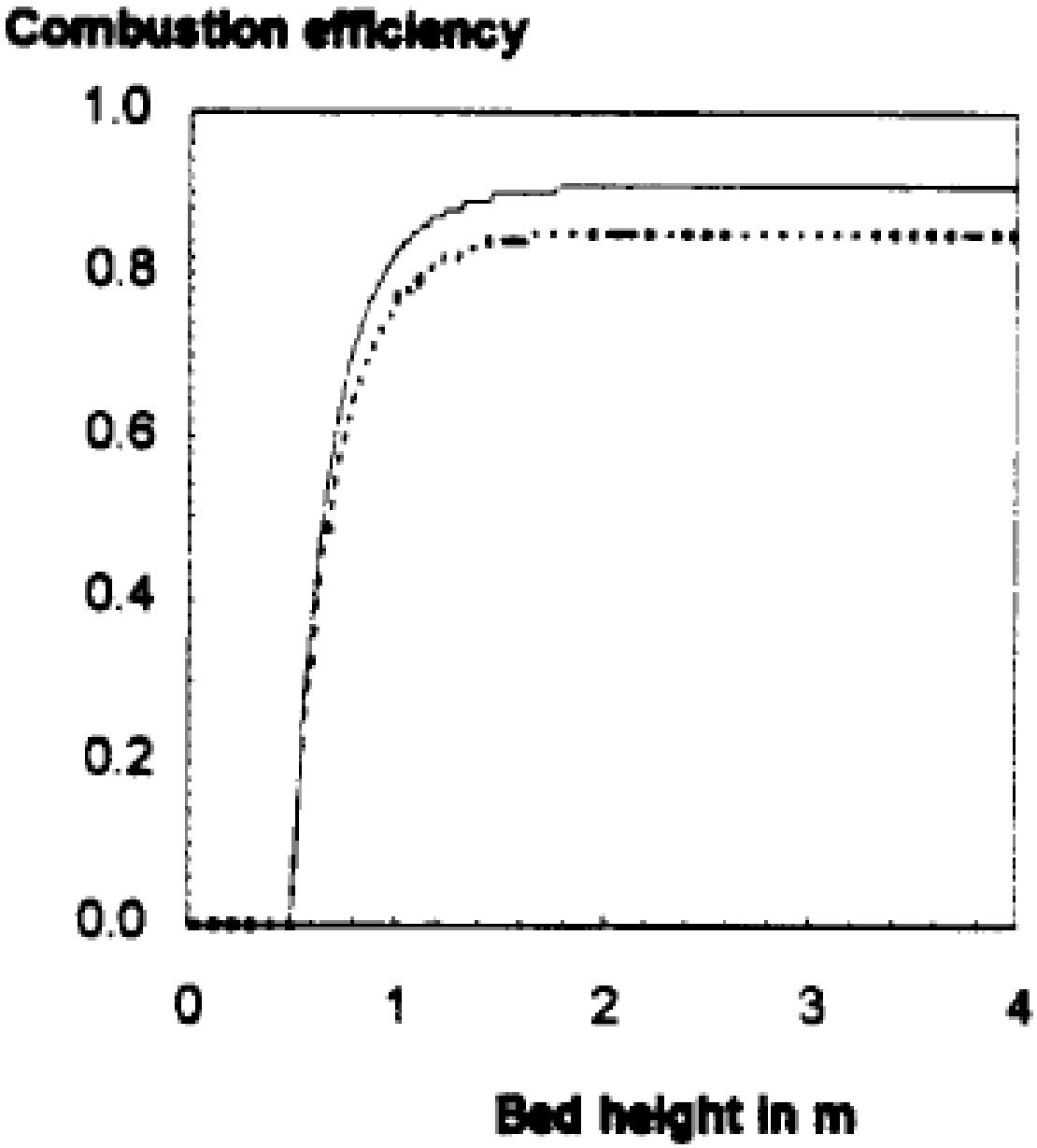

Fig. 18. Combustion efficiency comparison of two differing char combustion modes [31].

2.4 Chemical Kinetics

This model also shows the many global chemical reactions that are possibly taking place within the CFB as seen in Table 6 below also by Desroches-Ducarne et al., but it is encouraging to see that chemical kinetic information is available for many key reactions.

Table 6

Chemical reactions and rates in a CFB combustor [31].

Reaction	Catalyst
$C + \gamma O_2 = (2\gamma - 1)CO_2 + (2 - 2\gamma)CO$	
$CO + 1/2O_2 = CO_2$	Homogeneous
$2H_2 + O_2 = 2H_2O$	Homogeneous
$CH_4 + 3/2O_2 = CO + H_2O$	Homogeneous
$SO_2 + 0.5O_2 = SO_3$	CaO
$CaO + SO_3 = CaSO_4$	
$CaO + 2HCl = CaCl_2$	CaO
$NO + CO = 1/2N_2 + CO_2$	Char
	CaO
	Solids
$NO + Char = 0.5N_2 + CO$	Char
$NH_3 + 5/4O_2 = NO + 3/2H_2O$	Char
	Solids
	CaO
$NH_3 + 3/4O_2 = 1/2N_2 + 3/2H_2O$	Char
	Solids
	CaO
	Homogeneous
$NO + NH_3 + 1/2O_2 = N_2 + 3/2H_2O$	Homogeneous
$HCN + 1/2O_2 = CNO$	
$CNO + 1/2O_2 = NO + CO$	
$CNO + NO = N_2O + CO$	
$N_2O + Char = N_2 + CO$	Char

Table 6

Continued [31].

Reaction rates	Kinetic constants
$k.cO_2$	$k = 0.554\exp(-10824/T)$
$k1.cCO.cO_2^{0.5}.cH_2O^{0.5}$	$k1 = 3.25\ 10^7\exp(-16098/T)$
$/(k2.cHCl + k3)$	$k2 = 2.93\ 10^{11}\exp(-22709/T)$
	$k3 = 11.2$
$k.cO_2.cH_2^{1.5}$	$k = 1.63\ 10^9 T^{1.5}\exp(-3420/T)$
$k.cO_2^{0.8}.cCH_4^{0.7}$	$k = 1.585\ 10^{10}\exp(-24157/T)$
$k.cSO_3$	$k = 6.79\ 10^2\exp(-20000/T)$
$k.cHCl$	$k = \dfrac{2.6\cdot10^3\cdot\exp(-41600/T)}{1+1.1\cdot10^9\cdot\exp\left(\dfrac{-10460}{T}\right)P_{H_2O}}$
KT.($k1.cNO(k2.cCO + k3$	$KT = 1.952\ 10^{10}\exp(-19000/T)$
$))/(k1.cNO + k2.cCO + k3)$	$k1 = 0.1826$, $k2 = 0.00786$, $k3 = 0.002531$
$k.cNO.cCO$	$k = 2.1\ T\exp(-8920/T)$
$k.cNO.cCO$	$k = 9.6\ 10^4\exp(-10000/T)$
$k.cNO$	$k = 5.85\ 10^7\exp(-12000/T)$
$k.cNH_3.cO_2/(cO_2 + k')$	$k = 3.38\ 10^7\exp(-10000/T)$
	$k' = 0.054$
$k.cNH_3.cO_2$	$k = 3.1\ 10^5\exp(-10000/T)$
$k.cNH_3.cO_2$	$k = 2.67\ 10^7\exp(-10000/T)$
$k.cNH_3.cO_2/(cO_2 + k')$	$k = 3.38\ 10^7\exp(-10000/T)$, $k' = 0.054$
$k.cNH_3.cO_2$	$k = 4.96\ 10^5\exp(-1000/T)$
$k.cNH_3.cO_2$	$k = 6.65\ 10^7\exp(-10000/T)$
$k.cNH_3.cO_2$	$k = 5.07\ 10^{14}\exp(-35200/T)$
$k\sqrt{cO_2}\sqrt{cNH_3}\sqrt{cNO}$	$k = 1.1\ 10^{12}\exp(-27680/T)$
$k.cO_2.cHCN$	$k = 2.14\ 10^5\exp(-10000/T)$
$k.cO_2.cHCN.(k1/(k1 + k2.cNO)$	$k2/k1 = 1.02\ 10^9\exp(-25460/T)$
$k.cO_2.cHCN.(k2.cNO/k1 + k2.cNO)$	
$k.cN_2O$	$2.9\ 10^9\exp(-16983/T)$

In addition, this model assumes the temperature of the gaseous phase to be homogeneous, SO_2 is released during devolitilization and can be captured by $CaCO_3$ added to MSW, and volatile Nitrogen is released as NH_3 and HCN [31].

2.5 Particle Sauter Mean Diameter

The fuel Sauter Mean Diameter ($d_{Fuel,0}$) and limestone Sauter Mean Diameter ($d_{LS\ CaCO_3}$), which are average volume-to-surface area ratios of different sized particles, were usually not given directly in the literature, but could be calculated via the particle size distribution that was normally supplied as follows [10,11,16,31,32,39,45,54]:

$$d_{Fuel,0} = \frac{1}{\sum_i \left(\frac{\frac{\Delta m_{F,Fuel,i}}{100\%}}{d_{cp,Fuel,i}} \right)} \quad (1)$$

$$d_{LS\ CaCO_3} = \frac{1}{\sum_i \left(\frac{\frac{\Delta m_{F,LS\ CaCO_3,i}}{100\%}}{d_{cp,LS\ CaCO_3,i}} \right)} \quad (2)$$

"Since the particle size distribution (PSD) is known to have a strong influence on the hydrodynamics and combustion behavior, its variations should not be neglected in the simulation of CFBs" [9,16,18,45]. However, considering a single particle average of many particles of different sizes is considered adequate for combustion modeling [39]. For coals, the Rosin-Rammler distribution parameters could be used to extrapolate a small sample to fit a well-known coal distribution so that continuously fed coal would supposedly have a better estimate of the Sauter Mean Diameter (SMD) than just a small sample [37,55].

2.6 Continuum Gas Mixture

In order for the gas mixture in the CFB to be considered a continuum fluid rather than discrete molecules interacting with the char and limestone particles, the mean distance between molecular collisions of the gas mixture (λ_{Mix}) must be much smaller than the diameter of the particles (d_{Fuel} and $d_{LS\ CaCO_3}$). This calculation is not

performed within the model, but assuming the gas mixture to be mostly composed of air under typical CFB combustion applications (approximately 1,150 K and 1 bar [17,19,23]) $\lambda_{Mix} \cong 0.3\ microns$. There is typically a negligible mass fraction of the char or limestone particles that is near that small of size in CFB combustion so it is considered a good assumption that $\lambda_{Mix} \ll d_{Fuel}$. The equation for λ_{Mix} is given below:

$$\lambda_{Air} = \frac{V'_{Air}}{\sqrt{2} * \pi * {\sigma'_{Air}}^2} \quad [56] \qquad (3)$$

2.7 Limestone Calcination and Sulfation

The type of limestone used in experimentation is never given in the literature in Table 3, but can have drastic effects on the average degree of conversion/sulfation ($X_{LS\ CaSO_3, LS\ CaO} x100$) [40,48]. If the limestone type is known, then such articles as by Hansen et al. with 19 common limestone as shown in Table 7 below can be used in conjunction with Fig. 19 below to arrive at a steady long term value of $X_{LS\ CaSO_3, LS\ CaO} x100$ for a CFB that has fuel and limestone that quickly go through oxidizing conditions in the riser and reducing conditions in the cyclone over a large number of cycles for a total lengthy period of time [66]. However, it should be noted that many fuels have ash containing CaO with biomass usually having a higher content that are not normally accounted for in the data published on Sulfur capture [17,23].

Table 7

Name and number of several limestones [66].

LS no.	Name	LS no.	Name
1	Faxe Industri	13	Gotland
2	Faxe Bryozo	14	Ignaberga
3	Faxe Bryozo (Fe)	15	Förby
4	Faxe Koral	16	Carmeuse
5	Faxe Koral (Fe)	17	Malaga Calcite
6	Katholm	18	Malaga Dolomite
7	Stevns Chalk	19	Sangstrup

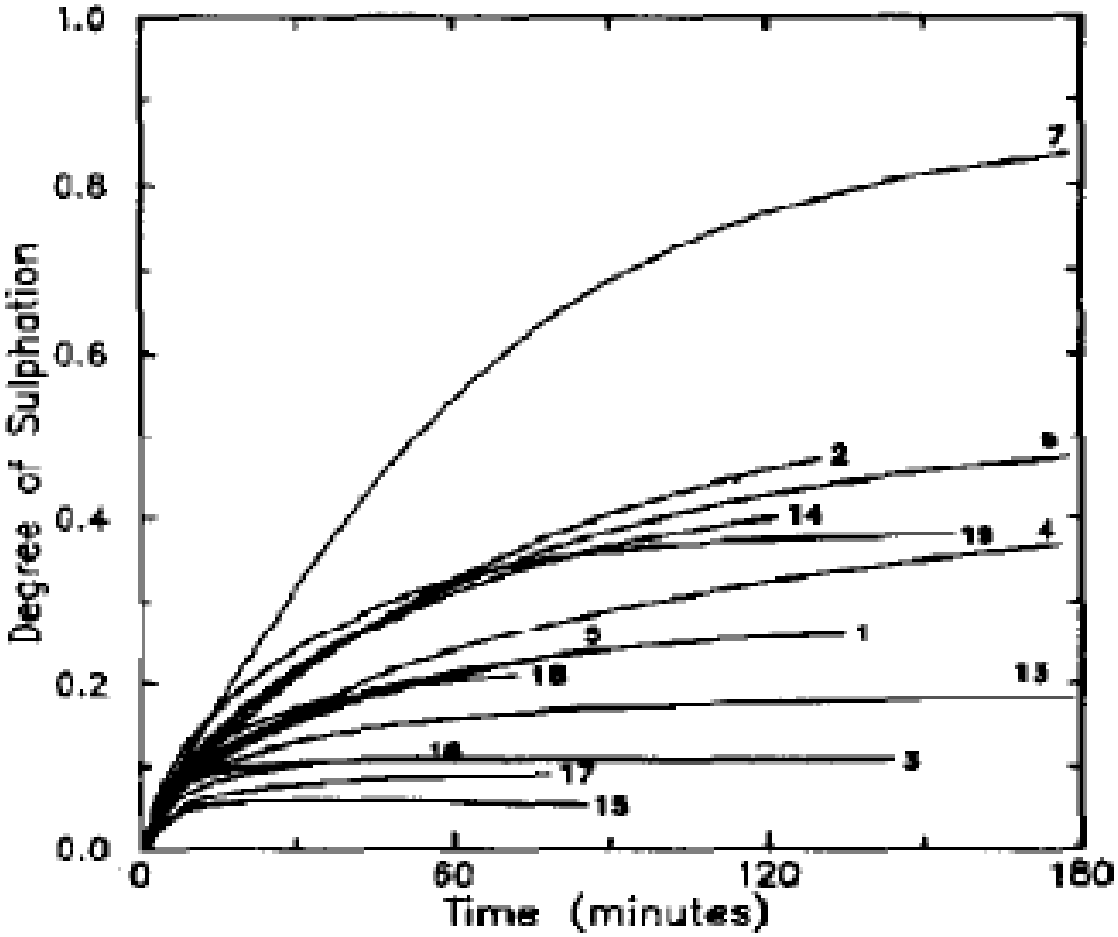

Fig. 19. Degree of sulfation versus time for several limestones under periodically changing oxidizing and reducing conditions [66].

Based on the stoichiometry of the Sulfur capture reaction with lime (CaO), a theoretical limestone feed of one mole Calcium per mole of Sulfur from the fuel would be enough for complete Sulfur capture [16]. The main reason that CaO cannot ever fully convert to $CaSO_3$ or $CaSO_4$ is that the CO_2 is fairly uniformly distributed throughout the original limestone (assumed to be only $CaCO_3$ [29,43,48,61,67-69]) so that when the temperature is high enough that calcination takes place causing CO_2 to be released

through newly formed passageways/pores the SO_2 then begins to react on the new pores as well as any other existing pores [17] closest to the surface and thereby blocking the core of the lime from reacting with SO_2 to form $CaSO_3$ or $CaSO_4$ [16,17,23,24,26,29,40]. A picture of this unreacted lime core is shown in Fig. 20 below by Anthony and Granatstein.

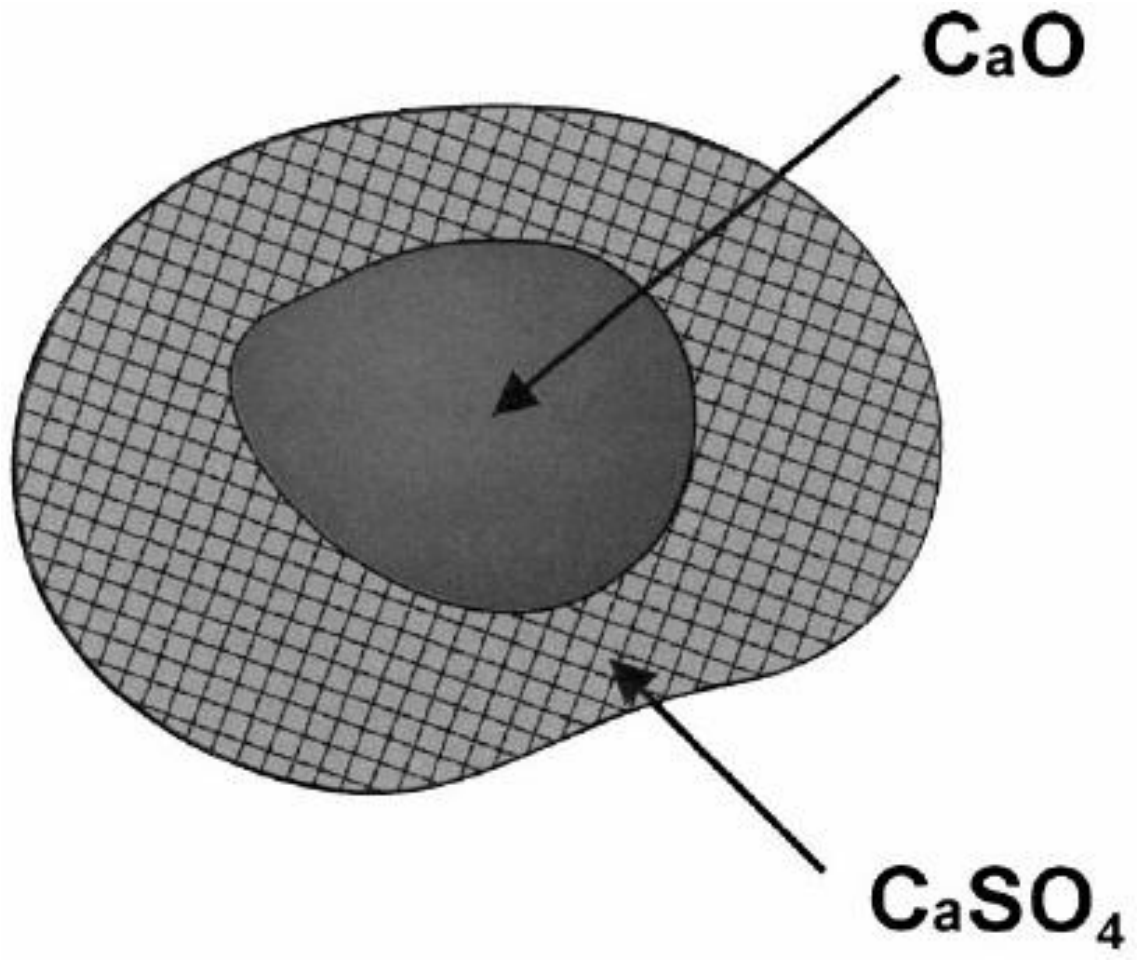

Fig. 20. Typical sulfation pattern for limestone particle [70].

Therefore, smaller diameter limestone particles with a higher surface area-to-volume ratio tend to have higher sulfation rates [13,16,48,54,66], but this also requires greater processing of the limestone for use. In addition, the stable form of Calcium Carbonate is commonly assumed to be calcite, of molar volume of about 36.9 $\frac{cm^3}{mol}$, and X-ray diffraction analysis reported of Stevns Chalk has demonstrated that all Calcium Carbonate is present as calcite. As for CaO, only one crystal form exists at moderate temperatures with a molar volume of about 16.9 $\frac{cm^3}{mol}$. However, the molar volume of $CaSO_4$ is about 52.2 $\frac{cm^3}{mol}$ which underlies another reason why complete sulfation does not occur due to longer average bond lengths [16,17,23,24,26,29,67,68]. Above normal CFB temperature, the rate of Sulfur capture versus the rate of Sulfur release becomes increasingly more important [66].

Limestone moisture was only furnished in two of the models in the literature, and pressure was rarely given in the literature probably due to the assumption that the CFB are atmospheric [17,33] since pressurized CFB haven't become popular until more recently.

2.8 US Government Regulations

Low emission levels of certain species from chemical reactions taking place in the CFB riser such as SO_x and NO_x are important due to government regulation such as the Clean Air Act of 1963 and its subsequent amendments. These regulations gave birth to such organizations as the US Environmental Protection Agency (EPA) which has the ability to enforce emission rates of certain species deemed pollutants such as SO_x and

NO_x from certain sources such as utility boilers [16,32,76]. According to US EPA 40 CFR Part 60, Clean Air Act Extension of 1970 gives US EPA authority to regulate emissions of stationary sources such as new or modified utility steam electric power plants/boilers built after September 18, 1978 called the New Source Performance Standards (NSPS). Coal-fired power plants in particular allow 260 g NO_x/GJ and 260 g SO_2/GJ (at least 70% SO_2 removal) or 520 g SO_2/GJ (at least 90% SO_2 removal).

2.9 Literature Deficiencies

None of these models are readily available, easily able to be applied with common software while taking minimal computation and troubleshooting time, user friendly, up to date with current combustion research, and validated against both laboratory and industrial scale CFB combustors for prominent combustion product species. Also, no known model has been used to predict the emission levels of tire as fuel likely due to the lack of experimentation and accompanying literature on tire combustion.

Although CFB combustor technology is becoming more common from the mentioned commercial applications, there are some significant uncertainties in predicting their performance in large-scale systems [27]. Moreover, the designs of existing CFB boilers for biomass and organic waste combustion are mainly based on experience from coal combustion because the mechanism of combustion of these solid fuels in CFB combustors is still not well understood. Fundamental work on understanding the basic mechanisms taking place during the conversion of these fuels has received little attention. However, rich knowledge is available from the great

number of works on CFB coal combustor modeling that can be used for biomass, although some differences exist between coals and biomasses, including the facts that biomasses are much more reactive and have higher volatile and moisture contents than coals [8,27]. This also seems to be the case for existing CFB boilers utilizing tire combustion. A good understanding of combustion and pollutant formation processes and modeling of the combustor can greatly avoid costly upsets of plants [27].

In addition, fuel cost is the single most important operating cost in a CFB boiler, and departure from ideal operating conditions, which often occurs in operating plants, throws the plant far off the designed performance. Proper combustion is essential for generation of the desired amount of steam at the least cost and for keeping the emission of harmful gases below statutory limits [24].

Utilities and power generation companies as well as laboratories also often would like to switch fuels when a certain fuel becomes cheaper than the currently used fuel. However, this is often not done because CFB combustors are built with a specific fuel in mind largely to minimize amounts of government regulated emissions. No model currently is known to exist that would account for departure from ideal operating conditions or a certain change in the combustion process such as switching fuel in order to determine if adverse emission levels would occur.

3. OBJECTIVES AND TASKS

This section presents an overview of the objectives and tasks of this thesis.

3.1 Objectives

In light of the lack of literature available on tire combustion and math modeling and simulation of CFB boilers:

1. A combustion model is to be developed and incorporated into Microsoft Excel software to enable quick and accurate estimates of emission levels produced by a CFB boiler when certain key parameters are varied.
2. The modelled program is to be then used to predict emission levels from tire fuel being fired in a CFB boiler.

3.2 Tasks

In order to achieve the objectives, the following tasks are to be performed:

1. Conduct an extensive literature review. The literature review covers such topics as current CFB boiler models, laboratory and industrial CFB boiler recorded emission levels and typical combustion parameters, key combustion product species and how they develop from fuel/limestone/air, appropriate chemical reaction rate equations, lignite and tire properties, and limestone properties. Where information is not readily available to provide adequate understanding, assumptions are to be made and documented for the model.
2. Create a combustion model specifically for CFB boilers using current combustion theory. The model is to be created backwards from the output

emissions toward the inputs in order to simplify the amount of calculations required to arrive at the desired end results.

3. Check the model to ensure that appropriate and minimal inputs are available for computation. Minimal inputs are allowed to give enough variability to the program to allow for a wide range of CFB combustion processes while not over burdening the user with acquiring large amounts of data that could be adequately estimated using other given parameters. Inputs are to be defined that are typically known, easily found, or varied through controls usually located on CFB boilers. Key inputs include fuel and limestone feed rates, excess air, temperature, pressure, CFB riser dimensions, and fuel properties. The output is to be emission levels of various species that are considered important in combustion as well as significant with respect to government regulations.
4. Develop the model in Microsoft Excel software readily available on most computers that requires little time to understand the basics of the program and that takes minimal time to compute results from varied parameters. Troubleshooting in Excel should be reduced because calculations can be seen step by step unlike other programming tools that require inputs and then show only outputs. The species' concentrations throughout the riser can also be simply graphed.
5. Validate the model by entering the required inputs found from documented data from operation of both an industrial scale CFB boiler using lignite coal fuel and a pilot/laboratory scale BFB boiler using subbituminous coal fuel to show

limitations of the model, and comparing the emission levels predicted by the model to emission levels available from these industrial setups.

6. Once sufficiently validated for the base case of lignite coal fuel in the anonymous CFB boiler, predict the performance using tire as the fuel assuming similar combustion characteristics to coal.
7. Perform a sensitivity analysis on the input parameters for tire fuel to develop emission level trends.

4. MODEL

Fuel and limestone (both assumed to be composed of perfectly spherical and solid particles) enter from the bottom of the combustor a little above the distributor where the primary air [13,19,22,35] is introduced (in the proposed model all air is introduced as primary air at this location so it is assumed there is no secondary air [38]). Sand is sometimes introduced into the CFB combustor to enhance fluidization if low ash fuels are used especially if no limestone is used such as in low sulfur fuels [5,18,27] or at startup where the sand is gradually supplemented and replaced by combustion ash when enough has been created [23], but the amount of this inert material is assumed to be negligible in the proposed model. The distributor helps to keep larger particles that aren't able to be fluidized from going back down into the primary air source and burn the char particles until they are able to be entrained by the air or continuously removed with the ash and limestone [5,29,31,77].

After the fuel and limestone enter the bed from their respective feed ports, they are assumed to immediately and completely become entrained in the primary air flow from the distributor and mixed throughout the entirety of the cross-sectional area of the CFB bed for a uniform blend of fuel and limestone. This assumption leads to the fuel and limestone particles immediately beginning to rise through the riser at a rate based on particle size so that larger particles tend to slowly creep upwards assuming that the primary air velocity is capable of such upward movement of very large particles ($V_{Bed\ Mix} - V_{term,d_{Fuel}} > 0$) while smaller particles move up the riser much more

quickly [13,21,23,24,75]. The proposed model assumes that the particles immediately reach their terminal velocity upon entry into the CFB combustor from their feed ports [21,23]. Also, it is assumed that the gases released from drying and devolatilization of the fuel particles as well as the gases released from the drying and calcination of limestone particles entering the CFB combustor instantaneously reach the velocity of the mixture of gases in the CFB bed.

Using the SMD of the fuel and the SMD of the limestone particles to account for one average particle size for each rather than following each range of particle sizes individually throughout the CFB riser, it greatly simplifies the computation required in the Excel program. The CFB bed described in the proposed model is the area of the CFB combustor near the feed ports [19] where the particles are at the largest average diameter because combustion has just begun to take place so the particles are moving the slowest at this point in the riser; and therefore, there is a greater amount of particles (dense region of CFB combustor [12,18,23]).

The fuel and limestone particles at this point just as they enter the riser from their respective feed ports also are assumed to immediately release all volatile matter and moisture (both fuel and limestone usually have moisture that is released as gaseous H_2O into the CFB combustor) in gaseous form [13,40,65] with negligible liquid (tar or oil) yields. The volatile matter is also assumed to immediately react to a certain degree in the bed. In fact, the bed portion of the proposed model is actually a snapshot of instantaneous actions that occur in the dense region of the CFB combustor just before entering the riser portion of the proposed model so that there is assumed to be a

negligible amount of time from the particles entering the bed to entering the riser while the riser portion of the proposed model follows time dependent actions above the bed all the way to the exit of the riser.

The shrinking core model is used in the riser portion of the proposed model for the fuel particles during combustion, and the diameter of the particles is assumed to only decrease during combustion of the fuel particles when Carbon and Nitrogen from the fixed Carbon react with Oxygen in the CFB riser gas mixture [8,12,14,16,22] while ash is assumed to immediately fall off at the same rate as the reactions taking place [12,16,24]. It is assumed that the ash is inert so that no chemical reactions occur with the constituents composing ash [24,36]. Also, the char particle density is assumed to remain constant [12,13,21,39]. Hence, fuel and limestone particle diameters in the proposed model neither decrease due to fragmentation that takes place as volatiles and moisture are released from within the burning fuel particles or calcinating limestone particles nor by attrition that occurs as particles collide with each other or the wall within the CFB combustor [10,22,29,31,38,39]. The fuel and limestone particle diameters in the proposed model don't increase either through agglomeration or sticking together of particles [45]. In fact, this means that the limestone particle SMD doesn't change at all in the proposed model since no chemical reactions are assumed to occur to cause the limestone particles to shrink [13].

4.1 Bed Model

4.1.1 Fuel pyrolysis

The volatile matter that is immediately released from the fuel particles entering the CFB combustor consists of all of the fuel Hydrogen [10,74,81], Oxygen [82], and Sulfur [10,54] as well as part of the fuel Carbon and part of the fuel Nitrogen. The remaining fuel Carbon and Nitrogen stay in what is now referred to as the char particle after devolatilization and drying of the original fuel particle [62]. The char particle consists of only the fixed Carbon (remaining fuel Carbon and Nitrogen) and ash [9,10,18,29,63,71]. The portion of fuel Nitrogen that remains in the char particle as fixed Nitrogen ($N_{FN,Fuel}x100$) is calculated based on what is left over after the volatile Nitrogen ($Y_{VN,N}x100$) is released [63]:

$$N_{FN,Fuel}x100 = \frac{Y_{N,Fuel}x100*\left(1-\frac{Y_{VN,N}x100}{100}\right)}{14.01} \quad (4)$$

The portion of fuel Carbon that remains in the char particle as fixed Carbon ($N_{FC,Fuel}x100$) is calculated based on how much fixed Nitrogen is in the char particle:

$$N_{FC,Fuel}x100 = \frac{Y_{FC,Fuel}x100-\left[Y_{N,Fuel}x100*\left(1-\frac{Y_{VN,N}x100}{100}\right)\right]}{12.01} \quad (5)$$

4.1.2 Fuel volatile combustion

As mentioned earlier, it is assumed that all fuel Nitrogen released as volatile matter immediately forms bonds to become N_2 [39] (that immediately joins with the N_2 from the primary air), NH_3 [77], or HCN [83] with the fraction of each depending upon the fuel used and operating conditions (heating rate and temperature being significant factors) of the CFB combustor [84]. Any fuel Carbon that is released as volatile matter

and isn't combined with volatile Hydrogen and volatile Nitrogen to form HCN is oxidized to form CO [8,10,38,39,77] immediately (along with all other volatile combustion that is assumed to occur instantaneously upon fuel entering the CFB combustor). Any fuel Hydrogen that is released as volatile matter and isn't combined with volatile Carbon and volatile Nitrogen to form either HCN or NH_3 is oxidized to form H_2O [8,10,27,31,39,77,84] immediately. Hence, water comes from three places in the bed being the moisture in the fuel, the moisture in the limestone [39,40], and the water that is formed from this volatile Hydrogen combustion. All fuel Sulfur that is released as volatile matter is oxidized to form SO_2 [10,12,13,21,23,31,39,54,61,77] immediately. Any fuel Oxygen that is released as volatile matter and isn't used to oxidize volatile Carbon, Hydrogen, or Sulfur to form CO, H_2O, or SO_2 joins as O_2 [11,39] with the primary air immediately.

The following is a summary of the fuel volatile combustion global reactions as described above (all of these are assumed to take place instantaneously as the fuel enters the CFB combustor and only in the forward direction):

$$Volatile\ C\ +\ \frac{1}{2}\ O_2\ (g)\ \rightarrow\ CO\ (g) \tag{6}$$

$$Volatile\ H\ +\ \frac{1}{2}\ O_2\ (g)\ \rightarrow\ H_2O\ (g) \tag{7}$$

$$Volatile\ O\ \rightarrow\ O_2\ (g) \tag{8}$$

$$Volatile\ N\ \rightarrow\ N_2\ (g) \tag{9}$$

$$Volatile\ N\ +\ Volatile\ H\ \rightarrow\ NH_3\ (g) \tag{10}$$

$$Volatile\ H\ +\ Volatile\ C\ +\ Volatile\ N\ \rightarrow\ HCN\ (g) \tag{11}$$

$$Volatile\ S\ +\ O_2\ (g)\ \rightarrow\ SO_2\ (g) \tag{12}$$

4.1.3 Limestone calcination and sulfation

The mass percent of limestone fed with respect to fuel fed into the CFB Riser (limestone/fuel feed mass ratio or $Y_{LS,Fuel}\ x100$) is computed as follows:

$$Y_{LS,Fuel}\ x100 = \frac{\left(CSR * N_{Vol\ SO_2,Fuel} x100\right) * (40.08+12.01+16*3)}{1-\frac{Y_{LS\ H_2O,LS} x100}{100}} \quad (13)$$

Immediately after entering the CFB combustor, the limestone releases its moisture along with the dry limestone ($CaCO_3$) instantaneously undergoing endothermic calcination where CO_2 is released and a porous lime (CaO) shell is left [10,12,13,16,21,23,31,33,40,48,54,61,66-69,85] to capture the SO_2 in the CFB combustor which is being formed concurrently from the devolatilizing fuel [12,13,16,21,54] to ultimately produce $CaSO_3$ [54,76,85] through exothermic sulfation reaction [66]. However, many others show the sulfation reaction to lead to $CaSO_4$ [10,12,13,16,21,33,40,66] which can be easily changed in the Excel program. Since there are no other reactions involving the limestone and Sulfur in the proposed model, these reactions are assumed to take place immediately [67] as the limestone enters the CFB combustor at an average sulfation rate of $X_{LS\ CaSO_3,LS\ CaO} x100$.

The following is a summary of the limestone calcination and sulfation global reactions as described above (both of these are assumed to take place instantaneously as the limestone enters the CFB combustor and only in the forward direction) which brings the total number of instantaneous bed chemical reactions to nine:

$$CaCO_3\ (s)\ \rightarrow\ CaO\ (s)\ +\ CO_2\ (g) \quad (14)$$

$$CaO\ (s)\ +\ SO_2\ (g)\ \rightarrow\ CaSO_3\ (s) \quad (15)$$

4.1.4 Combustion air

The stoichiometric chemical equation for determining the stoichiometric air required for complete combustion of the fuel [23] is as follows:

$$C_{N_{C,Fuel}x100}H_{N_{H,Fuel}x100}O_{N_{O,Fuel}x100}N_{N_{N,Fuel}x100}S_{N_{S,Fuel}x100}\,(s) + Moisture\,(l) + Ash\,(s) + \left(N_{C,Fuel}x100 + \frac{N_{H,Fuel}x100}{4} + N_{S,Fuel}x100 - \frac{N_{O,Fuel}x100}{2}\right)\left[O_2\,(g) + \left(\frac{X_{N_2,Air}x100}{X_{O_2,Air}x100}\right)N_2\,(g)\right] \rightarrow N_{C,Fuel}x100\,CO_2\,(g) + \left(\frac{N_{H,Fuel}x100}{2}\right)H_2O\,(g) + \left[\frac{N_{N,Fuel}x100}{2} + \left(N_{C,Fuel}x100 + \frac{N_{H,Fuel}x100}{4} + N_{S,Fuel}x100 - \frac{N_{O,Fuel}x100}{2}\right) * \left(\frac{X_{N_2,Air}x100}{X_{O_2,Air}x100}\right)\right]N_2\,(g) + N_{S,Fuel}x100\,SO_2\,(g) + Moisture\,(g) + Ash\,(s) \quad (16)$$

This means the kilogram-moles of O_2 required for stoichiometric combustion of 100 kilograms of fuel ($N_{Stoich\ O_2,Fuel}x100$) is easily calculated from the above stoichiometric chemical equation:

$$N_{Stoich\ O_2,Fuel}x100 = N_{C,Fuel}x100 + \frac{N_{H,Fuel}x100}{4} + N_{S,Fuel}x100 - \frac{N_{O,Fuel}x100}{2} \quad (17)$$

The equation for $N_{Stoich\ O_2,Fuel}x100$ is used to find the total kilograms of air needed for stoichiometric combustion of 100 kilograms of fuel ($m_{Stoich\ Air,Fuel}x100$):

$$m_{Stoich\ Air,Fuel}x100 = N_{Stoich\ O_2,Fuel}x100 * (16 * 2) + N_{Stoich\ O_2,Fuel}x100 * \left(\frac{X_{N_2,Air}x100}{X_{O_2,Air}x100}\right) * (14.01 * 2) \quad (18)$$

The equation for $m_{Stoich\ Air,Fuel}x100$ is then used in conjunction with the Stoichiometric Ratio (SR) or equivalence ratio (ϕ) to obtain the mass flow rate of air required for actual combustion ($\dot{m}_{Act\ Air}$):

$$SR = 1 + \frac{X_{Exc\ Air,Stoich\ Air} x100}{100} \quad (19)$$

$$\phi = \frac{1}{SR} \quad (20)$$

$$\dot{m}_{Act\ Air} = SR * \left(\frac{m_{Stoich\ Air,Fuel} x100}{100}\right) * \dot{m}_{Fuel} \quad (21)$$

Therefore, fuel rich (oxidizer lean) combustion will have $SR < 1$ and $\phi > 1$ and fuel lean (oxidizer rich) combustion will have $SR > 1$ and $\phi < 1$. If exact stoichiometric combustion is somehow achieved, then $SR = \phi = 1$.

4.1.5 Bed gas mixture total flow rate

The mass flow rate of actual combustion air combines with the mass flow rate of moisture and volatile matter released ($\dot{m}_{VF}$) by the fresh fuel particles (except for the Sulfur and Oxygen that is captured by the lime) as well as the mass flow rate of the moisture and CO_2 released ($\dot{m}_{VL}$) by the fresh limestone particles to amount to a total mass flow rate of the mixture of gases leaving the CFB bed ($\dot{m}_{Bed\ Mix}$) carrying the newly formed char particles. The mixture of gases leaving the CFB bed in the proposed model consist of the species CO, H_2O, O_2, N_2, NH_3, HCN, SO_2, and CO_2 in amounts that depend upon the fuel, limestone, and air properties:

$$\dot{m}_{VF} = \langle\left\{\frac{Y_{VM,Fuel} x100}{100} - \left[\left(\frac{N_{LS\ CaSO_3,Fuel} x100}{100}\right) * 32.07 + 2 * \left(\frac{N_{LS\ CaSO_3,Fuel} x100}{100}\right) * 16\right]\right\} + \frac{Y_{H_2O,Fuel} x100}{100}\rangle * \dot{m}_{Fuel} \quad (22)$$

$$\dot{m}_{VL} = \left[\left(\frac{Y_{LS\ H_2O,LS} x100}{100}\right) * \left(\frac{Y_{LS,Fuel}\ x100}{100}\right) + \left(\frac{N_{LS\ CO_2,Fuel} x100}{100}\right) * (12.01 + 16 * 2)\right] * \dot{m}_{Fuel} \quad (23)$$

$$\dot{m}_{Bed\ Mix} = \dot{m}_{Act\ Air} + \dot{m}_{VF} + \dot{m}_{VL} \quad (24)$$

4.1.6 Combustor effective cross-sectional area

The gas mixture leaving the CFB bed still encounters both char and limestone spherical particles as it travels up the riser and this has been accounted for by producing an effective cross-sectional area of the CFB riser ($a_{CS,Riser,Eff}$). The effective area is modeled by assuming that at any point in the CFB riser the gas mixture must go around both char and limestone particles thus decreasing the cross-sectional area available for the gas to flow through the CFB riser.

The number of char particles blocking the flow of the gas mixture at any point in the CFB riser is assumed to be the number of particles of char (same as the number of particles of fresh fuel) per cubic meter of the mixture of gases leaving the CFB bed ($n'''_{Char,Bed\ Mix}$) in a volume of the full cross-sectional area of the CFB riser ($a_{CS,Riser}$) by a depth of two times the SMD of the fresh fuel/char particles ($d_{Fuel,0}$) in order to account for some char particles that may be very close to one another causing a larger block while not being accounted for in a depth of only one $d_{Fuel,0}$. The fresh fuel particle SMD is equal to the char particle SMD just after devolatilization and drying because the particle size was found to decrease insignificantly during drying and devolatilization, with these processes mainly coinciding in time [23].

A similar assumption was used for the number of limestone particles obstructing the flow of the gas mixture at any point in the CFB riser to be the number of particles of dry limestone ($CaCO_3$) per cubic meter of the mixture of gases leaving the CFB bed ($n'''_{LS\ CaCO_3,Bed\ Mix}$) in a volume of the full cross-sectional area of the CFB riser

($a_{CS,Riser}$) by a depth of two times the SMD of the dry limestone ($d_{LS\ CaCO_3}$). The descriptions above are placed in the equations below:

$$a_{CS,Fuel,0} = \left[n'''_{Char,Bed\ Mix} * a_{CS,Riser} * (d_{Fuel,0} * 2)\right] * a'_{CS,Fuel,0} \quad (25)$$

$$a_{CS,LS\ CaCO_3} = \left[n'''_{LS\ CaCO_3,Bed\ Mix} * a_{CS,Riser} * (d_{LS\ CaCO_3} * 2)\right] * a'_{CS,LS\ CaCO_3} \quad (26)$$

$$a_{CS,Riser,Eff} = a_{CS,Riser} - a_{CS,Fuel,0} - a_{CS,LS\ CaCO_3} \quad (27)$$

4.1.7 Bed gas mixture average bulk velocity

With the $\dot{m}_{Bed\ Mix}$ and $a_{CS,Riser,Eff}$, the density of the mixture of gases leaving the CFB bed ($\rho_{Bed\ Mix}$) is used to calculate the average bulk velocity of the mixture of gases leaving the CFB bed ($V_{Bed\ Mix}$) based on the assumption that the gas mixture can be approximated as ideal gas which seems to be a good assumption considering the high temperature and low pressure of CFB combustion applications:

$$N'''_{Mix} = \frac{P_{Mix}}{0.08314 * T_{Mix}} \quad [10,76] \quad (28)$$

$$\rho_{Bed\ Mix} = \bar{m}_{Bed\ Mix} * N'''_{Mix} \quad [76] \quad (29)$$

$$V_{Bed\ Mix} = \frac{\dot{m}_{Bed\ Mix}}{\rho_{Bed\ Mix} * a_{CS,Riser,Eff}} \quad [86] \quad (30)$$

4.1.8 Gas mixture combustor residence time

Even though the char particles are reacting with the gas mixture throughout the CFB riser to form more gaseous species and smaller blockage nearer the riser top, it is assumed that the changes in the mass flow rate [15] and density of the gas mixture as well as the effective cross-sectional area of the CFB riser are negligible so $V_{Bed\ Mix}$ can be used throughout the CFB combustor [10,21,23] in order to more readily estimate the

residence time in the CFB riser of the mixture of gases from the time they leave the CFB bed until they just reach the exit at the top of the riser ($t_{Res,Bed\ Mix}$):

$$t_{Res,Bed\ Mix} = \frac{h_{Riser}}{V_{Bed\ Mix}} \quad [87] \tag{31}$$

4.1.9 Time step

Now that an approximate $t_{Res,Bed\ Mix}$ has been formulated, the time step (Δt) is determined to accurately capture the chemical kinetics taking place in the CFB riser. The time step is for smoothing incremental solving of chemical kinetics so it should be small enough to avoid too large of changes in values in the columns of the 'Riser' tab in the Excel program, but large enough to avoid excessive computation time. According to literature, the chemical kinetics of CFB combustion applications require a time step ranging from 0.001 seconds [88] to 0.000001 seconds [16]:

$$\Delta t = \frac{t_{Res,Bed\ Mix}}{\#\ of\ Chemical\ Kinetics\ Calculation\ Rows} \tag{32}$$

The 'Bed' tab of the Excel program can be viewed below in Table 8 which should not normally be altered by the user of the program, but it is a convenient way to track the intermediate CFB bed calculations of the program in a glance.

Table 8

Bed tab for anonymous CFB boiler firing lignite fuel.

Fuel Entering CFB Bed	
a'_CS,Fuel,0 (m^2 Fuel/Fuel Particle)	1.17766E-07
N_H2O,Fuel x 100 (kmol H2O/100 kg Fuel)	1.740119893
Ultimate/Elemental Fuel Analysis (Mole Basis)	
N_C,Fuel x 100 (kmol C/100 kg Fuel)	2.816819317
N_H,Fuel x 100 (kmol H/100 kg Fuel)	2.668650794
N_O,Fuel x 100 (kmol O/100 kg Fuel)	0.548125
N_N,Fuel x 100 (kmol N/100 kg Fuel)	0.047109208
N_S,Fuel x 100 (kmol S/100 kg Fuel)	0.048331774
Carbon & Nitrogen Retained in Fuel as Fixed Carbon	
N_FC,Fuel x 100 (kmol FC/100 kg Fuel)	1.785545379
N_FN,Fuel x 100 (kmol FN/100 kg Fuel)	0.031092077
	21.88
Y_FC,FC x 100 (kg FC/100 kg FC)	98.00914077
Y_FN,FC x 100 (kg FN/100 kg FC)	1.990859232
FCR (kg FN/kg FC)	0.020312995
Carbon, Hydrogen, Oxygen, Nitrogen, Sulfur Release from Fuel as Volatile Matter	
N_VC,Fuel x 100 (kmol VC/100 kg Fuel)	1.031273938
N_VH,Fuel x 100 (kmol VH/100 kg Fuel)	2.668650794
N_VO,Fuel x 100 (kmol VO/100 kg Fuel)	0.548125
N_VN,Fuel x 100 (kmol VN/100 kg Fuel)	0.016017131
N_VS,Fuel x 100 (kmol VS/100 kg Fuel)	0.048331774
	25.62
Nitrogen Release from Fuel as Volatile Matter & Split into N2, NH3, HCN	
N_N2,Fuel x 100 (kmol N2/100 kg Fuel)	0.000117773
N_NH3,Fuel x 100 (kmol N/100 kg Fuel)	0.004239829
N_HCN,Fuel x 100 (kmol N/100 kg Fuel)	0.011541756
	0.016017131
Air Entering CFB Bed	
N_Stoich O2,Fuel x 100 (kmol Stoich O2/100 kg Fuel)	3.25825129
SR (dimensionless)	1.076889942
	0.9286
N_Act O2,Fuel x 100 (kmol Act O2/100 kg Fuel)	3.508778042
N_Act N2,Fuel x 100 (kmol Act N2/100 kg Fuel)	13.19968883
	16.70846687
m_Stoich Air,Fuel x 100 (kg Stoich Air/100 kg Fuel)	447.7116551
Volatile Combustion	
N_Vol CO,Fuel x 100 (kmol Vol CO/100 kg Fuel)	1.019732182
N_Vol H2O,Fuel x 100 (kmol Vol H2O/100 kg Fuel)	1.322194776
N_Vol O2,Fuel x 100 (kmol Vol O2/100 kg Fuel)	2.563545289
N_Vol N2,Fuel x 100 (kmol Vol N2/100 kg Fuel)	13.1998066
N_Vol NH3,Fuel x 100 (kmol Vol NH3/100 kg Fuel)	0.004239829
N_Vol HCN,Fuel x 100 (kmol Vol HCN/100 kg Fuel)	0.011541756
N_Vol SO2,Fuel x 100 (kmol Vol SO2/100 kg Fuel)	0.048331774
Limestone Reactions	
a'_CS,LS CaCO3 (m^2 LS CaCO3/LS CaCO3 Particle)	1.76715E-08
Y_LS,Fuel x 100 (kg LS/100 kg Fuel)	10.69348136
N_LS H2O,Fuel x 100 (kmol LS H2O/100 kg Fuel)	0.029677735
N_LS CaCO3,Fuel x 100 (kmol LS CaCO3/100 kg Fuel)	0.101496726
N_LS CO2,Fuel x 100 (kmol LS CO2/100 kg Fuel)	0.101496726
N_LS CaO,Fuel x 100 (kmol LS CaO/100 kg Fuel)	0.101496726
N_LS CaSO3,Fuel x 100 (kmol LS CaSO3/100 kg Fuel)	0.017254443
	0.084242283
	35.7

Table 8

Continued.

Gaseous Species leaving CFB Bed	
mdot_Act Air (kg Act Air/s)	316.5540564
mdot_VL (kg VL/s)	3.283842661
mdot_VF (kg VF/s)	36.67871725
mdot_Bed Mix (kg Bed Mix/s)	356.5166163
N_Bed CO,Fuel x 100 (kmol Bed CO/100 kg Fuel)	1.019732182
N_Bed H2O,Fuel x 100 (kmol Bed H2O/100 kg Fuel)	3.091992404
N_Bed O2,Fuel x 100 (kmol Bed O2/100 kg Fuel)	2.563545289
N_Bed N2,Fuel x 100 (kmol Bed N2/100 kg Fuel)	13.1998066
N_Bed NH3,Fuel x 100 (kmol Bed NH3/100 kg Fuel)	0.004239829
N_Bed HCN,Fuel x 100 (kmol Bed HCN/100 kg Fuel)	0.011541756
N_Bed SO2,Fuel x 100 (kmol Bed SO2/100 kg Fuel)	0.031077331
N_Bed CO2,Fuel x 100 (kmol Bed CO2/100 kg Fuel)	0.101496726
N_Bed Mix,Fuel x 100 (kmol Bed Mix/100 kg Fuel)	20.02343211
X_Bed CO,Bed Mix x 100 (kmol Bed CO/100 kmol Bed Mix)	5.092694283
X_Bed H2O,Bed Mix x 100 (kmol Bed H2O/100 kmol Bed Mix)	15.44187024
X_Bed O2,Bed Mix x 100 (kmol Bed O2/100 kmol Bed Mix)	12.8027267
X_Bed N2,Bed Mix x 100 (kmol Bed N2/100 kmol Bed Mix)	65.92179863
X_Bed NH3,Bed Mix x 100 (kmol Bed NH3/100 kmol Bed Mix)	0.021174335
X_Bed HCN,Bed Mix x 100 (kmol Bed HCN/100 kmol Bed Mix)	0.057641247
X_Bed SO2,Bed Mix x 100 (kmol Bed SO2/100 kmol Bed Mix)	0.155204815
X_Bed CO2,Bed Mix x 100 (kmol Bed CO2/100 kmol Bed Mix)	0.506889755
	100
N'''_Mix (kmol Mix/m^3 Mix)	0.010551308
N'''_Bed CO (kmol Bed CO/m^3 Bed Mix)	0.000537346
N'''_Bed H2O (kmol Bed H2O/m^3 Bed Mix)	0.001629319
N'''_Bed O2 (kmol Bed O2/m^3 Bed Mix)	0.001350855
N'''_Bed N2 (kmol Bed N2/m^3 Bed Mix)	0.006955612
N'''_Bed NH3 (kmol Bed NH3/m^3 Bed Mix)	2.23417E-06
N'''_Bed HCN (kmol Bed HCN/m^3 Bed Mix)	6.08191E-06
N'''_Bed SO2 (kmol Bed SO2/m^3 Bed Mix)	1.63761E-05
N'''_Bed CO2 (kmol Bed CO2/m^3 Bed Mix)	5.34835E-05
	0.010551308
m_Bed CO,Fuel x 100 (kg Bed CO/100 kg Fuel)	28.56269843
m_Bed H2O,Fuel x 100 (kg Bed H2O/100 kg Fuel)	55.70533515
m_Bed O2,Fuel x 100 (kg Bed O2/100 kg Fuel)	82.03344924
m_Bed N2,Fuel x 100 (kg Bed N2/100 kg Fuel)	369.8585809
m_Bed NH3,Fuel x 100 (kg Bed NH3/100 kg Fuel)	0.072221242
m_Bed HCN,Fuel x 100 (kg Bed HCN/100 kg Fuel)	0.311950578
m_Bed SO2,Fuel x 100 (kg Bed SO2/100 kg Fuel)	1.991124587
m_Bed CO2,Fuel x 100 (kg Bed CO2/100 kg Fuel)	4.466870907
m_Bed Mix,Fuel x 100 (kg Bed Mix/100 kg Fuel)	543.002231
mbar_Bed Mix (kg Bed Mix/kmol Bed Mix)	27.11833955
rho_Bed Mix (kg Bed Mix/m^3 Bed Mix)	0.286133948
Solid Species leaving CFB Bed	
m'''_Fuel,Bed Mix (kg Fuel/m^3 Bed Mix)	0.052694802
m'''_Char,Bed Mix (kg Char/m^3 Bed Mix)	0.022674573
m'''_Char,Fuel (kg Char/m^3 Fuel)	688.48
m'''_FC,Fuel (kg FC/m^3 Fuel)	343.1104
m'_Char,0 (kg Char/Char Particle)	2.09307E-08
m'_FC,0 (kg FC/FC Particle)	1.0431E-08
CCR (kg Char/kg FC)	2.00658447
	2.11885E-10
n'''_Char,Bed Mix (Char Particles/m^3 Bed Mix)	1083318.228
m'''_LS CaCO3,Bed Mix (kg LS CaCO3/m^3 Bed Mix)	0.005353163
m'_LS CaCO3 (kg LS CaCO3/LS CaCO3 Particle)	4.78897E-09
n'''_LS CaCO3,Bed Mix (LS CaCO3 Particles/m^3 Bed Mix)	1117812.098
a_CS,Fuel,0 (m^2 Fuel)	0.012350344
a_CS,LS CaCO3 (m^2 LS CaCO3)	0.000740751
a_CS,Riser,Eff (m^2 Eff Riser)	124.9869089
V_Bed Mix (m Riser/s)	9.968868353
t_Res,Bed Mix (s)	3.671429766
delta t (s)	0.000734286

Table 8

Continued.

Gas Properties	
mu_CO (kg CO/(m CO*s))	4.35505E-05
mu_H2O (kg H2O/(m H2O*s))	4.03042E-05
mu_O2 (kg O2/(m O2*s))	5.19245E-05
mu_N2 (kg N2/(m N2*s))	4.2001E-05
mu_NH3 (kg NH3/(m NH3*s))	3.76217E-05
mu_HCN (kg HCN/(m HCN*s))	3.00371E-05
mu_SO2 (kg SO2/(m SO2*s))	4.25944E-05
mu_CO2 (kg CO2/(m CO2*s))	4.32664E-05
mu_H2 (kg H2/(m H2*s))	2.05904E-05
mu_NO (kg NO/(m NO*s))	4.90681E-05
phi_CO|CO (dimensionless)	1
phi_CO|H2O (dimensionless)	0.824720516
phi_CO|O2 (dimensionless)	0.978525655
phi_CO|N2 (dimensionless)	1.018545745
phi_CO|NH3 (dimensionless)	0.826832294
phi_CO|HCN (dimensionless)	1.191992817
phi_CO|SO2 (dimensionless)	1.484441167
phi_CO|CO2 (dimensionless)	1.245980395
phi_CO|H2 (dimensionless)	0.281615064
phi_CO|NO (dimensionless)	0.975302722
phi_H2O|CO (dimensionless)	1.186638532
phi_H2O|H2O (dimensionless)	1
phi_H2O|O2 (dimensionless)	1.150611674
phi_H2O|N2 (dimensionless)	1.209409548
phi_H2O|NH3 (dimensionless)	1.006340857
phi_H2O|HCN (dimensionless)	1.426169868
phi_H2O|SO2 (dimensionless)	1.704223693
phi_H2O|CO2 (dimensionless)	1.450112653
phi_H2O|H2 (dimensionless)	0.36711879
phi_H2O|NO (dimensionless)	1.15127626
phi_O2|CO (dimensionless)	1.021207339
phi_O2|H2O (dimensionless)	0.834562447
phi_O2|O2 (dimensionless)	1
phi_O2|N2 (dimensionless)	1.040669784
phi_O2|NH3 (dimensionless)	0.836439248
phi_O2|HCN (dimensionless)	1.222417693
phi_O2|SO2 (dimensionless)	1.545173746
phi_O2|CO2 (dimensionless)	1.28597569
phi_O2|H2 (dimensionless)	0.277505994
phi_O2|NO (dimensionless)	0.99597532
phi_N2|CO (dimensionless)	0.981954605
phi_N2|H2O (dimensionless)	0.810349964
phi_N2|O2 (dimensionless)	0.961351275
phi_N2|N2 (dimensionless)	1
phi_N2|NH3 (dimensionless)	0.81227219
phi_N2|HCN (dimensionless)	1.168602882
phi_N2|SO2 (dimensionless)	1.454825904
phi_N2|CO2 (dimensionless)	1.222227823
phi_N2|H2 (dimensionless)	0.277220589
phi_N2|NO (dimensionless)	0.95807553
phi_NH3|CO (dimensionless)	1.174516004
phi_NH3|H2O (dimensionless)	0.993516228
phi_NH3|O2 (dimensionless)	1.138503055
phi_NH3|N2 (dimensionless)	1.19682932
phi_NH3|NH3 (dimensionless)	1
phi_NH3|HCN (dimensionless)	1.409404384
phi_NH3|SO2 (dimensionless)	1.675091745
phi_NH3|CO2 (dimensionless)	1.429588126
phi_NH3/H2 (dimensionless)	0.369684361
phi_NH3|NO (dimensionless)	1.139491175

Table 8

Continued.

Gas Properties	
phi_HCN|CO (dimensionless)	0.851996315
phi_HCN|H2O (dimensionless)	0.708473624
phi_HCN|O2 (dimensionless)	0.837224626
phi_HCN|N2 (dimensionless)	0.866403421
phi_HCN|NH3 (dimensionless)	0.70918279
phi_HCN|HCN (dimensionless)	1
phi_HCN|SO2 (dimensionless)	1.236330765
phi_HCN|CO2 (dimensionless)	1.048653469
phi_HCN|H2 (dimensionless)	0.247848065
phi_HCN|NO (dimensionless)	0.833807371
phi_SO2|CO (dimensionless)	0.634717576
phi_SO2|H2O (dimensionless)	0.50644523
phi_SO2|O2 (dimensionless)	0.633072056
phi_SO2|N2 (dimensionless)	0.645234658
phi_SO2|NH3 (dimensionless)	0.50421368
phi_SO2|HCN (dimensionless)	0.739585066
phi_SO2|SO2 (dimensionless)	1
phi_SO2|CO2 (dimensionless)	0.817270837
phi_SO2|H2 (dimensionless)	0.15922395
phi_SO2|NO (dimensionless)	0.626134395
phi_CO2|CO (dimensionless)	0.787825675
phi_CO2|H2O (dimensionless)	0.637248783
phi_CO2|O2 (dimensionless)	0.779130075
phi_CO2|N2 (dimensionless)	0.801604625
phi_CO2|NH3 (dimensionless)	0.636338713
phi_CO2|HCN (dimensionless)	0.92765575
phi_CO2|SO2 (dimensionless)	1.208557697
phi_CO2|CO2 (dimensionless)	1
phi_CO2|H2 (dimensionless)	0.206516544
phi_CO2|NO (dimensionless)	0.77322719
phi_H2|CO (dimensionless)	1.849907969
phi_H2|H2O (dimensionless)	1.676058628
phi_H2|O2 (dimensionless)	1.74672646
phi_H2|N2 (dimensionless)	1.888899494
phi_H2|NH3 (dimensionless)	1.709557892
phi_H2|HCN (dimensionless)	2.277800565
phi_H2|SO2 (dimensionless)	2.446161361
phi_H2|CO2 (dimensionless)	2.145508151
phi_H2|H2 (dimensionless)	1
phi_H2|NO (dimensionless)	1.767296808
phi_NO|CO (dimensionless)	1.025634852
phi_NO|H2O (dimensionless)	0.841436283
phi_NO|O2 (dimensionless)	1.003598953
phi_NO|N2 (dimensionless)	1.045062368
phi_NO|NH3 (dimensionless)	0.843573234
phi_NO|HCN (dimensionless)	1.226746947
phi_NO|SO2 (dimensionless)	1.539938441
phi_NO|CO2 (dimensionless)	1.286001663
phi_NO|H2 (dimensionless)	0.282923216
phi_NO|NO (dimensionless)	1
D_O2|CO (m^2 CO/s)	0.000197468
D_O2|H2O (m^2 H2O/s)	0.000259327
D_O2|N2 (m^2 N2/s)	0.000193859
D_O2|NH3 (m^2 NH3/s)	0.000253223
D_O2|HCN (m^2 HCN/s)	0.00017717
D_O2|SO2 (m^2 SO2/s)	0.000135374
D_O2|CO2 (m^2 CO2/s)	0.000158387
D_O2|H2 (m^2 H2/s)	0.000730394
D_O2|NO (m^2 NO/s)	0.000202579

4.2 Riser Model

4.2.1 Two-phase flow

A major component of the proposed model is the approach to the flow field that follows the gases as it spends a certain time step (Δt) with each new shrunken fuel particle size (d_{Fuel}) that is calculated based on the reactions that occurred in the previous time step assuming the CFB combustor has reached steady-state [8,13,15]. Just above the CFB bed as the newly formed char particles, sulfated limestone particles, and gas mixture enter the riser section of the CFB, the CFB combustor is assumed to be a two-phase [18], one-dimensional plug flow (inviscid) reactor with the turbulent and well-mixed mixture only traveling upwards continuously with no backmixing anywhere across the CFB riser including the area closest to the CFB combustor walls where friction with the walls would normally occur.

To better illustrate this, a CFB combustor that has just begun feeding fresh fuel and limestone to the primary air current (before reaching steady-state) would immediately have uniform char and sulfated limestone particles as well as a newly formed gas mixture. This newly formed gas mixture immediately begins to raise this number of new particles (with both char and limestone having its own SMD size particle used for modeling and calculation purposes), but the gas mixture would only be in contact with this new group of particles for a very short time (Δt) and quickly pass the particles due to the more slowly moving average large sized particles.

However, immediately after the original layer of gas mixture has passed the original layer of particles then there is another layer of fresh gas mixture that is created

by the continuous flux of fresh fuel, limestone, and primary air that has passed the new group of particles that produced the new fresh gas mixture and is now in contact with the older layer of particles for a short time (Δt). This new fresh gas mixture has a slightly different composition when it encounters the older layer of particles though because it has already spent some time (Δt) in contact reacting with the new fresh particles layer.

The new fresh particles layer then becomes the older layer of particles because the same new fresh gas mixture spent the same time (Δt) with that new fresh particles layer, and the older layer of particles then becomes the oldest layer of particles as the newest layer of particles and gas mixture immediately follow. This pattern continues of fresh gas mixture layers rising through the riser lifting the particles for a short time (Δt) while chemical reactions take place between the char particles and the gas mixture causing an ever upwards yet shrinking size field of char particles [8,14,35] and an ever changing composition of gas mixture until a steady-state of the CFB combustor is reached. At this point in the model, there is now a set particle field that has an average/SMD particle size (d_{Fuel}) with an average particle upward velocity ($V_{Bed\ Mix} - V_{term,d_{Fuel}} > 0$) [14] at each point along the CFB riser that the gas mixture will encounter along its way from the bed to the riser exit.

4.2.2 Riser gas mixture properties

The Sherwood number for the mixture of gases around the char particle during any Δt ($Sh_{d_{Fuel}}$) is dependent upon the Reynolds number for the mixture of gases around the char particle ($Re_{d_{Fuel}}$) and the Schmidt number for the mixture of gases at the same Δt (Sc_{Mix}). These numbers in turn depend upon basic fluid properties during the Δt such

as the diffusivity of O_2 through the mixture of gases ($D_{O_2|Mix}$), the density of the mixture of gases (ρ_{Mix}), and the dynamic/absolute viscosity of the mixture of gases (μ_{Mix}). Wick's Law for determining the diffusivity of a certain gaseous species through a stagnant gas mixture is assumed to apply to O_2 diffusing through the gas mixture in the CFB riser because all species in the gas mixture are assumed to be traveling at the same bulk velocity so that relative to one another they are not moving:

$$Sh_{d_{Fuel}} = 2 + 0.6 * Re_{d_{Fuel}}{}^{\frac{1}{2}} * Sc_{Mix}{}^{\frac{1}{3}} \quad [24,54,91] \tag{33}$$

$$Re_{d_{Fuel}} = \frac{\rho_{Mix} * V_{term,d_{Fuel}} * d_{Fuel}}{\mu_{Mix}} \quad [76] \tag{34}$$

$$Sc_{Mix} = \frac{\mu_{Mix}}{\rho_{Mix} * D_{O_2|Mix}} \quad [90] \tag{35}$$

$$\rho_{Mix} = \bar{m}_{Mix} * N'''_{Mix} \tag{36}$$

$$\mu_{Mix} = \sum_i \left[\frac{X_{Mix\ i,Mix} * \mu_i}{\sum_j (X_{Mix\ j,Mix} * \phi_{i|j})} \right] \text{ (Chapman-Enskog Theory) [54]} \tag{37}$$

$$D_{O_2|Mix} = \frac{1 - Y_{Mix\ O_2,Mix}}{\sum_{i \neq O_2} \left(\frac{Y_{Mix\ i,Mix}}{D_{O_2|i}} \right)} \text{ (Wick's Law) [54]} \tag{38}$$

4.2.3 Particle terminal velocity

The $Re_{d_{Fuel}}$ and the $V_{term,d_{Fuel}}$ must be solved together. The terminal velocity of a certain size spherical char particle (d_{Fuel}) in the mixture of gas ($V_{term,d_{Fuel}}$) is obtained by a force balance on that certain size char particle with the downward direction being positive. The only forces acting on the char particle as it moves through the CFB riser are assumed to be gravity from the earth pulling the char downwards ($F'_{Gravity}$), and buoyancy ($F'_{Buoyancy}$) and drag (F'_{Drag}) from the gas mixture the char

particle is floating in pushing the char upwards with a combined effect accelerating (a'_{Fuel}) the char mass (m'_{Fuel}):

$$F'_{Gravity} - F'_{Buoyancy} - F'_{Drag} = m'_{Fuel} * a'_{Fuel} \tag{39}$$

Introducing the definitions of each force on the char particle, the force balance can be represented and reduced as:

$$m'_{Fuel} * 9.81 - m'_{Mix} * 9.81 - \frac{C_{Drag} * a'_{CS,Fuel} * \rho_{Mix} * V_{d_{Fuel}}{}^2}{2} = m'_{Fuel} * a'_{Fuel} \tag{40}$$

$$m'''_{Char,Fuel} * V'_{Fuel} * 9.81 - \rho_{Mix} * V'_{Fuel} * 9.81 -$$

$$\frac{C_{Drag} * \left(\frac{\pi * d_{Fuel}{}^2}{4}\right) * \left(\frac{\mu_{Mix} * Re_{d_{Fuel}}}{d_{Fuel}}\right) * V_{d_{Fuel}}}{2} = m'''_{Char,Fuel} * V'_{Fuel} * a'_{Fuel} \tag{41}$$

$$\left(m'''_{Char,Fuel} - \rho_{Mix}\right) * V'_{Fuel} * 9.81 - \frac{C_{Drag} * \pi * d_{Fuel} * \mu_{Mix} * Re_{d_{Fuel}} * V_{d_{Fuel}}}{8} =$$

$$m'''_{Char,Fuel} * V'_{Fuel} * a'_{Fuel} \tag{42}$$

$$\left(\frac{m'''_{Char,Fuel} - \rho_{Mix}}{m'''_{Char,Fuel}}\right) * 9.81 - \frac{C_{Drag} * \pi * d_{Fuel} * \mu_{Mix} * Re_{d_{Fuel}} * V_{d_{Fuel}}}{8 * m'''_{Char,Fuel} * V'_{Fuel}} = a'_{Fuel} \tag{43}$$

$$\left(\frac{m'''_{Char,Fuel} - \rho_{Mix}}{m'''_{Char,Fuel}}\right) * 9.81 - \frac{C_{Drag} * \pi * d_{Fuel} * \mu_{Mix} * Re_{d_{Fuel}} * V_{d_{Fuel}}}{8 * m'''_{Char,Fuel} * \left(\frac{1}{6} * \pi * d_{Fuel}{}^3\right)} = a'_{Fuel} \tag{44}$$

$$\left(\frac{m'''_{Char,Fuel} - \rho_{Mix}}{m'''_{Char,Fuel}}\right) * 9.81 - \frac{3 * C_{Drag} * \mu_{Mix} * Re_{d_{Fuel}} * V_{d_{Fuel}}}{4 * m'''_{Char,Fuel} * d_{Fuel}{}^2} = a'_{Fuel} \tag{45}$$

When solving for $V_{term,d_{Fuel}}$, the char is no longer accelerating:

$$\left(\frac{m'''_{Char,Fuel} - \rho_{Mix}}{m'''_{Char,Fuel}}\right) * 9.81 - \frac{3 * C_{Drag} * \mu_{Mix} * Re_{d_{Fuel}} * V_{term,d_{Fuel}}}{4 * m'''_{Char,Fuel} * d_{Fuel}{}^2} = 0 \tag{46}$$

$$\frac{3 * C_{Drag} * \mu_{Mix} * Re_{d_{Fuel}} * V_{term,d_{Fuel}}}{4 * m'''_{Char,Fuel} * d_{Fuel}{}^2} = \left(\frac{m'''_{Char,Fuel} - \rho_{Mix}}{m'''_{Char,Fuel}}\right) * 9.81 \tag{47}$$

$$V_{term,d_{Fuel}} = \frac{4 * d_{Fuel}{}^2 * \left(m'''_{Char,Fuel} - \rho_{Mix}\right) * 9.81}{3 * C_{Drag} * \mu_{Mix} * Re_{d_{Fuel}}} \tag{48}$$

However, C_{Drag} is dependent upon $Re_{d_{Fuel}}$ so that when $Re_{d_{Fuel}} \leq 2$ the flow of the gas mixture around the spherical char particle is in the Stoke's/Creeping Flow Region so $C_{Drag} = \frac{24}{Re_{d_{Fuel}}}$, when $2 < Re_{d_{Fuel}} \leq 500$ the flow of the gas mixture around the spherical char particle is in the Intermediate Region so $C_{Drag} = \frac{18.5}{Re_{d_{Fuel}}^{0.6}}$, and when $500 < Re_{d_{Fuel}} \leq 200{,}000$ the flow of the gas mixture around the spherical char particle is in the Newton's Law Region so $C_{Drag} = 0.44$ [76]. This results in the following three equations for $V_{term,d_{Fuel}}$ depending upon $Re_{d_{Fuel}}$:

$$V_{term,d_{Fuel}} = \frac{{d_{Fuel}}^2 * (m'''_{Char,Fuel} - \rho_{Mix}) * 9.81}{18 * \mu_{Mix}} \ (for\ Re_{d_{Fuel}} \leq 2) \quad (49)$$

$$V_{term,d_{Fuel}} = \frac{0.153 * {d_{Fuel}}^{1.14} * [(m'''_{Char,Fuel} - \rho_{Mix}) * 9.81]^{0.71}}{{\mu_{Mix}}^{0.43} * {\rho_{Mix}}^{0.29}} \ (for\ 2 < Re_{d_{Fuel}} \leq 500) \quad (50)$$

$$V_{term,d_{Fuel}} = 1.74 * \left[\frac{d_{Fuel} * (m'''_{Char,Fuel} - \rho_{Mix}) * 9.81}{\rho_{Mix}}\right]^{\frac{1}{2}} \ (for\ 500 < Re_{d_{Fuel}} \leq 200{,}000) \quad (51)$$

4.2.4 Kinetic-controlled reactions

The immediate chemical reactions that took place in the bed no longer take place, but rather new time dependent reactions (chemical kinetics) now with several key competing reactions that have inputs that can be changed to alter the rate of the reactions. These key time dependent, forward, global reactions taking place in the CFB riser are stated below:

$$NO\ (g)\ +\ C\ (s)\ \rightarrow \frac{1}{2}\ N_2\ (g)\ + CO\ (g) \quad (52)$$

$$CO\ (g)\ +\ \frac{1}{2}\ O_2\ (g)\ \rightarrow\ CO_2\ (g) \quad (53)$$

$$NH_3\,(g)\ +\ O_2\,(g)\ \rightarrow\ \mathrm{NO\,(g)}\ +\ H_2O\,(\mathrm{g})\ +\ \tfrac{1}{2}\,H_2\,(g) \tag{54}$$

$$NH_3\,(g)\ +\ NO\,(g)\ \rightarrow\ N_2\,(\mathrm{g})\ +\ H_2O\,(\mathrm{g})\ +\ \tfrac{1}{2}\,H_2\,(g) \tag{55}$$

$$HCN\,(g)\ +\ O_2\,(g)\ \rightarrow\ \mathrm{NO\,(g)}\ +\ CO\,(\mathrm{g})\ +\ \tfrac{1}{2}\,H_2\,(g) \tag{56}$$

$$HCN\,(g)\ +\ NO\,(g)\ \rightarrow\ N_2\,(\mathrm{g})\ +\ CO\,(\mathrm{g})\ +\ \tfrac{1}{2}\,H_2\,(g) \tag{57}$$

$$2\,H_2\,(g)\ +\ O_2\,(g)\rightarrow\ 2\,H_2O\,(g) \tag{58}$$

4.2.5 NO reduction by fixed Carbon

Besides char fixed Carbon and fixed Nitrogen oxidation, the reaction of NO with char fixed Carbon is the only other chemical reaction of the nine total CFB riser reactions that is heterogeneous (reaction between species of two different phases such as solid and gas in the case of these three reactions). The other six reactions in the CFB riser are homogeneous (reaction between species of the same phase such as gas and gas for the remaining six reactions). Thus, conservation of mass and chemical species is preserved by following the fuel, limestone, and air from their respective entries into the riser at the bed all the way to the exit of the riser at the cyclone [15].

However, the reaction of NO with char fixed Carbon is not considered to be diffusion-controlled in the proposed model because the majority of the NO being produced in the CFB riser is coming from the char fixed Nitrogen oxidizing on the surface of the char to form the NO [6,10,16,23,31,42,60,62-65,72,77] so that it is already at the surface of the char where much of the NO is reduced [6,16,17,31,32,42,60,62,63,65,72]. Instead of the char surface further catalyzing the reduction of NO by Carbon monoxide via $CO\,(g)\ +\ NO\,(g)\ \rightarrow\ CO_2\,(g)\ +\ \frac{1}{2}\,N_2\,(g)$,

it is believed that $CO\ (g)\ +\ \frac{1}{2}\ O_2\ (g)\ \rightarrow\ CO_2\ (g)$ at the surface quickly so that NO can have more free active sites to attach to the char fixed Carbon rather than O_2 attaching to the Carbon.

Therefore, an empirical average global rate equation [6,63] has been selected using the least-squares regression over 24 datasets by Aarna and Suuberg [89] for the reaction of NO with char fixed Carbon as noted previously even though there is a large variability in reported kinetics [16,32]. The extent of this reduction will depend on the combustion conditions and the structural characteristics of the char. In the case of the latter, factors such as porosity, active sites, reactivity towards various species, particle size, etc. need to be considered [62,63].

However, it is difficult to extract mechanistic information on Nitrogen oxide release from fluidized bed experiments, due to the coupling of parameters, which makes it difficult to determine the influence of a specific single parameter. The mechanisms proposed have not been proved unequivocally, but they are useful for the development of rate equations and understanding the surface chemistry [6,16,17,23,31,32,62].

Reduction of NO by H or hydrocarbon radicals, as utilized in reburning, does not take place to any great extent in FBC because the temperature is too low [6]. The NO and O_2 reacting on the surface of the char are assumed to not interfere with each other because of how quickly the reactions take place with respect to how relatively slowly the O_2 diffuses to the surface of the char so that both NO and O_2 are considered to have the entire surface area of the spherical char each to react on. The NO and O_2 reacting on the

surface of the char are also assumed to form only N_2 with negligible amounts of N_2O [6,17,42,63].

4.2.6 Diffusion-controlled reactions

The oxidation taking place on the char particle surface with the fixed Carbon and Nitrogen is assumed to be diffusion-controlled [12,13,23,24,29,35,37,63,73] which means that the oxidation occurs at a rate determined by how quickly the O_2 in the gas mixture can diffuse through the gas mixture to reach the char surface [29,35,65,71] because of how much quicker the chemical reactions are than the diffusion rate for the larger average sized particles found in FBC applications. Similar to the limestone, the fuel particles are assumed to have volatile matter and moisture fairly uniformly distributed throughout the original fuel particles [15] so that when devolatilization and drying takes place causing volatile matter and moisture to be released through newly formed passageways/pores in the remaining char particle shell (assumed to be only ash and fixed Carbon and Nitrogen uniformly distributed throughout [65]) the O_2 that diffuses to the char then begins to react on the surface as well as the pores closest to the surface [65]. This can agree with the assumption that the char particles are still solid sphere particles if the surface area lost by having a hole/pore in the surface is exactly compensated by allowing O_2 to react with the surface inside the hole/pore just far enough to be exactly the same area that the O_2 would have reacted with if the hole/pore was not created.

When the O_2 reaches the char surface, the O_2 is assumed to instantaneously react with the fixed Carbon or Nitrogen of the char and the new product leaves the surface of

the char particle rejoining the gas mixture [19,29,47,65]. The CO that is produced from fixed Carbon oxidizing then homogenously reacts in the gas mixture with O_2 again to form CO_2 [10,12,14,24,35,54,63,71], but the direct oxidation of fixed Carbon to CO_2 is considered negligible (especially above 800 K) [24,35,54,65] in the proposed model. Also, the direct oxidation of fixed Nitrogen to N_2O or NO_2 is considered negligible [6,23,55] in the proposed model. The global equations of the oxidation reactions at the char surface that are diffusion-controlled are as follows (assumed to only occur in the forward direction):

$$C\ (s)\ +\ \frac{1}{2}\ O_2\ (g)\ \rightarrow\ CO\ (g) \tag{59}$$

$$N\ (s)\ +\ \frac{1}{2}\ O_2\ (g)\ \rightarrow\ NO\ (g) \tag{60}$$

This brings the total number of key global reactions in the CFB riser for the proposed model to nine (including seven previously mentioned that are kinetics-controlled [37,73] and can have inputs changed) and the overall combustor reactions (including the nine instantaneous bed reactions) to 18 (all assumed to be forward reactions only). Also, these CFB riser reactions bring the number of gaseous species in the gas mixture at any time in the riser for the proposed model from eight (CO, H_2O, O_2, N_2, NH_3, HCN, SO_2, and CO_2) in the CFB bed up to now ten (CO, H_2O, O_2, N_2, NH_3, HCN, SO_2, CO_2, H_2, and NO) in the CFB riser.

4.2.7 Char burning

The rate at which the fixed Nitrogen is oxidized compared to the rate at which fixed Carbon is oxidized on the char surface is assumed to be proportional

[32,60,63,65,77] to the mass of fixed Nitrogen relative to the mass of fixed Carbon (Fixed Carbon Ratio or FCR) in the char particle:

$$FCR = \frac{Y_{FN,FC}}{Y_{FC,FC}} \tag{61}$$

$$\Delta m'_{FN,Surf} = \Delta m'_{FC,Surf} * FCR \tag{62}$$

The degree to which the char particle shrinks from its original SMD a time step (Δt) before ($d_{Fuel,i}$) to its new SMD (d_{Fuel}) when it is oxidized is derived from the change in the mass of the Carbon retained as fixed Carbon at the surface of the char particle during Δt ($\Delta m'_{FC,Surf}$). If the char particle SMD ever shrinks to zero, then the Excel program is coded to allow the six homogenous reactions to occur while stopping the three heterogeneous reactions:

$$\Delta m'_{FC,Surf} = m'_{FC,Surf} - m'_{FC,Surf,i} \tag{63}$$

$$\Delta m'_{FC,Surf} = m'''_{FC,Fuel} * V'_{Fuel} - m'''_{FC,Fuel} * V'_{Fuel,i} \tag{64}$$

$$\Delta m'_{FC,Surf} = m'''_{FC,Fuel} * \left(\frac{1}{6} * \pi * {d_{Fuel}}^3\right) - m'''_{FC,Fuel} * \left(\frac{1}{6} * \pi * {d_{Fuel,i}}^3\right) \tag{65}$$

$$\Delta m'_{FC,Surf} = \frac{1}{6} * \pi * m'''_{FC,Fuel} * \left({d_{Fuel}}^3 - {d_{Fuel,i}}^3\right) \tag{66}$$

$$\frac{6 * \Delta m'_{FC,Surf}}{\pi * m'''_{FC,Fuel}} = {d_{Fuel}}^3 - {d_{Fuel,i}}^3 \tag{67}$$

$$d_{Fuel} = \left({d_{Fuel,i}}^3 + \frac{6 * \Delta m'_{FC,Surf}}{\pi * m'''_{FC,Fuel}}\right)^{\frac{1}{3}} \tag{68}$$

The mass percent of char remaining from the time the char particle begins burning as it leaves the CFB bed ($m'_{FC,Surf,i}$) until it reaches the CFB riser exit ($m'_{FC,Surf,f}$) is calculated as follows:

$$mass\ \%\ char\ remaining = \left(\frac{\mathrm{m'}_{FC,Surf,f}}{\mathrm{m'}_{FC,Surf,i}}\right) * 100\% \tag{69}$$

$$mass\ \%\ char\ remaining = \left(\frac{\mathrm{m'''}_{FC,Fuel} * V'_{Fuel,f}}{\mathrm{m'''}_{FC,Fuel} * V'_{Fuel,i}}\right) * 100\% \tag{70}$$

$$mass\ \%\ char\ remaining = \left[\frac{\mathrm{m'''}_{FC,Fuel} * \left(\frac{1}{6} * \pi * {d_{Fuel,f}}^3\right)}{\mathrm{m'''}_{FC,Fuel} * \left(\frac{1}{6} * \pi * {d_{Fuel,i}}^3\right)}\right] * 100\% \tag{71}$$

$$mass\ \%\ char\ remaining = \left(\frac{{d_{Fuel,f}}^3}{{d_{Fuel,i}}^3}\right) * 100\% \tag{72}$$

The change in the mass of the Carbon retained as fixed Carbon at the surface of the char particle during Δt ($\Delta \mathrm{m'}_{FC,Surf}$) takes place due to the oxidation of the char fixed Carbon [31] as well as due to the reduction of NO on the char surface:

$$\Delta \mathrm{m'}_{FC,Surf} = (\dot{\mathrm{m}}'_{FC,Mix\ O_2} + \dot{\mathrm{m}}'_{FC,Mix\ NO}) * \Delta t \tag{73}$$

The reaction rate of the Carbon retained as fixed Carbon with the O_2 in the mixture of gases ($\dot{\mathrm{m}}'_{FC,Mix\ O_2}$) is derived from fundamental mass transfer principles [90] assuming there is no O_2 at the surface of the char particle at any time due to the O_2 reacting with the fixed Carbon or Nitrogen immediately as it reaches the char surface:

$$\dot{\mathrm{N}}'_{Mix\ O_2} = h_{avg,conv,m} * a'_{Surf,Fuel} * \left(\frac{\mathrm{N}_{Mix\ O_2,Surf}}{\mathrm{V}_{Mix}} - \frac{\mathrm{N}_{Mix\ O_2,Mix}}{\mathrm{V}_{Mix}}\right) \tag{74}$$

$$\dot{\mathrm{N}}'_{Mix\ O_2} = h_{avg,conv,m} * a'_{Surf,Fuel} * \left(\frac{0}{\mathrm{V}_{Mix}} - \frac{\mathrm{N}_{Mix\ O_2,Mix}}{\mathrm{V}_{Mix}}\right) \tag{75}$$

$$\dot{\mathrm{N}}'_{Mix\ O_2} = \frac{-h_{avg,conv,m} * a'_{Surf,Fuel} * \mathrm{N}_{Mix\ O_2,Mix}}{\mathrm{V}_{Mix}} \tag{76}$$

$$(16 * 2) * \dot{\mathrm{N}}'_{Mix\ O_2} = \frac{-h_{avg,conv,m} * a'_{Surf,Fuel} * \mathrm{N}_{Mix\ O_2,Mix} * (16*2)}{\mathrm{V}_{Mix}} \tag{77}$$

$$\left(\frac{\mathrm{m}_{Mix\ O_2}}{\mathrm{N}_{Mix\ O_2}}\right) * \dot{\mathrm{N}}'_{Mix\ O_2} = \frac{-h_{avg,conv,m} * a'_{Surf,Fuel} * \mathrm{N}_{Mix\ O_2,Mix} * \left(\frac{\mathrm{m}_{Mix\ O_2,Mix}}{\mathrm{N}_{Mix\ O_2,Mix}}\right)}{\mathrm{V}_{Mix}} \tag{78}$$

$$\dot{m}'_{Mix\ O_2} = \frac{-h_{avg,conv,m} * a'_{Surf,Fuel} * m_{Mix\ O_2,Mix}}{V_{Mix}} \quad (79)$$

$$\left[\frac{0.5*(16*2)}{1*12.01}\right] * \dot{m}'_{FC,Mix\ O_2} = \frac{-h_{avg,conv,m} * a'_{Surf,Fuel} * m_{Mix\ O_2,Mix}}{V_{Mix}} \text{ (Law of Stoichiometry) [54]} \quad (80)$$

$$\dot{m}'_{FC,Mix\ O_2} = \frac{-h_{avg,conv,m} * a'_{Surf,Fuel} * \left[\frac{m_{Mix\ O_2,Mix}}{\frac{0.5*(16*2)}{1*12.01}}\right]}{V_{Mix}} \quad (81)$$

$$\dot{m}'_{FC,Mix\ O_2} = \frac{-h_{avg,conv,m} * a'_{Surf,Fuel} * \left\{\left[\frac{\frac{m_{Mix\ O_2,Mix}}{m_{Mix}}}{\frac{0.5*(16*2)}{1*12.01}}\right] * m_{Mix}\right\}}{V_{Mix}} \quad (82)$$

$$\dot{m}'_{FC,Mix\ O_2} = \frac{-h_{avg,conv,m} * a'_{Surf,Fuel} * \left\{\left[\frac{Y_{Mix\ O_2,Mix}}{\frac{0.5*(16*2)}{1*12.01}}\right] * m_{Mix}\right\}}{V_{Mix}} \quad (83)$$

$$\dot{m}'_{FC,Mix\ O_2} = -h_{avg,conv,m} * a'_{Surf,Fuel} * \left[\frac{Y_{Mix\ O_2,Mix}}{\frac{0.5*(16*2)}{1*12.01}}\right] * \left(\frac{m_{Mix}}{V_{Mix}}\right) \quad (84)$$

$$\dot{m}'_{FC,Mix\ O_2} = -h_{avg,conv,m} * a'_{Surf,Fuel} * \left[\frac{Y_{Mix\ O_2,Mix}}{\frac{0.5*(16*2)}{1*12.01}}\right] * \rho_{Mix} \quad (85)$$

$$\dot{m}'_{FC,Mix\ O_2} = -\left(\frac{Sh_{d_{Fuel}} * D_{O_2|Mix}}{d_{Fuel}}\right) * \left(\pi * {d_{Fuel}}^2\right) * \left[\frac{Y_{Mix\ O_2,Mix}}{\frac{0.5*(16*2)}{1*12.01}}\right] * \rho_{Mix} \quad (86)$$

$$\dot{m}'_{FC,Mix\ O_2} = -Sh_{d_{Fuel}} * D_{O_2|Mix} * \left[\frac{Y_{Mix\ O_2,Mix}}{\frac{0.5*(16*2)}{1*12.01}}\right] * \rho_{Mix} * \pi * d_{Fuel} \quad (87)$$

The reaction rate of the Carbon retained as fixed Carbon with the NO in the mixture of gases ($\dot{m}'_{FC,Mix\ NO}$) is derived from the empirical average chemical rate equation as noted previously:

$$\dot{m}'_{FC,Mix\ NO} = \frac{\dot{N}'''_{Mix\ NO,1} * (14.01+16)}{\frac{1*(14.01+16)}{1*12.01} * n'''_{Char,Bed\ Mix}} \quad (88)$$

The reaction rate of the concentration of O_2 in the mixture of gases with Carbon retained as fixed Carbon ($\dot{N}'''_{Mix\ O_2,FC}$) and the reaction rate of the concentration of O_2 in the mixture of gases with Nitrogen retained as fixed Carbon ($\dot{N}'''_{Mix\ O_2,FN}$) are then derived as:

$$\dot{N}'''_{Mix\ O_2,FC} = \frac{\dot{m}'_{FC,Mix\ O_2} * \left[\frac{0.5*(16*2)}{1*12.01}\right] * n'''_{Char,Bed\ Mix}}{16*2} \quad (89)$$

$$\dot{N}'''_{Mix\ O_2,FN} = \frac{\left(\frac{\Delta m'_{FN,Surf}}{\Delta t}\right) * \left[\frac{0.5*(16*2)}{1*14.01}\right] * n'''_{Char,Bed\ Mix}}{16*2} \quad (90)$$

4.2.8 Particle recirculation

Limestone particles aren't assumed to react throughout the riser in the proposed model for simplicity so the limestone particles just circulate through the CFB combustor and cyclone once they have been calcinated and sulfated in the bed until they are removed from the bed along with the fuel ash, usually through the bottom of the combustor [9,18,43], that is assumed to immediately detach from the char particle due to frequent interparticle collisions in the combustor as the fixed Carbon reacts with the gas mixture [15,19,23]. However, the proposed model also assumes the cyclone has a 100% collection efficiency with negligible combustion occurring in the cyclone due to lack of oxygen so that all remaining char and limestone particles as well as ash at the top of the CFB riser is circulated back to the bottom of the CFB riser where it is immediately uniformly mixed with the fresh fuel feed [10,11,13,22,35,38] while all gas is allowed to escape through the cyclone. A 100% collection efficiency of the cyclone also means that the combustion efficiency of the CFB combustor is 100% because all char particles will

eventually be completely burned upon a number of circulations through the CFB and cyclone [13,21].

For recirculated particles, only char combustion would be considered since devolatilizations are complete in the first passage in the furnace [12,13,21]. However, the effects of the recirculated particles are assumed negligible in the proposed model. This modeling approach of the particle-gas flow field seems unique to those models presented in the literature review and greatly saves computation time by having a once through approach rather than an iterative approach to calculations.

The 'Riser' tab of the Excel program is not shown because there are usually several thousand rows necessary for the proper time step (Δt) of typical CFB combustion of coal. The calculations in this tab should not normally be altered by the user of the program, but it is a convenient way to quickly track the intermediate CFB riser calculations of the program. However, the graph of the mole fraction of species in the mixture of gases versus time after the mixture of gases leaves the CFB bed until they reach the CFB riser exit for all species is shown below in Fig. 21 and for trace species is shown below in Fig. 22.

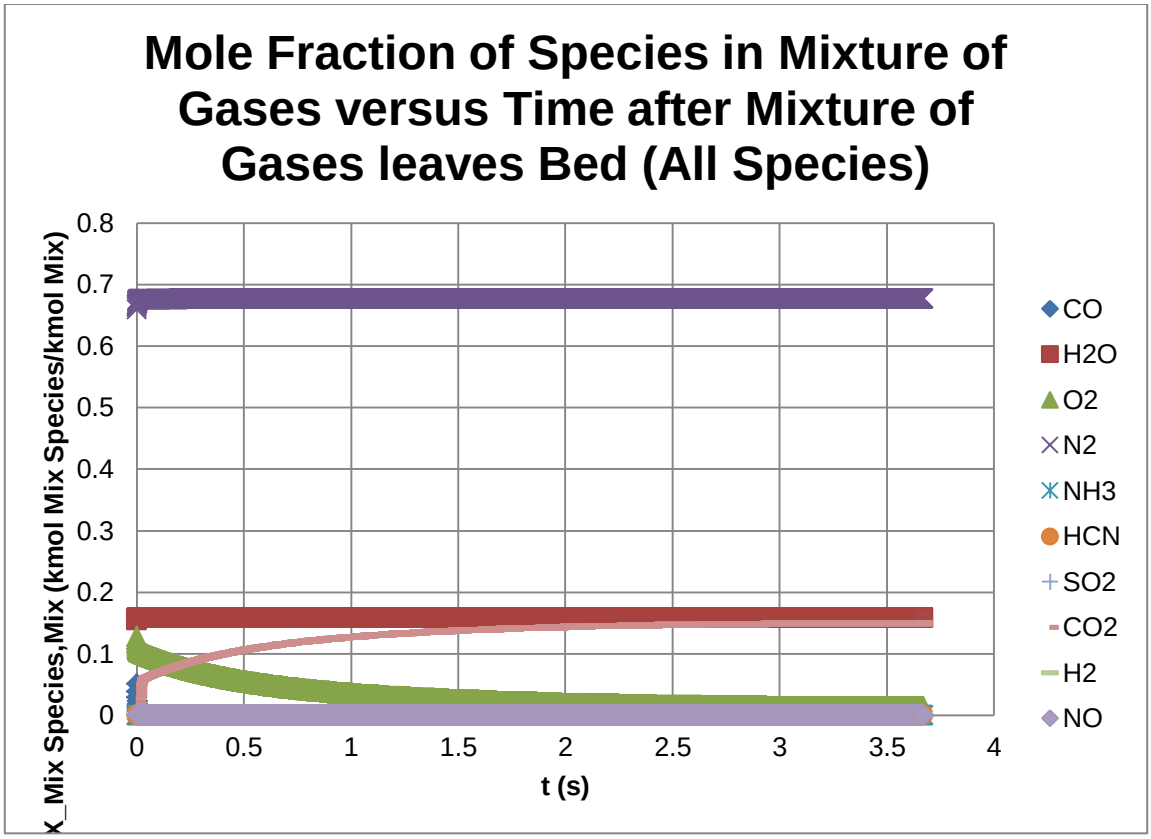

Fig. 21. Mole fraction of all species versus time for anonymous CFB boiler firing lignite fuel.

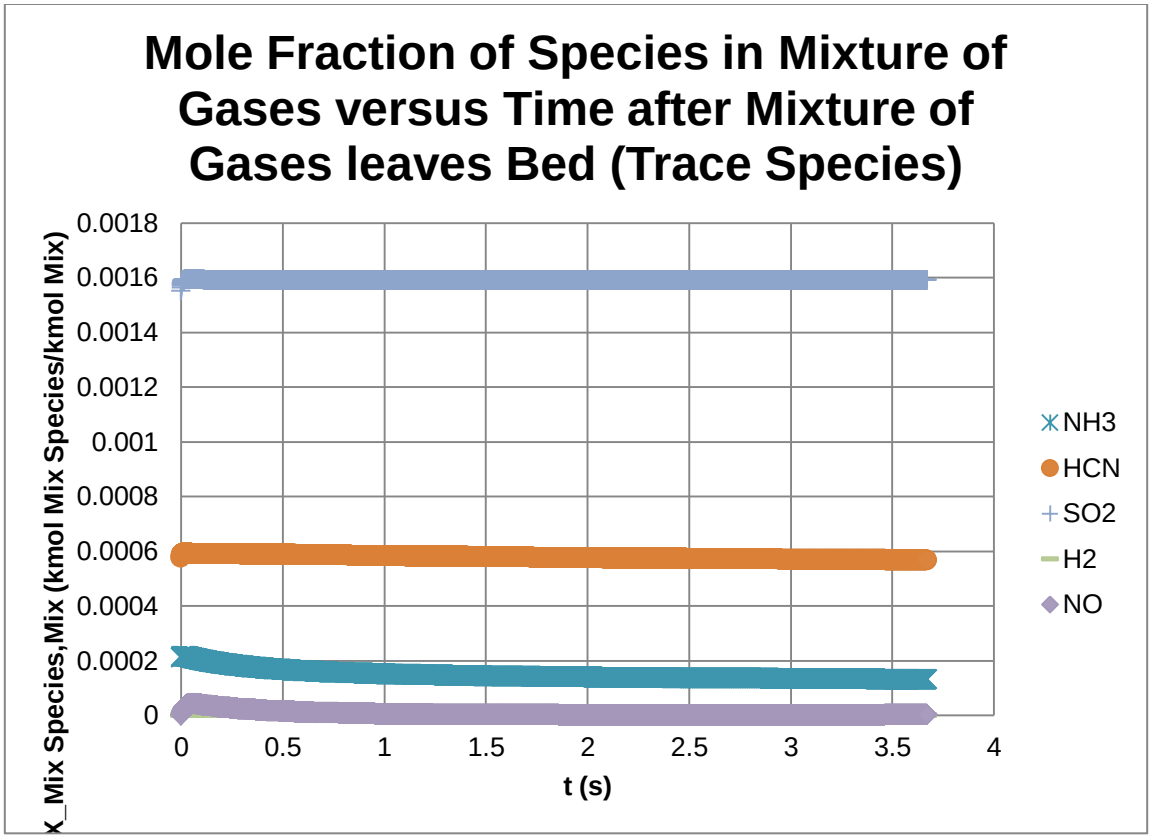

Fig. 22. Mole fraction of trace species versus time for anonymous CFB boiler firing lignite fuel.

4.3 Inputs

4.3.1 Fuel data

The mass flow rate of fuel (fuel feed rate or $\dot{m}_{Fuel}$), Calcium-Sulfur ratio (CSR), and mole percent of excess air with respect to stoichiometric air (simply known as excess air or $X_{Exc\ Air,Stoich\ Air}x100$) into the CFB combustor are inputs in the Excel program. It is assumed that these flows into the CFB combustor are constant throughout the run time [5].

The fuel is distinguished by its as received fuel particle density (ρ_{Fuel}), initial SMD of as received fuel particle ($d_{Fuel,0}$), as received fuel higher heating value (hhv_{Fuel}), as received proximate fuel analysis, as received ultimate fuel analysis, mass percent of Nitrogen in fuel released as volatile matter ($Y_{VN,N}x100$), mass percent of Nitrogen in fuel released as volatile matter and converted into N_2 ($Y_{N_2,N}x100$), mass percent of Nitrogen in fuel released as volatile matter and converted into NH_3 ($Y_{NH_3,N}x100$), and mass percent of Nitrogen in fuel released as volatile matter and converted into HCN ($Y_{HCN,N}x100$). These fuel/char particle properties are all inputs in the Excel program. It is assumed that the fuel/char particle properties are an average of several random samples taken for the fuel being put through the CFB during the run time.

The as received proximate fuel analysis consists of the mass percent of volatile matter in fuel/fresh feed ($Y_{VM,Fuel}x100$ consisting of volatile Carbon, Hydrogen, Oxygen, Nitrogen, and Sulfur), mass percent of fixed Carbon in fuel ($Y_{FC,Fuel}x100$ consisting of fixed Carbon and Nitrogen), mass percent of moisture in fuel ($Y_{H_2O,Fuel}x100$), and mass percent of ash in fuel ($Y_{Ash,Fuel}x100$). The as received ultimate fuel analysis consists of the mass percent of Carbon in fuel ($Y_{C,Fuel}x100$), mass percent of Hydrogen in fuel ($Y_{H,Fuel}x100$), mass percent of Oxygen in fuel ($Y_{O,Fuel}x100$), mass percent of Nitrogen in fuel ($Y_{N,Fuel}x100$), and mass percent of Sulfur in fuel ($Y_{S,Fuel}x100$).

Some basic checks that the user of the Excel program should watch for with respect to fuel/char particle properties is that the sum of $Y_{VM,Fuel}x100$, $Y_{FC,Fuel}x100$, $Y_{H_2O,Fuel}x100$, and $Y_{Ash,Fuel}x100$ should equal 100, the sum of $Y_{VM,Fuel}x100$ and $Y_{FC,Fuel}x100$ should equal the sum of $Y_{C,Fuel}x100$, $Y_{H,Fuel}x100$, $Y_{O,Fuel}x100$, $Y_{N,Fuel}x100$, and $Y_{S,Fuel}x100$, and the sum of $Y_{N_2,N}x100$, $Y_{NH_3,N}x100$, and $Y_{HCN,N}x100$ should equal $Y_{VN,N}x100$.

4.3.2 Limestone data

The limestone is distinguished by its Calcium Carbonate particle density (dry limestone particle density or ρ_{LSCaCO_3} which is approximately 2710 $\frac{kg}{m^3}$ [67,68]), SMD of limestone particle (d_{LSCaCO_3}), mass percent of moisture in limestone ($Y_{LS\ H_2O,LS}x100$), and mole percent of CaO in Limestone converted into $CaSO_3$ (average degree of conversion/sulfation from CaO to $CaSO_3$ or $X_{LS\ CaSO_3,LS\ CaO}x100$). These limestone particle properties are all inputs in the Excel program. It is assumed that the limestone particle properties are an average of several random samples taken for the limestone being put through the CFB during the run time.

4.3.3 Air data

The primary air is assumed to be completely dry and consist of only N_2 and O_2 [39]. It is assumed that there is no thermal NO formation (primary/combustion air N_2 oxidizing to form NO) in FBC because of the low combustion temperature even though it becomes more significant above 1,800 K [4-6,10,16,23,24,32,54,65], and a negligible amount of prompt NO may be formed [6,23,54,63]. However, the mole percent of N_2 in

the primary air ($X_{N_2,Air}x100$) and the mole percent of O_2 in the primary air ($X_{O_2,Air}x100$) can be varied as inputs in the Excel program as long as the sum of $X_{N_2,Air}x100$ and $X_{O_2,Air}x100$ equals 100. It is assumed that the air properties are an average of several random samples taken for the primary air being put through the CFB during the run time.

4.3.4 Operational data

The only operational data required as inputs in the Excel program are the pressure of the mixture of gases (P_{Mix}) and the temperature of the mixture of gases (T_{Mix}) in the CFB riser. Both of these are considered to be constant throughout the CFB riser. The pressure drop is low above the bed because of the increased space between the ever-shrinking particles (dilute region of CFB combustor [12,14,18]). The temperature is constant because the energy being produced from the combustion is being absorbed by the supposed uniform temperature tubes within the combustor walls to avoid erosion of tubes by the particles and obstruction within the riser [5,13,18,21,23]. The energy is then transferred to the water within the tubes to produce steam which typically goes through a Rankine cycle [17,78] steam turbine that ultimately converts the fluid energy into the desired electrical energy for distribution to consumers. This also satisfies the conservation of energy in a general way by extracting whatever energy that isn't used to maintain a constant temperature.

4.3.5 Riser data

The crucial geometrical data of the CFB can be captured by the inputs of cross-sectional area of the CFB riser/freeboard/lean region ($a_{CS,Riser}$) and the height of the

CFB riser from the top of the bed (at the location of the feed ports in the proposed model) to the centerline of the inlet of the cyclone at the top/exit of the riser (h_{Riser}) [13].

4.3.6 Chemical kinetics data

The chemical kinetics data for the most important global reactions taking place in the CFB riser are the last of the inputs in the Excel program. The number of rows in each column of the chemical kinetics in the 'Riser' tab of the Excel program is used to improve calculation "smoothness" (don't adjust this number without adding or deleting the number of rows in the 'Riser' tab of the Excel program to the new number indicated).

The riser chemical equations are restated along with rate equations and references for each below (all assumed to be only forward, global reactions):

$NO\ (g)\ +\ C\ (s)\ \rightarrow\ \frac{1}{2}\ N_2\ (g)\ +CO\ (g)$:

$$\dot{N}'''_{Mix\ NO,1} = -0.026 * e^{\left(\frac{-132,192.6}{8.314*T_{Mix}}\right)} * X_{Mix\ NO,Mix} * \left(\frac{P_{Mix}}{1.01325}\right) * \left(\frac{\pi * {d_{Fuel}}^2}{m'_{Char}}\right) * n'''_{Char,Bed\ Mix} \quad [63] \tag{91}$$

$CO\ (g)\ +\ \frac{1}{2}\ O_2\ (g)\ \rightarrow\ CO_2\ (g)$:

$$\dot{N}'''_{Mix\ CO,2} = -1.3 * 10^{11} * e^{\left(\frac{-125,520}{8.314*T_{Mix}}\right)} * N'''_{Mix\ CO} * {N'''_{Mix\ O_2}}^{\frac{1}{2}} * {N'''_{Mix\ H_2O}}^{\frac{1}{2}}$$

[65,79] (92)

$NH_3\ (g)\ +\ O_2\ (g)\ \rightarrow\ \mathrm{NO\ (g)}\ +\ H_2O\ \mathrm{(g)}\ +\ \frac{1}{2}\ H_2\ (g)$:

$$\dot{N}'''_{Mix\ NH_3,3} = \left[\frac{-3.48*10^{23}*e^{\left(\frac{-418,400}{8.314*T_{Mix}}\right)}*X_{Mix\ NH_3,Mix}*X_{Mix\ O_2,Mix}}{1+6.90*10^{-6}*e^{\left(\frac{175,728}{8.314*T_{Mix}}\right)}*X_{Mix\ O_2,Mix}}\right]*\left(\frac{\frac{P_{Mix}}{1.01325}}{82.057*T_{Mix}}\right) \quad [65] \quad (93)$$

$NH_3\ (g)\ +\ NO\ (g)\ \rightarrow\ N_2\ (\mathrm{g})\ +\ H_2O\ (\mathrm{g})\ +\ \frac{1}{2}\ H_2\ (g)$:

$$\dot{N}'''_{Mix\ NH_3,4} = -6.22*10^{17}*e^{\left(\frac{-230,120}{8.314*T_{Mix}}\right)}*X_{Mix\ NH_3,Mix}*X_{Mix\ NO,Mix}*\left(\frac{\frac{P_{Mix}}{1.01325}}{82.057*T_{Mix}}\right)$$

[65] (94)

$HCN\ (g)\ +\ O_2\ (g)\ \rightarrow\ \mathrm{NO}\ (\mathrm{g})\ +\ CO\ (\mathrm{g})\ +\ \frac{1}{2}\ H_2\ (g)$:

$$\dot{N}'''_{Mix\ HCN,5} = -1.0*10^{11}*e^{\left(\frac{-280,328}{8.314*T_{Mix}}\right)}*X_{Mix\ HCN,Mix}*{X_{Mix\ O_2,Mix}}^{b}*N'''_{Mix}$$

$$b\ =\ 0\ (for\ \ln\left(X_{Mix\ O_2,Mix}\right) \geq\ -3)$$

$$b = 233*e^{\left(\frac{-28}{X_{Mix\ O_2,Mix}+0.5}\right)}\ \left(for\ -5.67\ <\ \ln\left(X_{Mix\ O_2,Mix}\right)\ <\ -3\right)$$

$b = 1\ (for\ \ln\left(X_{Mix\ O_2,Mix}\right) \leq\ -5.67)$ [80] (95)

$HCN\ (g)\ +\ NO\ (g)\ \rightarrow\ N_2\ (\mathrm{g})\ +\ CO\ (\mathrm{g})\ +\ \frac{1}{2}\ H_2\ (g)$:

$$\dot{N}'''_{Mix\ HCN,6} = -3.0*10^{12}*e^{\left(\frac{-251,040}{8.314*T_{Mix}}\right)}*X_{Mix\ HCN,Mix}*X_{Mix\ NO,Mix}*N'''_{Mix}$$ [80] (96)

$2\ H_2\ (g)\ +\ O_2\ (g)\ \rightarrow\ 2\ H_2O\ (g)$:

$$\dot{N}'''_{Mix\ O_2,7} \cong -5.15*10^{13}*e^{\left(\frac{-28,433.88}{8.314*T_{Mix}}\right)}*{N'''}_{Mix\ O_2}*{N'''}_{Mix\ H_2}{}^{\frac{3}{2}}*{T_{Mix}}^{\frac{3}{2}}$$ [31] (97)

The 'Input' tab of the Excel program can be viewed below in Table 9 with the yellow cells indicating values that can be changed by the program user.

Table 9

Input tab for anonymous CFB boiler firing lignite fuel.

FUEL DATA	
Fuel	Texas Lignite
mdot_Fuel (kg Fuel/s)	65.65656566
Fuel/Char Particle Properties	
rho_Fuel (kg Fuel/m^3 Fuel)	1600
d_Fuel,0 (m Fuel)	0.000387226
hhv_Fuel (kJ/kg Fuel)	11365
	As Received (AR) Fuel
Proximate-equiv Fuel Analysis	
Y_VM,Fuel x 100 (kg VM/100 kg Fuel)	25.62
Y_FC,Fuel x 100 (kg FC/100 kg Fuel)	21.88
	47.5
Y_H2O,Fuel x 100 (kg H2O/100 kg Fuel)	31.35
Y_Ash,Fuel x 100 (kg Ash/100 kg Fuel)	21.15
	100
Ultimate/Elemental Fuel Analysis	
Y_C,Fuel x 100 (kg C/100 kg Fuel)	33.83
Y_H,Fuel x 100 (kg H/100 kg Fuel)	2.69
Y_O,Fuel x 100 (kg O/100 kg Fuel)	8.77
Y_N,Fuel x 100 (kg N/100 kg Fuel)	0.66
Y_S,Fuel x 100 (kg S/100 kg Fuel)	1.55
	47.5
Nitrogen Release from Fuel as Volatile Matter & Split into N2, NH3, HCN	
Y_VN,N x 100 (kg VN/100 kg N)	34
Y_N2,N x 100 (kg N2/100 kg N)	0.5
Y_NH3,N x 100 (kg N/100 kg N)	9
Y_HCN,N x 100 (kg N/100 kg N)	24.5
	34
AIR DATA	
X_Exc Air,Stoich Air x 100 (kmol Exc Air/100 kmol Stoich Air)	7.688994185
Air Properties	
X_N2,Air x 100 (kmol N2/100 kmol Air)	79
X_O2,Air x 100 (kmol O2/100 kmol Air)	21
	100
LIMESTONE DATA	
Limestone	Unknown
CSR (kmol LS CaCO3/kmol Vol SO2)	2.1
Limestone Particle Properties	
rho_LS CaCO3 (kg LS CaCO3/m^3 LS CaCO3)	2710
d_LS CaCO3 (m LS CaCO3)	0.00015
Y_LS H2O,LS x 100 (kg LS H2O/100 kg LS)	5
X_LS CaSO3,LS CaO x 100 (kmol LS CaSO3/100 kmol LS CaO)	17

Table 9

Continued.

OPERATIONAL DATA	
P_Mix (bar)	1
T_Mix (K)	1139.944444
RISER DATA	
a_CS,Riser (m^2 Riser)	125
h_Riser (m Riser)	36.6
CHEMICAL KINETICS DATA	
# of Chemical Kinetics Calculation Rows	5000
(1) NO + C -> 1/2 N2 + CO	
A_1 (1/s)	0.026
E_a,1 (kJ/kmol Mix NO)	132192.6
nu_Mix NO,1 (dimensionless)	1
(2) CO + 1/2 O2 -> CO2	
A_2 (m^3 Mix/(kmol*s))	1.3E+11
E_a,2 (kJ/kmol Mix CO)	125520
nu_Mix CO,2 (dimensionless)	1
nu_Mix O2,2 (dimensionless)	0.5
nu_Mix H2O,2 (dimensionless)	0.5
(3) NH3 + O2 -> NO + H2O + 1/2 H2	
A_3 (1/s)	3.48E+23
E_a,3 (kJ/kmol Mix NH3)	418400
nu_Mix NH3,3 (dimensionless)	1
nu_Mix O2,3 (dimensionless)	1
A_3,other (dimensionless)	0.0000069
E_a,3,other (kJ/kmol Mix NH3)	175728
nu_Mix O2,3,other (dimensionless)	1
(4) NH3 + NO -> N2 + H2O + 1/2 H2	
A_4 (1/s)	6.22E+17
E_a,4 (kJ/kmol Mix NH3)	230120
nu_Mix NH3,4 (dimensionless)	1
nu_Mix NO,4 (dimensionless)	1
(5) HCN + O2 -> NO + CO + 1/2 H2	
A_5 (1/s)	1E+11
E_a,5 (kJ/kmol Mix HCN)	280328
nu_Mix HCN,5 (dimensionless)	1
(6) HCN + NO -> N2 + CO + 1/2 H2	
A_6 (1/s)	3E+12
E_a,6 (kJ/kmol Mix HCN)	251040
nu_Mix HCN,6 (dimensionless)	1
nu_Mix NO,6 (dimensionless)	1
(7) 2 H2 + O2 -> 2 H2O	
A_7 (m^4.5 Mix/(kmol^1.5*K^1.5*s))	5.15451E+13
E_a,7 (kJ/kmol Mix O2)	28433.88
nu_Mix O2,7 (dimensionless)	1
nu_Mix H2,7 (dimensionless)	1.5
k_7 (dimensionless)	1.5

4.4 Outputs

The amount of each gaseous species CO, H_2O, O_2, N_2, NH_3, HCN, SO_2, CO_2, H_2, and NO exiting the CFB riser can be interpreted in many different ways. The proposed model displays a variety of the most common forms of species concentration evaluation.

4.4.1 Dry basis

The mole percent of each species exiting on a wet basis with respect to the actual percent O_2 in the exiting gas mixture ($X_{Mix\ i,Mix}x100$) is used to formulate the mole percent of each species exiting on a dry basis with respect to the actual percent O_2 in the exiting gas mixture ($X_{Mix\ i,Dry\ Mix}x100$) where the concentration of H_2O is set at zero as the description implies. The dry basis ensures that the variability in moisture based on the environment that the fuel came from or was stored in doesn't skew the emission results:

$$X_{Mix\ i,Dry\ Mix}x100 = \left(\frac{X_{Mix\ i,Mix}x100}{1-X_{Mix\ H_2O,Mix}}\right)_{i\neq H_2O} \quad (98)$$

The mole percent is typically reported for larger concentration species while the smaller/trace concentration species are normally reported in parts per million (ppm) [54]. The ppm of each species exiting on a dry basis with respect to the actual percent O_2 in the exiting gas mixture ($X_{Mix\ i,Dry\ Mix}x1{,}000{,}000$) is formulated in a similar manner to the dry basis mole percent except using the ppm of each species exiting on a wet basis with respect to the actual percent O_2 in the exiting gas mixture ($X_{Mix\ i,Mix}x1{,}000{,}000$):

$$X_{Mix\ i,Dry\ Mix}x1{,}000{,}000 = \left(\frac{X_{Mix\ i,Mix}x1{,}000{,}000}{1-X_{Mix\ H_2O,Mix}}\right)_{i\neq H_2O} \quad (99)$$

4.4.2 Standard percent O_2

Often times, the mole percent and ppm concentrations for both the wet basis and dry basis are corrected or normalized to a standard percent O_2 in the exiting gas mixture so that reported emissions can be compared more easily as actual percent O_2 can vary between different CFB combustor designs or even within the same CFB during operation [54] especially if the fuel was to be switched. This means that the O_2 mole percent or ppm is set at some selected value, and N_2 must be calculated from what is left over after the specified O_2 and the other eight species found from one of the below formulas [54] are added up:

$$\mathrm{X}_{Mix\ i,Mix,std}x100 = \left[\left(\frac{\frac{\mathrm{X}_{O_2,Air}x100}{100}-\mathrm{X}_{Mix\ O_2,Mix,std}}{\frac{\mathrm{X}_{O_2,Air}x100}{100}-\mathrm{X}_{Mix\ O_2,Mix}}\right)*\mathrm{X}_{Mix\ i,Mix}x100\right]_{i\neq O_2,N_2} \quad (100)$$

$$\mathrm{X}_{Mix\ i,Dry\ Mix,std}x100 = \left[\left(\frac{\frac{\mathrm{X}_{O_2,Air}x100}{100}-\mathrm{X}_{Mix\ O_2,Mix,std}}{\frac{\mathrm{X}_{O_2,Air}x100}{100}-\mathrm{X}_{Mix\ O_2,Dry\ Mix}}\right)*\mathrm{X}_{Mix\ i,Dry\ Mix}x100\right]_{i\neq O_2,N_2} \quad (101)$$

$$\mathrm{X}_{Mix\ i,Mix,std}x1{,}000{,}000 = \left[\left(\frac{\frac{\mathrm{X}_{O_2,Air}x100}{100}-\mathrm{X}_{Mix\ O_2,Mix,std}}{\frac{\mathrm{X}_{O_2,Air}x100}{100}-\mathrm{X}_{Mix\ O_2,Mix}}\right)*\mathrm{X}_{Mix\ i,Mix}x1{,}000{,}000\right]_{i\neq O_2,N_2} \quad (102)$$

$$\mathrm{X}_{Mix\ i,Dry\ Mix,std}x1{,}000{,}000 =$$

$$\left[\left(\frac{\frac{\mathrm{X}_{O_2,Air}x100}{100}-\mathrm{X}_{Mix\ O_2,Mix,std}}{\frac{\mathrm{X}_{O_2,Air}x100}{100}-\mathrm{X}_{Mix\ O_2,Dry\ Mix}}\right)*\mathrm{X}_{Mix\ i,Dry\ Mix}x1{,}000{,}000\right]_{i\neq O_2,N_2} \quad (103)$$

4.4.3 Grams of species emitted per gigajoule

Lastly, another form of correction or normalization for both the wet basis ($\frac{g_{Mix\ i,Mix}}{GJ_{Fuel}}$) and dry basis ($\frac{g_{Mix\ i,Dry\ Mix}}{GJ_{Fuel}}$) is the grams of species emitted per gigajoule produced by completely combusting one kilogram of fuel [54]. However, the molar mass of NO_2 is normally used for the molar mass of NO because NO is eventually converted to NO_2 in the atmosphere:

$$\frac{g_{Mix\ i,Mix}}{GJ_{Fuel}} = \frac{1{,}000*\left(\frac{Y_{C,Fuel}x100}{100}\right)*X_{Mix\ i,Mix}*\overline{m}_{Mix\ i}}{\left(X_{Mix\ CO_2,Mix}+X_{Mix\ CO,Mix}\right)*12.01*\left(\frac{hhv_{Fuel}}{1{,}000{,}000}\right)} \tag{104}$$

$$\frac{g_{Mix\ i,Dry\ Mix}}{GJ_{Fuel}} = \frac{1{,}000*\left(\frac{Y_{C,Fuel}x100}{100}\right)*X_{Mix\ i,Dry\ Mix}*\overline{m}_{Mix\ i}}{\left(X_{Mix\ CO_2,Dry\ Mix}+X_{Mix\ CO,Dry\ Mix}\right)*12.01*\left(\frac{hhv_{Fuel}}{1{,}000{,}000}\right)} \tag{105}$$

The 'Output' tab of the Excel program is shown below in Table 10. The red cells indicate the output cells for each species' concentration in the gaseous mixture leaving the CFB riser in each form of emissions reporting discussed above while the yellow cell indicates the cell that can be changed by the user of the Excel program to a desired standard percent O_2 for correction/normalization purposes.

Table 10

Output tab for anonymous CFB boiler firing lignite fuel.

WET BASIS CONCENTRATION OF SPECIES IN MIXTURE OF GASES LEAVING CFB RISER										
	CO	H2O	O2	N2	NH3	HCN	SO2	CO2	H2	NO
ppm (Actual % O2)	0.040373401	158467.0758	13633.15811	676744.0055	130.426466	566.5980334	1591.308718	148865.1704	0.004903618	2.211675493
Mole % (Actual % O2)	4.03734E-06	15.84670758	1.363315811	67.67440055	0.013042647	0.056659803	0.159130872	14.88651704	4.90362E-07	0.000221168
ppm (Standard % O2)	0.037008347	145259.1149	30000	686183.6998	119.5556421	519.3730522	1458.675846	136457.512	0.00449491	2.027336107
Mole % (Standard % O2)	3.70083E-06	14.52591149	3	F7/10000	0.011955564	0.051937305	0.145867585	13.6457512	4.49491E-07	0.000202734
g/GJ	0.018828025	47532.83861	7263.44719	315710.3953	36.98952065	254.9677824	1697.483258	109078.9129	0.00016459	1.694220656

DRY BASIS CONCENTRATION OF SPECIES IN MIXTURE OF GASES LEAVING CFB RISER										
	CO	H2O	O2	N2	NH3	HCN	SO2	CO2	H2	NO
ppm (Actual % O2)	0.04797602	0	16200.38589	804180.0695	154.9867655	673.2927698	1890.964301	176897.6188	0.005827007	2.628150877
Mole % (Actual % O2)	4.7976E-06	0	1.620038589	80.41800695	0.015498677	0.067329277	0.18909643	17.68976188	5.82701E-07	0.000262815
ppm (Standard % O2)	0.04455986	0	30000	803170.3694	143.9508428	625.350567	1756.31709	164301.5211	0.005412091	2.441011867
Mole % (Standard % O2)	4.45599E-06	0	3	F16/10000	0.014395084	0.062535057	0.175631709	16.43015211	5.41209E-07	0.000244101
g/GJ	0.018828025	0	7263.44719	315710.3953	36.98952065	254.9677824	1697.483258	109078.9129	0.00016459	1.694220656

5. RESULTS AND DISCUSSION

5.1 Model Validation

The proposed model was validated against two combustors to demonstrate the limitations of the model and corresponding Excel program.

5.1.1 Validation against anonymous CFB boiler

The first combustor that the model was validated against is an industrial scale CFB boiler with data provided by a company who wishes to remain anonymous. This CFB boiler is using lignite coal as the fuel and secondary air is injected above the combustor bed with inputs as seen earlier in Table 9. Almost all of the fuel, air, limestone, operational, and riser data were provided as requested. The only exceptions were the $d_{Fuel,0}$, $Y_{VN,N}x100$, $Y_{N_2,N}x100$, $Y_{NH_3,N}x100$, $Y_{HCN,N}x100$, and $X_{LS\ CaSO_3,LS\ CaO}x100$.

The $d_{Fuel,0}$ was calculated by performing a sieve analysis on a sample of the lignite provided by the company to determine the mass fraction in each particle size range. The $Y_{VN,N}x100$, $Y_{N_2,N}x100$, $Y_{NH_3,N}x100$, and $Y_{HCN,N}x100$ were all obtained by utilizing Kambara's coal data as described in the literature review earlier. It was determined that the coal in Table 5 that best matches the company's lignite based on the proximate and ultimate analyses comparison is coal 'R'. With a pyrolysis temperature near 1,000 K, Fig. 5, Fig. 6, and Fig. 7 were used in conjunction with coal 'R' to determine the desired values. The $X_{LS\ CaSO_3,LS\ CaO}x100$ was determined by manipulating the value until the company provided emission of 1600 ppm of SO_2 (wet basis and

uncorrected) at the cyclone inlet was obtained (this manipulation has little effect on the other concentration values due to Sulfur not being directly involved with any other chemical reactions).

The number of chemical kinetics calculation rows in the Excel program were chosen to be 5,000 which means the Δt is about 0.0007 seconds since the $V_{Bed\ Mix}$ is almost 10 meters per second meaning the $t_{Res,Bed\ Mix}$ is about 3.7 seconds with the given inputs. The $V_{Bed\ Mix}$ being 10 meters per second is also a strong indication of a circulating bed especially with such a low SMD. Other intermediate calculations can be viewed as described in detail earlier in the 'Bed' (Table 8) and 'Riser' tabs of the Excel program.

Also, the graph of the mole fraction of species in the mixture of gases versus time after the mixture of gases leaves the CFB bed until they reach the CFB riser exit for all species in Fig. 21 and trace species in Fig. 22 were shown previously with little variation except for at the bottom of the riser where O_2 is most abundant since the key reactions of combustion require O_2. The most notable trends are the CO drastically decreasing to almost nonexistent immediately due to the quick kinetics of CO oxidation, the O_2 also rapidly decreasing near the bottom of the riser with the many O_2 consuming reactions, and the CO_2 closely matching the O_2 trend but increasing due to the main reaction being the oxidation of the fixed Carbon in the char.

When no chemical kinetics data are modified, the 'Output' tab (Table 10) of the Excel program described in detail earlier is the result. However, the company was not able to provide the concentration of CO, NH_3, HCN, and H_2 at the cyclone inlet/riser

exit, but commented that most of these concentrations should be almost nonexistent at this location. All of the other desired species' concentrations were given by the company on an uncorrected wet basis in mole percent for dominant species (H_2O, O_2, N_2, and CO_2) and ppm for trace species (SO_2 and NO).

The company provided H_2O concentration is 13.01% compared to the model predicted 15.85% which is about a 22% difference. This difference may be due to the proximate analysis of the fuel and measurement of moisture in the limestone being performed at a different time than the emission concentration measurement so that the fuel and limestone may be more dry/evaporated due to their storage environment. There may also be some difference due to the neglected recirculated particles that had already released moisture in the initial pass and now only have burning char remaining. The company provided O_2 concentration of 1.5% is very close to the model predicted 1.4% being off less than 7%. This difference is acceptable and may be attributed to slight variations in chemical kinetics data or deviation in supplied combustion air. The company provided N_2 concentration of 71.48% is even closer to the model predicted 67.67% which is only a 5% difference. This difference is also acceptable and may be attributed to slight variations in chemical kinetics data especially that of the many complex nitrogenous reactions and assumptions or perhaps deviation in supplied combustion air. The company provided CO_2 concentration of 13.9% is similarly close to the model predicted 14.9% being off about 7%. This difference should come as no surprise since the O_2 concentration is closely tied to the CO_2 concentration due to the

fact that CO_2 is the main product of combustion; and therefore, the main consumer of O_2.

As for the trace species, the company provided SO_2 concentration is 1600 ppm which is very high for a CFB boiler with limestone, but this is no surprise since there is also a scrubber downstream of the boiler that further reduces the SO_2 concentration to below regulatory statutes. The use of the scrubber downstream rather than more limestone inside the combustor seems to be due to economics and perhaps the retrofitting of the unit from a scrubber initially to now some limestone to reduce the SO_2 to the appropriate levels. Either way with a CSR of 2.1 in the combustor and still having a 1600 ppm emission of SO_2 means that the $X_{LS\ CaSO_3,LS\ CaO}x100$ is only about 17% which leads to less than 36% SO_2 capture in the combustor. Using a more reactive limestone with a $X_{LS\ CaSO_3,LS\ CaO}x100$ of around 43% is fairly common and at the same CSR of 2.1 could lead to over 90% SO_2 capture in the combustor so that only 240 ppm is at the cyclone inlet/riser exit. This also means that a scrubber would no longer be necessary because the SO_2 concentration is about 256 g SO_2/GJ which is less than the US EPA regulation of 260 g SO_2/GJ (at least 70% SO_2 removal). However, cost of taking the scrubber out of service and the cost of a higher quality limestone may not be worth it. Another way to achieve the lower combustor SO_2 concentration is to increase the current limestone CSR to about 5.5, but this is an unusually large increase in limestone which obviously more than doubles the limestone loading and unloading.

The company provided NO concentration is 30 ppm compared to the model predicted 2 ppm which is the worst difference of about 93%. This difference along with

the NH_3 and HCN concentrations predicted by the model being far from nonexistent is likely due to the chemical kinetics of the reactions $NO\ (g)\ +\ C\ (s)\ \rightarrow \frac{1}{2}\ N_2\ (g)\ +\ CO\ (g)$ and $HCN\ (g)\ +\ O_2\ (g)\ \rightarrow$ NO (g) $+\ CO$ (g) $+\ \frac{1}{2}\ H_2\ (g)$ which also seem to have the greatest variation in the literature review. Therefore, the pre-exponential factor of the first reaction was changed from 0.026 to 0.00026 (a factor of 100) and the second reaction was changed from 10^{11} to 10^{14} (a factor of 1,000).

The new graph of the mole fraction of species in the mixture of gases versus time after the mixture of gases leaves the CFB bed until they reach the CFB riser exit for all species in Fig. 23 and trace species in Fig. 24 with the modified chemical kinetics for only these two reactions are shown below with minimal effects on the concentration of species other than NH_3, HCN, and NO. The NH_3 and HCN concentrations now both decrease very rapidly with the higher oxidation rate of HCN as well as the much greater amount of NO available to react with since the NO is being produced more quickly than it is being reduced on the surface of the char while in the more O_2 rich bottom portion of the riser. However, the NO concentration then peaks and begins to decline as the O_2 continues to decrease so that the remaining char more effectively reduces the NO.

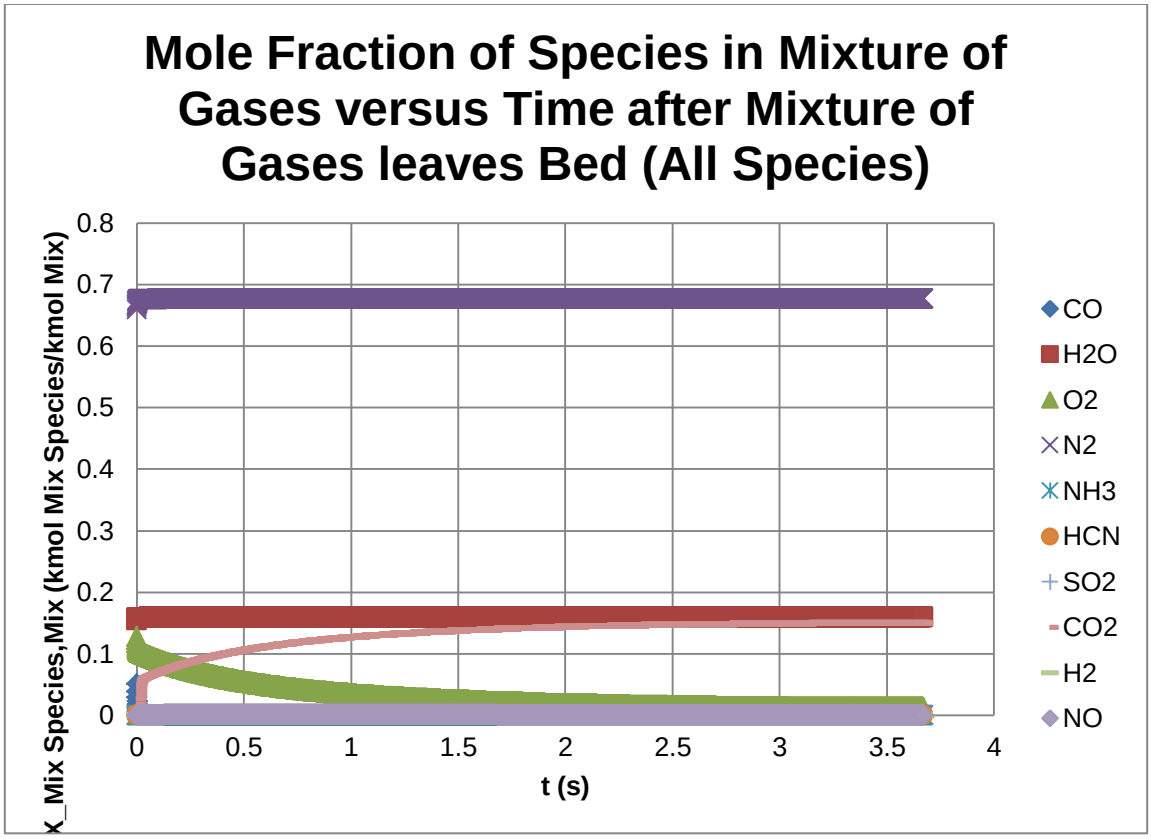

Fig. 23. Mole fraction of all species versus time for anonymous CFB boiler firing lignite fuel with modified kinetics.

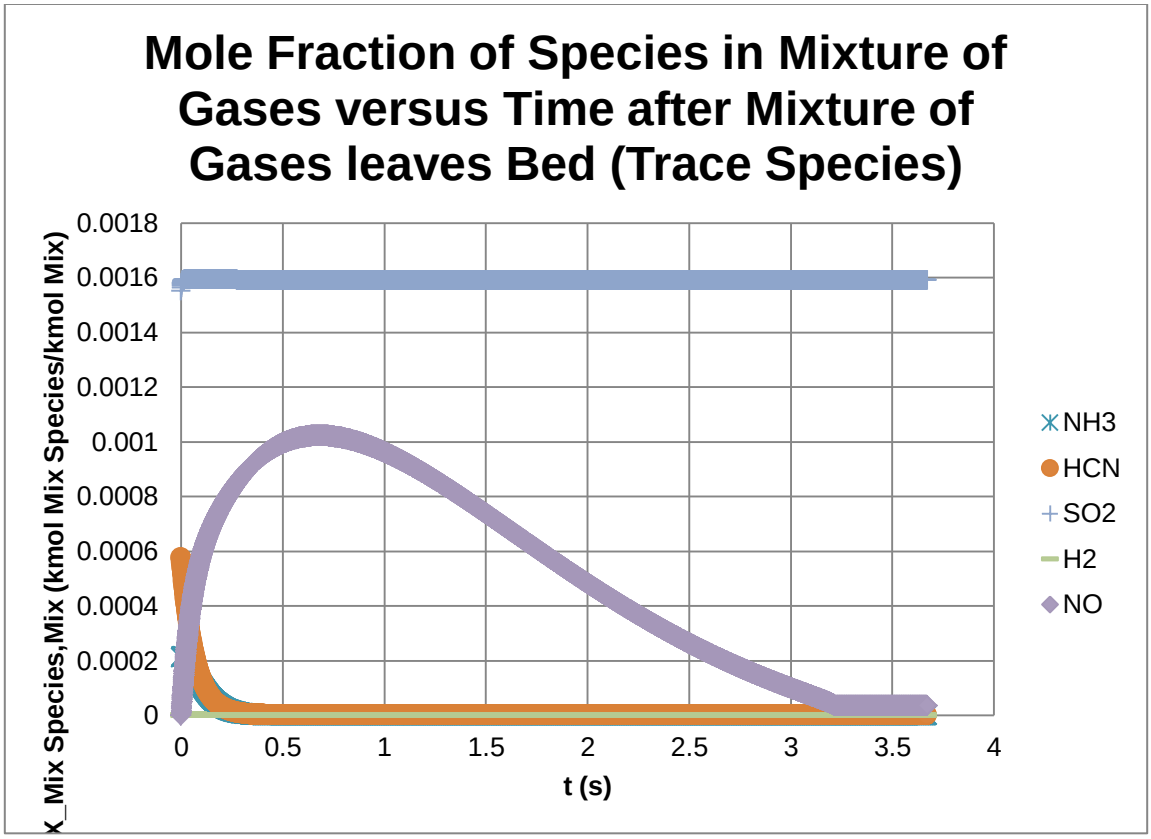

Fig. 24. Mole fraction of trace species versus time for anonymous CFB boiler firing lignite fuel with modified kinetics.

The new 'Output' tab of the Excel program with the modified chemical kinetics for only these two reactions is shown below in Table 11.

Table 11

Output tab for anonymous CFB boiler firing lignite fuel with modified kinetics.

WET BASIS CONCENTRATION OF SPECIES IN MIXTURE OF GASES LEAVING CFB RISER										
	CO	H2O	O2	N2	NH3	HCN	SO2	CO2	H2	NO
ppm (Actual % O2)	6.24101E-17	158963.3569	12812.43767	677150.3437	1.22302E-13	8.69531E-16	1591.482294	149448.1085	6.46584E-16	34.27102115
Mole % (Actual % O2)	6.24101E-21	15.89633569	1.281243767	67.71503437	1.22302E-17	8.69531E-20	0.159148229	14.94481085	6.46584E-20	0.003427102
ppm (Standard % O2)	5.69702E-17	145107.5509	30000	686986.7171	1.11642E-13	7.9374E-16	1452.763093	136421.6851	5.90225E-16	31.28383826
Mole % (Standard % O2)	5.69702E-21	14.51075509	3	F7/10000	1.11642E-17	7.9374E-20	0.145276309	13.64216851	5.90225E-20	0.003128384
g/GJ	2.89913E-17	47495.72552	6799.560959	314667.8421	3.45502E-14	3.89761E-16	1691.04694	109078.9425	2.16179E-17	26.15040419

DRY BASIS CONCENTRATION OF SPECIES IN MIXTURE OF GASES LEAVING CFB RISER										
	CO	H2O	O2	N2	NH3	HCN	SO2	CO2	H2	NO
ppm (Actual % O2)	7.42062E-17	0	15234.1016	805137.7419	1.45419E-13	1.03388E-15	1892.28651	177695.1215	7.68794E-16	40.74854696
Mole % (Actual % O2)	7.42062E-21	0	1.52341016	80.51377419	1.45419E-17	1.03388E-19	0.189228651	17.76951215	7.68794E-20	0.004074855
ppm (Standard % O2)	6.85803E-17	0	30000	803990.0956	1.34394E-13	9.55498E-16	1748.825511	164223.4197	7.10509E-16	37.65925407
Mole % (Standard % O2)	6.85803E-21	0	3	F16/10000	1.34394E-17	9.55498E-20	0.174882551	16.42234197	7.10509E-20	0.003765925
g/GJ	2.89913E-17	0	6799.560959	314667.8421	3.45502E-14	3.89761E-16	1691.04694	109078.9425	2.16179E-17	26.15040419

As can be seen, the concentration of CO, NH_3, HCN, and H_2 at the cyclone inlet/riser exit are now all practically nonexistent while the dominant species changed only slightly (except for O_2 which decreased more due to the drastically increased oxidation rate of HCN causing the predicted value of O_2 to be closer to 13% different than the company reported). In addition, the NO concentration is now estimated by the model to be about 34 ppm which is only a 13% difference from the company reported 30 ppm. With fine tuning of the chemical kinetics, the precise concentrations that the company has reported could possibly be obtained.

5.1.2 Validation against Babcock and Wilcox BFB boiler

The second combustor that the model was validated against is a pilot/laboratory scale once-through (non-circulating) boiler as seen below in Fig. 25 with its much smaller dimensions and throughput with data measurements by Babcock and Wilcox (test number 26) and presented in modeling articles by de Souza-Santos [36,40].

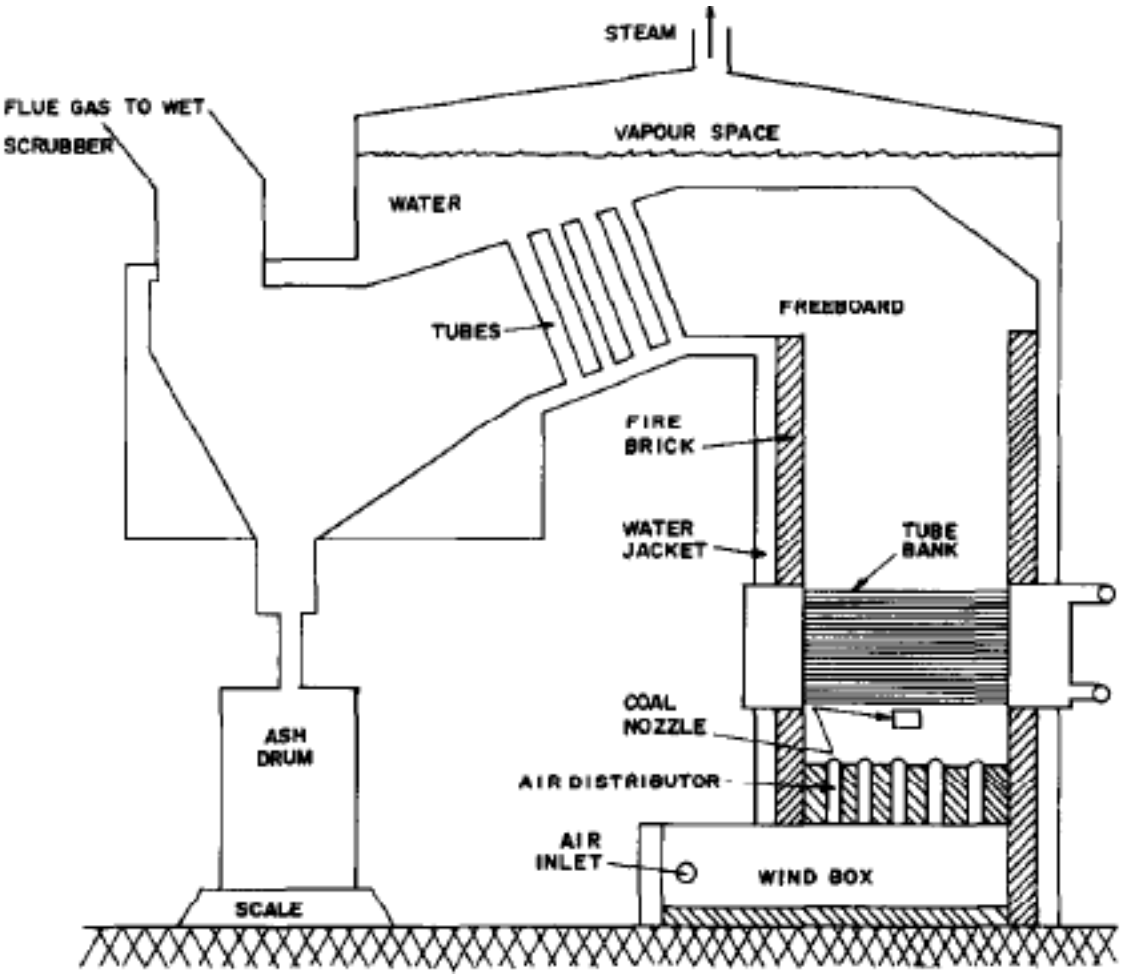

Fig. 25. Schematic of Babcock and Wilcox test unit [40].

This boiler uses a subbituminous coal as the fuel with inputs as seen in the 'Input' tab of the Excel program below in Table 12.

Table 12

Input tab for Babcock and Wilcox BFB boiler.

FUEL DATA	
Fuel	Subbituminous Coal
mdot_Fuel (kg Fuel/s)	0.0585
Fuel/Char Particle Properties	
rho_Fuel (kg Fuel/m^3 Fuel)	1400
d_Fuel,0 (m Fuel)	0.000421698
hhv_Fuel (kJ/kg Fuel)	29601.00725
	As Received (AR) Fuel
Proximate-equiv Fuel Analysis	
Y_VM,Fuel x 100 (kg VM/100 kg Fuel)	38
Y_FC,Fuel x 100 (kg FC/100 kg Fuel)	47.595
	85.595
Y_H2O,Fuel x 100 (kg H2O/100 kg Fuel)	5
Y_Ash,Fuel x 100 (kg Ash/100 kg Fuel)	9.405
	100
Ultimate/Elemental Fuel Analysis	
Y_C,Fuel x 100 (kg C/100 kg Fuel)	69.54
Y_H,Fuel x 100 (kg H/100 kg Fuel)	4.845
Y_O,Fuel x 100 (kg O/100 kg Fuel)	7.505
Y_N,Fuel x 100 (kg N/100 kg Fuel)	0.855
Y_S,Fuel x 100 (kg S/100 kg Fuel)	2.85
	85.595
Nitrogen Release from Fuel as Volatile Matter & Split into N2, NH3, HCN	
Y_VN,N x 100 (kg VN/100 kg N)	6
Y_N2,N x 100 (kg N2/100 kg N)	0
Y_NH3,N x 100 (kg N/100 kg N)	2.5
Y_HCN,N x 100 (kg N/100 kg N)	3.5
	6
AIR DATA	
X_Exc Air,Stoich Air x 100 (kmol Exc Air/100 kmol Stoich Air)	26.32629259
Air Properties	
X_N2,Air x 100 (kmol N2/100 kmol Air)	79
X_O2,Air x 100 (kmol O2/100 kmol Air)	21
	100
LIMESTONE DATA	
Limestone	Unknown
CSR (kmol LS CaCO3/kmol Vol SO2)	2.2
Limestone Particle Properties	
rho_LS CaCO3 (kg LS CaCO3/m^3 LS CaCO3)	2710
d_LS CaCO3 (m LS CaCO3)	0.000751644
Y_LS H2O,LS x 100 (kg LS H2O/100 kg LS)	0.4
X_LS CaSO3,LS CaO x 100 (kmol LS CaSO3/100 kmol LS CaO)	28.09

Table 12

Continued.

OPERATIONAL DATA	
P_Mix (bar)	1.013
T_Mix (K)	955
RISER DATA	
a_CS,Riser (m^2 Riser)	0.981688014
h_Riser (m Riser)	3.137
CHEMICAL KINETICS DATA	
# of Chemical Kinetics Calculation Rows	5000
(1) NO + C -> 1/2 N2 + CO	
A_1 (1/s)	0.026
E_a,1 (kJ/kmol Mix NO)	132192.6
nu_Mix NO,1 (dimensionless)	1
(2) CO + 1/2 O2 -> CO2	
A_2 (m^3 Mix/(kmol*s))	1.3E+11
E_a,2 (kJ/kmol Mix CO)	125520
nu_Mix CO,2 (dimensionless)	1
nu_Mix O2,2 (dimensionless)	0.5
nu_Mix H2O,2 (dimensionless)	0.5
(3) NH3 + O2 -> NO + H2O + 1/2 H2	
A_3 (1/s)	3.48E+23
E_a,3 (kJ/kmol Mix NH3)	418400
nu_Mix NH3,3 (dimensionless)	1
nu_Mix O2,3 (dimensionless)	1
A_3,other (dimensionless)	0.0000069
E_a,3,other (kJ/kmol Mix NH3)	175728
nu_Mix O2,3,other (dimensionless)	1
(4) NH3 + NO -> N2 + H2O + 1/2 H2	
A_4 (1/s)	6.22E+17
E_a,4 (kJ/kmol Mix NH3)	230120
nu_Mix NH3,4 (dimensionless)	1
nu_Mix NO,4 (dimensionless)	1
(5) HCN + O2 -> NO + CO + 1/2 H2	
A_5 (1/s)	1E+11
E_a,5 (kJ/kmol Mix HCN)	280328
nu_Mix HCN,5 (dimensionless)	1
(6) HCN + NO -> N2 + CO + 1/2 H2	
A_6 (1/s)	3E+12
E_a,6 (kJ/kmol Mix HCN)	251040
nu_Mix HCN,6 (dimensionless)	1
nu_Mix NO,6 (dimensionless)	1
(7) 2 H2 + O2 -> 2 H2O	
A_7 (m^4.5 Mix/(kmol^1.5*K^1.5*s))	5.15451E+13
E_a,7 (kJ/kmol Mix O2)	28433.88
nu_Mix O2,7 (dimensionless)	1
nu_Mix H2,7 (dimensionless)	1.5
k_7 (dimensionless)	1.5

This unit was chosen due to the abundance of key parameters required for simulation purposes and comparison as well as most of the desired species' concentrations. Unlike most articles, almost all of the fuel, air, limestone, operational, and riser data are available directly. The only exceptions are the $d_{Fuel,0}$, hhv_{Fuel}, $Y_{VN,N}x100$, $Y_{N_2,N}x100$, $Y_{NH_3,N}x100$, $Y_{HCN,N}x100$, $X_{Exc\ Air,Stoich\ Air}x100$, $d_{LS\ CaCO_3}$, T_{Mix}, and h_{Riser}.

Both the $d_{Fuel,0}$ and $d_{LS\ CaCO_3}$ were calculated by performing the SMD calculation on each of the respective supplied particle size distributions. The hhv_{Fuel} was estimated using the Boie equation. The $Y_{VN,N}x100$, $Y_{N_2,N}x100$, $Y_{NH_3,N}x100$, and $Y_{HCN,N}x100$ were all obtained by utilizing Kambara's coal data as described in the literature review earlier. It was determined that the coal in Table 5 that best matches the subbituminous coal based on the proximate and ultimate analyses comparison is coal 'L'. With a pyrolysis temperature near 850 K, Fig. 5, Fig. 6, and Fig. 7 were used in conjunction with coal 'L' to determine the desired values. The $X_{Exc\ Air,Stoich\ Air}x100$ was determined by computing the stoichiometric air required and comparing it to the actual air provided to the combustor. The T_{Mix} was taken as the average of the average temperature at bed top and average temperature at freeboard top. The h_{Riser} was derived from the difference between the freeboard height and the fuel and limestone feeding position.

The number of chemical kinetics calculation rows in the Excel program were chosen to stay at 5,000 which means the Δt is about 0.0003 seconds since the $V_{Bed\ Mix}$ is only 2.1 meters per second meaning the $t_{Res,Bed\ Mix}$ is only about 1.5 seconds with the

given inputs. The $V_{Bed\ Mix}$ being 2.1 meters per second is also a strong indication of a bubbling fluidized bed (BFB) especially with the computed particles' SMD. Compared to the measured value of 2.5 meters per second, the predicted $V_{Bed\ Mix}$ is only off by about 16% which is not a bad estimation considering that it is estimated based on initial values of the mixture of gases leaving the bed as well as an effective cross-sectional area assuming that the particles are small enough to immediately begin moving upwards upon entering the combustor. This is especially true due to the fact that the measurement of 2.5 meters per second was likely taken in the dense bed region as pointed out by de Souza-Santos [40]. Since this is a BFB boiler, there is more of a visual bed at the base of the combustor due to the low $V_{Bed\ Mix}$ and relatively large $d_{Fuel,0}$. This means that there are some particles that will just hover or even sink closer to the distributor upon entry into the combustor which is contrary to what is assumed in the proposed model described earlier. This is likely the largest contributor to the increase in actual from predicted $V_{Bed\ Mix}$ due to a more dense bed than predicted so that a smaller effective cross-sectional area of the combustor is available for the gas mixture to move through. Other intermediate calculations can be viewed in the 'Bed' tab of the Excel program below in Table 13.

Table 13

Bed tab for Babcock and Wilcox BFB boiler.

Fuel Entering CFB Bed	
a'_CS,Fuel,0 (m^2 Fuel/Fuel Particle)	1.39667E-07
N_H2O,Fuel x 100 (kmol H2O/100 kg Fuel)	0.277531083
Ultimate/Elemental Fuel Analysis (Mole Basis)	
N_C,Fuel x 100 (kmol C/100 kg Fuel)	5.790174854
N_H,Fuel x 100 (kmol H/100 kg Fuel)	4.806547619
N_O,Fuel x 100 (kmol O/100 kg Fuel)	0.4690625
N_N,Fuel x 100 (kmol N/100 kg Fuel)	0.061027837
N_S,Fuel x 100 (kmol S/100 kg Fuel)	0.088868101
Carbon & Nitrogen Retained in Fuel as Fixed Carbon	
N_FC,Fuel x 100 (kmol FC/100 kg Fuel)	3.89602831
N_FN,Fuel x 100 (kmol FN/100 kg Fuel)	0.057366167
	47.595
Y_FC,FC x 100 (kg FC/100 kg FC)	98.31137725
Y_FN,FC x 100 (kg FN/100 kg FC)	1.688622754
FCR (kg FN/kg FC)	0.01717627
Carbon, Hydrogen, Oxygen, Nitrogen, Sulfur Release from Fuel as Volatile Matter	
N_VC,Fuel x 100 (kmol VC/100 kg Fuel)	1.894146545
N_VH,Fuel x 100 (kmol VH/100 kg Fuel)	4.806547619
N_VO,Fuel x 100 (kmol VO/100 kg Fuel)	0.4690625
N_VN,Fuel x 100 (kmol VN/100 kg Fuel)	0.00366167
N_VS,Fuel x 100 (kmol VS/100 kg Fuel)	0.088868101
	38
Nitrogen Release from Fuel as Volatile Matter & Split into N2, NH3, HCN	
N_N2,Fuel x 100 (kmol N2/100 kg Fuel)	0
N_NH3,Fuel x 100 (kmol N/100 kg Fuel)	0.001525696
N_HCN,Fuel x 100 (kmol N/100 kg Fuel)	0.002135974
	0.00366167
Air Entering CFB Bed	
N_Stoich O2,Fuel x 100 (kmol Stoich O2/100 kg Fuel)	6.84614861
SR (dimensionless)	1.263262926
	0.791600845
N_Act O2,Fuel x 100 (kmol Act O2/100 kg Fuel)	8.648485724
N_Act N2,Fuel x 100 (kmol Act N2/100 kg Fuel)	32.53477963
	41.18326535
m_Stoich Air,Fuel x 100 (kg Stoich Air/100 kg Fuel)	940.7195003
Volatile Combustion	
N_Vol CO,Fuel x 100 (kmol Vol CO/100 kg Fuel)	1.89201057
N_Vol H2O,Fuel x 100 (kmol Vol H2O/100 kg Fuel)	2.399917278
N_Vol O2,Fuel x 100 (kmol Vol O2/100 kg Fuel)	6.648184949
N_Vol N2,Fuel x 100 (kmol Vol N2/100 kg Fuel)	32.53477963
N_Vol NH3,Fuel x 100 (kmol Vol NH3/100 kg Fuel)	0.001525696
N_Vol HCN,Fuel x 100 (kmol Vol HCN/100 kg Fuel)	0.002135974
N_Vol SO2,Fuel x 100 (kmol Vol SO2/100 kg Fuel)	0.088868101
Limestone Reactions	
a'_CS,LS CaCO3 (m^2 LS CaCO3/LS CaCO3 Particle)	4.43726E-07
Y_LS,Fuel x 100 (kg LS/100 kg Fuel)	19.64716678
N_LS H2O,Fuel x 100 (kmol LS H2O/100 kg Fuel)	0.00436216
N_LS CaCO3,Fuel x 100 (kmol LS CaCO3/100 kg Fuel)	0.195509822
N_LS CO2,Fuel x 100 (kmol LS CO2/100 kg Fuel)	0.195509822
N_LS CaO,Fuel x 100 (kmol LS CaO/100 kg Fuel)	0.195509822
N_LS CaSO3,Fuel x 100 (kmol LS CaSO3/100 kg Fuel)	0.054918709
	0.140591113
	61.798

Table 13

Continued.

Gaseous Species leaving CFB Bed	
mdot Act Air (kg Act Air/s)	0.6952
mdot VL (kg VL/s)	0.005079541
mdot VF (kg VF/s)	0.023096595
mdot Bed Mix (kg Bed Mix/s)	0.723376136
N Bed CO,Fuel x 100 (kmol Bed CO/100 kg Fuel)	1.89201057
N Bed H2O,Fuel x 100 (kmol Bed H2O/100 kg Fuel)	2.681810522
N Bed O2,Fuel x 100 (kmol Bed O2/100 kg Fuel)	6.648184949
N Bed N2,Fuel x 100 (kmol Bed N2/100 kg Fuel)	32.53477963
N_Bed NH3,Fuel x 100 (kmol Bed NH3/100 kg Fuel)	0.001525696
N_Bed HCN,Fuel x 100 (kmol Bed HCN/100 kg Fuel)	0.002135974
N_Bed SO2,Fuel x 100 (kmol Bed SO2/100 kg Fuel)	0.033949392
N_Bed CO2,Fuel x 100 (kmol Bed CO2/100 kg Fuel)	0.195509822
N_Bed Mix,Fuel x 100 (kmol Bed Mix/100 kg Fuel)	43.98990655
X_Bed CO,Bed Mix x 100 (kmol Bed CO/100 kmol Bed Mix)	4.30101066
X_Bed H2O,Bed Mix x 100 (kmol Bed H2O/100 kmol Bed Mix)	6.096422411
X Bed O2,Bed Mix x 100 (kmol Bed O2/100 kmol Bed Mix)	15.11297811
X Bed N2,Bed Mix x 100 (kmol Bed N2/100 kmol Bed Mix)	73.95964706
X Bed NH3,Bed Mix x 100 (kmol Bed NH3/100 kmol Bed Mix)	0.003468286
X Bed HCN,Bed Mix x 100 (kmol Bed HCN/100 kmol Bed Mix)	0.004855601
X Bed SO2,Bed Mix x 100 (kmol Bed SO2/100 kmol Bed Mix)	0.077175413
X Bed CO2,Bed Mix x 100 (kmol Bed CO2/100 kmol Bed Mix)	0.444442459
	100
N''' Mix (kmol Mix/m^3 Mix)	0.012758395
N'''_Bed CO (kmol Bed CO/m^3 Bed Mix)	0.00054874
N'''_Bed H2O (kmol Bed H2O/m^3 Bed Mix)	0.000777806
N'''_Bed O2 (kmol Bed O2/m^3 Bed Mix)	0.001928173
N'''_Bed N2 (kmol Bed N2/m^3 Bed Mix)	0.009436064
N'''_Bed NH3 (kmol Bed NH3/m^3 Bed Mix)	4.42498E-07
N'''_Bed HCN (kmol Bed HCN/m^3 Bed Mix)	6.19497E-07
N'''_Bed SO2 (kmol Bed SO2/m^3 Bed Mix)	9.84634E-06
N'''_Bed CO2 (kmol Bed CO2/m^3 Bed Mix)	5.67037E-05
	0.012758395
m Bed CO,Fuel x 100 (kg Bed CO/100 kg Fuel)	52.99521607
m Bed H2O,Fuel x 100 (kg Bed H2O/100 kg Fuel)	48.31549836
m Bed O2,Fuel x 100 (kg Bed O2/100 kg Fuel)	212.7419184
m Bed N2,Fuel x 100 (kg Bed N2/100 kg Fuel)	911.6245252
m Bed NH3,Fuel x 100 (kg Bed NH3/100 kg Fuel)	0.025988704
m Bed HCN,Fuel x 100 (kg Bed HCN/100 kg Fuel)	0.057731113
m Bed SO2,Fuel x 100 (kg Bed SO2/100 kg Fuel)	2.175137543
m_Bed CO2,Fuel x 100 (kg Bed CO2/100 kg Fuel)	8.604387278
m_Bed Mix,Fuel x 100 (kg Bed Mix/100 kg Fuel)	1236.540403
mbar_Bed Mix (kg Bed Mix/kmol Bed Mix)	28.10963922
rho_Bed Mix (kg Bed Mix/m^3 Bed Mix)	0.358633889
Solid Species leaving CFB Bed	
m'''_Fuel,Bed Mix (kg Fuel/m^3 Bed Mix)	0.029003006
m'''_Char,Bed Mix (kg Char/m^3 Bed Mix)	0.016531713
m''' Char,Fuel (kg Char/m^3 Fuel)	798
m''' FC,Fuel (kg FC/m^3 Fuel)	655.0782
m' Char,0 (kg Char/Char Particle)	3.13333E-08
m' FC,0 (kg FC/FC Particle)	2.57215E-08
CCR (kg Char/kg FC)	1.218175174
	4.41799E-10
n''' Char,Bed Mix (Char Particles/m^3 Bed Mix)	527608.8128
m'''_LS CaCO3,Bed Mix (kg LS CaCO3/m^3 Bed Mix)	0.005675476
m'_LS CaCO3 (kg LS CaCO3/LS CaCO3 Particle)	6.02566E-07
n'''_LS CaCO3,Bed Mix (LS CaCO3 Particles/m^3 Bed Mix)	9418.843569
a_CS,Fuel,0 (m^2 Fuel)	6.10112E-05
a_CS,LS CaCO3 (m^2 LS CaCO3)	6.16776E-06
a CS,Riser,Eff (m^2 Eff Riser)	0.981620835
V Bed Mix (m Riser/s)	2.054797762
t Res,Bed Mix (s)	1.526670925
delta t (s)	0.000305334

Table 13

Continued.

Gas Properties	
mu_CO (kg CO/(m CO*s))	3.91428E-05
mu_H2O (kg H2O/(m H2O*s))	3.4118E-05
mu_O2 (kg O2/(m O2*s))	4.65499E-05
mu_N2 (kg N2/(m N2*s))	3.78875E-05
mu_NH3 (kg NH3/(m NH3*s))	3.22139E-05
mu_HCN (kg HCN/(m HCN*s))	2.57034E-05
mu_SO2 (kg SO2/(m SO2*s))	3.70909E-05
mu_CO2 (kg CO2/(m CO2*s))	3.82785E-05
mu_H2 (kg H2/(m H2*s))	1.86145E-05
mu_NO (kg NO/(m NO*s))	4.39167E-05
phi_CO|CO (dimensionless)	1
phi_CO|H2O (dimensionless)	0.849085503
phi_CO|O2 (dimensionless)	0.979745073
phi_CO|N2 (dimensionless)	1.016680692
phi_CO|NH3 (dimensionless)	0.846718635
phi_CO|HCN (dimensionless)	1.224453862
phi_CO|SO2 (dimensionless)	1.510801741
phi_CO|CO2 (dimensionless)	1.256447031
phi_CO|H2 (dimensionless)	0.280912032
phi_CO|NO (dimensionless)	0.977315592
phi_H2O|CO (dimensionless)	1.150634424
phi_H2O|H2O (dimensionless)	1
phi_H2O|O2 (dimensionless)	1.118035363
phi_H2O|N2 (dimensionless)	1.170204103
phi_H2O|NH3 (dimensionless)	1.000547266
phi_H2O|HCN (dimensionless)	1.417538238
phi_H2O|SO2 (dimensionless)	1.676964403
phi_H2O|CO2 (dimensionless)	1.415699361
phi_H2O|H2 (dimensionless)	0.356575144
phi_H2O|NO (dimensionless)	1.119408671
phi_O2|CO (dimensionless)	1.019865839
phi_O2|H2O (dimensionless)	0.858814879
phi_O2|O2 (dimensionless)	1
phi_O2|N2 (dimensionless)	1.037337319
phi_O2|NH3 (dimensionless)	0.856012808
phi_O2|HCN (dimensionless)	1.254728801
phi_O2|SO2 (dimensionless)	1.570982119
phi_O2|CO2 (dimensionless)	1.295249995
phi_O2|H2 (dimensionless)	0.276478415
phi_O2|NO (dimensionless)	0.996802819
phi_N2|CO (dimensionless)	0.98372504
phi_N2|H2O (dimensionless)	0.835535351
phi_N2|O2 (dimensionless)	0.964226795
phi_N2|N2 (dimensionless)	1
phi_N2|NH3 (dimensionless)	0.83310397
phi_N2|HCN (dimensionless)	1.202544156
phi_N2|SO2 (dimensionless)	1.483432942
phi_N2|CO2 (dimensionless)	1.234767798
phi_N2|H2 (dimensionless)	0.276962834
phi_N2|NO (dimensionless)	0.961730178
phi_NH3|CO (dimensionless)	1.145845992
phi_NH3|H2O (dimensionless)	0.999168664
phi_NH3|O2 (dimensionless)	1.112852072
phi_NH3|N2 (dimensionless)	1.165191174
phi_NH3|NH3 (dimensionless)	1
phi_NH3|HCN (dimensionless)	1.409897303
phi_NH3|SO2 (dimensionless)	1.659211576
phi_NH3|CO2 (dimensionless)	1.404581532
phi_NH3/H2 (dimensionless)	0.360978208
phi_NH3|NO (dimensionless)	1.114574576

Table 13

Continued.

Gas Properties	
phi_HCN|CO (dimensionless)	0.83325779
phi_HCN|H2O (dimensionless)	0.711845597
phi_HCN|O2 (dimensionless)	0.820270074
phi_HCN|N2 (dimensionless)	0.845763306
phi_HCN|NH3 (dimensionless)	0.708985421
phi_HCN|HCN (dimensionless)	1
phi_HCN|SO2 (dimensionless)	1.225386671
phi_HCN|CO2 (dimensionless)	1.031917459
phi_HCN|H2 (dimensionless)	0.242678878
phi_HCN|NO (dimensionless)	0.817400414
phi_SO2|CO (dimensionless)	0.625866268
phi_SO2|H2O (dimensionless)	0.512639393
phi_SO2|O2 (dimensionless)	0.625194796
phi_SO2|N2 (dimensionless)	0.635115684
phi_SO2|NH3 (dimensionless)	0.507912272
phi_SO2|HCN (dimensionless)	0.745950937
phi_SO2|SO2 (dimensionless)	1
phi_SO2|CO2 (dimensionless)	0.811154128
phi_SO2|H2 (dimensionless)	0.157002143
phi_SO2|NO (dimensionless)	0.618730277
phi_CO2|CO (dimensionless)	0.782003249
phi_CO2|H2O (dimensionless)	0.650203753
phi_CO2|O2 (dimensionless)	0.774440427
phi_CO2|N2 (dimensionless)	0.794256024
phi_CO2|NH3 (dimensionless)	0.645987619
phi_CO2|HCN (dimensionless)	0.94378349
phi_CO2|SO2 (dimensionless)	1.218691232
phi_CO2|CO2 (dimensionless)	1
phi_CO2|H2 (dimensionless)	0.204738908
phi_CO2|NO (dimensionless)	0.76912452
phi_H2|CO (dimensionless)	1.85606551
phi_H2|H2O (dimensionless)	1.738553619
phi_H2|O2 (dimensionless)	1.754907519
phi_H2|N2 (dimensionless)	1.891277707
phi_H2|NH3 (dimensionless)	1.762450027
phi_H2|HCN (dimensionless)	2.356231624
phi_H2|SO2 (dimensionless)	2.504116157
phi_H2|CO2 (dimensionless)	2.173496625
phi_H2|H2 (dimensionless)	1
phi_H2|NO (dimensionless)	1.777264248
phi_NO|CO (dimensionless)	1.023433384
phi_NO|H2O (dimensionless)	0.865022656
phi_NO|O2 (dimensionless)	1.002776282
phi_NO|N2 (dimensionless)	1.040851676
phi_NO|NH3 (dimensionless)	0.862475471
phi_NO|HCN (dimensionless)	1.257832027
phi_NO|SO2 (dimensionless)	1.564055111
phi_NO|CO2 (dimensionless)	1.294067816
phi_NO|H2 (dimensionless)	0.281678563
phi_NO|NO (dimensionless)	1
D_O2|CO (m^2 CO/s)	0.000146695
D_O2|H2O (m^2 H2O/s)	0.000187723
D_O2|N2 (m^2 N2/s)	0.000144296
D_O2|NH3 (m^2 NH3/s)	0.000184324
D_O2|HCN (m^2 HCN/s)	0.000128929
D_O2|SO2 (m^2 SO2/s)	9.92218E-05
D_O2|CO2 (m^2 CO2/s)	0.000116825
D_O2|H2 (m^2 H2/s)	0.000544364
D_O2|NO (m^2 NO/s)	0.00015018

Also, the graphs of the mole fraction of species in the mixture of gases versus time after the mixture of gases leaves the BFB bed until they reach the BFB riser exit for all species in Fig. 26 and trace species in Fig. 27 are shown below. The trends are fairly similar to the first combustor except they are not as steep likely due to the much lower average T_{Mix} causing slower reaction rates.

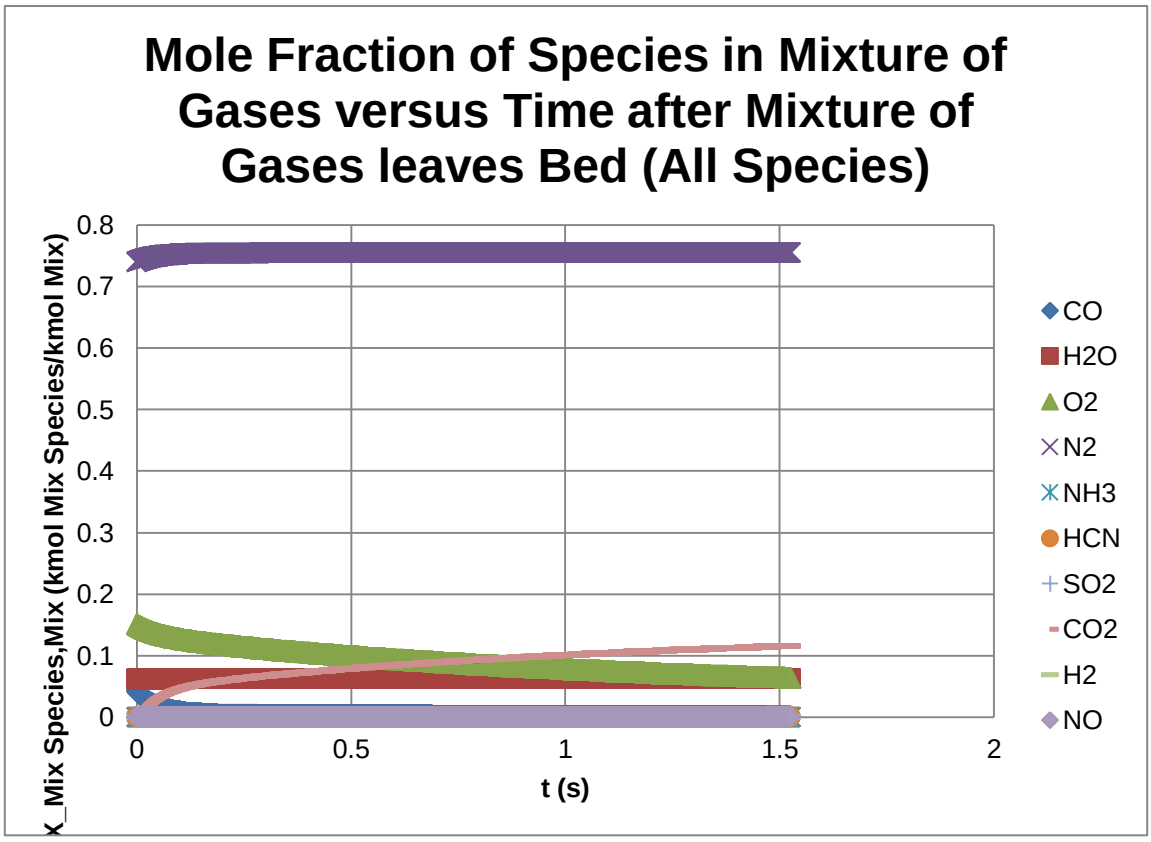

Fig. 26. Mole fraction of all species versus time for Babcock and Wilcox BFB boiler.

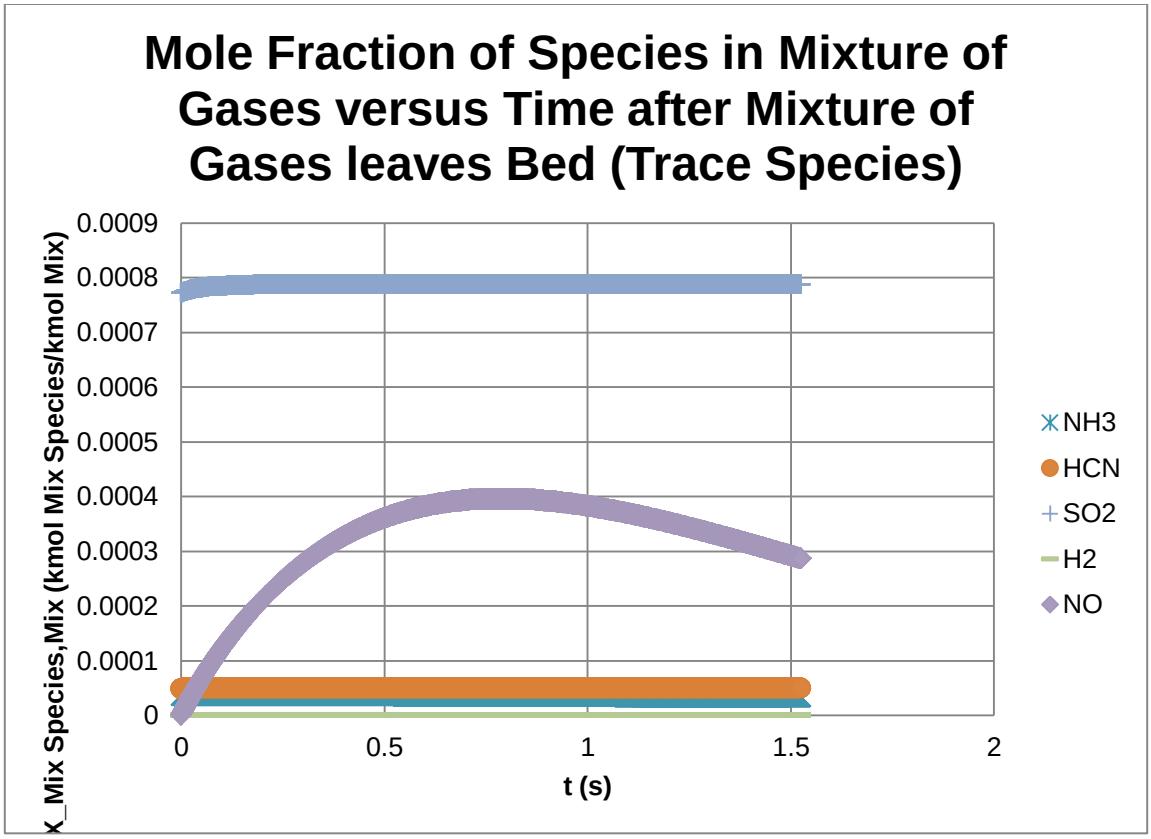

Fig. 27. Mole fraction of trace species versus time for Babcock and Wilcox BFB boiler.

When no chemical kinetics data are modified, the 'Output' tab of the Excel program below in Table 14 is the result.

Table 14

Output tab for Babcock and Wilcox BFB boiler.

WET BASIS CONCENTRATION OF SPECIES IN MIXTURE OF GASES LEAVING CFB RISER										
	CO	H2O	O2	N2	NH3	HCN	SO2	CO2	H2	NO
ppm (Actual % O2)	1621.577669	62225.83773	63753.7466	755220.4444	32.68981434	49.55266046	787.6736016	116022.3629	0.000235095	286.1144008
Mole % (Actual % O2)	0.162157767	6.222583773	6.37537466	75.52204444	0.003268981	0.004955266	0.07876736	11.60223629	2.35095E-08	0.02861144
ppm (Standard % O2)	1896.047078	72758.22802	39000	749333.6317	38.22291595	57.93997961	920.995805	135660.3919	0.000274887	334.5423311
Mole % (Standard % O2)	0.189604708	7.275822802	3.9	F7/10000	0.003822292	0.005793998	0.09209958	13.56603919	2.74887E-08	0.033454233
g/GJ	755.2078412	18639.95038	33921.20855	351849.9518	9.258587251	22.26878455	839.1056421	84900.19762	7.88042E-06	218.8807546
DRY BASIS CONCENTRATION OF SPECIES IN MIXTURE OF GASES LEAVING CFB RISER										
	CO	H2O	O2	N2	NH3	HCN	SO2	CO2	H2	NO
ppm (Actual % O2)	1729.177167	0	67984.11512	805332.9627	34.85894115	52.84071843	839.9395433	123721.0061	0.000250694	305.0994709
Mole % (Actual % O2)	0.172917717	0	6.798411512	80.53329627	0.003485894	0.005284072	0.083993954	12.37210061	2.50694E-08	0.030509947
ppm (Standard % O2)	2082.086069	0	39000	808462.2771	41.97332532	63.62501533	1011.363356	148971.3074	0.000301859	367.3674221
Mole % (Standard % O2)	0.208208607	0	3.9	F16/10000	0.004197333	0.006362502	0.101136336	14.89713074	3.01859E-08	0.036736742
g/GJ	755.2078412	0	33921.20855	351849.9518	9.258587251	22.26878455	839.1056421	84900.19762	7.88042E-06	218.8807546

Experimental concentration measurements were not provided for H_2O, NH_3, HCN, and H_2 (CO was given in a range without a specific value), but these species were predicted by de Souza-Santos [36,40]. The H_2O concentration predicted by de Souza-Santos [40] is believed to be erroneous at a value of nearly 15.0% meaning a difference from the proposed model predicted 6.2% of about 59%. This doesn't seem possible with the inputs provided since the proposed model assumes all fuel and limestone moisture is immediately released in the bed upon entry into the combustor and all volatile Hydrogen not used to produce NH_3 or HCN is oxidized to form H_2O while in the combustor as a whole H_2O is assumed to not be consumed in any chemical reaction. As for NH_3, HCN, and H_2, the concentrations are so small that they can't be compared since de Souza-Santos has these values listed as basically nonexistent [36], and the proposed model also predicts small concentrations of these species. All of the other desired species' concentrations are believed to be given on an uncorrected dry basis in mole percent (CO, O_2, N_2, SO_2, CO_2, and NO).

The measured CO concentration is between 0% and 0.9% compared to the model predicted 0.2% which is within the expected range. On the other hand, the measured O_2 concentration of 3.9% is not too close to the model predicted 6.8% being off more than 74%. This is the largest discrepancy between the model and the measured concentrations, and is likely attributed to the fact that the BFB has a greater portion of particles in the dense bed region of the combustor that don't become entrained due to the low $V_{Bed\ Mix}$ so that the O_2 has much more char to react with than is predicted by a CFB model that assumes that all of the particles immediately become entrained moving continually upwards. The measured N_2 concentration of 81.2% is very close to the model predicted 80.5% which is less than a 1% difference. This difference is also acceptable and may be attributed to slight variations in chemical kinetics data especially that of the many complex nitrogenous reactions and assumptions or perhaps deviation in supplied combustion air.

As for SO_2, the measured and predicted concentrations are both 0.08% due to all of the important limestone data being provided and no other Sulfur reactions. The 0.08% concentration is somewhat high for a boiler with limestone, but this is no surprise since there is also a scrubber downstream of the boiler as shown in the schematic of the boiler in Fig. 25 that further reduces the SO_2 concentration to below regulatory statutes. With a CSR of 2.2 and a $X_{LS\ CaSO_3,LS\ CaO}x100$ of 28.09% in the combustor and still having a 0.08% emission of SO_2, only about 62% SO_2 is captured in the combustor. Using a more reactive limestone with a $X_{LS\ CaSO_3,LS\ CaO}x100$ of around 41% is fairly common and at the same CSR of 2.2 could lead to over 90% SO_2 capture in the

combustor so that only 0.02% SO_2 is at the cyclone inlet/riser exit. This also means that a scrubber would no longer be necessary because the SO_2 concentration is about 215 g SO_2/GJ which is less than the US EPA regulation of 260 g SO_2/GJ (at least 70% SO_2 removal). However, cost of taking the scrubber out of service and the cost of a higher quality limestone may not be worth it. Alternatively, the CSR can be increased to about 3.2 to achieve similarly low levels of SO_2.

The measured CO_2 concentration of 13.8% is fairly close to the model predicted 12.4% being just more than 10% different. This difference should come as no surprise since the O_2 concentration is closely tied to the CO_2 concentration due to the fact that CO_2 is the main product of combustion; and therefore, the main consumer of O_2. As discussed previously with the O_2 comparison, the less O_2 consumed is likely caused by the model having less char in the dense region oxidizing to form CO_2. The measured NO concentration of 0.03% amazingly matches the model predicted 0.03% without any chemical kinetics modifications.

5.2 Anonymous CFB Boiler Fuel Switch to Tire

The first combustor validated with modified kinetics was then used to observe the changes that take place when the fuel is switched from lignite to tire (assuming metal wiring removed). When the lignite fuel is used, the total heat generated by combustion is almost 750 MW. In order to maintain similar heat output with the tire fuel that has a hhv_{Fuel} of over three times that of the lignite, the $\dot{m}_{Fuel}$ must be reduced accordingly to less than a third of that of the lignite. According to Atal and Levendis, the density of tire is approximately 0.33 times the density of lignite [1]. The proximate and ultimate analyses for the tire were provided by Dai et al. [3]. Due to the changes in the proximate and ultimate analyses from lignite to tire fuel, the $Y_{VN,N}x100$, $Y_{N_2,N}x100$, $Y_{NH_3,N}x100$, and $Y_{HCN,N}x100$ were all obtained by utilizing Kambara's coal data as described in the literature review earlier. It was determined that the coal in Table 5 that best matches the tire fuel based mostly on the Carbon amount in the ultimate analysis comparison is coal 'B'. With a pyrolysis temperature near 1,000 K, Fig. 5, Fig. 6, and Fig. 7 were used in conjunction with coal 'B' to determine the desired values. All other inputs were kept the same. The new 'Input' tab of the Excel program utilizing the tire fuel can be seen below in Table 15.

Table 15

Input tab for anonymous CFB boiler firing tire fuel.

FUEL DATA	
Fuel	Waste Tire
mdot_Fuel (kg Fuel/s)	20.46422041
Fuel/Char Particle Properties	
rho_Fuel (kg Fuel/m^3 Fuel)	528
d_Fuel,0 (m Fuel)	0.000387226
hhv_Fuel (kJ/kg Fuel)	36463
	As Received (AR) Fuel
Proximate-equiv Fuel Analysis	
Y_VM,Fuel x 100 (kg VM/100 kg Fuel)	68.7
Y_FC,Fuel x 100 (kg FC/100 kg Fuel)	27.2
	95.9
Y_H2O,Fuel x 100 (kg H2O/100 kg Fuel)	0.8
Y_Ash,Fuel x 100 (kg Ash/100 kg Fuel)	3.3
	100
Ultimate/Elemental Fuel Analysis	
Y_C,Fuel x 100 (kg C/100 kg Fuel)	82.1376
Y_H,Fuel x 100 (kg H/100 kg Fuel)	7.5392
Y_O,Fuel x 100 (kg O/100 kg Fuel)	4.464
Y_N,Fuel x 100 (kg N/100 kg Fuel)	0.496
Y_S,Fuel x 100 (kg S/100 kg Fuel)	1.2896
	95.9264
Nitrogen Release from Fuel as Volatile Matter & Split into N2, NH3, HCN	
Y_VN,N x 100 (kg VN/100 kg N)	14
Y_N2,N x 100 (kg N2/100 kg N)	0
Y_NH3,N x 100 (kg N/100 kg N)	4
Y_HCN,N x 100 (kg N/100 kg N)	10
	14
AIR DATA	
X_Exc Air,Stoich Air x 100 (kmol Exc Air/100 kmol Stoich Air)	7.688994185
Air Properties	
X_N2,Air x 100 (kmol N2/100 kmol Air)	79
X_O2,Air x 100 (kmol O2/100 kmol Air)	21
	100
LIMESTONE DATA	
Limestone	Unknown
CSR (kmol LS CaCO3/kmol Vol SO2)	2.1
Limestone Particle Properties	
rho_LS CaCO3 (kg LS CaCO3/m^3 LS CaCO3)	2710
d_LS CaCO3 (m LS CaCO3)	0.00015
Y_LS H2O,LS x 100 (kg LS H2O/100 kg LS)	5
X_LS CaSO3,LS CaO x 100 (kmol LS CaSO3/100 kmol LS CaO)	17

Table 15

Continued.

OPERATIONAL DATA	
P_Mix (bar)	1
T_Mix (K)	1139.944444
RISER DATA	
a_CS,Riser (m^2 Riser)	125
h_Riser (m Riser)	36.6
CHEMICAL KINETICS DATA	
# of Chemical Kinetics Calculation Rows	5000
(1) NO + C -> 1/2 N2 + CO	
A_1 (1/s)	0.00026
E_a,1 (kJ/kmol Mix NO)	132192.6
nu_Mix NO,1 (dimensionless)	1
(2) CO + 1/2 O2 -> CO2	
A_2 (m^3 Mix/(kmol*s))	1.3E+11
E_a,2 (kJ/kmol Mix CO)	125520
nu_Mix CO,2 (dimensionless)	1
nu_Mix O2,2 (dimensionless)	0.5
nu_Mix H2O,2 (dimensionless)	0.5
(3) NH3 + O2 -> NO + H2O + 1/2 H2	
A_3 (1/s)	3.48E+23
E_a,3 (kJ/kmol Mix NH3)	418400
nu_Mix NH3,3 (dimensionless)	1
nu_Mix O2,3 (dimensionless)	1
A_3,other (dimensionless)	0.0000069
E_a,3,other (kJ/kmol Mix NH3)	175728
nu_Mix O2,3,other (dimensionless)	1
(4) NH3 + NO -> N2 + H2O + 1/2 H2	
A_4 (1/s)	6.22E+17
E_a,4 (kJ/kmol Mix NH3)	230120
nu_Mix NH3,4 (dimensionless)	1
nu_Mix NO,4 (dimensionless)	1
(5) HCN + O2 -> NO + CO + 1/2 H2	
A_5 (1/s)	1E+14
E_a,5 (kJ/kmol Mix HCN)	280328
nu_Mix HCN,5 (dimensionless)	1
(6) HCN + NO -> N2 + CO + 1/2 H2	
A_6 (1/s)	3E+12
E_a,6 (kJ/kmol Mix HCN)	251040
nu_Mix HCN,6 (dimensionless)	1
nu_Mix NO,6 (dimensionless)	1
(7) 2 H2 + O2 -> 2 H2O	
A_7 (m^4.5 Mix/(kmol^1.5*K^1.5*s))	5.15451E+13
E_a,7 (kJ/kmol Mix O2)	28433.88
nu_Mix O2,7 (dimensionless)	1
nu_Mix H2,7 (dimensionless)	1.5
k_7 (dimensionless)	1.5

The number of chemical kinetics calculation rows in the Excel program remained at 5,000 which means the Δt is almost 0.001 seconds since the $V_{Bed\ Mix}$ decreased to about 7.5 meters per second due to the greatly decreased $\dot{m}_{Fuel}$ even though the $N_{Stoich\ O_2,Fuel}x100$ over doubled from a large increase in $Y_{C,Fuel}x100$. This means the $t_{Res,Bed\ Mix}$ is now about 4.9 seconds with the new inputs. The $V_{Bed\ Mix}$ being 7.5 meters per second still indicates a circulating bed especially since the same SMD as the lignite fuel is used.

In just less than 2 seconds or only a little over a third of the way up the riser, the SMD size tire particle appears to be completely burned. This is different from the lignite SMD size particle which didn't completely burn until a little over 3 seconds or almost 90% of the way up the riser. This difference can be greatly attributed to the great variance in densities between the two fuels. This relative decrease in density of the tire from lignite may also be a key in allowing an increased SMD of the tire to be burned in the combustor in order to cut back on the amount of costly processing to reduce the tire particle size. Other intermediate calculations can be viewed in the 'Bed' tab of the Excel program below in Table 16.

Table 16

Bed tab for anonymous CFB boiler firing tire fuel.

Fuel Entering CFB Bed	
a'_CS,Fuel,0 (m^2 Fuel/Fuel Particle)	1.17766E-07
N_H2O,Fuel x 100 (kmol H2O/100 kg Fuel)	0.044404973
Ultimate/Elemental Fuel Analysis (Mole Basis)	
N_C,Fuel x 100 (kmol C/100 kg Fuel)	6.839100749
N_H,Fuel x 100 (kmol H/100 kg Fuel)	7.479365079
N_O,Fuel x 100 (kmol O/100 kg Fuel)	0.279
N_N,Fuel x 100 (kmol N/100 kg Fuel)	0.035403283
N_S,Fuel x 100 (kmol S/100 kg Fuel)	0.040212036
Carbon & Nitrogen Retained in Fuel as Fixed Carbon	
N_FC,Fuel x 100 (kmol FC/100 kg Fuel)	2.229262281
N_FN,Fuel x 100 (kmol FN/100 kg Fuel)	0.030446824
	27.2
Y_FC,FC x 100 (kg FC/100 kg FC)	98.43176471
Y_FN,FC x 100 (kg FN/100 kg FC)	1.568235294
FCR (kg FN/kg FC)	0.015932207
Carbon, Hydrogen, Oxygen, Nitrogen, Sulfur Release from Fuel as Volatile Matter	
N_VC,Fuel x 100 (kmol VC/100 kg Fuel)	4.609838468
N_VH,Fuel x 100 (kmol VH/100 kg Fuel)	7.479365079
N_VO,Fuel x 100 (kmol VO/100 kg Fuel)	0.279
N_VN,Fuel x 100 (kmol VN/100 kg Fuel)	0.00495646
N_VS,Fuel x 100 (kmol VS/100 kg Fuel)	0.040212036
	68.7264
Nitrogen Release from Fuel as Volatile Matter & Split into N2, NH3, HCN	
N_N2,Fuel x 100 (kmol N2/100 kg Fuel)	0
N_NH3,Fuel x 100 (kmol N/100 kg Fuel)	0.001416131
N_HCN,Fuel x 100 (kmol N/100 kg Fuel)	0.003540328
	0.00495646
Air Entering CFB Bed	
N_Stoich O2,Fuel x 100 (kmol Stoich O2/100 kg Fuel)	8.609654055
SR (dimensionless)	1.076889942
	0.9286
N_Act O2,Fuel x 100 (kmol Act O2/100 kg Fuel)	9.271649855
N_Act N2,Fuel x 100 (kmol Act N2/100 kg Fuel)	34.87906374
	44.1507136
m_Stoich Air,Fuel x 100 (kg Stoich Air/100 kg Fuel)	1183.040264
Volatile Combustion	
N_Vol CO,Fuel x 100 (kmol Vol CO/100 kg Fuel)	4.60629814
N_Vol H2O,Fuel x 100 (kmol Vol H2O/100 kg Fuel)	3.735788179
N_Vol O2,Fuel x 100 (kmol Vol O2/100 kg Fuel)	5.19989466
N_Vol N2,Fuel x 100 (kmol Vol N2/100 kg Fuel)	34.87906374
N_Vol NH3,Fuel x 100 (kmol Vol NH3/100 kg Fuel)	0.001416131
N_Vol HCN,Fuel x 100 (kmol Vol HCN/100 kg Fuel)	0.003540328
N_Vol SO2,Fuel x 100 (kmol Vol SO2/100 kg Fuel)	0.040212036
Limestone Reactions	
a'_CS,LS CaCO3 (m^2 LS CaCO3/LS CaCO3 Particle)	1.76715E-08
Y_LS,Fuel x 100 (kg LS/100 kg Fuel)	8.896976495
N_LS H2O,Fuel x 100 (kmol LS H2O/100 kg Fuel)	0.024691875
N_LS CaCO3,Fuel x 100 (kmol LS CaCO3/100 kg Fuel)	0.084445276
N_LS CO2,Fuel x 100 (kmol LS CO2/100 kg Fuel)	0.084445276
N_LS CaO,Fuel x 100 (kmol LS CaO/100 kg Fuel)	0.084445276
N_LS CaSO3,Fuel x 100 (kmol LS CaSO3/100 kg Fuel)	0.014355697
	0.070089579
	35.7

Table 16

Continued.

Gaseous Species leaving CFB Bed	
mdot Act Air (kg Act Air/s)	260.7150196
mdot VL (kg VL/s)	0.85157462
mdot VF (kg VF/s)	14.03440952
mdot Bed Mix (kg Bed Mix/s)	275.6010037
N Bed CO,Fuel x 100 (kmol Bed CO/100 kg Fuel)	4.60629814
N Bed H2O,Fuel x 100 (kmol Bed H2O/100 kg Fuel)	3.804885027
N Bed O2,Fuel x 100 (kmol Bed O2/100 kg Fuel)	5.19989466
N Bed N2,Fuel x 100 (kmol Bed N2/100 kg Fuel)	34.87906374
N Bed NH3,Fuel x 100 (kmol Bed NH3/100 kg Fuel)	0.001416131
N_Bed HCN,Fuel x 100 (kmol Bed HCN/100 kg Fuel)	0.003540328
N_Bed SO2,Fuel x 100 (kmol Bed SO2/100 kg Fuel)	0.025856339
N_Bed CO2,Fuel x 100 (kmol Bed CO2/100 kg Fuel)	0.084445276
N_Bed Mix,Fuel x 100 (kmol Bed Mix/100 kg Fuel)	48.60539964
X_Bed CO,Bed Mix x 100 (kmol Bed CO/100 kmol Bed Mix)	9.476926789
X_Bed H2O,Bed Mix x 100 (kmol Bed H2O/100 kmol Bed Mix)	7.828111805
X Bed O2,Bed Mix x 100 (kmol Bed O2/100 kmol Bed Mix)	10.69818312
X Bed N2,Bed Mix x 100 (kmol Bed N2/100 kmol Bed Mix)	71.7596481
X Bed NH3,Bed Mix x 100 (kmol Bed NH3/100 kmol Bed Mix)	0.002913527
X Bed HCN,Bed Mix x 100 (kmol Bed HCN/100 kmol Bed Mix)	0.007283817
X Bed SO2,Bed Mix x 100 (kmol Bed SO2/100 kmol Bed Mix)	0.053196434
X Bed CO2,Bed Mix x 100 (kmol Bed CO2/100 kmol Bed Mix)	0.173736409
	100
N''' Mix (kmol Mix/m^3 Mix)	0.010551308
N''' Bed CO (kmol Bed CO/m^3 Bed Mix)	0.00099994
N'''_Bed H2O (kmol Bed H2O/m^3 Bed Mix)	0.000825968
N'''_Bed O2 (kmol Bed O2/m^3 Bed Mix)	0.001128798
N'''_Bed N2 (kmol Bed N2/m^3 Bed Mix)	0.007571581
N'''_Bed NH3 (kmol Bed NH3/m^3 Bed Mix)	3.07415E-07
N'''_Bed HCN (kmol Bed HCN/m^3 Bed Mix)	7.68538E-07
N'''_Bed SO2 (kmol Bed SO2/m^3 Bed Mix)	5.61292E-06
N'''_Bed CO2 (kmol Bed CO2/m^3 Bed Mix)	1.83315E-05
	0.010551308
m_Bed CO,Fuel x 100 (kg Bed CO/100 kg Fuel)	129.0224109
m Bed H2O,Fuel x 100 (kg Bed H2O/100 kg Fuel)	68.54880865
m Bed O2,Fuel x 100 (kg Bed O2/100 kg Fuel)	166.3966291
m Bed N2,Fuel x 100 (kg Bed N2/100 kg Fuel)	977.311366
m Bed NH3,Fuel x 100 (kg Bed NH3/100 kg Fuel)	0.024122381
m Bed HCN,Fuel x 100 (kg Bed HCN/100 kg Fuel)	0.095687994
m Bed SO2,Fuel x 100 (kg Bed SO2/100 kg Fuel)	1.656615656
m Bed CO2,Fuel x 100 (kg Bed CO2/100 kg Fuel)	3.716436595
m Bed Mix,Fuel x 100 (kg Bed Mix/100 kg Fuel)	1346.772077
mbar Bed Mix (kg Bed Mix/kmol Bed Mix)	27.70828112
rho_Bed Mix (kg Bed Mix/m^3 Bed Mix)	0.292358603
Solid Species leaving CFB Bed	
m'''_Fuel,Bed Mix (kg Fuel/m^3 Bed Mix)	0.021708098
m'''_Char,Bed Mix (kg Char/m^3 Bed Mix)	0.00662097
m'''_Char,Fuel (kg Char/m^3 Fuel)	161.04
m'''_FC,Fuel (kg FC/m^3 Fuel)	141.3637632
m' Char,0 (kg Char/Char Particle)	4.89582E-09
m' FC,0 (kg FC/FC Particle)	4.29764E-09
CCR (kg Char/kg FC)	1.139188688
	6.84709E-11
n''' Char,Bed Mix (Char Particles/m^3 Bed Mix)	1352371.819
m''' LS CaCO3,Bed Mix (kg LS CaCO3/m^3 Bed Mix)	0.001834796
m' LS CaCO3 (kg LS CaCO3/LS CaCO3 Particle)	4.78897E-09
n'''_LS CaCO3,Bed Mix (LS CaCO3 Particles/m^3 Bed Mix)	383129.9768
a_CS,Fuel,0 (m^2 Fuel)	0.015417683
a_CS,LS CaCO3 (m^2 LS CaCO3)	0.000253892
a_CS,Riser,Eff (m^2 Eff Riser)	124.9843284
V_Bed Mix (m Riser/s)	7.542396429
t_Res,Bed Mix (s)	4.852569119
delta t (s)	0.000970514

Table 16

Continued.

Gas Properties	
mu_CO (kg CO/(m CO*s))	4.35505E-05
mu_H2O (kg H2O/(m H2O*s))	4.03042E-05
mu_O2 (kg O2/(m O2*s))	5.19245E-05
mu_N2 (kg N2/(m N2*s))	4.2001E-05
mu_NH3 (kg NH3/(m NH3*s))	3.76217E-05
mu_HCN (kg HCN/(m HCN*s))	3.00371E-05
mu_SO2 (kg SO2/(m SO2*s))	4.25944E-05
mu_CO2 (kg CO2/(m CO2*s))	4.32664E-05
mu_H2 (kg H2/(m H2*s))	2.05904E-05
mu_NO (kg NO/(m NO*s))	4.90681E-05
phi_CO|CO (dimensionless)	1
phi_CO|H2O (dimensionless)	0.824720516
phi_CO|O2 (dimensionless)	0.978525655
phi_CO|N2 (dimensionless)	1.018545745
phi_CO|NH3 (dimensionless)	0.826832294
phi_CO|HCN (dimensionless)	1.191992817
phi_CO|SO2 (dimensionless)	1.484441167
phi_CO|CO2 (dimensionless)	1.245980395
phi_CO|H2 (dimensionless)	0.281615064
phi_CO|NO (dimensionless)	0.975302722
phi_H2O|CO (dimensionless)	1.186638532
phi_H2O|H2O (dimensionless)	1
phi_H2O|O2 (dimensionless)	1.150611674
phi_H2O|N2 (dimensionless)	1.209409548
phi_H2O|NH3 (dimensionless)	1.006340857
phi_H2O|HCN (dimensionless)	1.426169868
phi_H2O|SO2 (dimensionless)	1.704223693
phi_H2O|CO2 (dimensionless)	1.450112653
phi_H2O|H2 (dimensionless)	0.36711879
phi_H2O|NO (dimensionless)	1.15127626
phi_O2|CO (dimensionless)	1.021207339
phi_O2|H2O (dimensionless)	0.834562447
phi_O2|O2 (dimensionless)	1
phi_O2|N2 (dimensionless)	1.040669784
phi_O2|NH3 (dimensionless)	0.836439248
phi_O2|HCN (dimensionless)	1.222417693
phi_O2|SO2 (dimensionless)	1.545173746
phi_O2|CO2 (dimensionless)	1.28597569
phi_O2|H2 (dimensionless)	0.277505994
phi_O2|NO (dimensionless)	0.99597532
phi_N2|CO (dimensionless)	0.981954605
phi_N2|H2O (dimensionless)	0.810349964
phi_N2|O2 (dimensionless)	0.961351275
phi_N2|N2 (dimensionless)	1
phi_N2|NH3 (dimensionless)	0.81227219
phi_N2|HCN (dimensionless)	1.168602882
phi_N2|SO2 (dimensionless)	1.454825904
phi_N2|CO2 (dimensionless)	1.222227823
phi_N2|H2 (dimensionless)	0.277220589
phi_N2|NO (dimensionless)	0.95807553
phi_NH3|CO (dimensionless)	1.174516004
phi_NH3|H2O (dimensionless)	0.993516228
phi_NH3|O2 (dimensionless)	1.138503055
phi_NH3|N2 (dimensionless)	1.19682932
phi_NH3|NH3 (dimensionless)	1
phi_NH3|HCN (dimensionless)	1.409404384
phi_NH3|SO2 (dimensionless)	1.675091745
phi_NH3|CO2 (dimensionless)	1.429588126
phi_NH3/H2 (dimensionless)	0.369684361
phi_NH3|NO (dimensionless)	1.139491175

Table 16

Continued.

Gas Properties	
phi_HCN|CO (dimensionless)	0.851996315
phi_HCN|H2O (dimensionless)	0.708473624
phi_HCN|O2 (dimensionless)	0.837224626
phi_HCN|N2 (dimensionless)	0.866403421
phi_HCN|NH3 (dimensionless)	0.70918279
phi_HCN|HCN (dimensionless)	1
phi_HCN|SO2 (dimensionless)	1.236330765
phi_HCN|CO2 (dimensionless)	1.048653469
phi_HCN|H2 (dimensionless)	0.247848065
phi_HCN|NO (dimensionless)	0.833807371
phi_SO2|CO (dimensionless)	0.634717576
phi_SO2|H2O (dimensionless)	0.50644523
phi_SO2|O2 (dimensionless)	0.633072056
phi_SO2|N2 (dimensionless)	0.645234658
phi_SO2|NH3 (dimensionless)	0.50421368
phi_SO2|HCN (dimensionless)	0.739585066
phi_SO2|SO2 (dimensionless)	1
phi_SO2|CO2 (dimensionless)	0.817270837
phi_SO2|H2 (dimensionless)	0.15922395
phi_SO2|NO (dimensionless)	0.626134395
phi_CO2|CO (dimensionless)	0.787825675
phi_CO2|H2O (dimensionless)	0.637248783
phi_CO2|O2 (dimensionless)	0.779130075
phi_CO2|N2 (dimensionless)	0.801604625
phi_CO2|NH3 (dimensionless)	0.636338713
phi_CO2|HCN (dimensionless)	0.92765575
phi_CO2|SO2 (dimensionless)	1.208557697
phi_CO2|CO2 (dimensionless)	1
phi_CO2|H2 (dimensionless)	0.206516544
phi_CO2|NO (dimensionless)	0.77322719
phi_H2|CO (dimensionless)	1.849907969
phi_H2|H2O (dimensionless)	1.676058628
phi_H2|O2 (dimensionless)	1.74672646
phi_H2|N2 (dimensionless)	1.888899494
phi_H2|NH3 (dimensionless)	1.709557892
phi_H2|HCN (dimensionless)	2.277800565
phi_H2|SO2 (dimensionless)	2.446161361
phi_H2|CO2 (dimensionless)	2.145508151
phi_H2|H2 (dimensionless)	1
phi_H2|NO (dimensionless)	1.767296808
phi_NO|CO (dimensionless)	1.025634852
phi_NO|H2O (dimensionless)	0.841436283
phi_NO|O2 (dimensionless)	1.003598953
phi_NO|N2 (dimensionless)	1.045062368
phi_NO|NH3 (dimensionless)	0.843573234
phi_NO|HCN (dimensionless)	1.226746947
phi_NO|SO2 (dimensionless)	1.539938441
phi_NO|CO2 (dimensionless)	1.286001663
phi_NO|H2 (dimensionless)	0.282923216
phi_NO|NO (dimensionless)	1
D_O2|CO (m^2 CO/s)	0.000197468
D_O2|H2O (m^2 H2O/s)	0.000259327
D_O2|N2 (m^2 N2/s)	0.000193859
D_O2|NH3 (m^2 NH3/s)	0.000253223
D_O2|HCN (m^2 HCN/s)	0.00017717
D_O2|SO2 (m^2 SO2/s)	0.000135374
D_O2|CO2 (m^2 CO2/s)	0.000158387
D_O2|H2 (m^2 H2/s)	0.000730394
D_O2|NO (m^2 NO/s)	0.000202579

Also, the graphs of the mole fraction of species in the mixture of gases versus time after the mixture of gases leaves the CFB bed until they reach the CFB riser exit for all species in Fig. 28 and trace species in Fig. 29 are shown below. The trends are very similar to the lignite fuel except that they happen much sooner in the riser as the tire char burns much more quickly as stated.

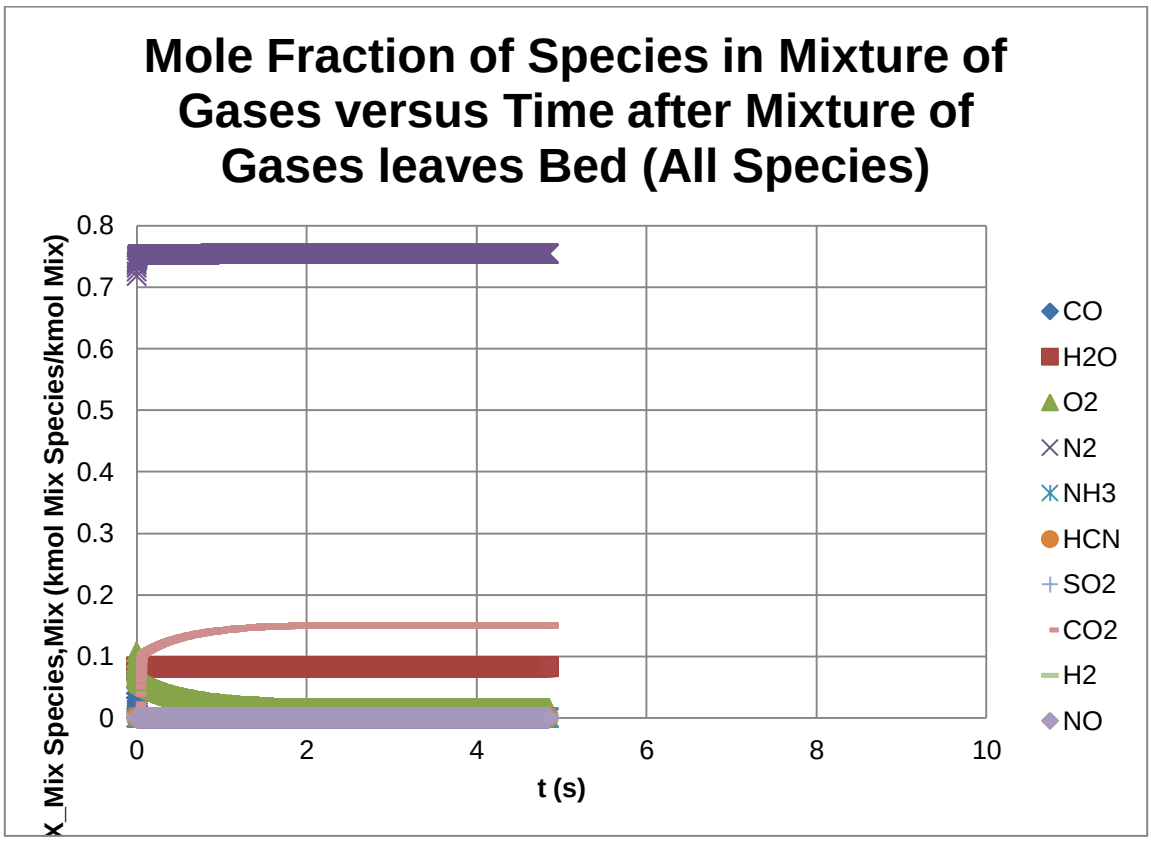

Fig. 28. Mole fraction of all species versus time for anonymous CFB boiler firing tire fuel.

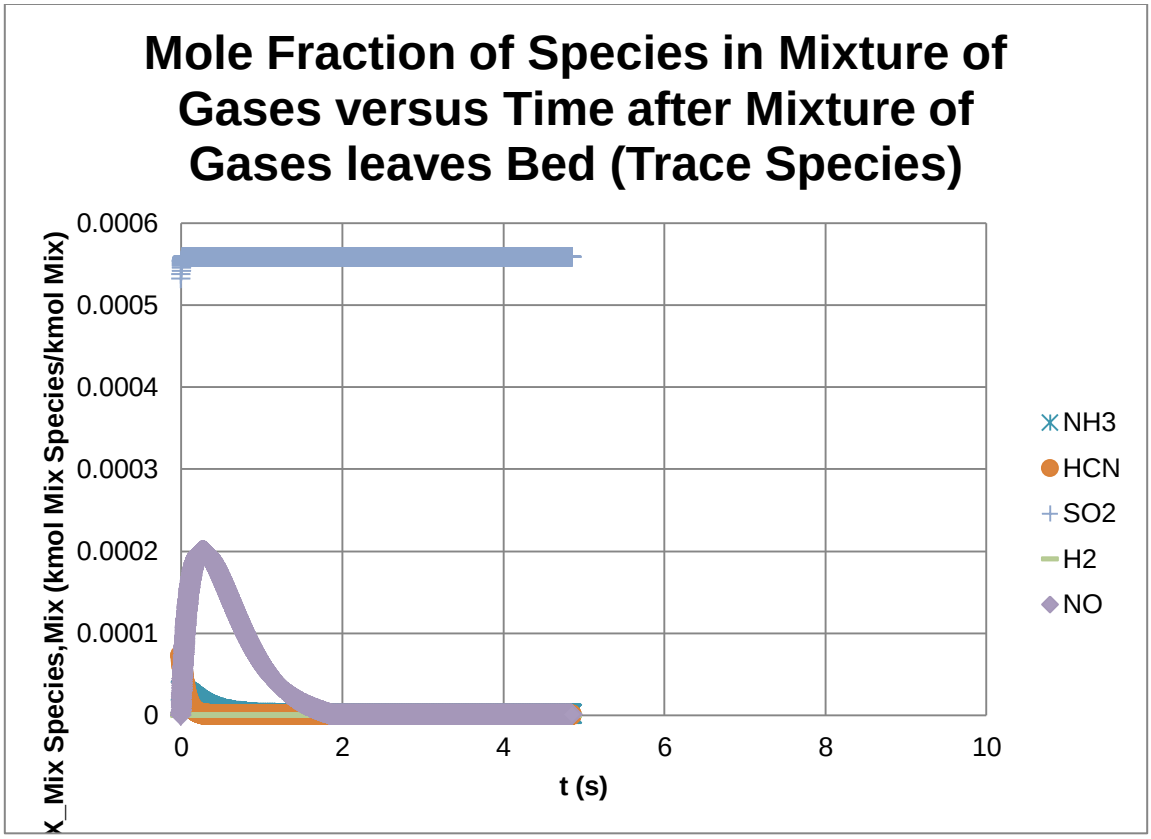

Fig. 29. Mole fraction of trace species versus time for anonymous CFB boiler firing tire fuel.

The 'Output' tab of the Excel program is shown below in Table 17.

Table 17

Output tab for anonymous CFB boiler firing tire fuel.

WET BASIS CONCENTRATION OF SPECIES IN MIXTURE OF GASES LEAVING CFB RISER										
	CO	H2O	O2	N2	NH3	HCN	SO2	CO2	H2	NO
ppm (Actual % O2)	9.61988E-21	82231.03742	14293.42046	753433.4251	1.300571751	7.9979E-20	558.2481491	149481.9787	2.51741E-05	0.589611374
Mole % (Actual % O2)	9.61988E-25	8.223103742	1.429342046	75.34334251	0.000130057	7.9979E-24	0.055824815	14.94819787	2.51741E-09	5.89611E-05
ppm (Standard % O2)	8.84783E-21	75631.52333	30000	756368.1032	1.196193382	7.35603E-20	513.4455217	137485.1894	2.31537E-05	0.542291668
Mole % (Standard % O2)	8.84783E-25	7.563152333	3	F7/10000	0.000119619	7.35603E-24	0.051344552	13.74851894	2.31537E-09	5.42292E-05
g/GJ	3.38096E-21	18588.82371	5739.101608	264893.182	0.277976912	2.71236E-20	448.7864975	82546.36864	6.36798E-07	0.340389263

DRY BASIS CONCENTRATION OF SPECIES IN MIXTURE OF GASES LEAVING CFB RISER										
	CO	H2O	O2	N2	NH3	HCN	SO2	CO2	H2	NO
ppm (Actual % O2)	1.04818E-20	0	15574.0944	820940.1884	1.417101476	8.71451E-20	608.2665375	162875.3911	2.74296E-05	0.642439871
Mole % (Actual % O2)	1.04818E-24	0	1.55740944	82.09401884	0.00014171	8.71451E-24	0.060826654	16.28753911	2.74296E-09	6.4244E-05
ppm (Standard % O2)	9.70409E-21	0	30000	818644.5055	1.311956166	8.06791E-20	563.134714	150790.4531	2.53944E-05	0.594772474
Mole % (Standard % O2)	9.70409E-25	0	3	F16/10000	0.000131196	8.06791E-24	0.056313471	15.07904531	2.53944E-09	5.94772E-05
g/GJ	3.38096E-21	0	5739.101608	264893.182	0.277976912	2.71236E-20	448.7864975	82546.36864	6.36798E-07	0.340389263

The CO, NH_3, HCN, and H_2 at the cyclone inlet/riser exit are still almost nonexistent. The CO decreased mostly due to the increased time after complete burning of the SMD size tire particle to oxidize as well as the decreased amount of NO and HCN that was available to form CO. The lower NO is due to the less dense tire fuel that in turn allows quicker shrinking of the fuel particle when similar mass is lost from both NO and O_2 reacting with the char which greatly enhances combustion as seen in the graphs. The decreased HCN is greatly due to the smaller amount of $Y_{VN,N}x100$ as well as less $Y_{HCN,N}x100$. However, the NH_3 concentration actually increased even though the $Y_{VN,N}x100$ and $Y_{NH_3,N}x100$ are smaller due to NH_3 being more sensitive to reacting with NO as seen by the much higher reaction pre-exponential factor. Therefore, the lower NO concentration means less consumption of NH_3. The H_2 amount has increased tremendously due to the relatively higher oxidation rates of NH_3 and HCN compared to that of H_2 from higher O_2 concentrations left after the tire is completely burned. The H_2O concentration greatly decreased from that of lignite fuel not directly due to the

decreased $Y_{H_2O,Fuel}x100$ from over 30% in the lignite fuel to less than 1% in the tire fuel even though $Y_{H,Fuel}x100$ for the tire almost tripled, but it was merely due to the fact that the greatly increased air required for complete combustion of the tire caused the relative concentration of H_2O to be lower. The similar O_2 concentration is due to both fuels' SMD size particle being completely burned in the riser and having the same $X_{Exc\ Air,Stoich\ Air}x100$. Even though the $Y_{O,Fuel}x100$ of the tire fuel is about half that of lignite fuel, the $N_{Stoich\ O_2,Fuel}x100$ of the tire is over double that of the lignite. The $N_{Stoich\ O_2,Fuel}x100$ of the tire being over double that of the lignite is also the reason the N_2 concentration greatly increases with the tire fuel because of the fixed ratio of these constituents in the actual combustion air. The CO_2 concentration follows the reasoning behind the CO and O_2 concentrations being the chief product of CO oxidization. Therefore, the CO_2 concentration from the tire was able to almost exactly match that of the lignite CO_2 level due to also finishing complete burning of the tire particles, but also having extra time to oxidize more CO after the SMD particles were all burned.

As for SO_2, the greatly decreased concentration is similarly due to the fact that the greatly increased air required for complete combustion of the tire caused the relative concentration of SO_2 to be lower like H_2O. However, a SO_2 concentration of 558 ppm wet based and uncorrected is still high for regulatory statutes even though the grams of SO_2 per gigajoule was cut to a third being 449 now because of the hhv_{Fuel} tripling. Therefore, the scrubber downstream can still be used to reduce the SO_2 to the appropriate levels. However, a more reactive limestone with a $X_{LS\ CaSO_3,LS\ CaO}x100$ of around 34% is fairly common and at the same CSR of 2.1 could lead to almost double

the SO_2 capture in the combustor to 71% so that only 248 ppm is at the cyclone inlet/riser exit. This also means that a scrubber would no longer be necessary because the SO_2 concentration is about 200 g SO_2/GJ which is less than the US EPA regulation of 260 g SO_2/GJ (at least 70% SO_2 removal). However, cost of taking the scrubber out of service and the cost of a higher quality limestone may not be worth it. Another way to achieve the lower combustor SO_2 concentration is to increase the current limestone CSR to about 4.2, but this is an unusually large increase in limestone which obviously doubles the limestone loading and unloading.

5.3 Parametric Analysis of Anonymous CFB Boiler Firing Tire Fuel

With the tire now being used as the fuel in the first combustor validated with modified kinetics, the inputs have been varied separately in order to study the effects of these key parameters on the outputs.

The hhv_{Fuel} was not varied since in the proposed model/program this input only affects the grams of species emitted per gigajoule produced by completely combusting one kilogram of fuel. Therefore, this value is always inversely proportional to hhv_{Fuel} as shown earlier and will always increase for all species when hhv_{Fuel} decreases and vice versa.

The proximate and ultimate analyses were not varied either seeing that a brief overview was already given when switching fuels from lignite to tire.

The d_{LSCaCO_3} was not varied since in the proposed model/program this input only affects the number of limestone particles in the combustor which perfectly balances with

the change in limestone diameter to not affect the effective cross-sectional area of the riser or anything else.

5.3.1 Fuel mass flow rate

The first input modified was $\dot{m}_{Fuel}$. Changing of the mass flow rate of the fuel without affecting temperatures such as T_{Mix} can only be achieved by increasing water flows through the tubes within the combustor walls to produce more steam which is assumed to be able to be handled by this combustor's tubes. Adding ten kilograms per second of fuel at a constant average hhv_{Fuel} while holding other inputs unmodified, raises the total heat generated by combustion to over 1100 MW. The increase in $\dot{m}_{Fuel}$ increases the $\dot{m}_{Bed\ Mix}$ due to the more fuel and limestone volatile matter being released from more fuel and limestone as well as the more actual combustion air needed to maintain the same $X_{Exc\ Air,Stoich\ Air}x100$. The increase in $\dot{m}_{Bed\ Mix}$ in turn increases the $V_{Bed\ Mix}$ which decreases the $t_{Res,Bed\ Mix}$ and Δt. This translates into the SMD size tire fuel not completely burning until higher up the riser at over half way. However, the trends are almost exactly the same just shortened due to less time spent in the riser as seen in the trends below in the graphs of the mole fraction of species in the mixture of gases versus time after the mixture of gases leaves the CFB bed until they reach the CFB riser exit for all species in Fig. 30 and trace species in Fig. 31.

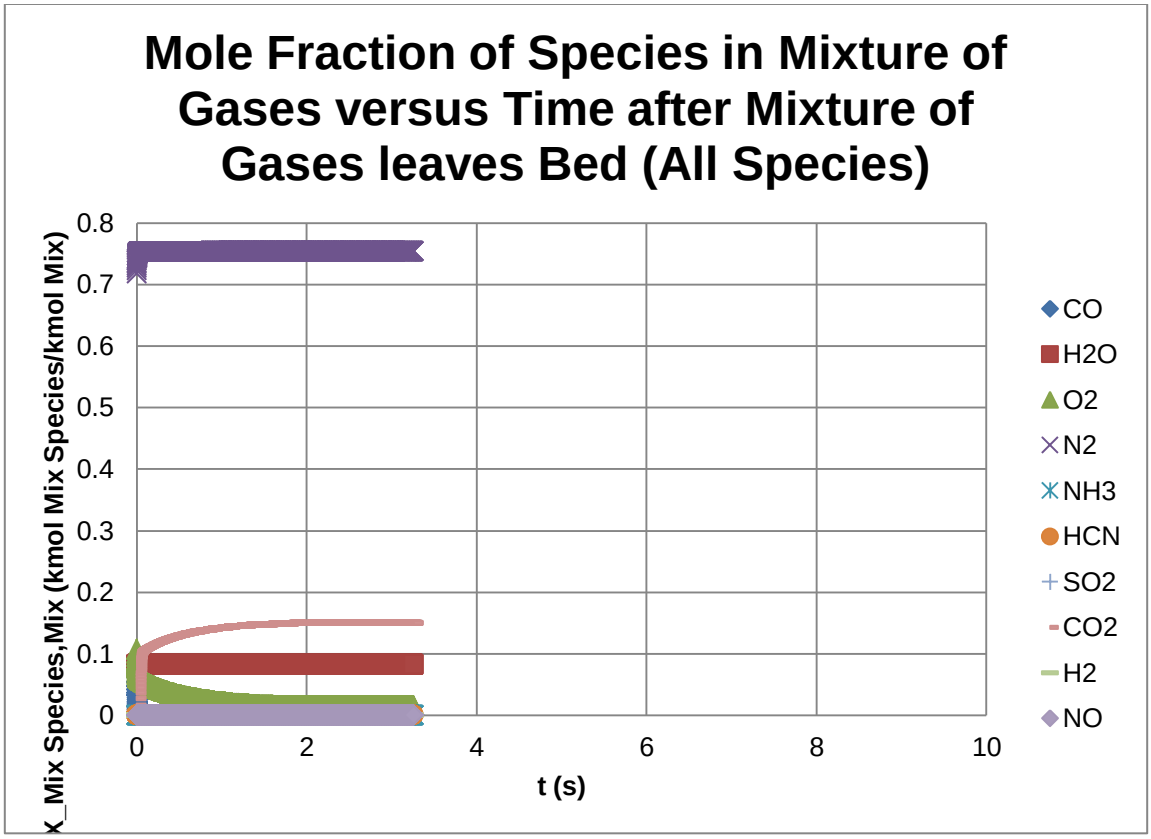

Fig. 30. Mole fraction of all species versus time for anonymous CFB boiler firing tire fuel with increased fuel mass flow rate.

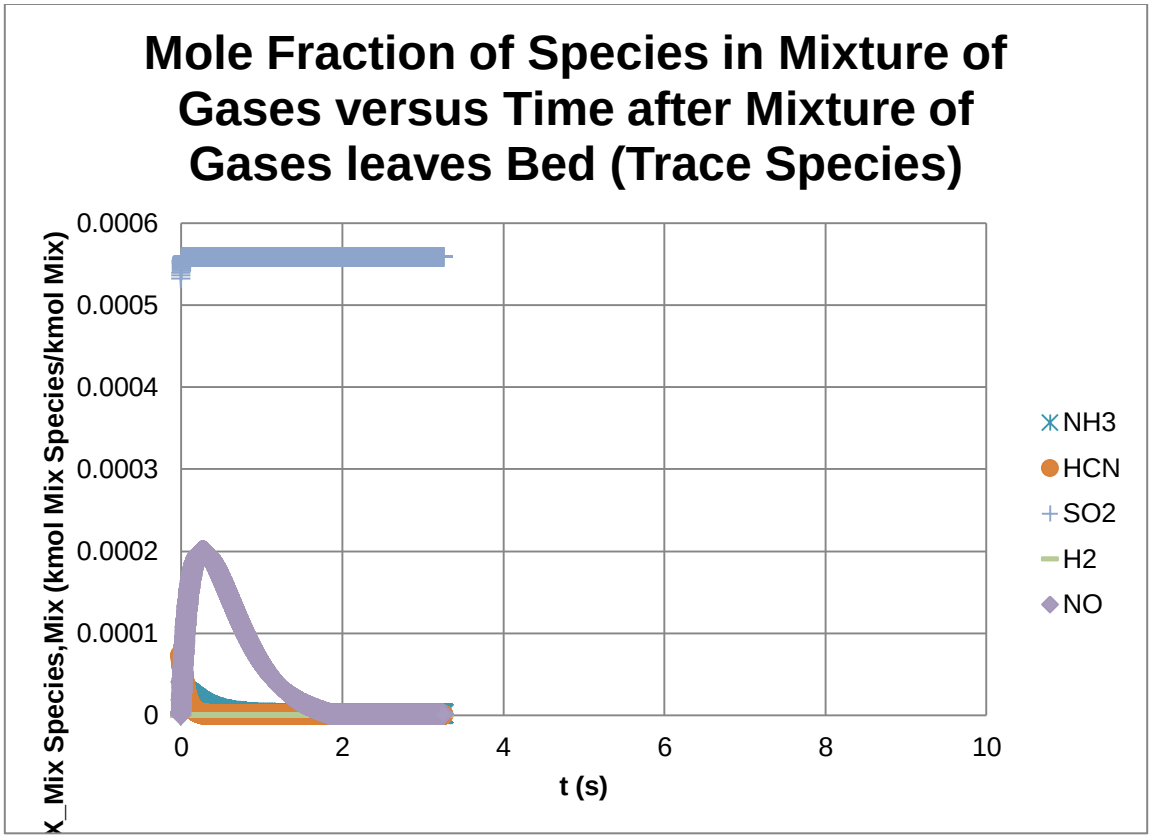

Fig. 31. Mole fraction of trace species versus time for anonymous CFB boiler firing tire fuel with increased fuel mass flow rate.

The nearly matching trends are greatly evident in the 'Output' tab of the Excel program as shown below in Table 18 where all species are basically unchanged with only trace species noticeably different such as CO and HCN which increase due to the less time available to react. Continuing to increase $\dot{m}_{Fuel}$ can begin to have drastic effects on the concentration of the species as less and less time is given for reactions to take place in the combustor.

Table 18

Output tab for anonymous CFB boiler firing tire fuel with increased fuel mass flow rate.

WET BASIS CONCENTRATION OF SPECIES IN MIXTURE OF GASES LEAVING CFB RISER										
	CO	H2O	O2	N2	NH3	HCN	SO2	CO2	H2	NO
ppm (Actual % O2)	8.48099E-15	82230.90868	14293.51197	753433.4239	1.387600025	7.05099E-14	558.2481612	149481.9819	1.76054E-05	0.537746261
Mole % (Actual % O2)	8.48099E-19	8.223090868	1.429351197	75.34334239	0.00013876	7.05099E-18	0.055824816	14.94819819	1.76054E-09	5.37746E-05
ppm (Standard % O2)	7.80034E-15	75631.44028	30000	756368.0864	1.276237733	6.48511E-14	513.445773	137485.2567	1.61924E-05	0.49458926
Mole % (Standard % O2)	7.80034E-19	7.563144028	3	F7/10000	0.000127624	6.48511E-18	0.051344577	13.74852567	1.61924E-09	4.94589E-05
g/GJ	2.98069E-15	18588.7942	5739.138226	264893.1758	0.296577841	2.39123E-14	448.7864975	82546.36864	4.45342E-07	0.310446944
DRY BASIS CONCENTRATION OF SPECIES IN MIXTURE OF GASES LEAVING CFB RISER										
	CO	H2O	O2	N2	NH3	HCN	SO2	CO2	H2	NO
ppm (Actual % O2)	9.24087E-15	0	15574.19193	820940.072	1.511927171	7.68275E-14	608.2664654	162875.3718	1.91828E-05	0.585927622
Mole % (Actual % O2)	9.24087E-19	0	1.557419193	82.0940072	0.000151193	7.68275E-18	0.060826647	16.28753718	1.91828E-09	5.85928E-05
ppm (Standard % O2)	8.55523E-15	0	30000	818644.412	1.399746738	7.11271E-14	563.1349298	150790.5108	1.77595E-05	0.542453561
Mole % (Standard % O2)	8.55523E-19	0	3	F16/10000	0.000139975	7.11271E-18	0.056313493	15.07905108	1.77595E-09	5.42454E-05
g/GJ	2.98069E-15	0	5739.138226	264893.1758	0.296577841	2.39123E-14	448.7864975	82546.36864	4.45342E-07	0.310446944

A decrease in $\dot{m}_{Fuel}$ without affecting temperatures such as T_{Mix} can only be achieved by decreasing water flows through the tubes within the combustor walls to produce less steam. Subtracting ten kilograms per second of fuel at a constant average hhv_{Fuel} while holding other inputs unmodified, lowers the total heat generated by combustion to only about 380 MW. The decrease in $\dot{m}_{Fuel}$ decreases the $\dot{m}_{Bed\ Mix}$ due to less fuel and limestone volatile matter being released from less fuel and limestone as well as less actual combustion air needed to maintain the same $X_{Exc\ Air,Stoich\ Air}x100$. The decrease in $\dot{m}_{Bed\ Mix}$ in turn decreases the $V_{Bed\ Mix}$ which increases the $t_{Res,Bed\ Mix}$ and Δt. This translates into the SMD size tire fuel completely burning lower in the riser at less than a fifth of the way. However, the problem with such a decrease in $V_{Bed\ Mix}$ to less than 4 meters per second is that the combustor is less like a CFB and more like a BFB so that it becomes more difficult for particles to become entrained in the slower moving gases. This means that more particles are stationary or maybe even move down upon entry into the combustor rather than continually moving up as assumed in the

proposed model. Since the proposed model is geared more towards a CFB combustor, there will begin to be skewed results for a BFB as seen earlier in the second combustor validated. Nevertheless, the trends according to the proposed model are almost exactly the same as before the decrease in $\dot{m}_{Fuel}$ except lengthened due to more time spent in the riser. These results are evident in the trends below in the graphs of the mole fraction of species in the mixture of gases versus time after the mixture of gases leaves the CFB bed until they reach the CFB riser exit for all species in Fig. 32 and trace species in Fig. 33.

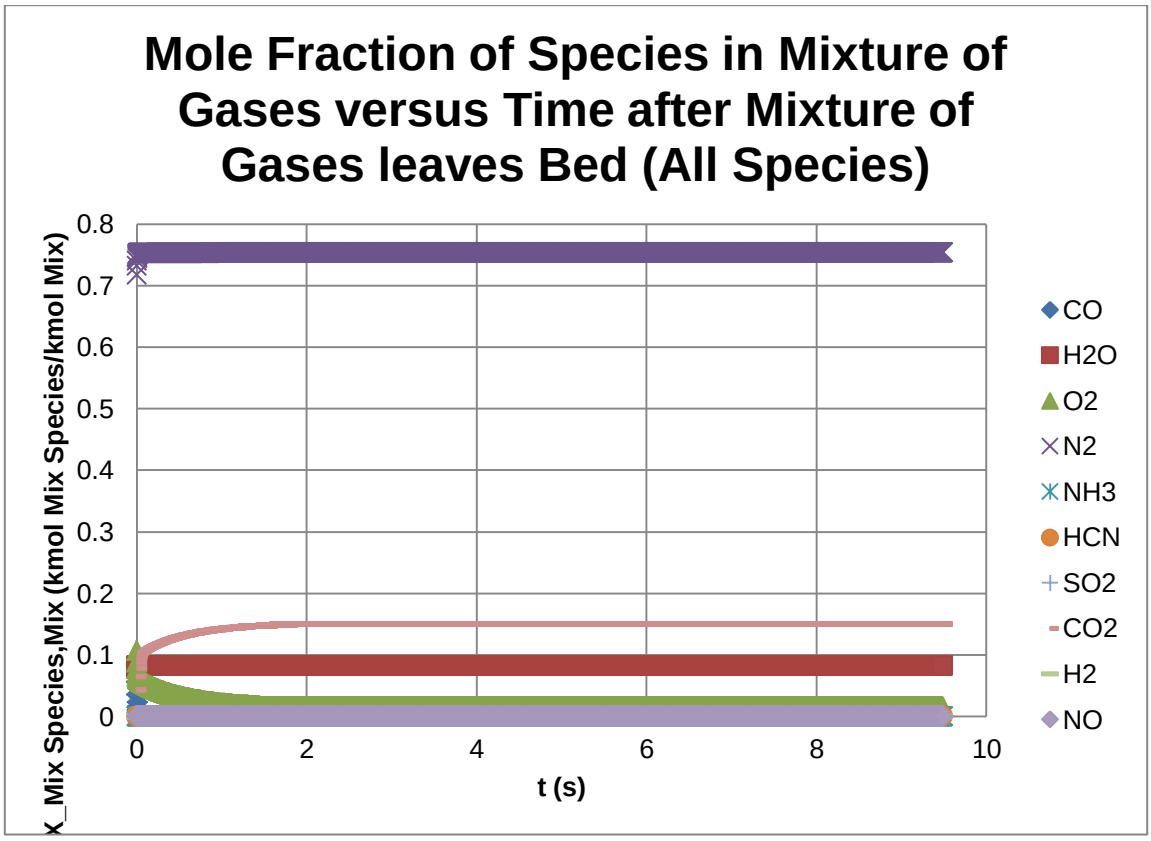

Fig. 32. Mole fraction of all species versus time for anonymous CFB boiler firing tire fuel with decreased fuel mass flow rate.

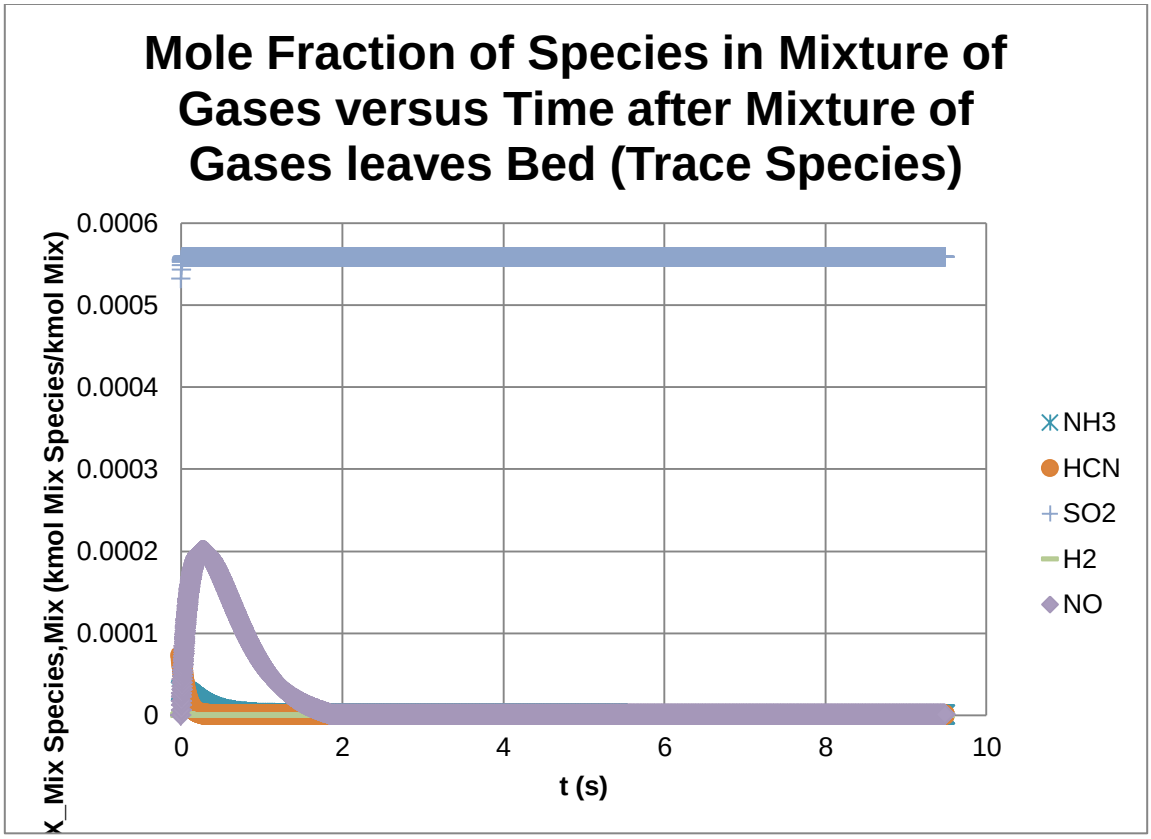

Fig. 33. Mole fraction of trace species versus time for anonymous CFB boiler firing tire fuel with decreased fuel mass flow rate.

The nearly matching trends are greatly evident in the 'Output' tab of the Excel program as shown below in Table 19 where all species are basically unchanged with only trace species noticeably different such as CO and HCN which decrease due to the more time available to react. Continuing to decrease $\dot{m}_{Fuel}$ can begin to have drastic effects on the accuracy of the concentrations of the species predicted by the proposed model as more and more time is spent by the fuel particles in the bottom of the

combustor so that eventually the combustor is not even fluidized anymore, but is a stationary combustor instead.

Table 19

Output tab for anonymous CFB boiler firing tire fuel with decreased fuel mass flow rate.

WET BASIS CONCENTRATION OF SPECIES IN MIXTURE OF GASES LEAVING CFB RISER										
	CO	H2O	O2	N2	NH3	HCN	SO2	CO2	H2	NO
ppm (Actual % O2)	3.81606E-38	82231.38532	14293.17749	753433.4326	1.065406992	3.1727E-37	558.2481163	149481.9699	4.28061E-05	0.721142026
Mole % (Actual % O2)	3.81606E-42	8.223138532	1.429317749	75.34334326	0.000106541	3.1727E-41	0.055824812	14.94819699	4.28061E-09	7.21142E-05
ppm (Standard % O2)	3.5098E-38	75631.74941	30000	756368.1519	0.979900732	2.91807E-37	513.4448541	137485.0107	3.93706E-05	0.663265404
Mole % (Standard % O2)	3.5098E-42	7.563174941	3	F7/10000	9.79901E-05	2.91807E-41	0.051344485	13.74850107	3.93706E-09	6.63265E-05
g/GJ	1.34118E-38	18588.90344	5739.004387	264893.2002	0.227714128	1.07597E-37	448.7864975	82546.36864	1.08281E-06	0.416323409
DRY BASIS CONCENTRATION OF SPECIES IN MIXTURE OF GASES LEAVING CFB RISER										
	CO	H2O	O2	N2	NH3	HCN	SO2	CO2	H2	NO
ppm (Actual % O2)	4.15798E-38	0	15573.83556	820940.5078	1.160866666	3.45697E-37	608.2667323	162875.4432	4.66414E-05	0.785755816
Mole % (Actual % O2)	4.15798E-42	0	1.557383556	82.09405078	0.000116087	3.45697E-41	0.060826673	16.28754432	4.66414E-09	7.85756E-05
ppm (Standard % O2)	3.84946E-38	0	30000	818644.763	1.074731894	3.20047E-37	563.1341447	150790.3006	4.31807E-05	0.727453773
Mole % (Standard % O2)	3.84946E-42	0	3	F16/10000	0.000107473	3.20047E-41	0.056313414	15.07903006	4.31807E-09	7.27454E-05
g/GJ	1.34118E-38	0	5739.004387	264893.2002	0.227714128	1.07597E-37	448.7864975	82546.36864	1.08281E-06	0.416323409

5.3.2 Fuel density

Returning the $\dot{m}_{Fuel}$ to its original value, the ρ_{Fuel} was then modified. Adding 400 kilograms per cubic meter to the density of the as-received fuel almost doubles the amount of fixed Carbon and Nitrogen in each char particle. However, the increase in $V_{term,d_{Fuel}}$ from having a denser particle with larger $Re_{d_{Fuel}}$ leading to larger $Sh_{d_{Fuel}}$ which increases the amount of fixed Carbon and Nitrogen oxidized per particle does not increase as much. Therefore, the particle is shrinking slower than before because the mass being removed is relatively less than what was added throughout the char. This coupled with the fact that there are now less particles/surface area to react with due to each particle now containing more of the mass hinders the combustion rate of the char particles. This translates into the SMD size tire fuel not completely burning until higher up the riser at almost two thirds of the way. However, the trends are still closely similar

except for less steep as combustion is drawn out as seen in the trends below in the graph of the mole fraction of species in the mixture of gases versus time after the mixture of gases leaves the CFB bed until they reach the CFB riser exit for all species in Fig. 34.

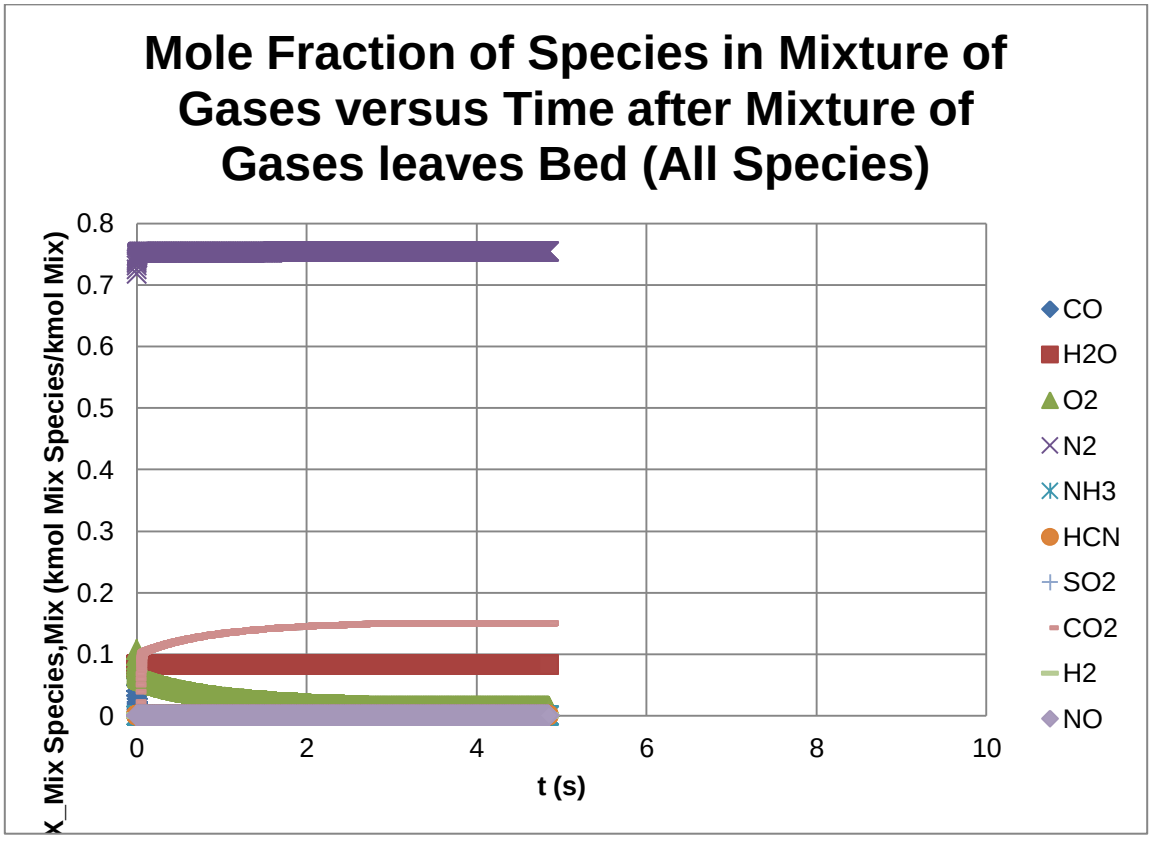

Fig. 34. Mole fraction of all species versus time for anonymous CFB boiler firing tire fuel with increased fuel density.

The NO concentration is even more so affected by the reduced number of char particles to react with as seen not only by the lengthening out of the trend, but also the larger concentration achieved at the peak due to lack of reducing surfaces as seen below

in the graph of the mole fraction of species in the mixture of gases versus time after the mixture of gases leaves the CFB bed until they reach the CFB riser exit for trace species in Fig. 35.

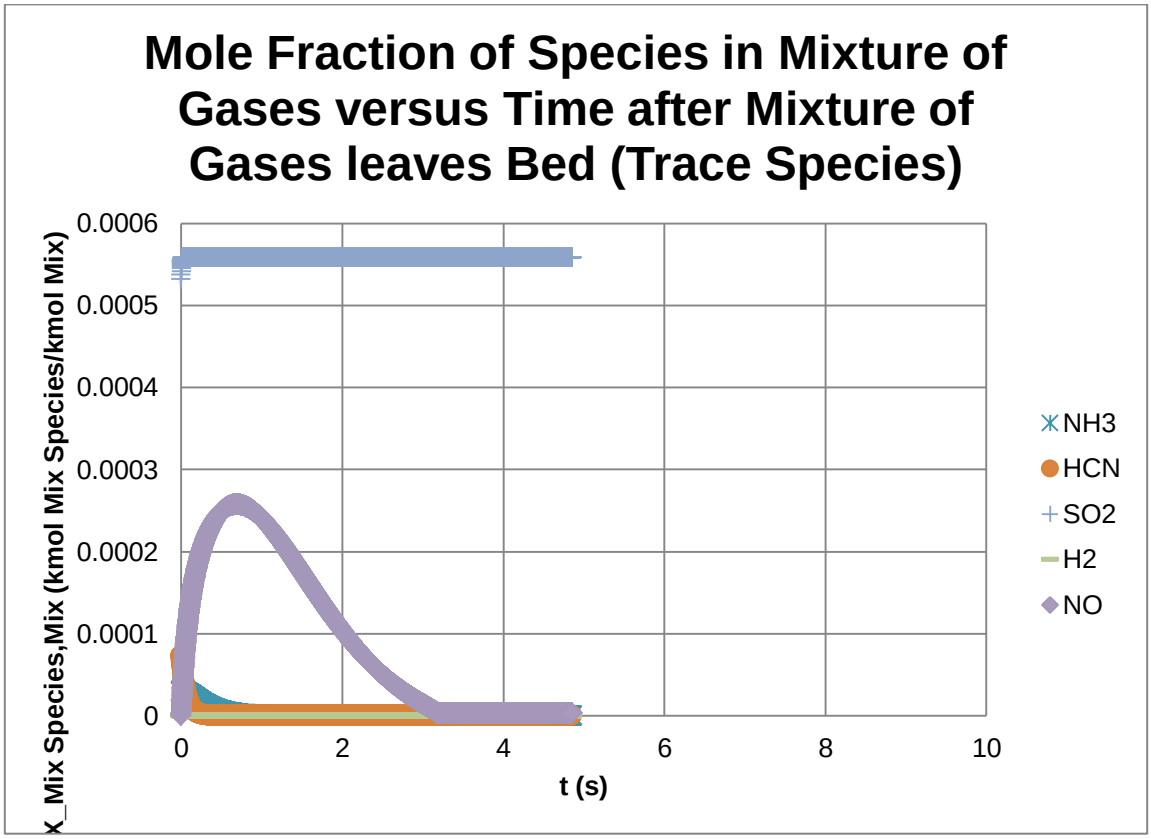

Fig. 35. Mole fraction of trace species versus time for anonymous CFB boiler firing tire fuel with increased fuel density.

The nearly matching concentrations at the riser exit are greatly evident in the 'Output' tab of the Excel program as shown below in Table 20 where all species are basically unchanged. Continuing to increase ρ_{Fuel} can begin to have more drastic

effects on the concentration of the species as more and more time is required to burn the fewer and fewer particles and the heavier particles begin to stay longer in the bottom of the combustor rather than be entrained upwards.

Table 20

Output tab for anonymous CFB boiler firing tire fuel with increased fuel density.

WET BASIS CONCENTRATION OF SPECIES IN MIXTURE OF GASES LEAVING CFB RISER										
	CO	H2O	O2	N2	NH3	HCN	SO2	CO2	H2	NO
ppm (Actual % O2)	8.96826E-23	82232.95277	14291.05194	753432.4356	0.005949892	7.45728E-22	558.2479684	149481.9303	2.64888E-07	3.375441198
Mole % (Actual % O2)	8.96826E-27	8.223295277	1.429105194	75.34324356	5.94989E-07	7.45728E-26	0.055824797	14.94819303	2.64888E-11	0.000337544
ppm (Standard % O2)	8.24841E-23	75632.36962	30000	756367.6002	0.005472313	6.8587E-22	513.4391417	137483.4811	2.43627E-07	3.10450504
Mole % (Standard % O2)	8.24841E-27	7.563236962	3	F7/10000	5.47231E-07	6.8587E-26	0.051343914	13.74834811	2.43627E-11	0.000310451
g/GJ	3.15195E-23	18589.2627	5738.152456	264892.9199	0.001271697	2.52902E-22	448.7864975	82546.36864	6.70056E-09	1.948680713
DRY BASIS CONCENTRATION OF SPECIES IN MIXTURE OF GASES LEAVING CFB RISER										
	CO	H2O	O2	N2	NH3	HCN	SO2	CO2	H2	NO
ppm (Actual % O2)	9.77183E-23	0	15571.54616	820940.8236	0.006483009	8.12546E-22	608.2676101	162875.6783	2.88623E-07	3.6778845
Mole % (Actual % O2)	9.77183E-27	0	1.557154616	82.09408236	6.48301E-07	8.12546E-26	0.060826761	16.28756783	2.88623E-11	0.000367788
ppm (Standard % O2)	9.04667E-23	0	30000	818644.7181	0.006001907	7.52247E-22	563.1283264	150788.7426	2.67204E-07	3.404950237
Mole % (Standard % O2)	9.04667E-27	0	3	F16/10000	6.00191E-07	7.52247E-26	0.056312833	15.07887426	2.67204E-11	0.000340495
g/GJ	3.15195E-23	0	5738.152456	264892.9199	0.001271697	2.52902E-22	448.7864975	82546.36864	6.70056E-09	1.948680713

Subtracting 400 kilograms per cubic meter from the density of the as-received fuel almost reduces to a fourth the amount of fixed Carbon and Nitrogen in each char particle. However, the decrease in $V_{term,d_{Fuel}}$ from having a less dense particle with smaller $Re_{d_{Fuel}}$ leading to smaller $Sh_{d_{Fuel}}$ which decreases the amount of fixed Carbon and Nitrogen oxidized per particle does not decrease as much. Therefore, the particle is shrinking faster than before because the mass being removed is relatively more than what was subtracted throughout the char. This coupled with the fact that there are now more particles/surface area to react with due to each particle now containing less of the mass enhances the combustion rate of the char particles. This translates into the SMD size tire fuel completely burning at only a tenth of the way up the riser. However, the

trends are still closely similar except for more steep as combustion is quickened as seen in the trends below in the graph of the mole fraction of species in the mixture of gases versus time after the mixture of gases leaves the CFB bed until they reach the CFB riser exit for all species in Fig. 36.

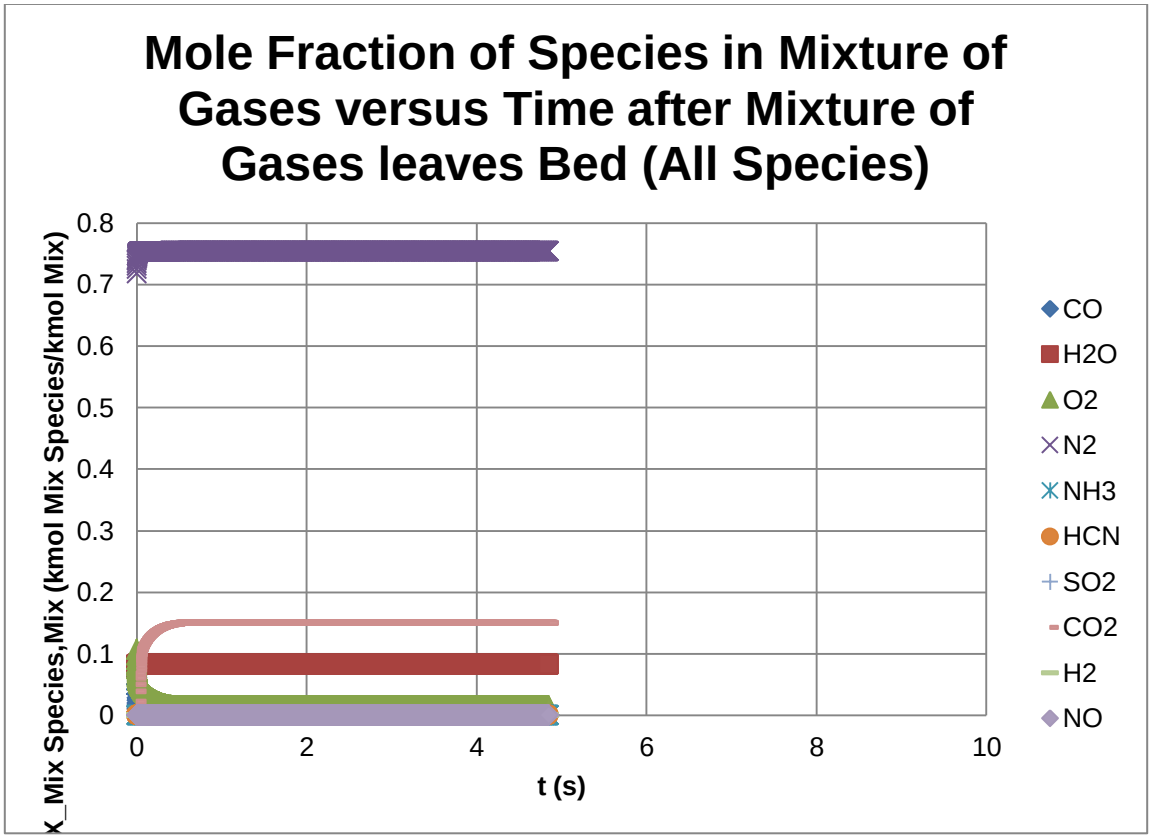

Fig. 36. Mole fraction of all species versus time for anonymous CFB boiler firing tire fuel with decreased fuel density.

The NO concentration is even more so affected by the increased number of char particles to react with as seen not only by the shortening out of the trend, but also the smaller concentration achieved at the peak due to abundance of reducing surfaces. Interestingly, the NO concentration is nevertheless slightly higher at the riser exit likely due to the reduced time to react with char particles and the relatively much slower reaction rates with NH_3 and HCN. The CO is increased due to the increased reaction rate of NO with char fixed Carbon. On the other hand, the NH_3 and HCN have increased due to the lack of NO available to react with. These trends are seen below in the graph of the mole fraction of species in the mixture of gases versus time after the mixture of gases leaves the CFB bed until they reach the CFB riser exit for trace species in Fig. 37.

The nearly matching concentrations at the riser exit are greatly evident in the 'Output' tab of the Excel program as shown below in Table 21 where all species are basically unchanged. Continuing to decrease ρ_{Fuel} can begin to have more drastic effects on the concentration of the trace species (especially increasing NO) as less and less time is required to burn the more and more particles and the lighter particles begin to stay shorter in the combustor being entrained upwards at basically the same speed as the gas mixture.

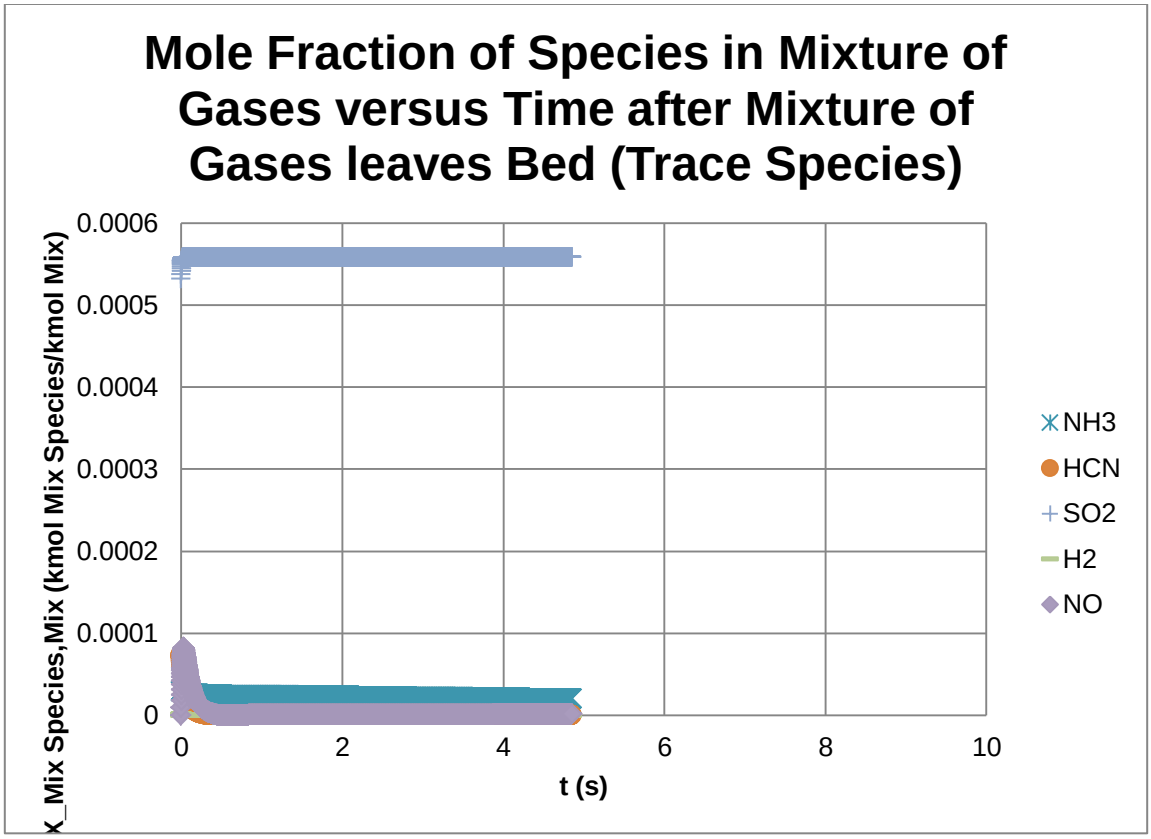

Fig. 37. Mole fraction of trace species versus time for anonymous CFB boiler firing tire fuel with decreased fuel density.

Table 21

Output tab for anonymous CFB boiler firing tire fuel with decreased fuel density.

WET BASIS CONCENTRATION OF SPECIES IN MIXTURE OF GASES LEAVING CFB RISER										
	CO	H2O	O2	N2	NH3	HCN	SO2	CO2	H2	NO
ppm (Actual % O2)	1.45057E-18	82203.27924	14307.1779	753427.1963	20.06282347	1.20477E-17	558.2507674	149482.6798	0.000526419	1.352678738
Mole % (Actual % O2)	1.45057E-22	8.220327924	1.43071779	75.34271963	0.002006282	1.20477E-21	0.055825077	14.94826798	5.26419E-08	0.000135268
ppm (Standard % O2)	1.33425E-18	75611.3081	30000	756360.0095	18.45396365	1.10816E-17	513.484026	137495.4997	0.000484205	1.244205946
Mole % (Standard % O2)	1.33425E-22	7.56113081	3	F7/10000	0.001845396	1.10816E-21	0.051348403	13.74954997	4.84205E-08	0.000124421
g/GJ	5.0981E-19	18582.46164	5744.598559	264889.7497	4.288095254	4.08578E-18	448.7864975	82546.36864	1.33161E-05	0.780912952
DRY BASIS CONCENTRATION OF SPECIES IN MIXTURE OF GASES LEAVING CFB RISER										
	CO	H2O	O2	N2	NH3	HCN	SO2	CO2	H2	NO
ppm (Actual % O2)	1.58049E-18	0	15588.61301	820908.5729	21.85976809	1.31268E-17	608.2509937	162871.2289	0.000573568	1.473832611
Mole % (Actual % O2)	1.58049E-22	0	1.558861301	82.09085729	0.002185977	1.31268E-21	0.060825099	16.28712289	5.73568E-08	0.000147383
ppm (Standard % O2)	1.46334E-18	0	30000	818617.3727	20.23934049	1.21537E-17	563.1623773	150797.8604	0.00053105	1.364579895
Mole % (Standard % O2)	1.46334E-22	0	3	F16/10000	0.002023934	1.21537E-21	0.056316238	15.07978604	5.3105E-08	0.000136458
g/GJ	5.0981E-19	0	5744.598559	264889.7497	4.288095254	4.08578E-18	448.7864975	82546.36864	1.33161E-05	0.780912952

5.3.3 Fuel Sauter Mean Diameter

Returning the ρ_{Fuel} to its original value, the $d_{Fuel,0}$ was then altered. Multiplying by ten times the initial SMD of the as-received fuel increased the amount of fixed Carbon and Nitrogen in each char particle by a factor of 1,000. However, the increase in $V_{term,d_{Fuel}}$ from having a larger particle with larger $Re_{d_{Fuel}}$ leading to larger $Sh_{d_{Fuel}}$ which increases the amount of fixed Carbon and Nitrogen oxidized per particle does not increase as much similar to what occurred with the increase in ρ_{Fuel}. Therefore, the particle is shrinking slower than before because the mass being removed is relatively less than what was added with the increased size of the char. This coupled with the fact that there are now only one-one thousandth as many particles/surface area to react with due to each particle now containing more of the mass hinders the combustion rate of the char particles. This translates into the SMD size tire fuel not completely burning in the riser. In fact, almost 73% of the tire is still left unburned at the exit of the riser. This also means that there will still likely need to be a significant amount of processing of the tire fuel in order to be able to have a SMD size particle that allows for more complete burning of the tire in the combustor. This lack of complete burning is especially apparent in the O_2 and CO_2 trends that are never quite leveled out, but instead maintain a fairly gradual slope throughout the riser as seen below in the graph of the mole fraction of species in the mixture of gases versus time after the mixture of gases leaves the CFB bed until they reach the CFB riser exit for all species in Fig. 38.

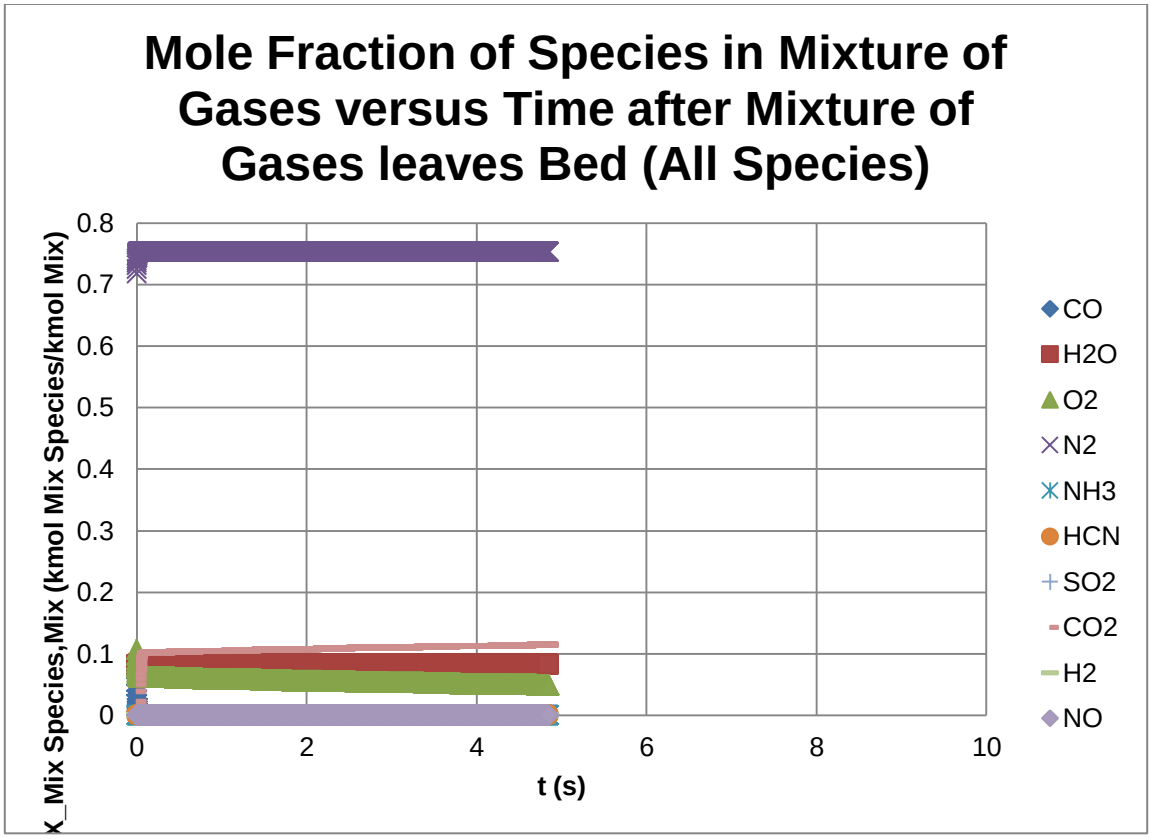

Fig. 38. Mole fraction of all species versus time for anonymous CFB boiler firing tire fuel with increased fuel SMD.

The NO concentration is once again even more so affected by the reduced number of char particles to react with as the slope is steep in the beginning with high O_2 concentration, and then the NO continues steadily increasing with the prolonged burning of the tire. Therefore, the larger NO concentration achieved is due to lack of reducing surfaces. Not as nearly noticeable, the lower amounts of NH_3 and HCN are attributed to the increased concentration of NO to react with. These trends can be viewed below in the graph of the mole fraction of species in the mixture of gases versus time after the

mixture of gases leaves the CFB bed until they reach the CFB riser exit for trace species in Fig. 39.

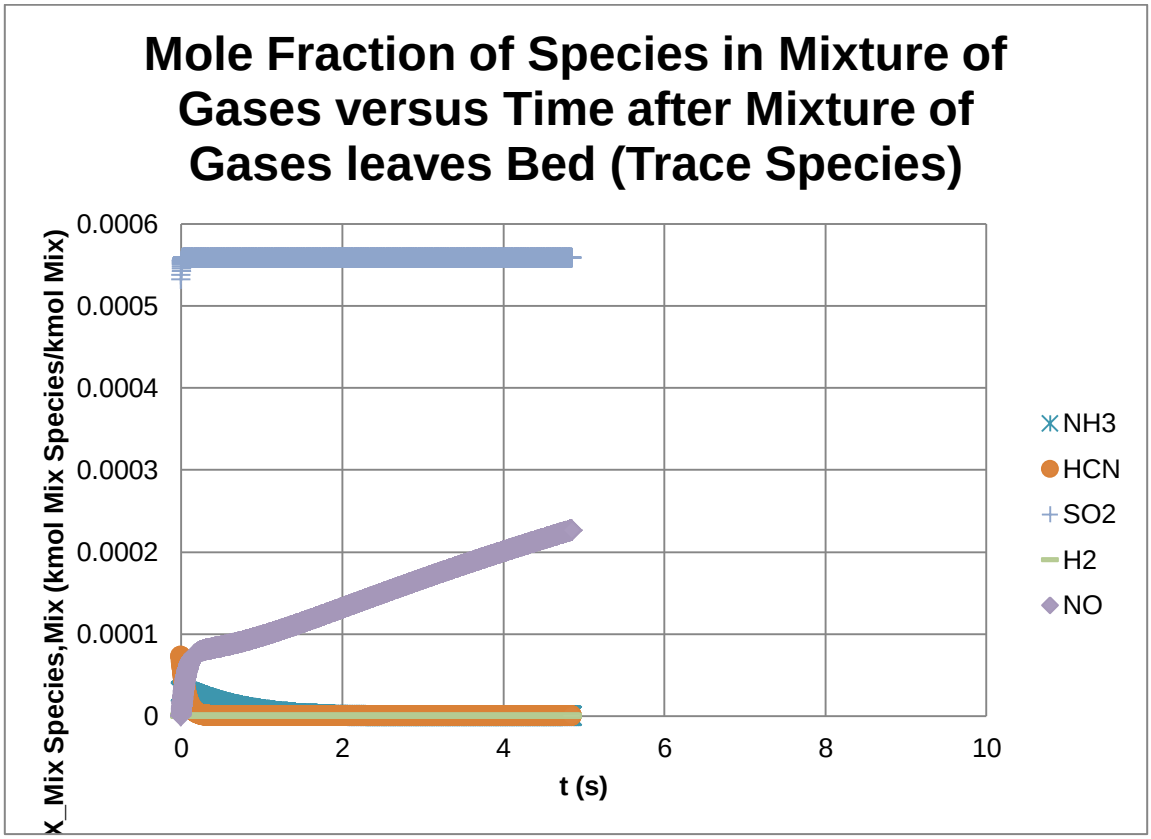

Fig. 39. Mole fraction of trace species versus time for anonymous CFB boiler firing tire fuel with increased fuel SMD.

The concentrations at the riser exit are more affected due to the lack of burning taking place as seen in the 'Output' tab of the Excel program below in Table 22. The lack of burning of the char is most easily seen in the increased amount of O_2 and decreased amount of CO_2 left at the exit of the riser. The CO concentration has

increased due to both a more continual formation from fixed Carbon oxidation and NO reduction as well as a lower oxidation rate due to a lower average of CO since the oxidation of CO is more highly dependent upon its concentration than that of O_2. Continuing to increase $d_{Fuel,0}$ will continue to have more drastic effects on the concentration of the species (especially the O_2 and CO_2) as more and more time is required to burn the fewer and fewer particles and the heavier particles begin to stay longer in the bottom of the combustor rather than be entrained upwards. If the fuel particles are too big, then there may be feeding issues also.

Table 22

Output tab for anonymous CFB boiler firing tire fuel with increased fuel SMD.

WET BASIS CONCENTRATION OF SPECIES IN MIXTURE OF GASES LEAVING CFB RISER										
	CO	H2O	O2	N2	NH3	HCN	SO2	CO2	H2	NO
ppm (Actual % O2)	14.79148502	82252.00189	49179.37779	753256.3793	4.69611E-05	1.2819E-30	558.3772255	114512.5527	9.71761E-08	226.519549
Mole % (Actual % O2)	0.001479149	8.225200189	4.917937779	75.32563793	4.69611E-09	1.2819E-34	0.055837723	11.45125527	9.71761E-12	0.022651955
ppm (Standard % O2)	16.55550929	92061.3298	30000	748874.3556	5.25616E-05	1.43478E-30	624.9689822	128169.2559	1.08765E-07	253.5341442
Mole % (Standard % O2)	0.001655551	9.20613298	3	F7/10000	5.25616E-09	1.43478E-34	0.062496898	12.81692559	1.08765E-11	0.025353414
g/GJ	6.785194498	24268.46257	25773.32335	345659.3935	1.31006E-05	5.67421E-31	585.8950578	82535.70758	3.20839E-09	170.6849919
DRY BASIS CONCENTRATION OF SPECIES IN MIXTURE OF GASES LEAVING CFB RISER										
	CO	H2O	O2	N2	NH3	HCN	SO2	CO2	H2	NO
ppm (Actual % O2)	16.11715313	0	53587.01724	820766.0282	5.11699E-05	1.39679E-30	608.421077	124775.5952	1.05885E-07	246.8210767
Mole % (Actual % O2)	0.001611715	0	5.358701724	82.07660282	5.11699E-09	1.39679E-34	0.060842108	12.47755952	1.05885E-11	0.024682108
ppm (Standard % O2)	18.54761359	0	30000	825405.5334	5.88863E-05	1.60742E-30	700.1707399	143591.7066	1.21853E-07	284.0415995
Mole % (Standard % O2)	0.001854761	0	3	F16/10000	5.88863E-09	1.60742E-34	0.070017074	14.35917066	1.21853E-11	0.02840416
g/GJ	6.785194498	0	25773.32335	345659.3935	1.31006E-05	5.67421E-31	585.8950578	82535.70758	3.20839E-09	170.6849919

Dividing by ten the initial SMD of the as-received fuel decreased the amount of fixed Carbon and Nitrogen in each char particle by a factor of 1,000. However, the decrease in $V_{term,d_{Fuel}}$ from having a smaller particle with smaller $Re_{d_{Fuel}}$ leading to smaller $Sh_{d_{Fuel}}$ which decreases the amount of fixed Carbon and Nitrogen oxidized per particle does not decrease as much similar to what also occurred with the decrease in ρ_{Fuel}. Therefore, the particle is shrinking faster than before because the mass being removed is relatively more than what was subtracted with the decreased size of the char. This coupled with the fact that there are now 1,000 times as many particles/surface area to react with due to each particle now containing less of the mass enhances the combustion rate of the char particles. This translates into the SMD size tire fuel completely burning less than 1% of the way up the riser. This incredible rate of complete burning is especially apparent in the O_2 and CO_2 trends that almost instantaneously leveled out as seen below in the graph of the mole fraction of species in the mixture of gases versus time after the mixture of gases leaves the CFB bed until they reach the CFB riser exit for all species in Fig. 40.

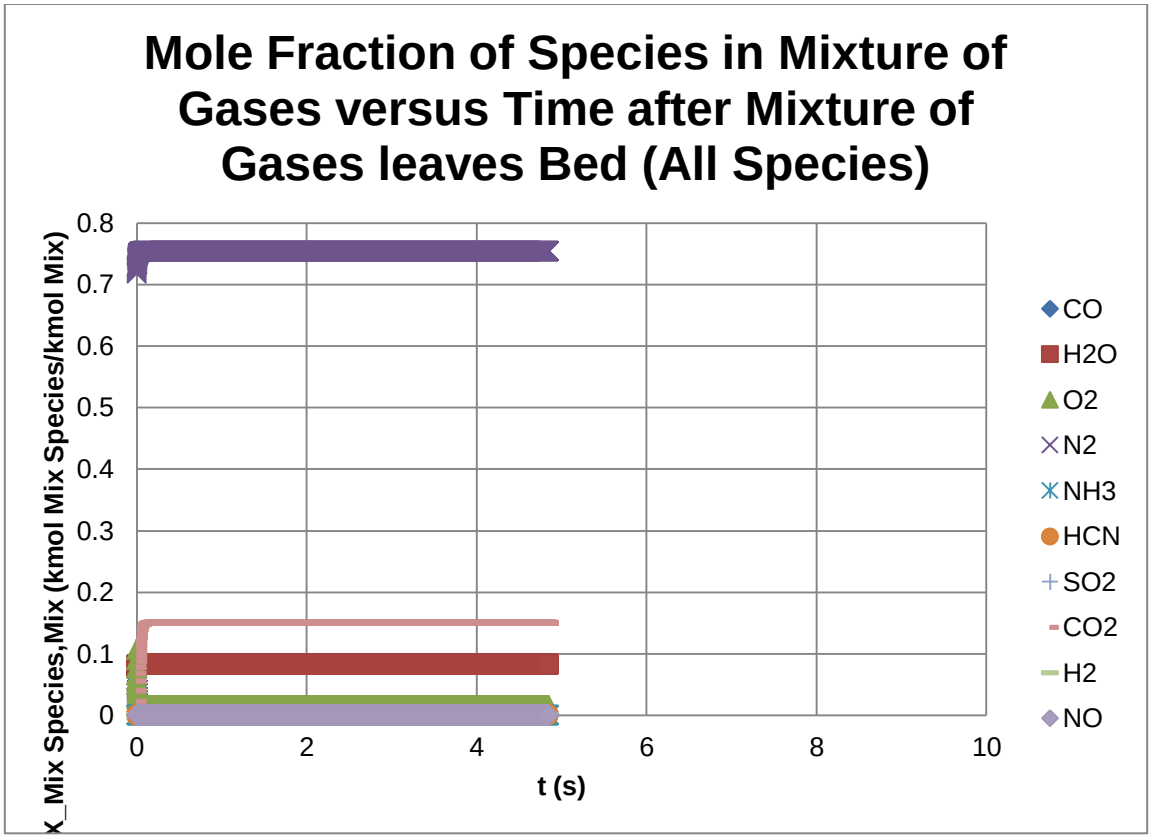

Fig. 40. Mole fraction of all species versus time for anonymous CFB boiler firing tire fuel with decreased fuel SMD.

The NO concentration is once again even more so affected by the enlarged number of char particles to react with as the slope is extremely steep in the beginning with high O_2 concentration leading to high fixed Nitrogen oxidation rates, and then the NO quickly levels off after the char is all burned while only slightly decreasing with NH_3 and HCN reactions. Therefore, the smaller peak NO concentration achieved is due to abundance of reducing surfaces for a short amount of time. However, the higher NO concentration at the exit of the riser is attributed to the NO not having the continued char

particle surfaces to be reduced on. This trend can be viewed below in the graph of the mole fraction of species in the mixture of gases versus time after the mixture of gases leaves the CFB bed until they reach the CFB riser exit for trace species in Fig. 41.

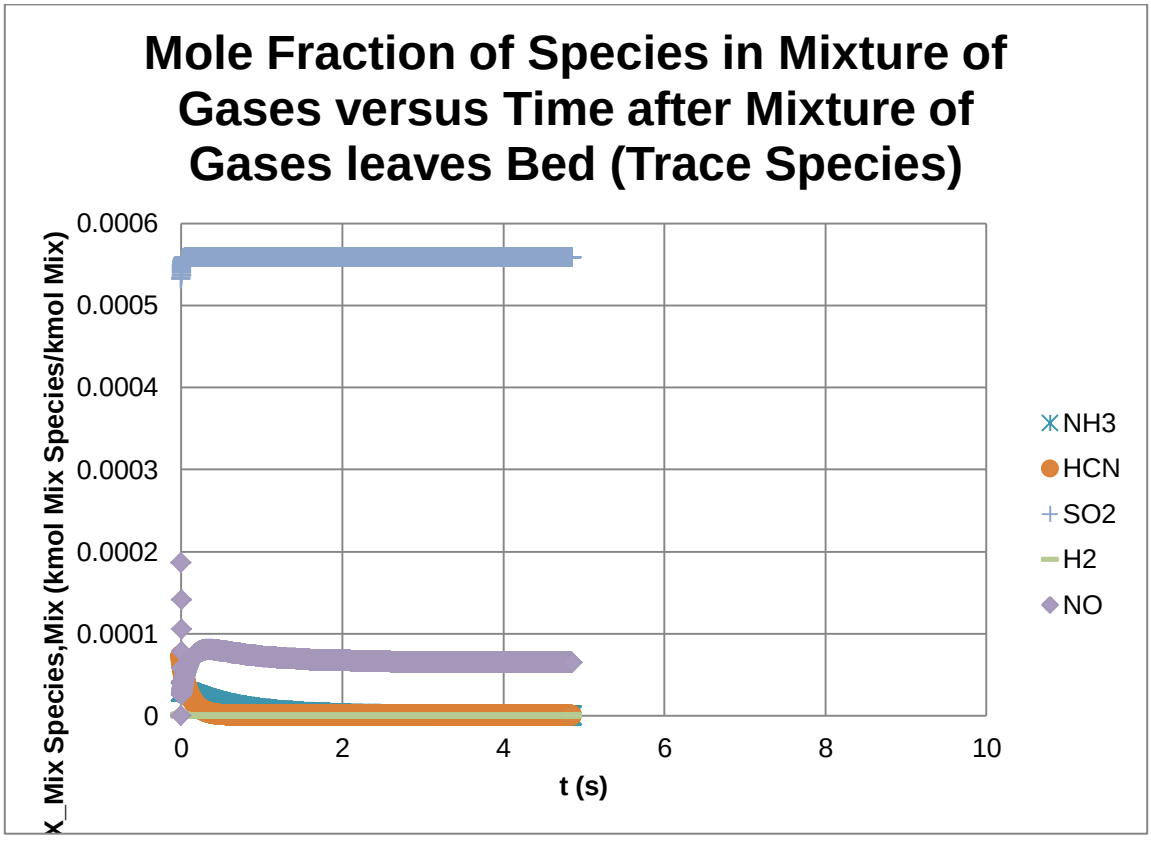

Fig. 41. Mole fraction of trace species versus time for anonymous CFB boiler firing tire fuel with decreased fuel SMD.

The nearly matching trends are greatly evident in the 'Output' tab of the Excel program as shown below in Table 23 where most species are basically unchanged. Continuing to decrease $d_{Fuel,0}$ can begin to have more drastic effects on the

concentration of the trace species (especially increasing NO) as less and less time is required to burn the more and more particles and the lighter particles begin to stay shorter in the combustor being entrained upwards at basically the same speed as the gas mixture. If the fuel particles are too small (approaching 0.3 microns), then the mean free path of the gas mixture (λ_{Mix}) becomes increasingly important since fuel particles could then begin to slip by gas particles so that the gas mixture can no longer be considered a continuum fluid. Instead, discrete molecule interactions would need to be considered with the char and limestone particles.

Table 23

Output tab for anonymous CFB boiler firing tire fuel with decreased fuel SMD.

WET BASIS CONCENTRATION OF SPECIES IN MIXTURE OF GASES LEAVING CFB RISER										
	CO	H2O	O2	N2	NH3	HCN	SO2	CO2	H2	NO
ppm (Actual % O2)	8.2393E-18	82232.87707	14260.21405	753401.5432	0.057089851	6.86317E-17	558.2479755	149481.9322	3.44202E-05	65.12833368
Mole % (Actual % O2)	8.2393E-22	8.223287707	1.426021405	75.34015432	5.70899E-06	6.86317E-21	0.055824798	14.94819322	3.44202E-09	0.006512833
ppm (Standard % O2)	7.57676E-18	75620.38449	30000	756344.4905	0.052499154	6.31129E-17	513.3582583	137461.8229	3.16524E-05	59.891248
Mole % (Standard % O2)	7.57676E-22	7.562038449	3	F7/10000	5.24992E-06	6.31129E-21	0.051335826	13.74618229	3.16524E-09	0.005989125
g/GJ	2.89575E-18	18589.24535	5725.770332	264882.0553	0.012202068	2.32754E-17	448.7864975	82546.36864	8.70686E-07	37.59932958
DRY BASIS CONCENTRATION OF SPECIES IN MIXTURE OF GASES LEAVING CFB RISER										
	CO	H2O	O2	N2	NH3	HCN	SO2	CO2	H2	NO
ppm (Actual % O2)	8.97755E-18	0	15537.94388	820907.0955	0.062205161	7.47811E-17	608.2675677	162875.6669	3.75043E-05	70.96389929
Mole % (Actual % O2)	8.97755E-22	0	1.553794388	82.09070955	6.22052E-06	7.47811E-21	0.060826757	16.28756669	3.75043E-09	0.00709639
ppm (Standard % O2)	8.30989E-18	0	30000	818608.5486	0.057578991	6.92197E-17	563.0309808	150762.6764	3.47151E-05	65.68634585
Mole % (Standard % O2)	8.30989E-22	0	3	F16/10000	5.7579E-06	6.92197E-21	0.056303098	15.07626764	3.47151E-09	0.006568635
g/GJ	2.89575E-18	0	5725.770332	264882.0553	0.012202068	2.32754E-17	448.7864975	82546.36864	8.70686E-07	37.59932958

5.3.4 Volatile Nitrogen to N_2

Returning the $d_{Fuel,0}$ to its original value, the $Y_{N_2,N}x100$ was then altered. In order to alter the $Y_{N_2,N}x100$, the $Y_{VN,N}x100$ must also be changed so that the other volatile Nitrogen conversions to NH_3 and HCN remain the same. Since $Y_{N_2,N}x100$ is originally 0%, this value is only to be increased for the parametric study of the proposed

model seeing that a negative value would be unrealistic and meaningless. Therefore, adding 4% to the mass percent of fuel Nitrogen released as volatile matter and subsequently converted to N_2 also requires adding 4% to the total mass percent of fuel Nitrogen released as volatile matter (which includes what is converted to NH_3 and HCN). Very little change can be seen in the resulting concentrations of the species, but basically the more volatile Nitrogen converted to N_2 means there is less fixed Nitrogen available to be oxidized to NO. However, this also means less NO is available to react with NH_3 so that NH_3 increases. The less fixed Nitrogen is replaced by more fixed Carbon (leading to slightly longer burn time required since fixed Nitrogen oxidizes proportionally to that of fixed Carbon); and therefore, less volatile Carbon so that CO decreases which leads to higher O_2. Even though N_2 actually increases from the combustor bed, the new kilogram-moles of the mixture of gases per cubic meter of the mixture of gases (N'''_{Mix}) at the riser exit causes the concentration to be lower than before. The almost identical trends are shown below in the graphs of the mole fraction of species in the mixture of gases versus time after the mixture of gases leaves the CFB bed until they reach the CFB riser exit for all species in Fig. 42 and trace species in Fig. 43.

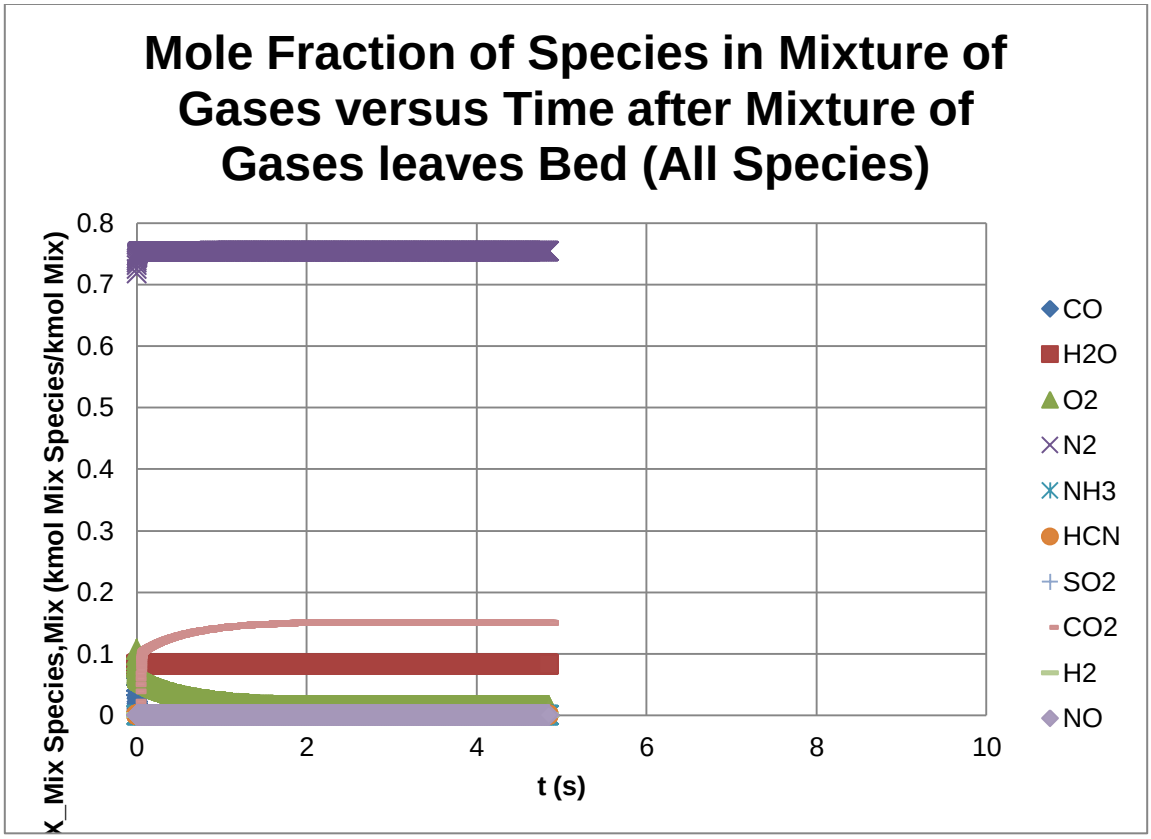

Fig. 42. Mole fraction of all species versus time for anonymous CFB boiler firing tire fuel with 4% increase in volatile Nitrogen to N_2.

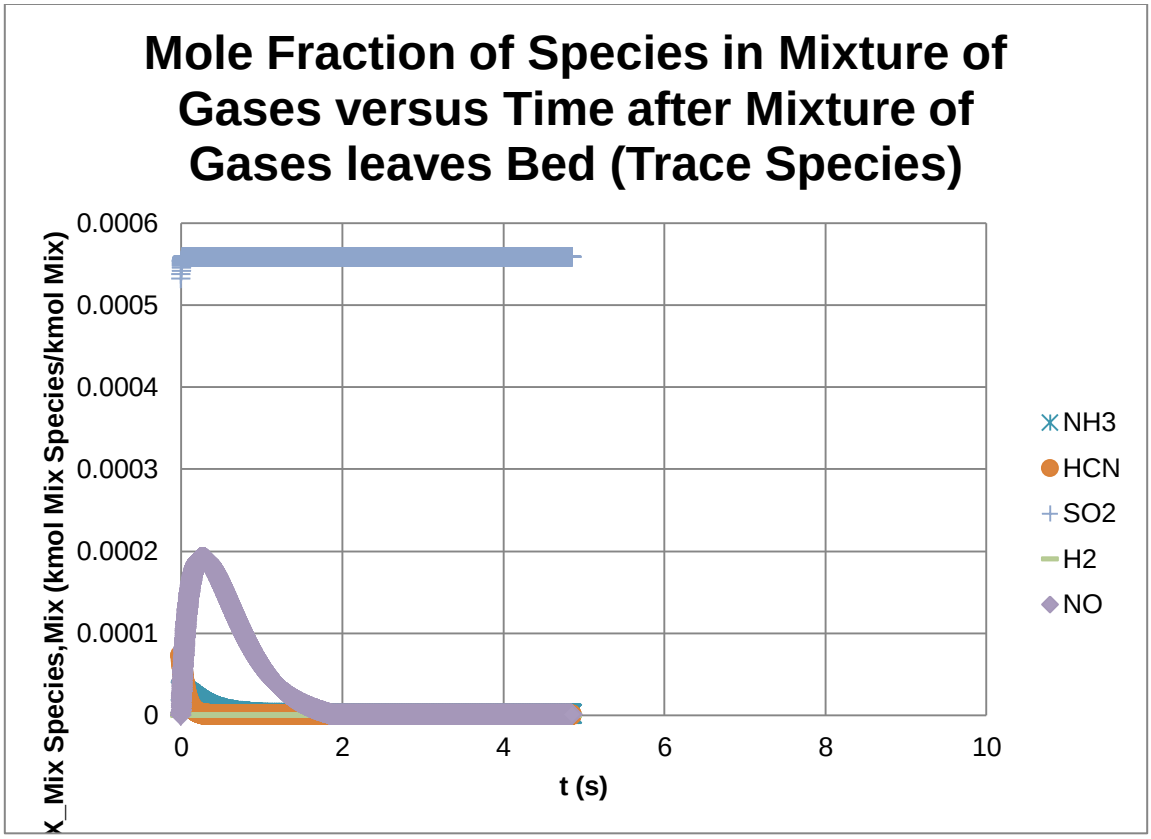

Fig. 43. Mole fraction of trace species versus time for anonymous CFB boiler firing tire fuel with 4% increase in volatile Nitrogen to N_2.

The nearly identical trends are greatly evident in the 'Output' tab of the Excel program as shown below in Table 24 where all species are basically unchanged.

Table 24

Output tab for anonymous CFB boiler firing tire fuel with 4% increase in volatile Nitrogen to N_2.

WET BASIS CONCENTRATION OF SPECIES IN MIXTURE OF GASES LEAVING CFB RISER										
	CO	H2O	O2	N2	NH3	HCN	SO2	CO2	H2	NO
ppm (Actual % O2)	9.5237E-21	82230.77963	14293.55694	753433.3759	1.474821499	7.91791E-20	558.2481734	149481.9852	2.84091E-05	0.579267647
Mole % (Actual % O2)	9.5237E-25	8.223077963	1.429355694	75.34333759	0.000147482	7.91791E-24	0.055824817	14.94819852	2.84091E-09	5.79268E-05
ppm (Standard % O2)	8.75938E-21	75631.33897	30000	756368.0346	1.35645953	7.28246E-20	513.4459022	137485.2913	2.61291E-05	0.532778455
Mole % (Standard % O2)	8.75938E-25	7.563133897	3	F7/10000	0.000135646	7.28246E-24	0.05134459	13.74852913	2.61291E-09	5.32778E-05
g/GJ	3.34716E-21	18588.76462	5739.156159	264893.1532	0.315220062	2.68523E-20	448.7864975	82546.36864	7.1863E-07	0.334417698

DRY BASIS CONCENTRATION OF SPECIES IN MIXTURE OF GASES LEAVING CFB RISER										
	CO	H2O	O2	N2	NH3	HCN	SO2	CO2	H2	NO
ppm (Actual % O2)	1.0377E-20	0	15574.23874	820939.9043	1.606963348	8.62734E-20	608.2663931	162875.3524	3.09545E-05	0.63116918
Mole % (Actual % O2)	1.0377E-24	0	1.557423874	82.09399043	0.000160696	8.62734E-24	0.060826639	16.28753524	3.09545E-09	6.31169E-05
ppm (Standard % O2)	9.60707E-21	0	30000	818644.2637	1.487731877	7.98722E-20	563.1349984	150790.5292	2.86577E-05	0.584338473
Mole % (Standard % O2)	9.60707E-25	0	3	F16/10000	0.000148773	7.98722E-24	0.0563135	15.07905292	2.86577E-09	5.84338E-05
g/GJ	3.34716E-21	0	5739.156159	264893.1532	0.315220062	2.68523E-20	448.7864975	82546.36864	7.1863E-07	0.334417698

Increasing both $Y_{N_2,N}x100$ and $Y_{VN,N}x100$ by another 4%, the same trends can be seen to continue below in the graphs of the mole fraction of species in the mixture of gases versus time after the mixture of gases leaves the CFB bed until they reach the CFB riser exit for all species in Fig. 44 and trace species in Fig. 45.

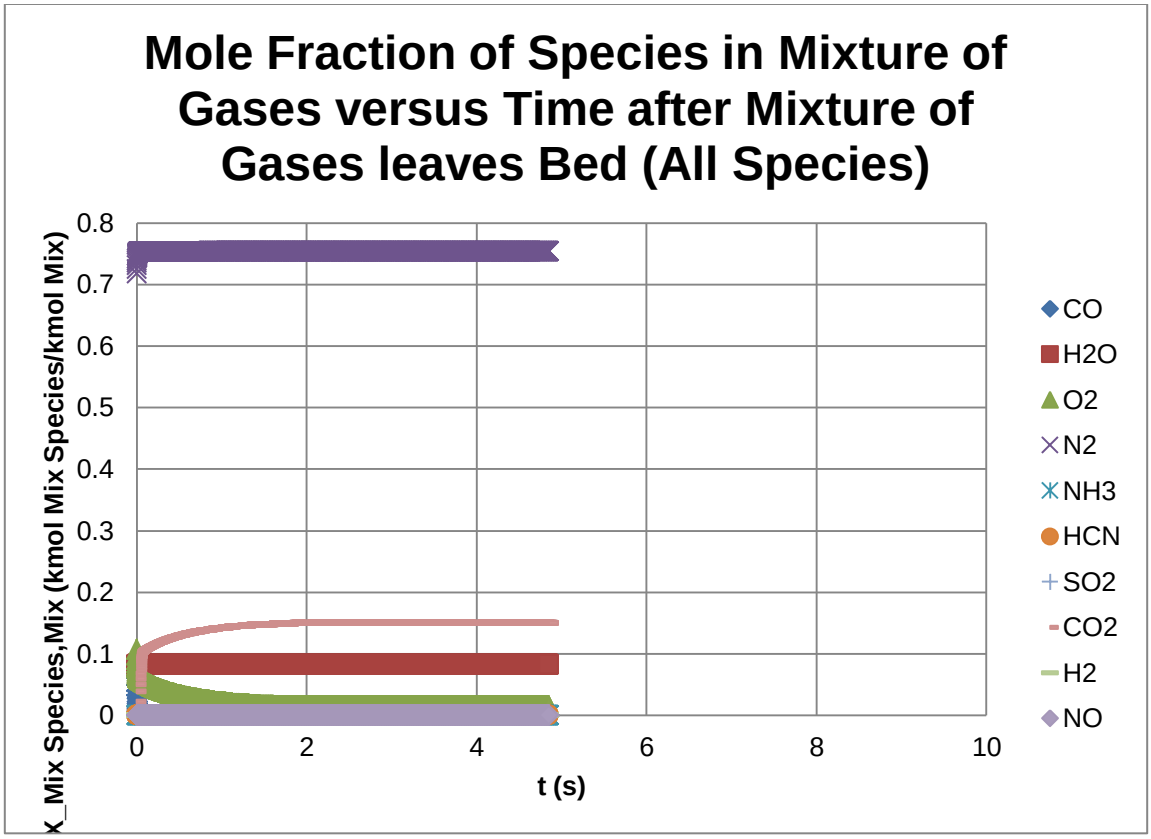

Fig. 44. Mole fraction of all species versus time for anonymous CFB boiler firing tire fuel with 8% increase in volatile Nitrogen to N_2.

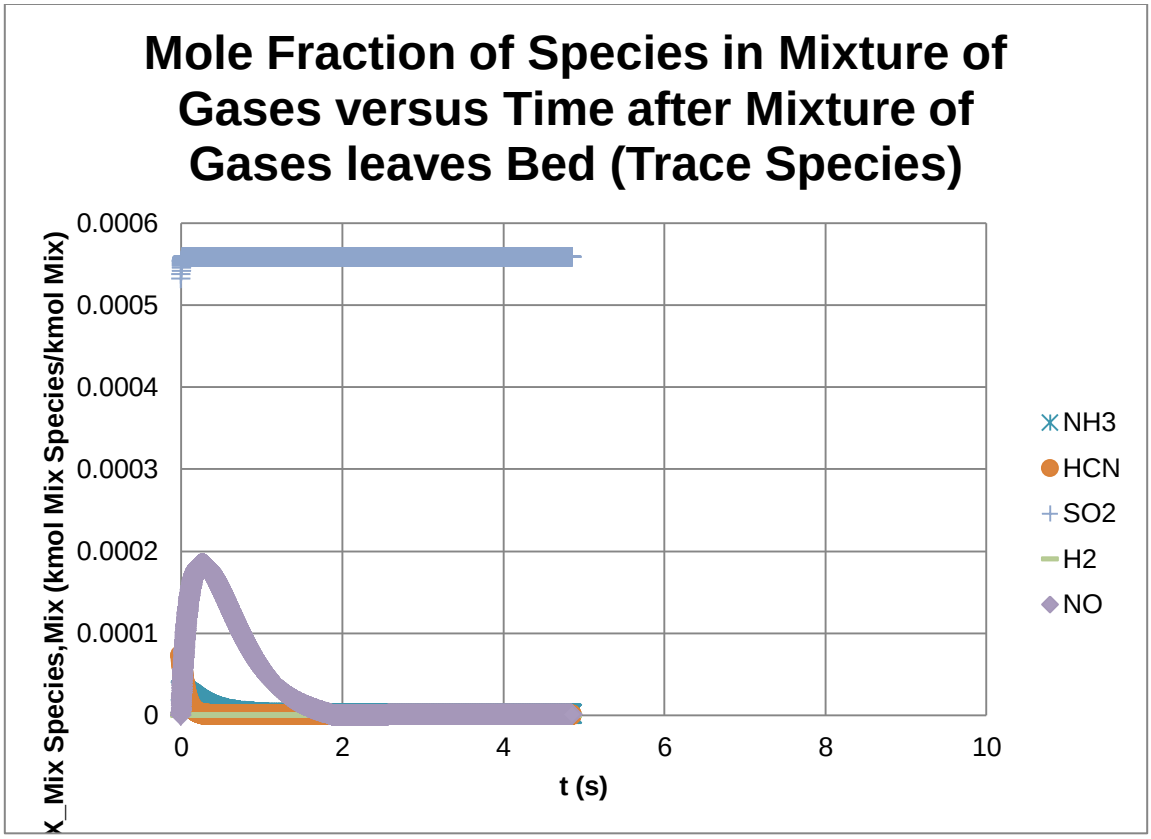

Fig. 45. Mole fraction of trace species versus time for anonymous CFB boiler firing tire fuel with 8% increase in volatile Nitrogen to N_2.

The nearly identical trends are again greatly evident in the 'Output' tab of the Excel program as shown below in Table 25 where all species are basically unchanged. Continuing to increase $Y_{N_2,N}x100$ exemplifies the continued effects of the trends except for NO. Even though NO has a continued decrease in its peak concentration due to less and less fixed Nitrogen available to form NO, it begins to have a higher and higher concentration at the exit of the riser due to its lower average concentration slowing down its reduction from NH_3 and HCN reactions.

Table 25

Output tab for anonymous CFB boiler firing tire fuel with 8% increase in volatile Nitrogen to N_2.

WET BASIS CONCENTRATION OF SPECIES IN MIXTURE OF GASES LEAVING CFB RISER										
	CO	H2O	O2	N2	NH3	HCN	SO2	CO2	H2	NO
ppm (Actual % O2)	9.42931E-21	82230.48595	14293.71685	753433.3244	1.673321173	7.83938E-20	558.2482011	149481.9926	3.19206E-05	0.558619053
Mole % (Actual % O2)	9.42931E-25	8.223048595	1.429371685	75.34333244	0.000167332	7.83938E-24	0.05582482	14.94819926	3.19206E-09	5.58619E-05
ppm (Standard % O2)	8.67256E-21	75631.13066	30000	756367.9597	1.539029848	7.21024E-20	513.4463472	137485.4105	2.93588E-05	0.513787437
Mole % (Standard % O2)	8.67256E-25	7.563113066	3	F7/10000	0.000153903	7.21024E-24	0.051344635	13.74854105	2.93588E-09	5.13787E-05
g/GJ	3.31399E-21	18588.69731	5739.220081	264893.1219	0.357646249	2.6586E-20	448.7864975	82546.36864	8.07457E-07	0.322497018

DRY BASIS CONCENTRATION OF SPECIES IN MIXTURE OF GASES LEAVING CFB RISER										
	CO	H2O	O2	N2	NH3	HCN	SO2	CO2	H2	NO
ppm (Actual % O2)	1.02742E-20	0	15574.40799	820939.5855	1.823247719	8.54177E-20	608.2662287	162875.3084	3.47806E-05	0.608670309
Mole % (Actual % O2)	1.02742E-24	0	1.557440799	82.09395855	0.000182325	8.54177E-24	0.060826623	16.28753084	3.47806E-09	6.0867E-05
ppm (Standard % O2)	9.51186E-21	0	30000	818643.9934	1.687970118	7.90801E-20	563.1353364	150790.6197	3.22001E-05	0.563509435
Mole % (Standard % O2)	9.51186E-25	0	3	F16/10000	0.000168797	7.90801E-24	0.056313534	15.07906197	3.22001E-09	5.63509E-05
g/GJ	3.31399E-21	0	5739.220081	264893.1219	0.357646249	2.6586E-20	448.7864975	82546.36864	8.07457E-07	0.322497018

5.3.5 Volatile Nitrogen to NH_3

Returning the $Y_{N_2,N}x100$ to its original value, the $Y_{NH_3,N}x100$ was then altered. In order to alter the $Y_{NH_3,N}x100$, the $Y_{VN,N}x100$ must similarly be changed so that the other volatile Nitrogen conversions to N_2 and HCN remain the same. Adding 4% to the mass percent of fuel Nitrogen released as volatile matter and subsequently converted to NH_3 also requires adding 4% to the total mass percent of fuel Nitrogen released as volatile matter (which includes what is converted to N_2 and HCN). Still very little change can be seen in the resulting concentrations of the species, but similar trends apply with more volatile Nitrogen converted to NH_3 meaning less fixed Nitrogen available to be oxidized to NO. This results in a lower peak NO concentration. This also means a lower average of NO is available to react with NH_3 so that NH_3 increases along with the addition of NH_3 from the volatile Nitrogen. The NO concentration at the riser exit nonetheless increases because the NO destroyed by NH_3 and HCN due to lower average NO is not as much as the NO created by the oxidation of NH_3 and HCN due to higher O_2 and NH_3. The less fixed Nitrogen is replaced by more fixed Carbon (leading to slightly longer burn time required since fixed Nitrogen oxidizes proportionally to that of fixed Carbon); and therefore, less volatile Carbon so that CO decreases which leads to higher O_2. Slightly less H_2O is seen as a result of more volatile Hydrogen being used to form NH_3 rather than H_2O (this also results in slightly more O_2). The almost identical trends are shown below in the graphs of the mole fraction of species in the mixture of gases versus time after the mixture of gases leaves the CFB bed until they reach the CFB riser exit for all species in Fig. 46 and trace species in Fig. 47.

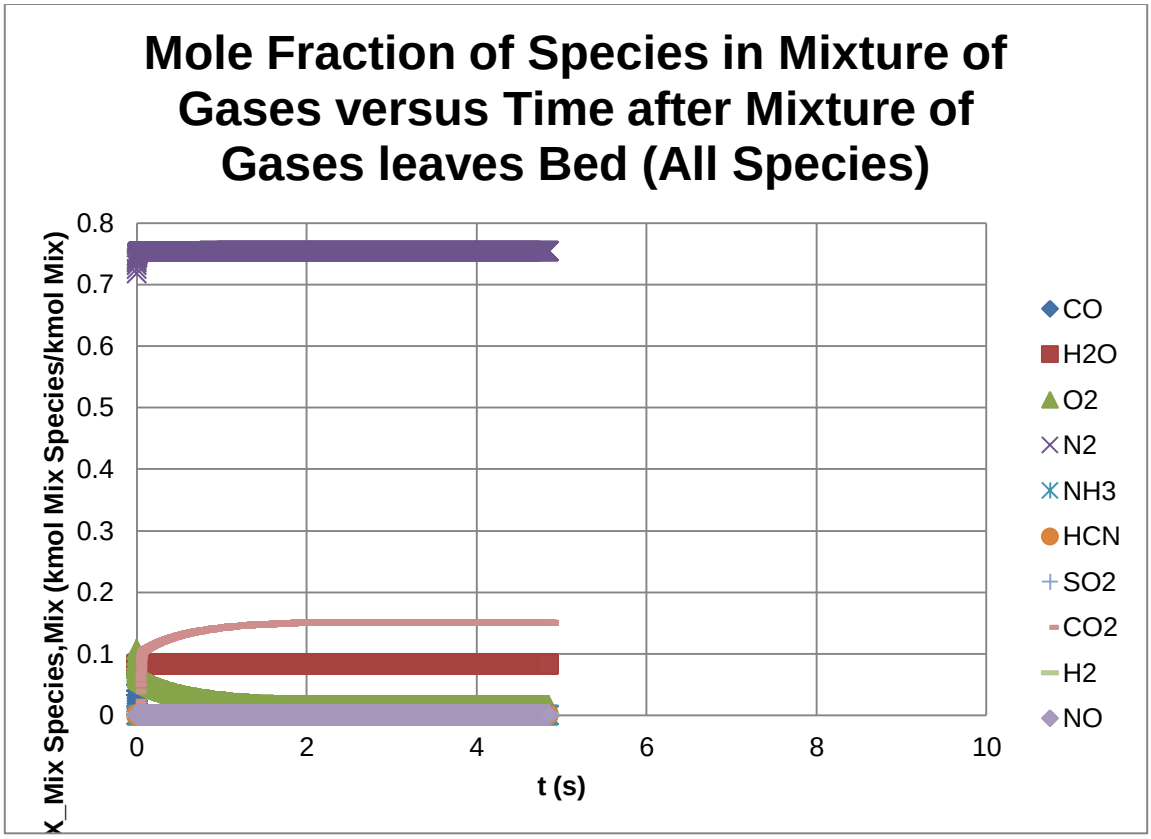

Fig. 46. Mole fraction of all species versus time for anonymous CFB boiler firing tire fuel with increased volatile Nitrogen to NH_3.

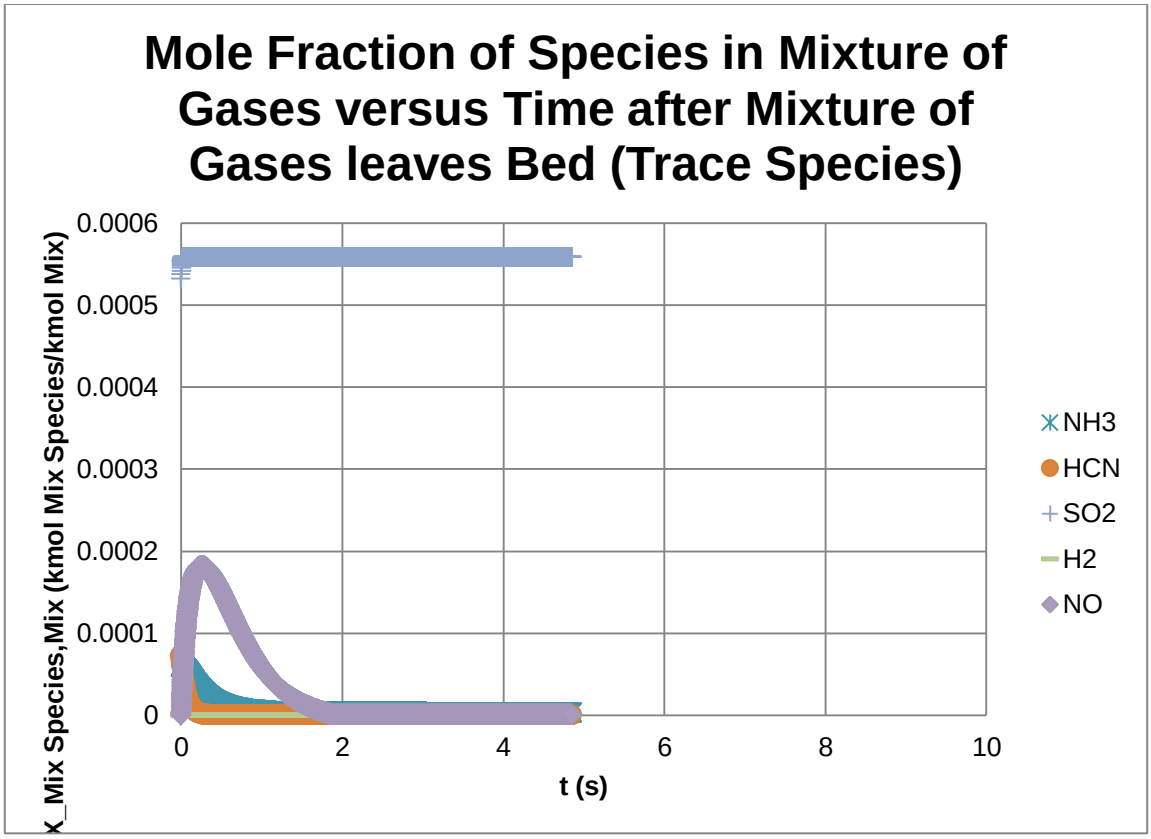

Fig. 47. Mole fraction of trace species versus time for anonymous CFB boiler firing tire fuel with increased volatile Nitrogen to NH_3.

The nearly identical trends are again greatly evident in the 'Output' tab of the Excel program as shown below in Table 26 where all species are basically unchanged. Continuing to increase $Y_{NH_3,N}x100$ further illustrates the continued effects of the trends of all species (especially the increase of NH_3).

Table 26

Output tab for anonymous CFB boiler firing tire fuel with increased volatile Nitrogen to NH_3.

WET BASIS CONCENTRATION OF SPECIES IN MIXTURE OF GASES LEAVING CFB RISER										
	CO	H2O	O2	N2	NH3	HCN	SO2	CO2	H2	NO
ppm (Actual % O2)	9.45082E-21	82228.03066	14294.90954	753432.7492	3.332907483	7.85666E-20	558.2484327	149482.0546	6.70676E-05	0.674521106
Mole % (Actual % O2)	9.45082E-25	8.222803066	1.429490954	75.34327492	0.000333291	7.85666E-24	0.055824843	14.94820546	6.70676E-09	6.74521E-05
ppm (Standard % O2)	8.69241E-21	75629.33332	30000	756367.2257	3.065445797	7.22617E-20	513.4496893	137486.3054	6.16856E-05	0.620391625
Mole % (Standard % O2)	8.69241E-25	7.562933332	3	F7/10000	0.000306545	7.22617E-24	0.051344969	13.74863054	6.16856E-09	6.20392E-05
g/GJ	3.32155E-21	18588.13456	5739.696587	264892.8098	0.712356591	2.66446E-20	448.7864975	82546.36864	1.69653E-06	0.389408406
DRY BASIS CONCENTRATION OF SPECIES IN MIXTURE OF GASES LEAVING CFB RISER										
	CO	H2O	O2	N2	NH3	HCN	SO2	CO2	H2	NO
ppm (Actual % O2)	1.02976E-20	0	15575.66587	820936.7625	3.631520241	8.56058E-20	608.2648538	162874.9402	7.30766E-05	0.734955008
Mole % (Actual % O2)	1.02976E-24	0	1.557566587	82.09367625	0.000363152	8.56058E-24	0.060826485	16.28749402	7.30766E-09	7.34955E-05
ppm (Standard % O2)	9.53359E-21	0	30000	818641.5653	3.362097889	7.92547E-20	563.1377068	150791.2544	6.7655E-05	0.680428724
Mole % (Standard % O2)	9.53359E-25	0	3	F16/10000	0.00033621	7.92547E-24	0.056313771	15.07912544	6.7655E-09	6.80429E-05
g/GJ	3.32155E-21	0	5739.696587	264892.8098	0.712356591	2.66446E-20	448.7864975	82546.36864	1.69653E-06	0.389408406

Subtracting 4% from the mass percent of fuel Nitrogen released as volatile matter and subsequently converted to NH_3 also requires subtracting 4% from the total mass percent of fuel Nitrogen released as volatile matter (which includes what is converted to N_2 and HCN). This means that there is no NH_3 at any time in the combustor because all NH_3 is assumed to evolve from the volatile Nitrogen. Still very little change can be seen in the resulting concentrations of the species, but similar trends apply with less volatile Nitrogen converted to NH_3 meaning more fixed Nitrogen available to be oxidized to NO. This results in a higher peak NO concentration. The NO concentration at the riser nonetheless decreases because the NO destroyed by HCN due to higher average NO is more than the NO created by the oxidation of HCN due to lower O_2. The increase in fixed Nitrogen causes a decrease in fixed Carbon (leading to slightly shorter burn time required since fixed Nitrogen oxidizes proportionally to that of fixed Carbon); and therefore, more volatile Carbon so that CO increases which leads to lower O_2. Slightly more H_2O is seen as a result of less volatile Hydrogen being used to form NH_3 rather

than H_2O (this also results in slightly less O_2). The almost identical trends are shown below in the graphs of the mole fraction of species in the mixture of gases versus time after the mixture of gases leaves the CFB bed until they reach the CFB riser exit for all species in Fig. 48 and trace species in Fig. 49.

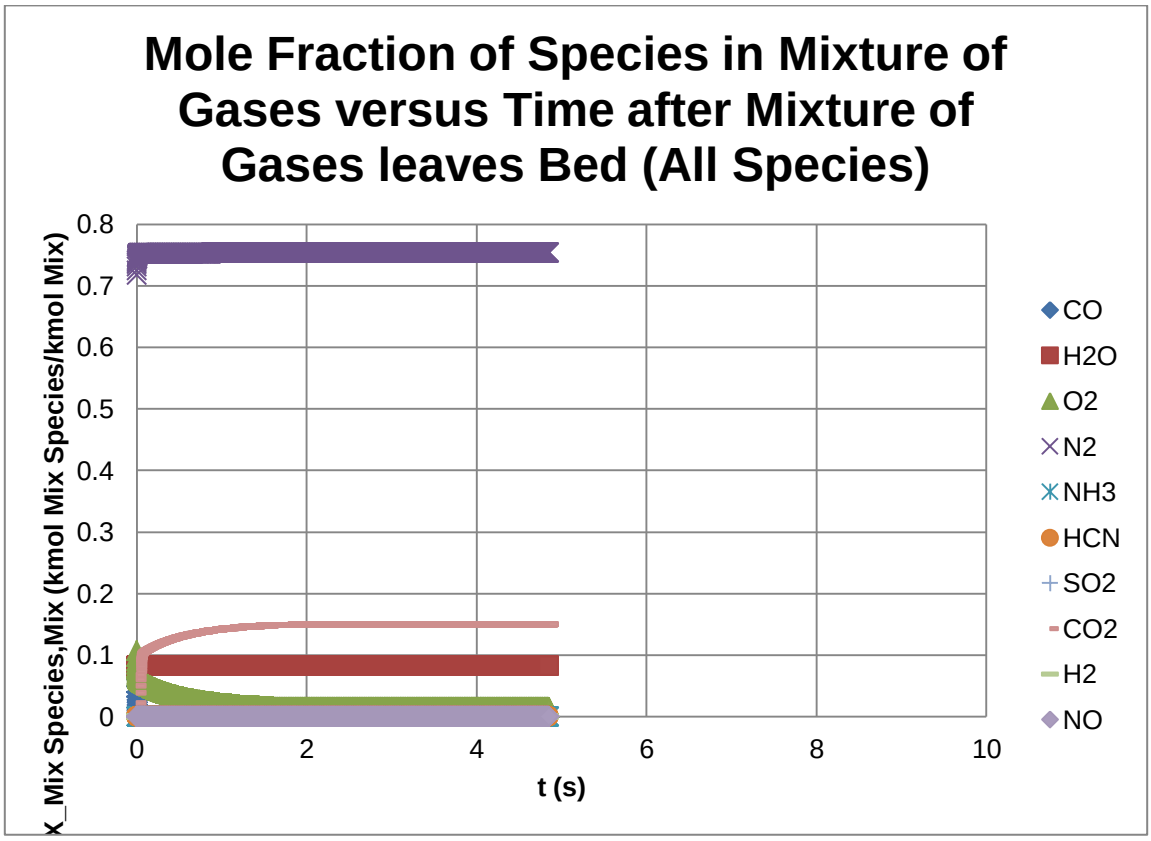

Fig. 48. Mole fraction of all species versus time for anonymous CFB boiler firing tire fuel with decreased volatile Nitrogen to NH_3.

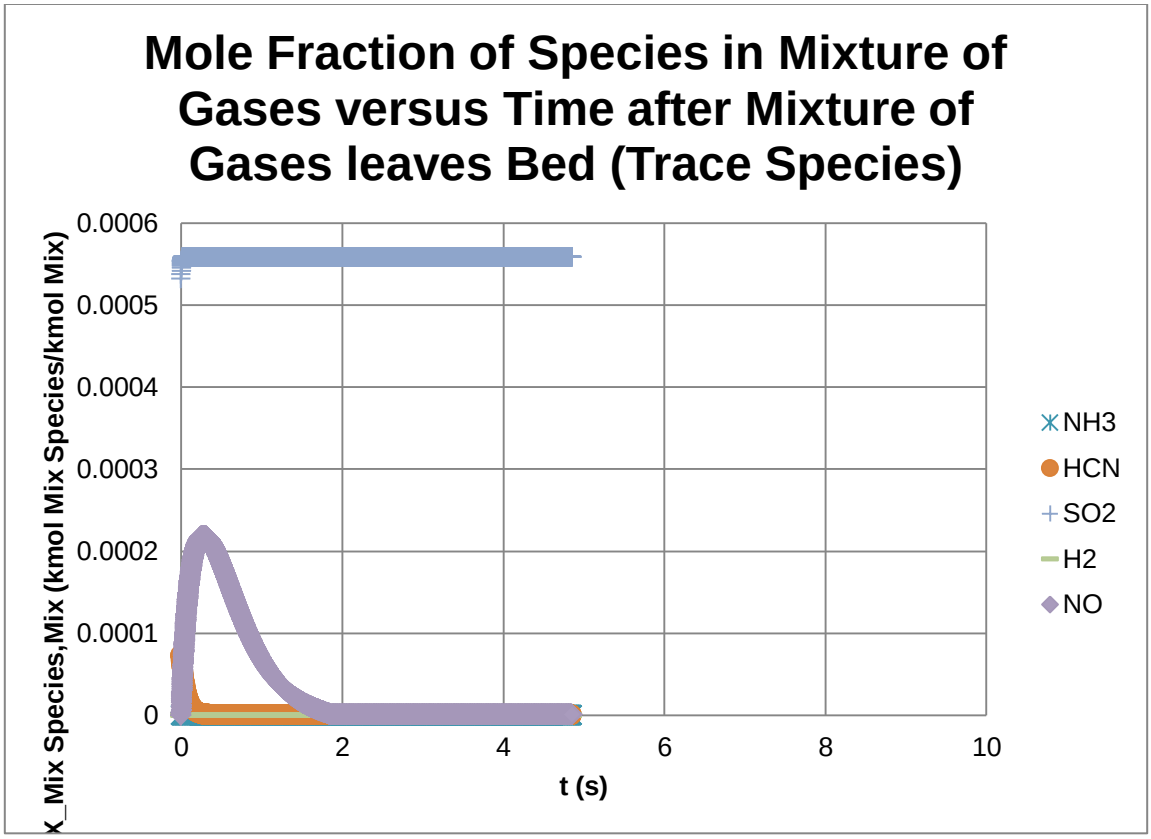

Fig. 49. Mole fraction of trace species versus time for anonymous CFB boiler firing tire fuel with decreased volatile Nitrogen to NH_3.

The nearly identical trends are again greatly evident in the 'Output' tab of the Excel program as shown below in Table 27 where all species are basically unchanged. Continuing to decrease $Y_{NH_3,N}x100$ further to a negative percentage is unrealistic and meaningless since there is already no NH_3 in the CFB combustor.

Table 27

Output tab for anonymous CFB boiler firing tire fuel with decreased volatile Nitrogen to NH_3.

WET BASIS CONCENTRATION OF SPECIES IN MIXTURE OF GASES LEAVING CFB RISER										
	CO	H2O	O2	N2	NH3	HCN	SO2	CO2	H2	NO
ppm (Actual % O2)	9.77781E-21	82232.96157	14292.46025	753433.8503	0	8.1296E-20	558.2479676	149481.9301	1.21204E-18	0.549855722
Mole % (Actual % O2)	9.77781E-25	8.223296157	1.429246025	75.34338503	0	8.1296E-24	0.055824797	14.94819301	1.21204E-22	5.49856E-05
ppm (Standard % O2)	8.99304E-21	75632.92197	30000	756368.6593	0	7.47712E-20	513.4428356	137484.4702	1.11476E-18	0.505724154
Mole % (Standard % O2)	8.99304E-25	7.563292197	3	F7/10000	0	7.47712E-24	0.051344284	13.74844702	1.11476E-22	5.05724E-05
g/GJ	3.43647E-21	18589.26471	5738.717929	264893.4176	0	2.75703E-20	448.7864975	82546.36864	3.06595E-20	0.317437982

DRY BASIS CONCENTRATION OF SPECIES IN MIXTURE OF GASES LEAVING CFB RISER										
	CO	H2O	O2	N2	NH3	HCN	SO2	CO2	H2	NO
ppm (Actual % O2)	1.06539E-20	0	15573.08081	820942.3729	0	8.85803E-20	608.267615	162875.6796	1.32064E-18	0.599123414
Mole % (Actual % O2)	1.06539E-24	0	1.557308081	82.09423729	0	8.85803E-24	0.060826761	16.28756796	1.32064E-22	5.99123E-05
ppm (Standard % O2)	9.86337E-21	0	30000	818646.3785	0	8.20074E-20	563.1327758	150789.9341	1.22264E-18	0.554667096
Mole % (Standard % O2)	9.86337E-25	0	3	F16/10000	0	8.20074E-24	0.056313278	15.07899341	1.22264E-22	5.54667E-05
g/GJ	3.43647E-21	0	5738.717929	264893.4176	0	2.75703E-20	448.7864975	82546.36864	3.06595E-20	0.317437982

5.3.6 Volatile Nitrogen to HCN

Returning the $Y_{NH_3,N}x100$ to its original value, the $Y_{HCN,N}x100$ was then altered. In order to alter the $Y_{HCN,N}x100$, the $Y_{VN,N}x100$ must similarly be changed so that the other volatile Nitrogen conversions to N_2 and NH_3 remain the same. Adding 4% to the mass percent of fuel Nitrogen released as volatile matter and subsequently converted to HCN also requires adding 4% to the total mass percent of fuel Nitrogen released as volatile matter (which includes what is converted to N_2 and NH_3). Still very little change can be seen in the resulting concentrations of the species, but this time trends appear to be opposite even though more volatile Nitrogen converted to HCN still means less fixed Nitrogen available to be oxidized to NO. The key seems to be HCN being more reactive with O_2 than NH_3. Therefore, the increased HCN causes increased production of NO while O_2 is plentiful near the bottom of the combustor, but then begins

to taper off as the O_2 begins to be depleted. Thus, the result is a higher peak NO concentration. Yet HCN and NO are still relatively higher at the end of the complete burning of the tire, so that the trend is reversed to end up with a lower NO concentration at the riser exit. The higher peak of NO also more greatly reduces NH_3 so that NH_3 also ends up lower. The greater reaction rates of HCN also lead to higher CO, H_2O (indirectly since H_2 quickly oxidizes), and N_2 as well as reduced O_2 at the riser exit. Even though HCN is more reactive, the increase in the original concentration from the volatile Nitrogen carries over to a higher concentration in the end. The less fixed Nitrogen is still replaced by more fixed Carbon which leads to slightly longer burn time required since fixed Nitrogen oxidizes proportionally to that of fixed Carbon. The almost identical trends are shown below in the graphs of the mole fraction of species in the mixture of gases versus time after the mixture of gases leaves the CFB bed until they reach the CFB riser exit for all species in Fig. 50 and trace species in Fig. 51.

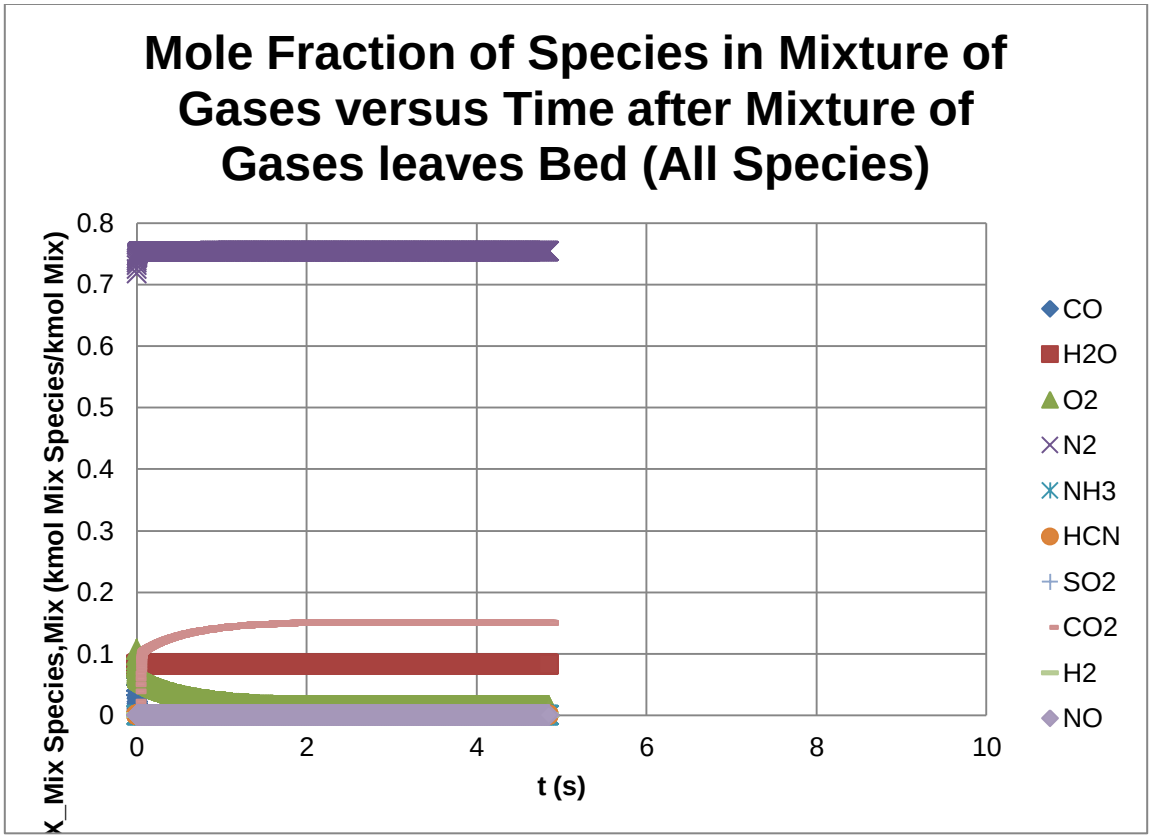

Fig. 50. Mole fraction of all species versus time for anonymous CFB boiler firing tire fuel with increased volatile Nitrogen to HCN.

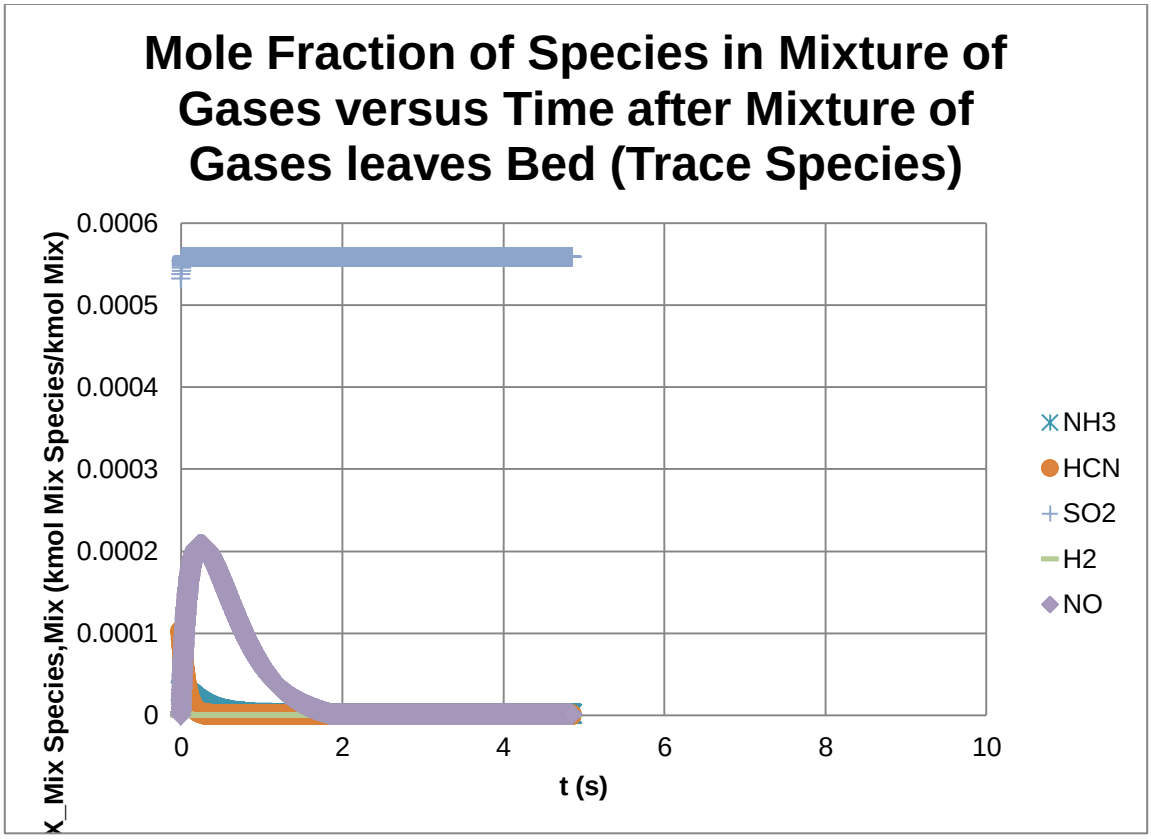

Fig. 51. Mole fraction of trace species versus time for anonymous CFB boiler firing tire fuel with increased volatile Nitrogen to HCN.

The nearly identical trends are again greatly evident in the 'Output' tab of the Excel program as shown below in Table 28 where all species are basically unchanged. Continuing to increase $Y_{HCN,N}x100$ merely continues the trend of each species.

Table 28

Output tab for anonymous CFB boiler firing tire fuel with increased volatile Nitrogen to HCN.

WET BASIS CONCENTRATION OF SPECIES IN MIXTURE OF GASES LEAVING CFB RISER										
	CO	H2O	O2	N2	NH3	HCN	SO2	CO2	H2	NO
ppm (Actual % O2)	1.33944E-20	82231.09285	14293.40569	753433.4502	1.263105798	1.11363E-19	558.2481439	149481.9773	2.41416E-05	0.562679047
Mole % (Actual % O2)	1.33944E-24	8.223109285	1.429340569	75.34334502	0.000126311	1.11363E-23	0.055824814	14.94819773	2.41416E-09	5.62679E-05
ppm (Standard % O2)	1.23194E-20	75631.5686	30000	756368.1289	1.161734199	1.02425E-19	513.4454782	137485.1778	2.22041E-05	0.517520775
Mole % (Standard % O2)	1.23194E-24	7.56315686	3	F7/10000	0.000116173	1.02425E-23	0.051344548	13.74851778	2.22041E-09	5.17521E-05
g/GJ	4.70754E-21	18588.83641	5739.095732	264893.1933	0.269969152	3.77669E-20	448.7864975	82546.36864	6.10682E-07	0.324840931
DRY BASIS CONCENTRATION OF SPECIES IN MIXTURE OF GASES LEAVING CFB RISER										
	CO	H2O	O2	N2	NH3	HCN	SO2	CO2	H2	NO
ppm (Actual % O2)	1.45945E-20	0	15574.07925	820940.2654	1.376278699	1.21341E-19	608.2665685	162875.3994	2.63047E-05	0.613094476
Mole % (Actual % O2)	1.45945E-24	0	1.557407925	82.09402654	0.000137628	1.21341E-23	0.060826657	16.28753994	2.63047E-09	6.13094E-05
ppm (Standard % O2)	1.35116E-20	0	30000	818644.5745	1.274162236	1.12337E-19	563.1346989	150790.449	2.43529E-05	0.567604387
Mole % (Standard % O2)	1.35116E-24	0	3	F16/10000	0.000127416	1.12337E-23	0.05631347	15.0790449	2.43529E-09	5.67604E-05
g/GJ	4.70754E-21	0	5739.095732	264893.1933	0.269969152	3.77669E-20	448.7864975	82546.36864	6.10682E-07	0.324840931

Subtracting 4% from the mass percent of fuel Nitrogen released as volatile matter and subsequently converted to HCN also requires subtracting 4% from the total mass percent of fuel Nitrogen released as volatile matter (which includes what is converted to N_2 and NH_3). Still very little change can be seen in the resulting concentrations of the species, and the trends appear to remain opposite even though less volatile Nitrogen converted to HCN still means more fixed Nitrogen available to be oxidized to NO. The key seems to remain HCN being more reactive with O_2 than NH_3. Therefore, the decreased HCN causes decreased production of NO through O_2 near the bottom of the combustor. Thus, the result is a lower peak NO concentration. The lower HCN concentration also attributes to less NO reduction at the end of the complete burning of the tire so that the trend is reversed to end up with a higher NO concentration at the riser exit. The lower peak of NO also decreases its reaction rate with NH_3 so that NH_3 also ends up higher. The lesser reaction rates of HCN also lead to lower CO, H_2O (indirectly since H_2 quickly oxidizes), and N_2 as well as increased O_2 at the riser exit. Even though

HCN is less reactive, the decrease in the original concentration from the volatile Nitrogen carries over to a lower concentration in the end. The more fixed Nitrogen replaces fixed Carbon which leads to slightly shorter burn time required since fixed Nitrogen oxidizes proportionally to that of fixed Carbon. The almost identical trends are shown below in the graphs of the mole fraction of species in the mixture of gases versus time after the mixture of gases leaves the CFB bed until they reach the CFB riser exit for all species in Fig. 52 and trace species in Fig. 53.

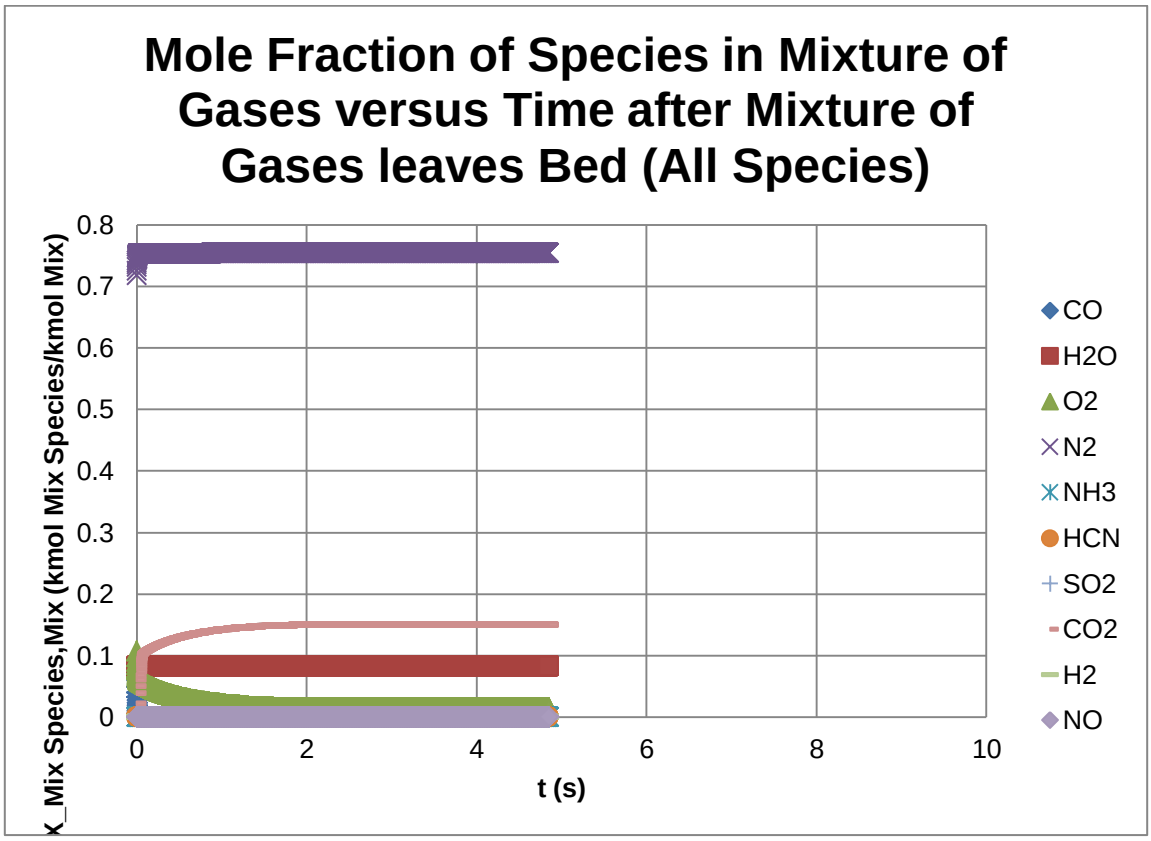

Fig. 52. Mole fraction of all species versus time for anonymous CFB boiler firing tire fuel with decreased volatile Nitrogen to HCN.

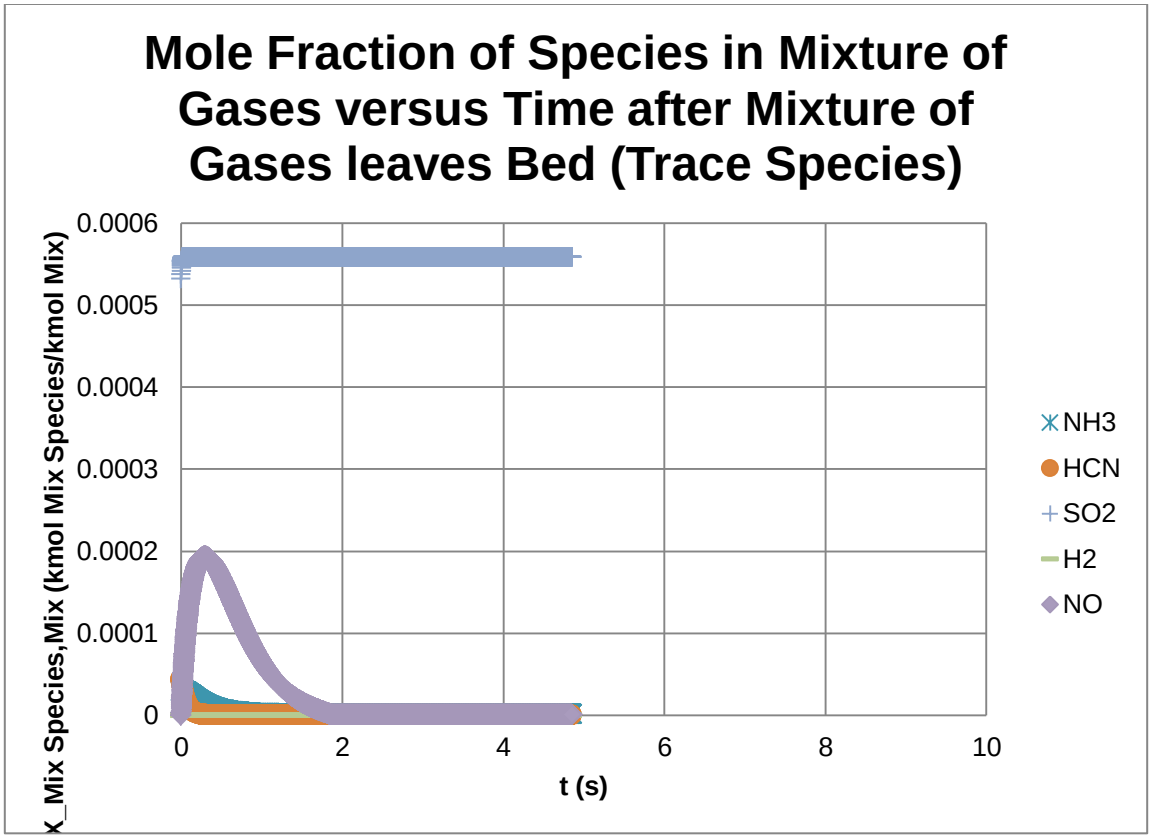

Fig. 53. Mole fraction of trace species versus time for anonymous CFB boiler firing tire fuel with decreased volatile Nitrogen to HCN.

The nearly identical trends are again greatly evident in the 'Output' tab of the Excel program as shown below in Table 29 where all species are basically unchanged. Continuing to decrease $Y_{HCN,N}x100$ merely continues the trend of each species until there is no more HCN.

Table 29

Output tab for anonymous CFB boiler firing tire fuel with decreased volatile Nitrogen to HCN.

WET BASIS CONCENTRATION OF SPECIES IN MIXTURE OF GASES LEAVING CFB RISER										
	CO	H2O	O2	N2	NH3	HCN	SO2	CO2	H2	NO
ppm (Actual % O2)	5.80357E-21	82230.98066	14293.435	753433.3987	1.338940821	4.82494E-20	558.2481544	149481.9801	2.62645E-05	0.618370323
Mole % (Actual % O2)	5.80357E-25	8.223098066	1.4293435	75.34333987	0.000133894	4.82494E-24	0.055824815	14.94819801	2.62645E-09	6.1837E-05
ppm (Standard % O2)	5.3378E-21	75631.47674	30000	756368.0765	1.231483205	4.43771E-20	513.4455648	137485.201	2.41566E-05	0.568742588
Mole % (Standard % O2)	5.3378E-25	7.563147674	3	F7/10000	0.000123148	4.43771E-24	0.051344556	13.7485201	2.41566E-09	5.68743E-05
g/GJ	2.0397E-21	18588.8107	5739.107389	264893.1702	0.286177699	1.6363E-20	448.7864975	82546.36864	6.64382E-07	0.356992124
DRY BASIS CONCENTRATION OF SPECIES IN MIXTURE OF GASES LEAVING CFB RISER										
	CO	H2O	O2	N2	NH3	HCN	SO2	CO2	H2	NO
ppm (Actual % O2)	6.32356E-21	0	15574.10927	820940.109	1.45890828	5.25724E-20	608.2665057	162875.3825	2.86178E-05	0.673775547
Mole % (Actual % O2)	6.32356E-25	0	1.557410927	82.0940109	0.000145891	5.25724E-24	0.060826651	16.28753825	2.86178E-09	6.73776E-05
ppm (Standard % O2)	5.85437E-21	0	30000	818644.4341	1.350661115	4.86717E-20	563.1347277	150790.4567	2.64944E-05	0.62378317
Mole % (Standard % O2)	5.85437E-25	0	3	F16/10000	0.000135066	4.86717E-24	0.056313473	15.07904567	2.64944E-09	6.23783E-05
g/GJ	2.0397E-21	0	5739.107389	264893.1702	0.286177699	1.6363E-20	448.7864975	82546.36864	6.64382E-07	0.356992124

5.3.7 Excess air

Returning the $Y_{HCN,N}x100$ to its original value, the $X_{Exc\ Air,Stoich\ Air}x100$ was then altered. Excess air realistically has an effect on the temperatures of the combustor such as T_{Mix} with the closer to stoichiometric combustion (no excess air) leading to higher temperatures while the further away (more or less excess air) has the opposite effect. More excess air usually leads to more air being required to be heated while not providing more fuel to provide the heat so that the temperature decreases. Less excess air usually leads to not enough air to fully burn the given fuel so that the full heating value of the fuel is not realized which also leads to decrease in temperature. Therefore, changing of the excess air without affecting temperatures such as T_{Mix} can only be achieved by decreasing water flow through the tubes within the combustor walls to

produce less steam the further the combustor is run from stoichiometric combustion.

Adding 20% to the excess air, much more change is apparent in the resulting concentrations of the species. This is especially true for O_2 and N_2 which obviously increase due to their increase by definition in the primary combustion air. Even though the increase in air leads to higher $\dot{m}_{Bed\ Mix}$ in turn increasing the $V_{Bed\ Mix}$ which decreases the $t_{Res,Bed\ Mix}$ and Δt, the SMD size tire fuel completely burns lower in the riser at about a fifth of the way because of the much higher O_2. The mere increase in O_2 and N_2 causes a pseudo-deflation of such species as H_2O, SO_2, and CO_2. The greater concentration of O_2 also increases the reaction rate of CO oxidation so that CO has a lower concentration at the exit of the riser. The new trends are shown below in the graph of the mole fraction of species in the mixture of gases versus time after the mixture of gases leaves the CFB bed until they reach the CFB riser exit for all species in Fig. 54.

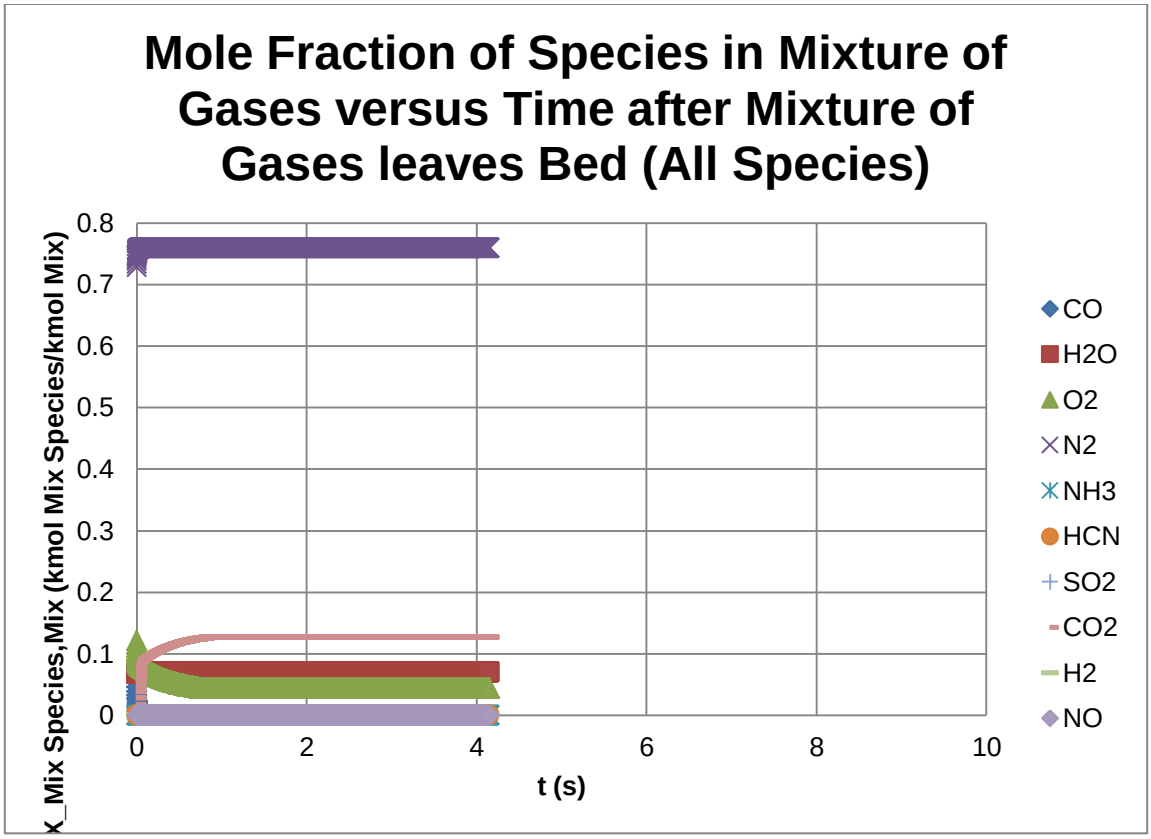

Fig. 54. Mole fraction of all species versus time for anonymous CFB boiler firing tire fuel with increased excess air.

Most of the trace species are highly dependent upon O_2 concentration. For instance, the higher oxidation rates from higher O_2 lead to lower concentrations of NH_3 and HCN. This in turn increases both the peak and riser exit concentrations of NO as well as increases the exit concentration of H_2 as these species are both products of NH_3 and HCN oxidation. The new trends are shown below in the graph of the mole fraction of species in the mixture of gases versus time after the mixture of gases leaves the CFB bed until they reach the CFB riser exit for trace species in Fig. 55.

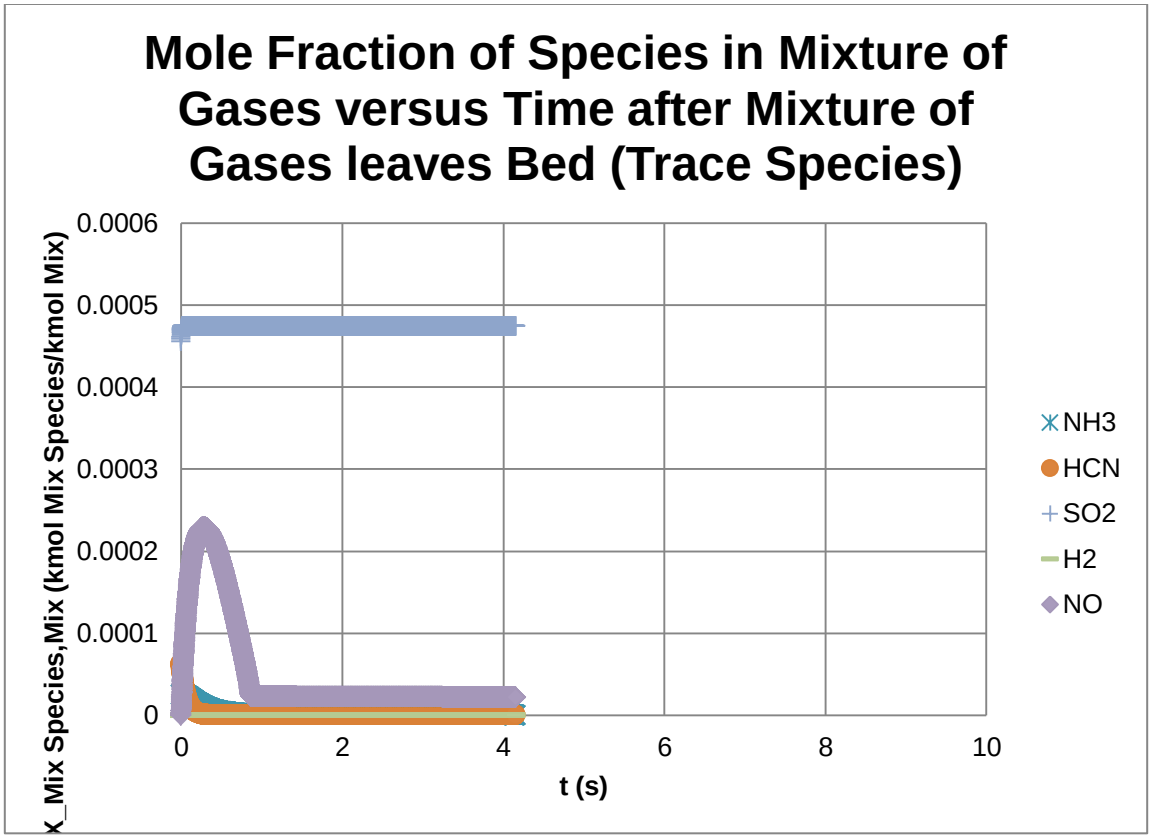

Fig. 55. Mole fraction of trace species versus time for anonymous CFB boiler firing tire fuel with increased excess air.

The new trends are evident in the 'Output' tab of the Excel program as shown below in Table 30. Continuing to increase $X_{Exc\ Air,Stoich\ Air}x100$ can begin to reverse some effects on the concentration of the species as less and less time is given for reactions to take place in the combustor and the O_2 diffusion to the char surface is not able to keep up.

Table 30

Output tab for anonymous CFB boiler firing tire fuel with increased excess air.

WET BASIS CONCENTRATION OF SPECIES IN MIXTURE OF GASES LEAVING CFB RISER										
	CO	H2O	O2	N2	NH3	HCN	SO2	CO2	H2	NO
ppm (Actual % O2)	2.2143E-26	69863.8558	43717.74969	758922.678	0.477116284	1.73126E-25	474.2837219	126998.8433	8.70008E-05	22.11230217
Mole % (Actual % O2)	2.2143E-30	6.98638558	4.371774969	75.8922678	4.77116E-05	1.73126E-29	0.047428372	12.69988433	8.70008E-09	0.00221123
ppm (Standard % O2)	2.39697E-26	75627.39872	30000	756358.8991	0.51647684	1.87409E-25	513.4106003	137475.8385	9.41781E-05	23.93649582
Mole % (Standard % O2)	2.39697E-30	7.562739872	3	F7/10000	5.16477E-05	1.87409E-29	0.05134106	13.74758385	9.41781E-09	0.00239365
g/GJ	9.16E-27	18589.07427	20661.15597	314059.9087	0.120029424	6.91073E-26	448.7864975	82546.36864	2.59036E-06	15.02564183

DRY BASIS CONCENTRATION OF SPECIES IN MIXTURE OF GASES LEAVING CFB RISER										
	CO	H2O	O2	N2	NH3	HCN	SO2	CO2	H2	NO
ppm (Actual % O2)	2.38061E-26	0	47001.45238	815926.4455	0.51295317	1.8613E-25	509.9078505	136537.908	9.35355E-05	23.7731888
Mole % (Actual % O2)	2.38061E-30	0	4.700145238	81.59264455	5.12953E-05	1.8613E-29	0.050990785	13.6537908	9.35355E-09	0.002377319
ppm (Standard % O2)	2.62892E-26	0	30000	818630.6857	0.566456401	2.05544E-25	563.0934412	150779.4014	0.000103292	26.25283505
Mole % (Standard % O2)	2.62892E-30	0	3	F16/10000	5.66456E-05	2.05544E-29	0.056309344	15.07794014	1.03292E-08	0.002625284
g/GJ	9.16E-27	0	20661.15597	314059.9087	0.120029424	6.91073E-26	448.7864975	82546.36864	2.59036E-06	15.02564183

Subtracting 20% from the excess air, the oxygen becomes deficient (negative excess air) since there is less O_2 available than is needed for stoichiometric combustion of the tire. The reverse trends are apparent especially with O_2 and N_2 which obviously decrease due to their decrease by definition in the primary combustion air. Even though the decrease in air leads to lower $\dot{m}_{Bed\ Mix}$ in turn decreasing the $V_{Bed\ Mix}$ which increases the $t_{Res,Bed\ Mix}$ and Δt, the SMD size tire fuel fails to completely burn in the riser with about 50% of the tire left unburned at the exit. This should come as no surprise considering the combustor lacks the O_2 required to burn all of the fuel. The mere decrease in O_2 and N_2 causes a pseudo-inflation of such species as H_2O, SO_2, and CO_2. The lower concentration of O_2 also decreases the reaction rate of CO oxidation so that CO has a higher concentration at the exit of the riser. The new trends are shown below in the graph of the mole fraction of species in the mixture of gases versus time after the mixture of gases leaves the CFB bed until they reach the CFB riser exit for all species in Fig. 56.

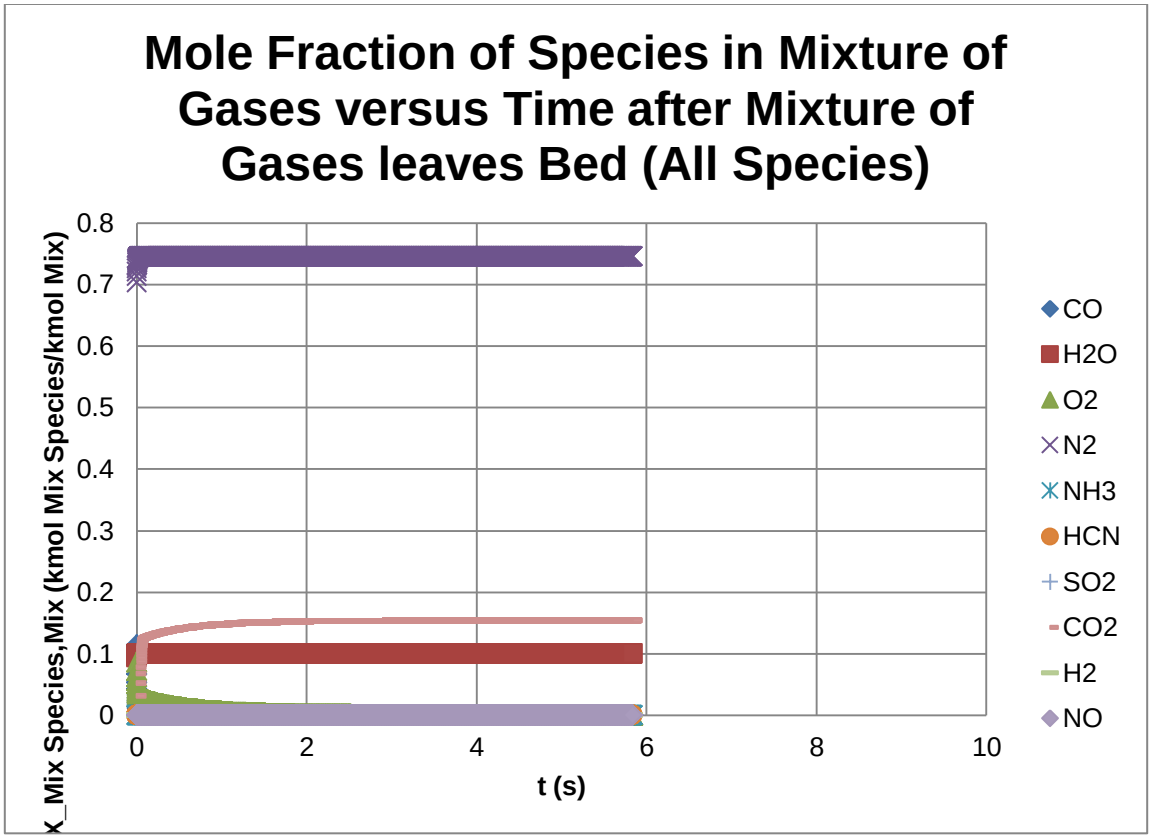

Fig. 56. Mole fraction of all species versus time for anonymous CFB boiler firing tire fuel with decreased excess air.

Most of the trace species are highly dependent upon O_2 concentration. For instance, the lower oxidation rates from lower O_2 lead to higher concentrations of NH_3 and HCN. This in turn decreases both the peak and riser exit concentrations of NO as well as decreases the exit concentration of H_2 as these species are both products of NH_3 and HCN oxidation. The new trends are shown below in the graph of the mole fraction of species in the mixture of gases versus time after the mixture of gases leaves the CFB bed until they reach the CFB riser exit for trace species in Fig. 57.

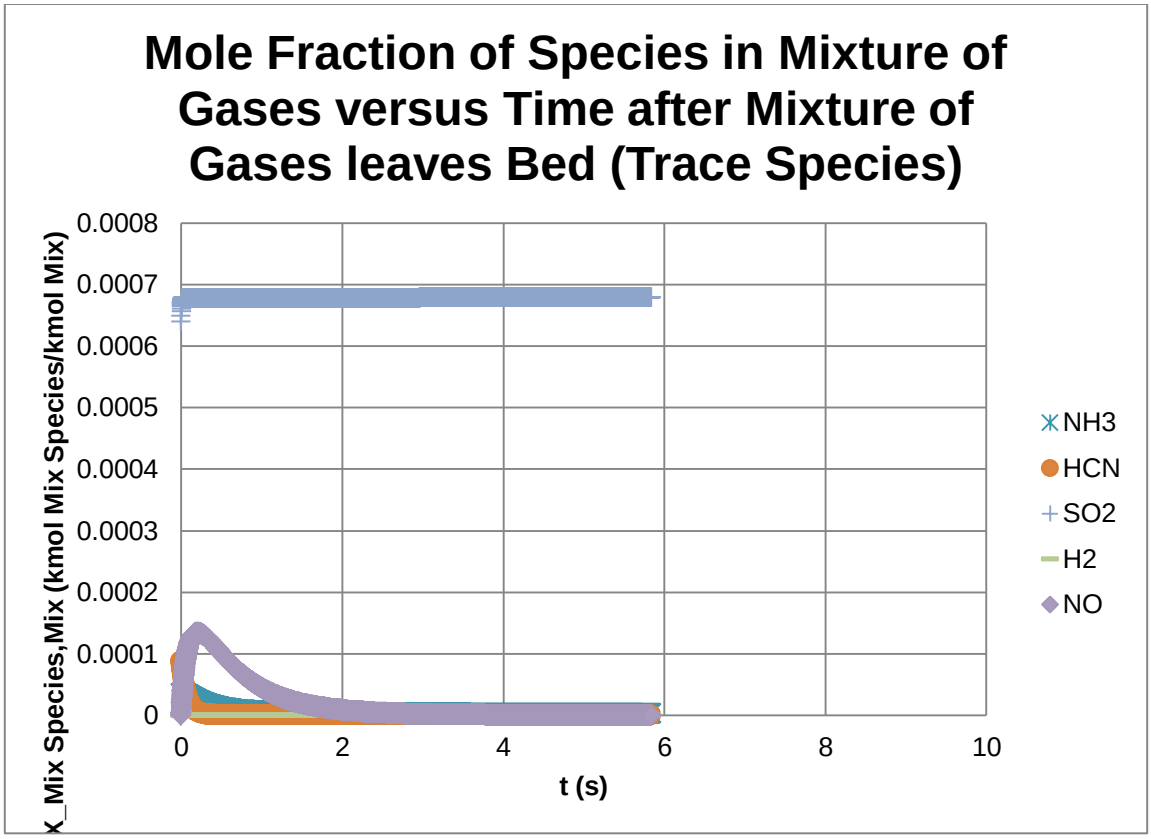

Fig. 57. Mole fraction of trace species versus time for anonymous CFB boiler firing tire fuel with decreased excess air.

The new trends are evident in the 'Output' tab of the Excel program as shown below in Table 31. Continuing to decrease $X_{Exc\ Air,Stoich\ Air}x100$ will begin to halt the combustion of tire altogether as O_2 begins to be more completely depleted in the combustor sooner and sooner since most reactions are dependent upon O_2. In fact, the volatile combustion that is assumed to take place immediately in the bed of the combustor may not even have enough O_2 at a low enough $X_{Exc\ Air,Stoich\ Air}x100$ value so that the combustor then begins to be a gasifier and the proposed program will begin to

show negative values of O_2 in the riser since the program is not modified to handle this yet.

Table 31

Output tab for anonymous CFB boiler firing tire fuel with decreased excess air.

WET BASIS CONCENTRATION OF SPECIES IN MIXTURE OF GASES LEAVING CFB RISER										
	CO	H2O	O2	N2	NH3	HCN	SO2	CO2	H2	NO
ppm (Actual % O2)	6.154274849	99935.84117	4.375419887	745516.3609	3.705775494	0.04947506	678.4639162	153855.0207	1.3905E-06	0.02832456
Mole % (Actual % O2)	0.000615427	9.993584117	0.000437542	74.55163609	0.000370578	4.94751E-06	0.067846392	15.38550207	1.3905E-10	2.83246E-06
ppm (Standard % O2)	5.275202638	85661.07721	30000	751870.372	3.176445177	0.042408078	581.5526164	131878.4798	1.19188E-06	0.0242787
Mole % (Standard % O2)	0.00052752	8.566107721	3	F7/10000	0.000317645	4.24081E-06	0.058155262	13.18784798	1.19188E-10	2.42787E-06
g/GJ	2.10139433	21948.11388	1.706818235	254649.5242	0.769508298	0.016301133	529.9062455	82543.06688	3.41726E-08	0.015886673
DRY BASIS CONCENTRATION OF SPECIES IN MIXTURE OF GASES LEAVING CFB RISER										
	CO	H2O	O2	N2	NH3	HCN	SO2	CO2	H2	NO
ppm (Actual % O2)	6.83759573	0	4.861231107	828292.4651	4.117234819	0.054968371	753.7950595	170937.8373	1.54489E-06	0.03146949
Mole % (Actual % O2)	0.00068376	0	0.000486123	82.82924651	0.000411723	5.49684E-06	0.075379506	17.09378373	1.54489E-10	3.14695E-06
ppm (Standard % O2)	5.860932013	0	30000	822822.8728	3.529140111	0.047116837	646.125008	146521.538	1.32422E-06	0.026974473
Mole % (Standard % O2)	0.000586093	0	3	F16/10000	0.000352914	4.71168E-06	0.064612501	14.6521538	1.32422E-10	2.69745E-06
g/GJ	2.10139433	0	1.706818235	254649.5242	0.769508298	0.016301133	529.9062455	82543.06688	3.41726E-08	0.015886673

5.3.8 Air O_2

Returning the $X_{Exc\ Air,Stoich\ Air}x100$ to its original value, the $X_{O_2,Air}x100$ was then altered. In order to modify the $X_{O_2,Air}x100$, the $X_{N_2,Air}x100$ must be inversely changed since O_2 and N_2 are assumed to be the only constituents of air in the proposed model. The $X_{O_2,Air}x100$ can also have an effect on the temperatures of the combustor such as T_{Mix} since N_2 is just an energy sink during combustion. This means as more N_2 is in the air compared to O_2 the more energy is wasted to merely raise the temperature of the N_2 due to its inertness unlike the O_2 which provides heat through exothermic combustion reactions. Therefore, more N_2 versus O_2 means lower overall T_{Mix}. Therefore, decreasing the mole percent of O_2 in the air without affecting temperatures such as T_{Mix} can only be achieved by decreasing water flow through the tubes within the

combustor walls to produce less steam. Whereas, increasing the mole percent of O_2 in the air without affecting temperatures such as T_{Mix} can only be achieved by increasing water flow through the tubes within the combustor walls to produce more steam which is assumed to be able to be handled by this combustor's tubes.

Adding 10% to the mole percent of O_2 in the air also requires removing 10% from the mole percent of N_2 in the air. The only real change taking place is the decrease in N_2 since the amount of O_2 is set by the excess air. The decrease in N_2 leads to lower $\dot{m}_{Bed\ Mix}$ in turn decreasing the $V_{Bed\ Mix}$ which increases the $t_{Res,Bed\ Mix}$ and Δt. The longer time in the combustor along with the relatively higher O_2 concentration enhances the complete burning of the SMD size tire fuel lower in the riser at less than a fifth of the way. The mere decrease in N_2 causes a pseudo-inflation of such species as O_2, H_2O, SO_2, and CO_2. However, the greater concentration of O_2 increases the reaction rate of CO oxidation so that CO has a lower concentration at the exit of the riser. The new trends are shown below in the graph of the mole fraction of species in the mixture of gases versus time after the mixture of gases leaves the CFB bed until they reach the CFB riser exit for all species in Fig. 58.

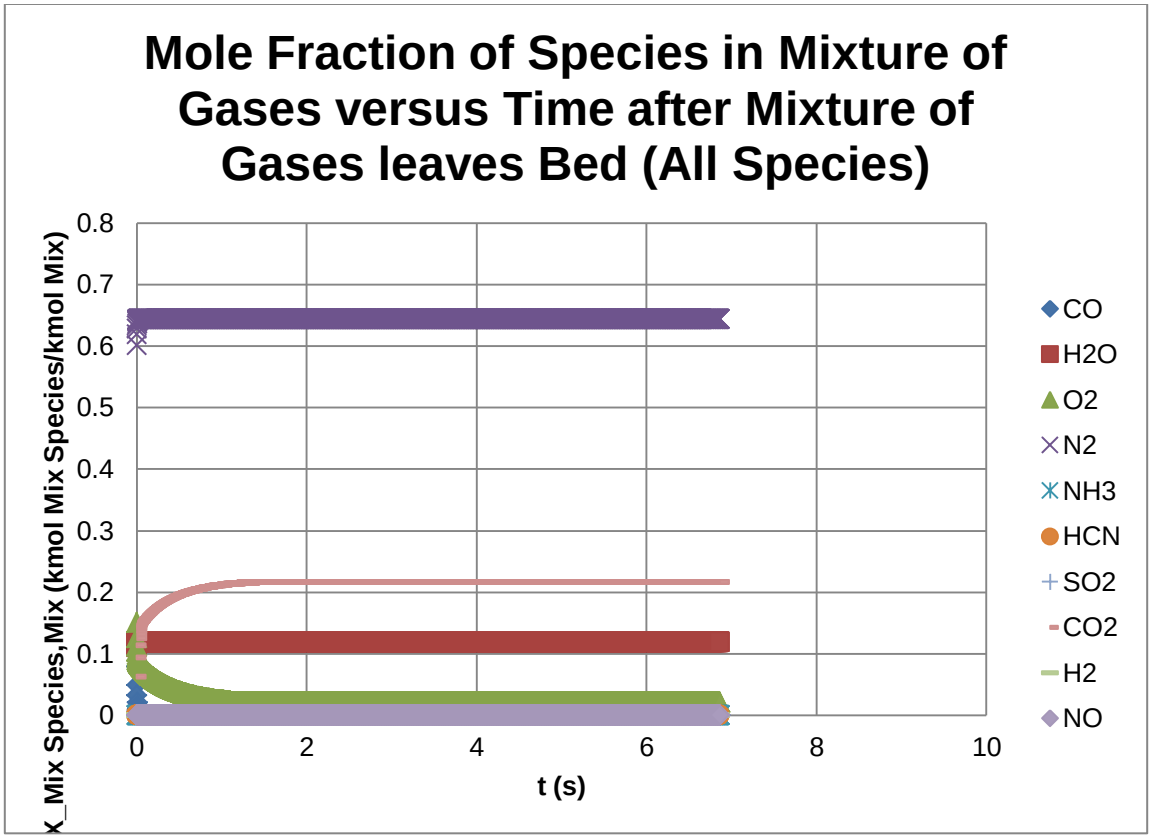

Fig. 58. Mole fraction of all species versus time for anonymous CFB boiler firing tire fuel with increased air O_2.

Most of the trace species are highly dependent upon O_2 concentration. For instance, the higher oxidation rate from higher O_2 leads to a lower concentration of HCN. This would be the case with NH_3 also except that it isn't as reactive as the HCN so that the inflation of the NH_3 concentration merely from the decrease in N_2 overshadows the loss of NH_3 from increased oxidation causing an overall higher NH_3. The increased oxidation rates of both NH_3 and HCN increases both the peak and riser exit concentrations of NO as well as increases the exit concentration of H_2 as these

species are both products of NH_3 and HCN oxidation. The new trends are shown below in the graph of the mole fraction of species in the mixture of gases versus time after the mixture of gases leaves the CFB bed until they reach the CFB riser exit for trace species in Fig. 59.

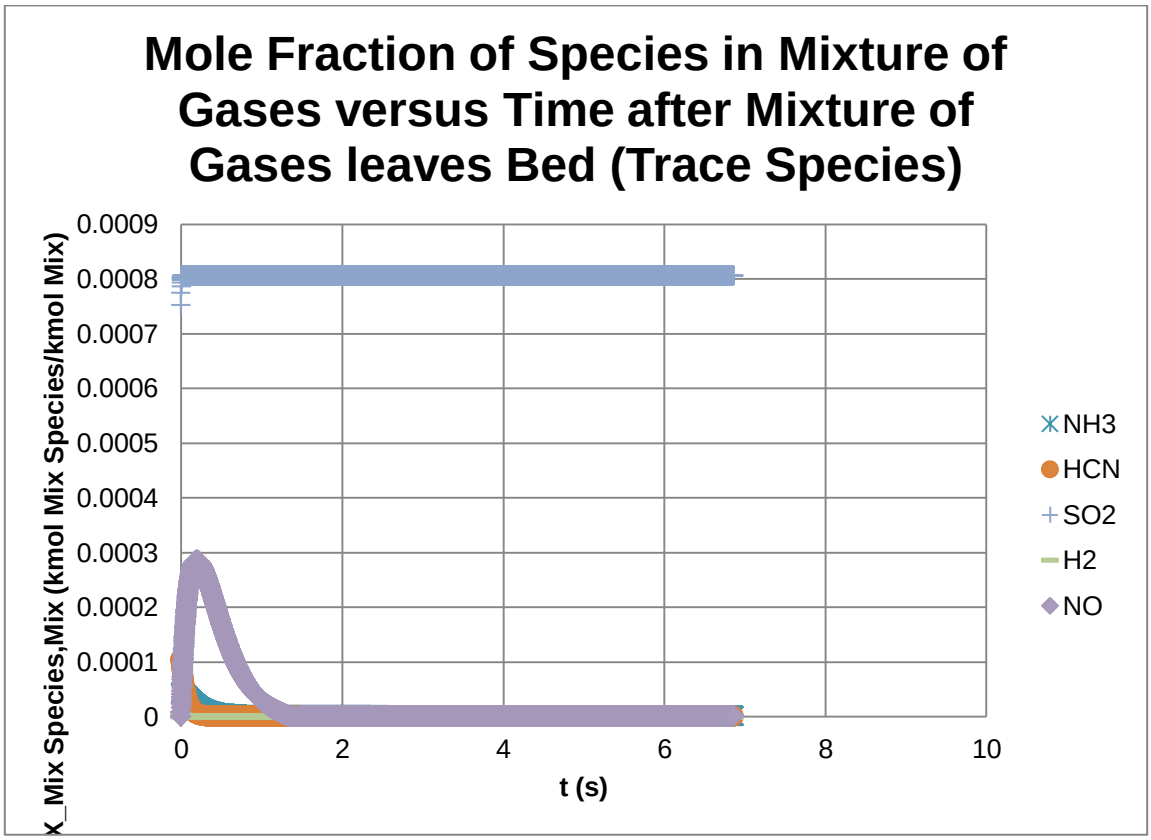

Fig. 59. Mole fraction of trace species versus time for anonymous CFB boiler firing tire fuel with increased air O_2.

The new trends are evident in the 'Output' tab of the Excel program as shown below in Table 32. Continuing to increase $X_{O_2,Air}x100$ will continue all of the trends

except for that of NH_3 which finally becomes lower at the exit as relatively more and more O_2 continues to increase the oxidation rate of NH_3 more quickly than it is inflated by the decreasing amount of N_2.

Table 32

Output tab for anonymous CFB boiler firing tire fuel with increased air O_2.

WET BASIS CONCENTRATION OF SPECIES IN MIXTURE OF GASES LEAVING CFB RISER										
	CO	H2O	O2	N2	NH3	HCN	SO2	CO2	H2	NO
ppm (Actual % O2)	2.59898E-37	118744.5941	20639.87517	643950.5044	1.547517249	2.13905E-36	806.127165	215856.4859	4.96426E-05	0.86578882
Mole % (Actual % O2)	2.59898E-41	11.87445941	2.063987517	64.39505044	0.000154752	2.13905E-40	0.080612717	21.58564859	4.96426E-09	8.65789E-05
ppm (Standard % O2)	2.51491E-37	114903.4835	30000	645440.0981	1.497458677	2.06986E-36	780.0508323	208874.0322	4.80367E-05	0.837782572
Mole % (Standard % O2)	2.51491E-41	11.49034835	3	F7/10000	0.000149746	2.06986E-40	0.078005083	20.88740322	4.80367E-09	8.37783E-05
g/GJ	6.32554E-38	18588.90132	5739.030678	156784.1372	0.229051765	5.02362E-37	448.7864975	82546.36864	8.69613E-07	0.346135153

DRY BASIS CONCENTRATION OF SPECIES IN MIXTURE OF GASES LEAVING CFB RISER										
	CO	H2O	O2	N2	NH3	HCN	SO2	CO2	H2	NO
ppm (Actual % O2)	2.94918E-37	0	23420.99127	730719.4941	1.75603717	2.42728E-36	914.7486184	244942.0275	5.63316E-05	0.982449372
Mole % (Actual % O2)	2.94918E-41	0	2.342099127	73.07194941	0.000175604	2.42728E-40	0.091474862	24.49420275	5.63316E-09	9.82449E-05
ppm (Standard % O2)	2.88148E-37	0	30000	729784.6946	1.715723736	2.37155E-36	893.7486883	239318.881	5.50384E-05	0.959895232
Mole % (Standard % O2)	2.88148E-41	0	3	F16/10000	0.000171572	2.37155E-40	0.089374869	23.9318881	5.50384E-09	9.59895E-05
g/GJ	6.32554E-38	0	5739.030678	156784.1372	0.229051765	5.02362E-37	448.7864975	82546.36864	8.69613E-07	0.346135153

Subtracting 10% from the mole percent of O_2 in the air also requires adding 10% to the mole percent of N_2 in the air. The only real change taking place is the increase in N_2 since the amount of O_2 is set by the excess air. The increase in N_2 leads to higher $\dot{m}_{Bed\ Mix}$ in turn increasing the $V_{Bed\ Mix}$ which decreases the $t_{Res,Bed\ Mix}$ and Δt. The shorter time in the combustor along with the relatively lower O_2 concentration reduces the burning effectiveness so that almost 5% of the SMD size tire fuel is still unburned at the riser exit. The mere increase in N_2 causes a pseudo-deflation of such species as O_2, H_2O, SO_2, and CO_2. However, the smaller concentration of O_2 decreases the reaction rate of CO oxidation so that CO has a higher concentration at the exit of the riser. The new trends are shown below in the graph of the mole fraction of species in the mixture

of gases versus time after the mixture of gases leaves the CFB bed until they reach the CFB riser exit for all species in Fig. 60.

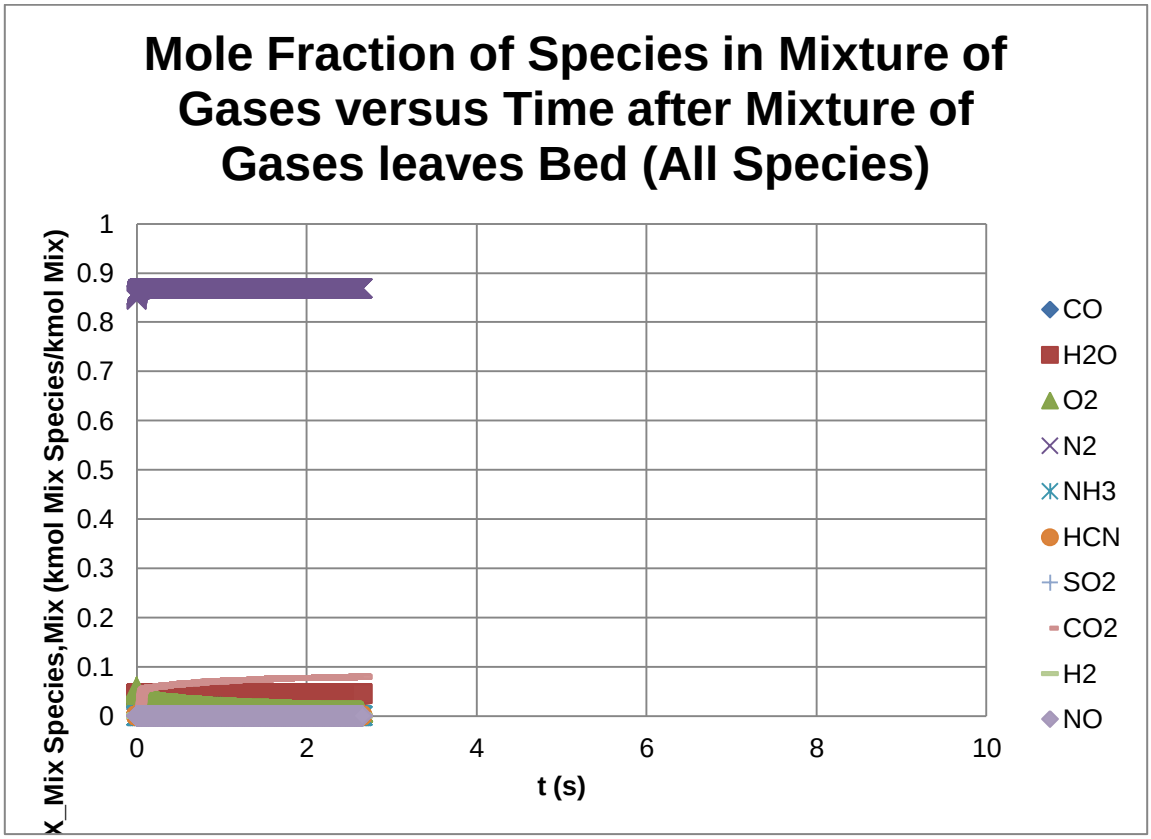

Fig. 60. Mole fraction of all species versus time for anonymous CFB boiler firing tire fuel with decreased air O_2.

Most of the trace species are highly dependent upon O_2 concentration. For instance, the lower oxidation rate from lower O_2 leads to a higher concentration of HCN. This would be the case with NH_3 also except that it isn't as reactive as the HCN so that the deflation of the NH_3 concentration merely from the increase in N_2 overshadows the

gain of NH_3 from decreased oxidation causing an overall lower NH_3. The decreased oxidation rates of both NH_3 and HCN decreases the peak concentration of NO. However, the NO concentration at the riser exit increases because the NO is still being formed from the delayed combustion of tire at the exit. The new trends are shown below in the graph of the mole fraction of species in the mixture of gases versus time after the mixture of gases leaves the CFB bed until they reach the CFB riser exit for trace species in Fig. 61.

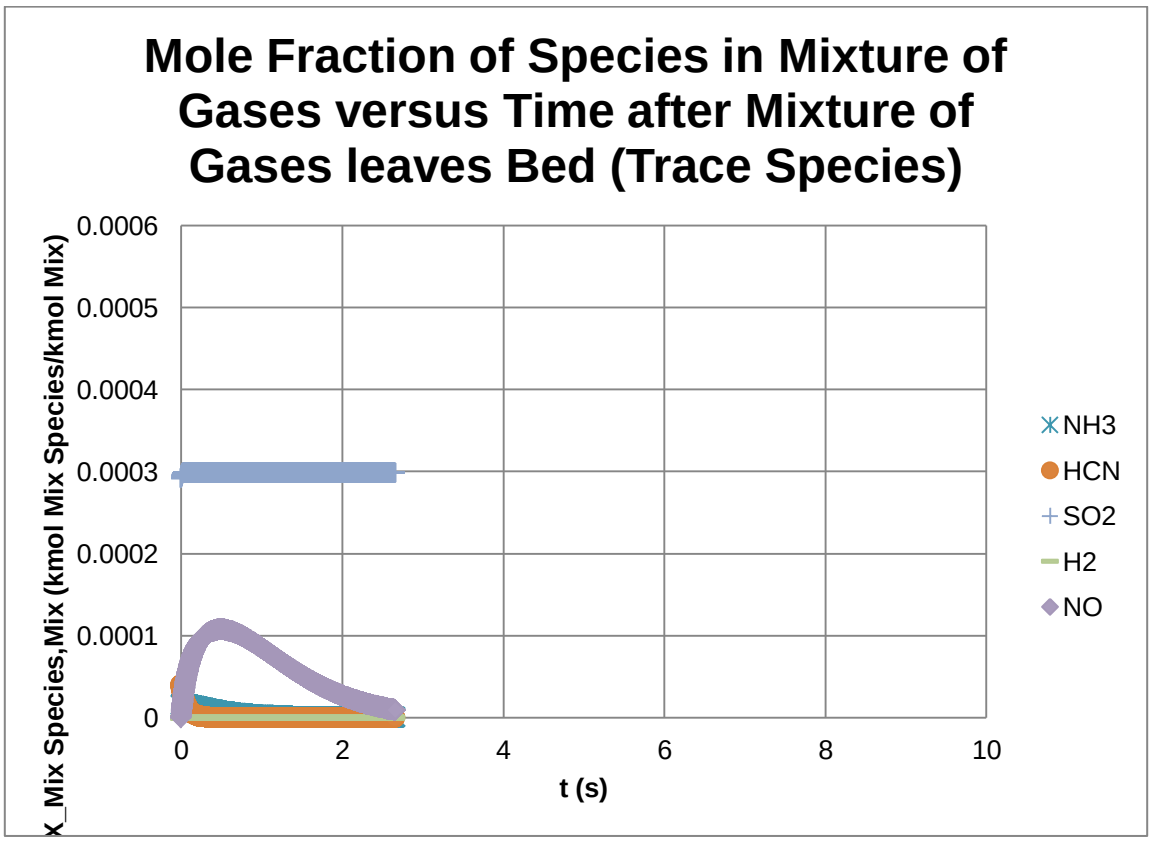

Fig. 61. Mole fraction of trace species versus time for anonymous CFB boiler firing tire fuel with decreased air O_2.

The new trends are evident in the 'Output' tab of the Excel program as shown below in Table 33. Continuing to decrease $X_{O_2,Air}x100$ will continue all of the trends except for that of NH_3 which finally becomes higher at the exit as relatively less and less O_2 continues to decrease the oxidation rate of NH_3 more quickly than it is deflated by the increasing amount of N_2. In fact, there is no more O_2 in the primary combustion air when $X_{O_2,Air}x100$ is 0% so that the only oxygen in the combustor is what comes from the tire fuel itself. Since the fuel oxygen is usually very small, the volatile combustion that is assumed to take place immediately in the bed of the combustor will likely not even have enough O_2 so that the combustor then begins to be a gasifier and the proposed program will cause errors since the program is not modified to handle this yet.

Table 33

Output tab for anonymous CFB boiler firing tire fuel with decreased air O_2.

WET BASIS CONCENTRATION OF SPECIES IN MIXTURE OF GASES LEAVING CFB RISER										
	CO	H2O	O2	N2	NH3	HCN	SO2	CO2	H2	NO
ppm (Actual % O2)	45.47803232	44053.5434	8571.185965	867878.9397	0.877784013	1.08578E-08	299.0715117	79141.34526	4.68933E-05	9.55827434
Mole % (Actual % O2)	0.004547803	4.40535434	0.857118596	86.78789397	8.77784E-05	1.08578E-12	0.029907151	7.914134526	4.68933E-09	0.000955827
ppm (Standard % O2)	35.86991152	34746.37366	30000	872552.4449	0.692335031	8.56389E-09	235.8868253	62421.19344	3.69862E-05	7.538902574
Mole % (Standard % O2)	0.003586991	3.474637366	3	F7/10000	6.92335E-05	8.56389E-13	0.023588683	6.242119344	3.69862E-09	0.00075389
g/GJ	30.17230283	18798.92012	6496.576837	575997.9846	0.354158764	6.95104E-09	453.8616138	82498.96118	2.23921E-06	10.4165861
DRY BASIS CONCENTRATION OF SPECIES IN MIXTURE OF GASES LEAVING CFB RISER										
	CO	H2O	O2	N2	NH3	HCN	SO2	CO2	H2	NO
ppm (Actual % O2)	47.57382801	0	8966.177871	907874.0067	0.918235543	1.13582E-08	312.8538315	82788.47075	4.90544E-05	9.998754924
Mole % (Actual % O2)	0.004757383	0	0.896617787	90.78740067	9.18236E-05	1.13582E-12	0.031285383	8.278847075	4.90544E-09	0.000999875
ppm (Standard % O2)	37.66962549	0	30000	904152.8896	0.727071805	8.99357E-09	247.7220597	65553.07441	3.88419E-05	7.917154643
Mole % (Standard % O2)	0.003766963	0	3	F16/10000	7.27072E-05	8.99357E-13	0.024772206	6.555307441	3.88419E-09	0.000791715
g/GJ	30.17230283	0	6496.576837	575997.9846	0.354158764	6.95104E-09	453.8616138	82498.96118	2.23921E-06	10.4165861

5.3.9 Calcium-Sulfur Ratio

Returning $X_{O_2,Air}x100$ to its original value, CSR was then altered. Increasing CSR by one, increases $Y_{LS,Fuel}\,x100$ which leads to more moisture immediately released during drying and more CO_2 immediately released during calcination. However, this also leaves more CaO available to immediately capture SO_2 so that almost 55% is captured. The SO_2 concentration is now less than 330 g SO_2/GJ, but this is still more than the US EPA regulation of 260 g SO_2/GJ (at least 70% SO_2 removal). The increases in H_2O and CO_2 increase $\dot{m}_{VL}$ while the decrease in SO_2 decreases $\dot{m}_{VF}$. However, the increase in $\dot{m}_{VL}$ is greater than the decrease in $\dot{m}_{VF}$ so there is an overall increase in $\dot{m}_{Bed\ Mix}$ in turn increasing $V_{Bed\ Mix}$ which decreases $t_{Res,Bed\ Mix}$ and Δt. The shorter time in the combustor inhibits the complete burning of the SMD size tire fuel only slightly higher in the riser. In fact, the changes are so small that other species are hardly affected by the increase in CSR. The almost identical trends are shown below in the graphs of the mole fraction of species in the mixture of gases versus time after the mixture of gases leaves the CFB bed until they reach the CFB riser exit for all species in Fig. 62 and trace species in Fig. 63.

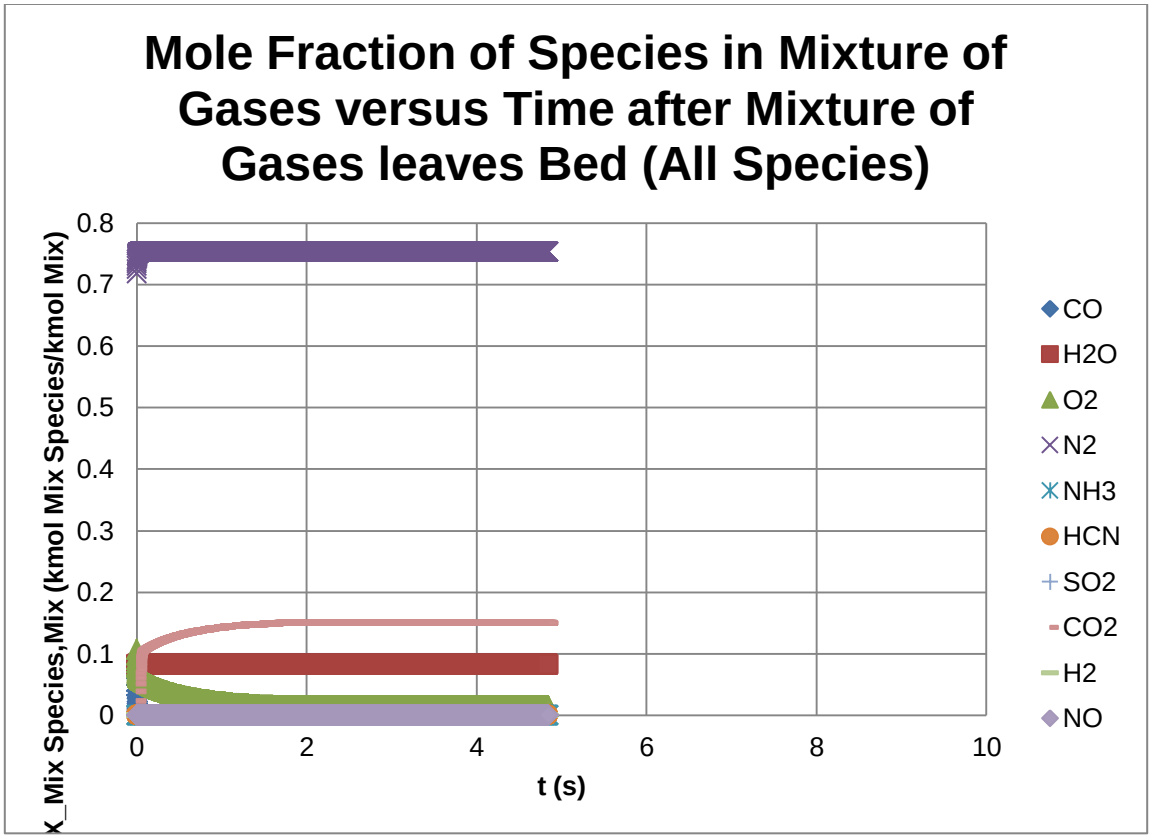

Fig. 62. Mole fraction of all species versus time for anonymous CFB boiler firing tire fuel with increased Calcium-Sulfur Ratio.

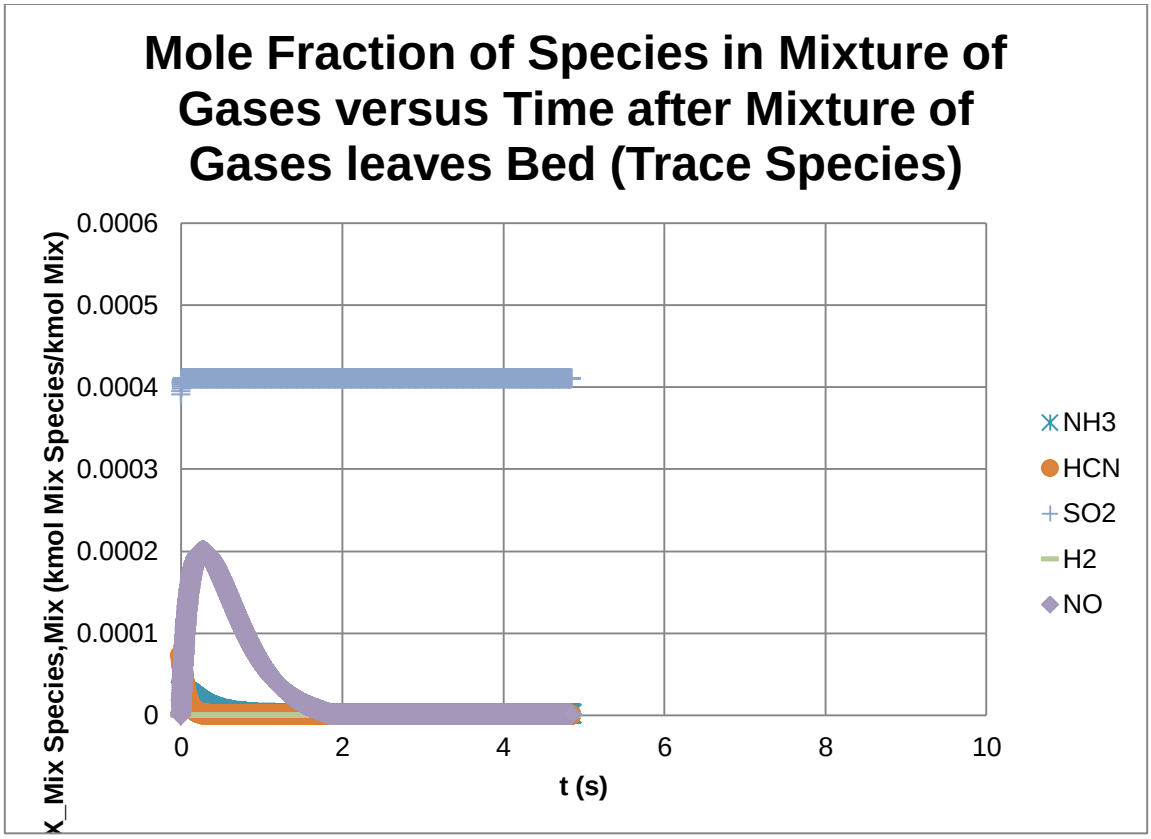

Fig. 63. Mole fraction of trace species versus time for anonymous CFB boiler firing tire fuel with increased Calcium-Sulfur Ratio.

The nearly identical trends are again greatly evident in the 'Output' tab of the Excel program as shown below in Table 34 where all species are basically unchanged except for SO_2. Continuing to increase CSR will end up flooding the combustor with limestone so that 100% of SO_2 may be captured, but the greater endothermic drying and calcination processes as well as the production of more and more energy sinks of H_2O and CO_2 will begin to greatly reduce heat output to the point of flame extinction. Also,

the shorter and shorter time in the combustor continues to inhibit the complete burning of the SMD size tire fuel to higher and higher in the riser.

Table 34

Output tab for anonymous CFB boiler firing tire fuel with increased Calcium-Sulfur Ratio.

WET BASIS CONCENTRATION OF SPECIES IN MIXTURE OF GASES LEAVING CFB RISER										
	CO	H2O	O2	N2	NH3	HCN	SO2	CO2	H2	NO
ppm (Actual % O2)	1.03543E-20	82404.59806	14279.50138	752699.9445	1.299143971	8.62664E-20	410.2555479	150203.8041	2.52108E-05	0.597318967
Mole % (Actual % O2)	1.03543E-24	8.240459806	1.427950138	75.26999445	0.000129914	8.62664E-24	0.041025555	15.02038041	2.52108E-09	5.97319E-05
ppm (Standard % O2)	9.52259E-21	75785.76468	30000	755695.9284	1.194795213	7.93374E-20	377.303344	138139.2594	2.31858E-05	0.549341611
Mole % (Standard % O2)	9.52259E-25	7.578576468	3	F7/10000	0.00011948	7.93374E-24	0.037730334	13.81392594	2.31858E-09	5.49342E-05
g/GJ	3.62158E-21	18538.5384	5705.959615	263363.5619	0.276337356	2.91153E-20	328.2274201	82546.36864	6.34663E-07	0.343181771
DRY BASIS CONCENTRATION OF SPECIES IN MIXTURE OF GASES LEAVING CFB RISER										
	CO	H2O	O2	N2	NH3	HCN	SO2	CO2	H2	NO
ppm (Actual % O2)	1.12841E-20	0	15561.87112	820296.1162	1.415813515	9.40136E-20	447.0985219	163692.8473	2.74749E-05	0.65096116
Mole % (Actual % O2)	1.12841E-24	0	1.556187112	82.02961162	0.000141581	9.40136E-24	0.044709852	16.36928473	2.74749E-09	6.50961E-05
ppm (Standard % O2)	1.04462E-20	0	30000	818046.4585	1.310681368	8.70326E-20	413.8989323	151537.7292	2.54347E-05	0.602623618
Mole % (Standard % O2)	1.04462E-24	0	3	F16/10000	0.000131068	8.70326E-24	0.041389893	15.15377292	2.54347E-09	6.02624E-05
g/GJ	3.62158E-21	0	5705.959615	263363.5619	0.276337356	2.91153E-20	328.2274201	82546.36864	6.34663E-07	0.343181771

Decreasing CSR by one, decreases $Y_{LS,Fuel}\ x100$ which leads to less moisture immediately released during drying and less CO_2 immediately released during calcination. However, this also leaves less CaO available to immediately capture SO_2 so that less than 20% is captured. The SO_2 concentration is now over 570 g SO_2/GJ which is more than the US EPA regulation of 260 g SO_2/GJ (at least 70% SO_2 removal). The decreases in H_2O and CO_2 decrease $\dot{m}_{VL}$ while the increase in SO_2 increases $\dot{m}_{VF}$. However, the decrease in $\dot{m}_{VL}$ is greater than the increase in $\dot{m}_{VF}$ so there is an overall decrease in $\dot{m}_{Bed\ Mix}$ in turn decreasing $V_{Bed\ Mix}$ which increases $t_{Res,Bed\ Mix}$ and Δt. The longer time in the combustor enhances the complete burning of the SMD size tire fuel only slightly lower in the riser. In fact, the changes are so small that other species

are hardly affected by the decrease in CSR. The almost identical trends are shown below in the graphs of the mole fraction of species in the mixture of gases versus time after the mixture of gases leaves the CFB bed until they reach the CFB riser exit for all species in Fig. 64 and trace species in Fig. 65.

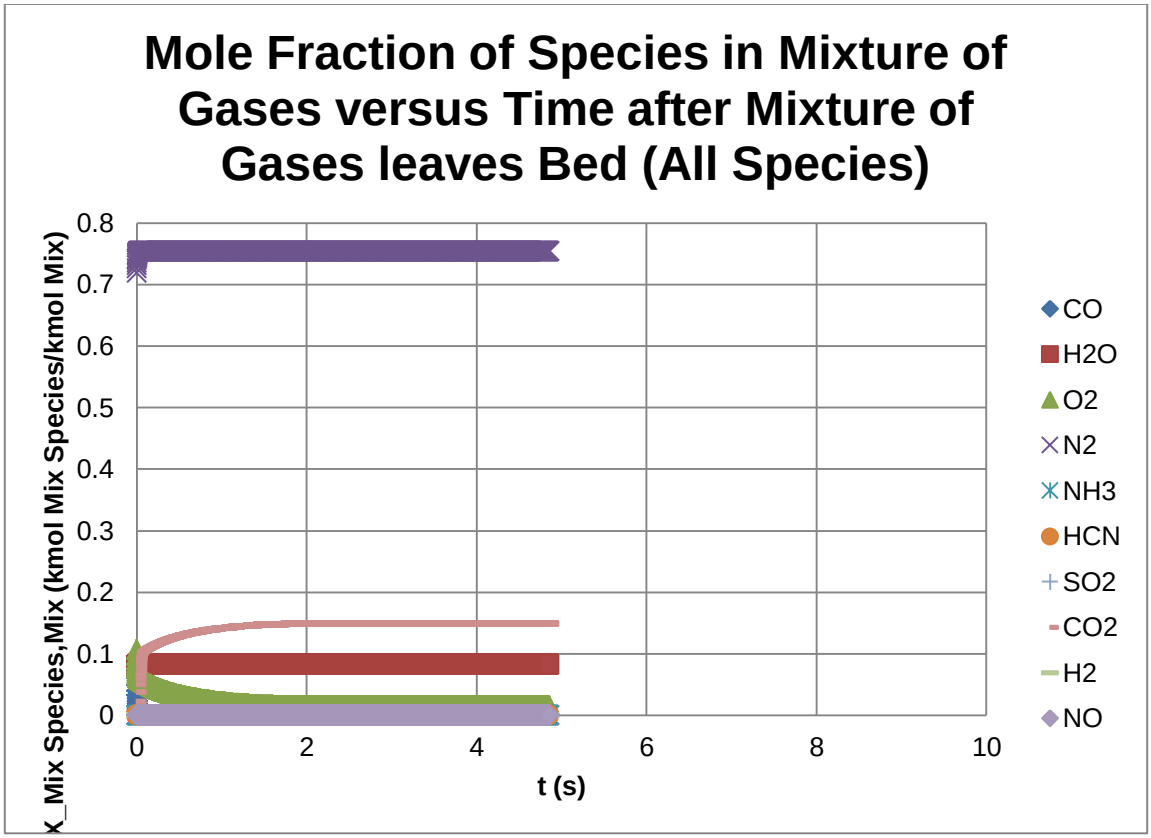

Fig. 64. Mole fraction of all species versus time for anonymous CFB boiler firing tire fuel with decreased Calcium-Sulfur Ratio.

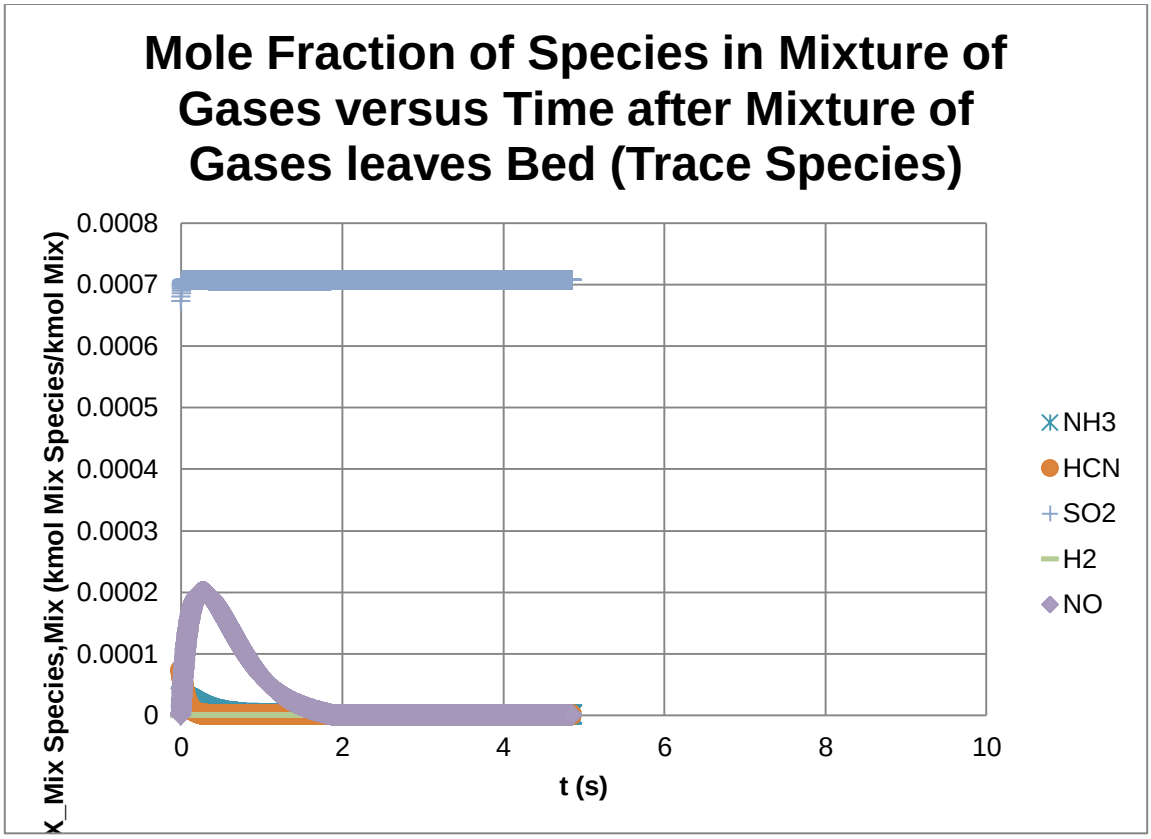

Fig. 65. Mole fraction of trace species versus time for anonymous CFB boiler firing tire fuel with decreased Calcium-Sulfur Ratio.

The nearly identical trends are again greatly evident in the 'Output' tab of the Excel program as shown below in Table 35 where all species are basically unchanged except for SO_2. Continuing to decrease CSR will end up with no limestone in the combustor so that 0% of SO_2 is captured. This leads to a maximum SO_2 concentration of over 700 g SO_2/GJ which is obviously more than the US EPA regulation of 260 g SO_2/GJ (at least 70% SO_2 removal). A CSR of zero also means that there is no $\dot{m}_{VL}$ so

that the longest time in the combustor is reached to enhance the complete burning of the SMD size tire fuel to still only slightly lower in the riser.

Table 35

Output tab for anonymous CFB boiler firing tire fuel with decreased Calcium-Sulfur Ratio.

WET BASIS CONCENTRATION OF SPECIES IN MIXTURE OF GASES LEAVING CFB RISER										
	CO	H2O	O2	N2	NH3	HCN	SO2	CO2	H2	NO
ppm (Actual % O2)	8.93459E-21	82057.13913	14307.36202	754168.3326	1.301372367	7.41248E-20	706.5294574	148758.7451	2.52237E-05	0.590297812
Mole % (Actual % O2)	8.93459E-25	8.205713913	1.430736202	75.41683326	0.000130137	7.41248E-24	0.070652946	14.87587451	2.52237E-09	5.90298E-05
ppm (Standard % O2)	8.21813E-21	75476.95813	30000	757041.6823	1.197015015	6.81807E-20	649.8726965	136829.7469	2.3201E-05	0.542961693
Mole % (Standard % O2)	8.21813E-25	7.547695813	3	F7/10000	0.000119702	6.81807E-24	0.06498727	13.68297469	2.3201E-09	5.42962E-05
g/GJ	3.15538E-21	18639.69675	5772.628941	266440.6726	0.279500328	2.52605E-20	570.7541731	82546.36864	6.41155E-07	0.342442378
DRY BASIS CONCENTRATION OF SPECIES IN MIXTURE OF GASES LEAVING CFB RISER										
	CO	H2O	O2	N2	NH3	HCN	SO2	CO2	H2	NO
ppm (Actual % O2)	9.73328E-21	0	15586.33181	821585.2693	1.4177052	8.0751E-20	769.6878396	162056.6502	2.74785E-05	0.643065965
Mole % (Actual % O2)	9.73328E-25	0	1.558633181	82.15852693	0.000141771	8.0751E-24	0.076968784	16.20566502	2.74785E-09	6.43066E-05
ppm (Standard % O2)	9.01166E-21	0	30000	819243.5636	1.312597711	7.47642E-20	712.6238212	150041.9045	2.54413E-05	0.595389587
Mole % (Standard % O2)	9.01166E-25	0	3	F16/10000	0.00013126	7.47642E-24	0.071262382	15.00419045	2.54413E-09	5.9539E-05
g/GJ	3.15538E-21	0	5772.628941	266440.6726	0.279500328	2.52605E-20	570.7541731	82546.36864	6.41155E-07	0.342442378

5.3.10 Dry limestone density

Returning CSR to its original value, ρ_{LSCaCO_3} was then altered. Adding 2,000 kilograms per cubic meter to the density of the dry limestone merely decreases the number of limestone particles in the combustor so that the effective cross-sectional area of the combustor is greater. The result is a decrease in $V_{Bed\ Mix}$ which increases $t_{Res,Bed\ Mix}$ and Δt. However, the effect is so small that the complete burning of the SMD size tire fuel is basically unaffected in the riser. In fact, the changes are so small that the difference in concentration is hardly noticeable even in trace species. The almost identical trends are shown below in the graphs of the mole fraction of species in

the mixture of gases versus time after the mixture of gases leaves the CFB bed until they reach the CFB riser exit for all species in Fig. 66 and trace species in Fig. 67.

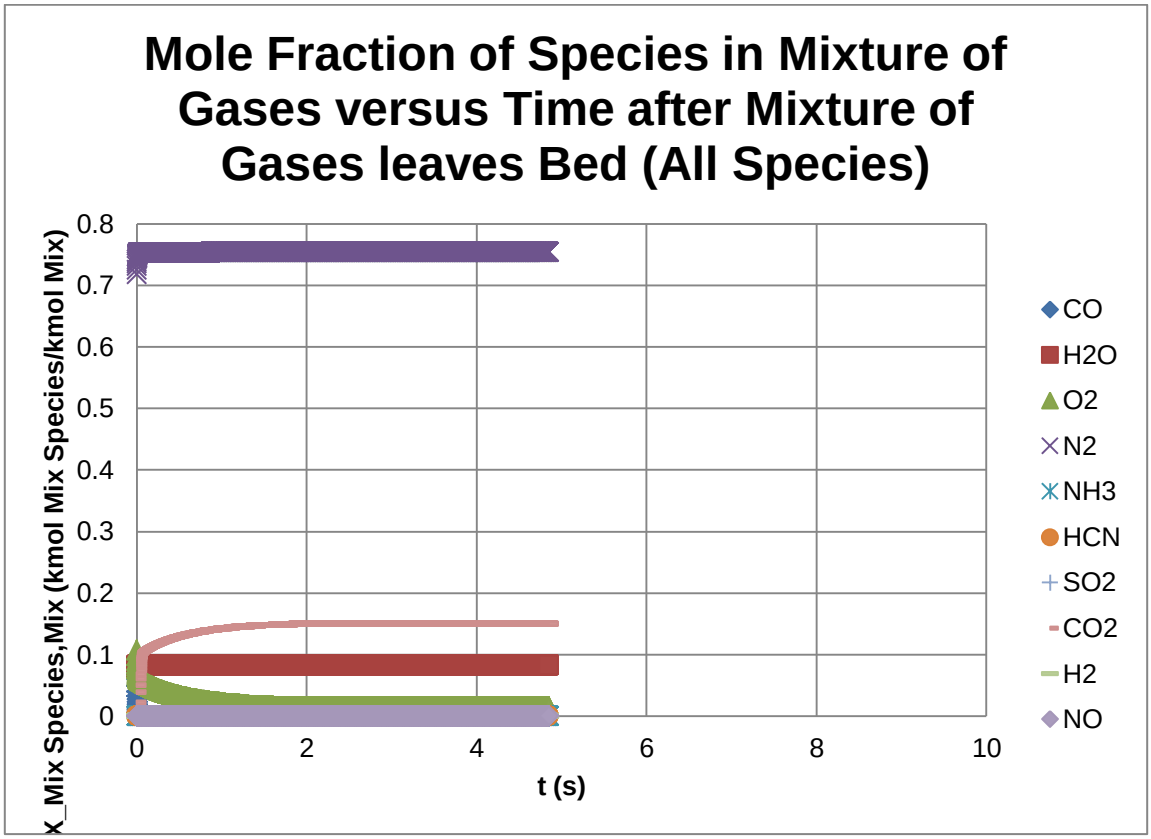

Fig. 66. Mole fraction of all species versus time for anonymous CFB boiler firing tire fuel with increased dry limestone density.

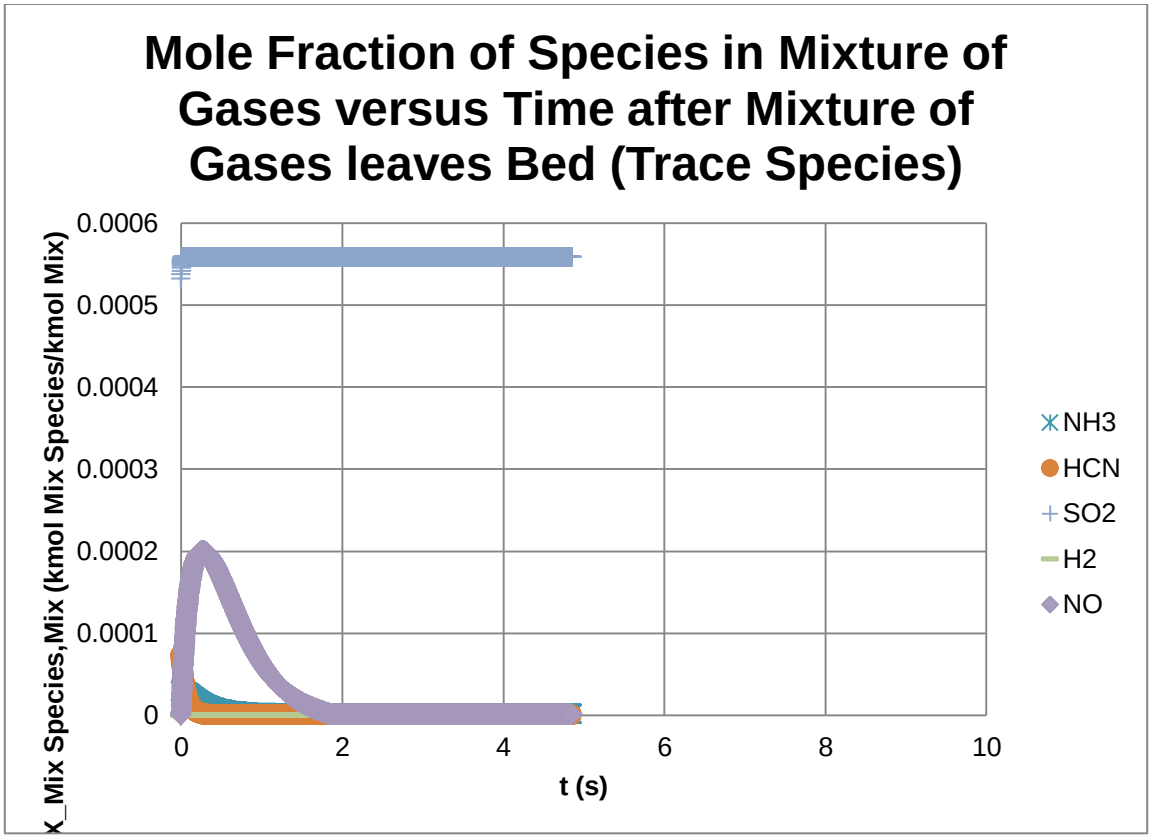

Fig. 67. Mole fraction of trace species versus time for anonymous CFB boiler firing tire fuel with increased dry limestone density.

The nearly matching concentrations at the riser exit are greatly evident in the 'Output' tab of the Excel program as shown below in Table 36 where all species are basically unchanged. Continuing to increase ρ_{LSCaCO_3} will slightly continue the stated trends until reaching an unrealistic density of limestone.

Table 36

Output tab for anonymous CFB boiler firing tire fuel with increased dry limestone density.

WET BASIS CONCENTRATION OF SPECIES IN MIXTURE OF GASES LEAVING CFB RISER										
	CO	H2O	O2	N2	NH3	HCN	SO2	CO2	H2	NO
ppm (Actual % O2)	9.61953E-21	82231.03743	14293.42044	753433.4251	1.300568777	7.99762E-20	558.2481491	149481.9787	2.51745E-05	0.589648163
Mole % (Actual % O2)	9.61953E-25	8.223103743	1.429342044	75.34334251	0.000130057	7.99762E-24	0.055824815	14.94819787	2.51745E-09	5.89648E-05
ppm (Standard % O2)	8.84751E-21	75631.52332	30000	756368.1032	1.196190646	7.35576E-20	513.4455217	137485.1894	2.31541E-05	0.542325504
Mole % (Standard % O2)	8.84751E-25	7.563152332	3	F7/10000	0.000119619	7.35576E-24	0.051344552	13.74851894	2.31541E-09	5.42326E-05
g/GJ	3.38084E-21	18588.82371	5739.101599	264893.182	0.277976276	2.71227E-20	448.7864975	82546.36864	6.36808E-07	0.340410502

DRY BASIS CONCENTRATION OF SPECIES IN MIXTURE OF GASES LEAVING CFB RISER										
	CO	H2O	O2	N2	NH3	HCN	SO2	CO2	H2	NO
ppm (Actual % O2)	1.04814E-20	0	15574.09438	820940.1884	1.417098235	8.71419E-20	608.2665375	162875.3911	2.74301E-05	0.642479957
Mole % (Actual % O2)	1.04814E-24	0	1.557409438	82.09401884	0.00014171	8.71419E-24	0.060826654	16.28753911	2.74301E-09	6.4248E-05
ppm (Standard % O2)	9.70374E-21	0	30000	818644.5055	1.311953166	8.06762E-20	563.134714	150790.453	2.53948E-05	0.594809585
Mole % (Standard % O2)	9.70374E-25	0	3	F16/10000	0.000131195	8.06762E-24	0.056313471	15.0790453	2.53948E-09	5.9481E-05
g/GJ	3.38084E-21	0	5739.101599	264893.182	0.277976276	2.71227E-20	448.7864975	82546.36864	6.36808E-07	0.340410502

Subtracting 2,000 kilograms per cubic meter from the density of the dry limestone merely increases the number of limestone particles in the combustor so that the effective cross-sectional area of the combustor is reduced. The result is an increase in $V_{Bed\ Mix}$ which decreases $t_{Res,Bed\ Mix}$ and Δt. However, the effect is so small that the complete burning of the SMD size tire fuel is basically unaffected in the riser. In fact, the changes are so small that the difference in concentration is hardly noticeable even in trace species. The almost identical trends are shown below in the graphs of the mole fraction of species in the mixture of gases versus time after the mixture of gases leaves the CFB bed until they reach the CFB riser exit for all species in Fig. 68 and trace species in Fig. 69.

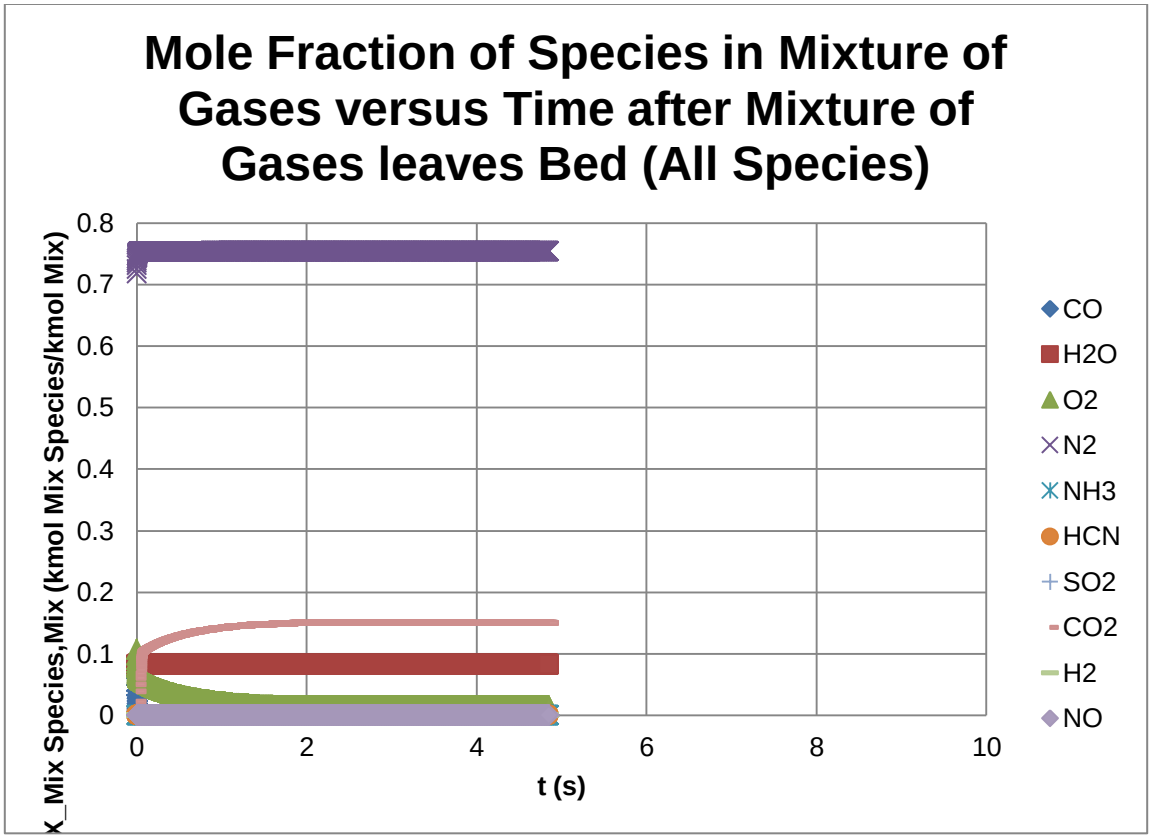

Fig. 68. Mole fraction of all species versus time for anonymous CFB boiler firing tire fuel with decreased dry limestone density.

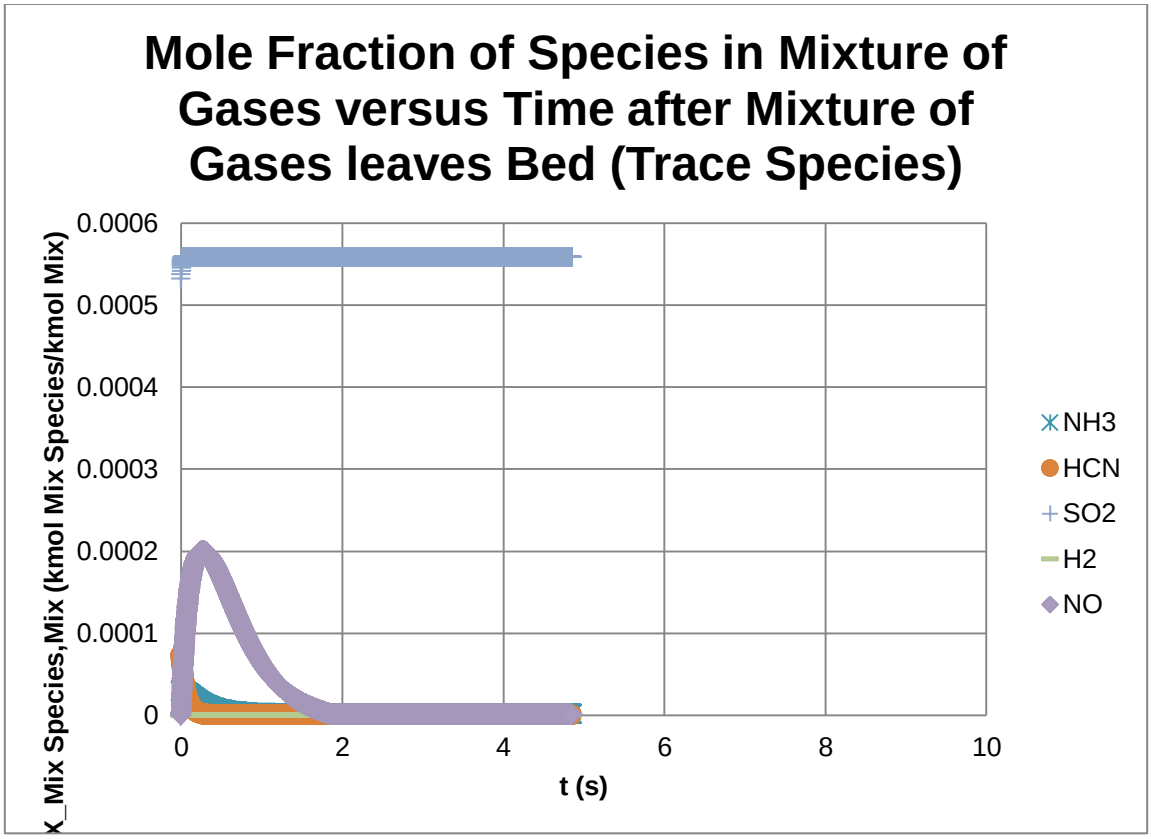

Fig. 69. Mole fraction of trace species versus time for anonymous CFB boiler firing tire fuel with decreased dry limestone density.

The nearly matching concentrations at the riser exit are greatly evident in the 'Output' tab of the Excel program as shown below in Table 37 where all species are basically unchanged. Continuing to decrease ρ_{LSCaCO_3} will slightly continue the stated trends until reaching an unrealistic density of limestone.

Table 37

Output tab for anonymous CFB boiler firing tire fuel with decreased dry limestone density.

WET BASIS CONCENTRATION OF SPECIES IN MIXTURE OF GASES LEAVING CFB RISER										
	CO	H2O	O2	N2	NH3	HCN	SO2	CO2	H2	NO
ppm (Actual % O2)	9.62218E-21	82231.0374	14293.42059	753433.4252	1.300589958	7.99981E-20	558.2481491	149481.9787	2.51716E-05	0.589387632
Mole % (Actual % O2)	9.62218E-25	8.22310374	1.429342059	75.34334252	0.000130059	7.99981E-24	0.055824815	14.94819787	2.51716E-09	5.89388E-05
ppm (Standard % O2)	8.84994E-21	75631.52335	30000	756368.1033	1.196210128	7.35778E-20	513.4455221	137485.1895	2.31515E-05	0.542085882
Mole % (Standard % O2)	8.84994E-25	7.563152335	3	F7/10000	0.000119621	7.35778E-24	0.051344552	13.74851895	2.31515E-09	5.42086E-05
g/GJ	3.38177E-21	18588.8237	5739.101658	264893.182	0.277980803	2.71301E-20	448.7864975	82546.36864	6.36737E-07	0.340260094
DRY BASIS CONCENTRATION OF SPECIES IN MIXTURE OF GASES LEAVING CFB RISER										
	CO	H2O	O2	N2	NH3	HCN	SO2	CO2	H2	NO
ppm (Actual % O2)	1.04843E-20	0	15574.09454	820940.1885	1.417121314	8.71659E-20	608.2665375	162875.3911	2.7427E-05	0.642196082
Mole % (Actual % O2)	1.04843E-24	0	1.557409454	82.09401885	0.000141712	8.71659E-24	0.060826654	16.28753911	2.7427E-09	6.42196E-05
ppm (Standard % O2)	9.70641E-21	0	30000	818644.5056	1.311974533	8.06984E-20	563.1347144	150790.4532	2.5392E-05	0.594546773
Mole % (Standard % O2)	9.70641E-25	0	3	F16/10000	0.000131197	8.06984E-24	0.056313471	15.07904532	2.5392E-09	5.94547E-05
g/GJ	3.38177E-21	0	5739.101658	264893.182	0.277980803	2.71301E-20	448.7864975	82546.36864	6.36737E-07	0.340260094

5.3.11 Limestone moisture

Returning ρ_{LSCaCO_3} to its original value, $Y_{LS\,H_2O,LS}x100$ was then altered. Increasing $Y_{LS\,H_2O,LS}x100$ by 5%, increases $Y_{LS,Fuel}\,x100$ which leads to more moisture immediately released during drying. The increase in H_2O increases $\dot{m}_{VL}$. Therefore, there is an increase in $\dot{m}_{Bed\ Mix}$ in turn increasing $V_{Bed\ Mix}$ which decreases $t_{Res,Bed\ Mix}$ and Δt. The shorter time in the combustor inhibits the complete burning of the SMD size tire fuel only slightly higher in the riser. In fact, the changes are so small that other species are hardly affected by the increase in $Y_{LS\,H_2O,LS}x100$. The almost identical trends are shown below in the graphs of the mole fraction of species in the mixture of gases versus time after the mixture of gases leaves the CFB bed until they reach the CFB riser exit for all species in Fig. 70 and trace species in Fig. 71.

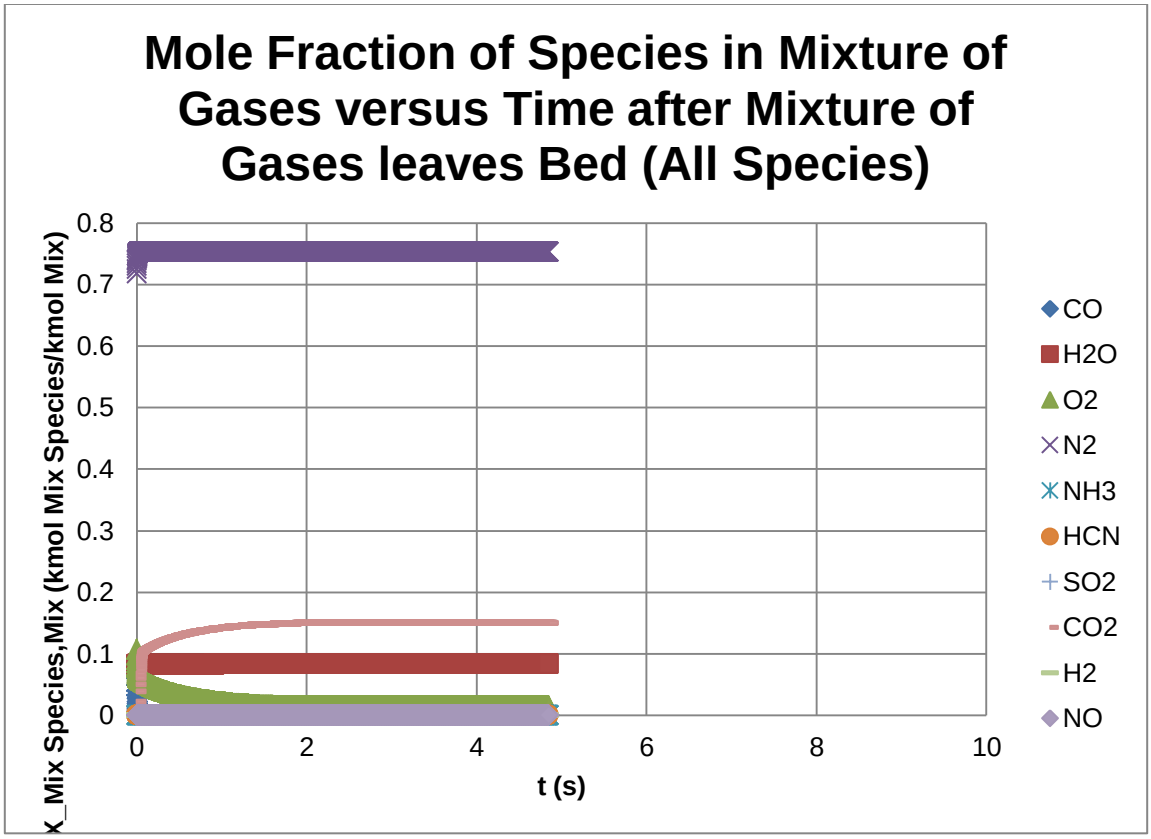

Fig. 70. Mole fraction of all species versus time for anonymous CFB boiler firing tire fuel with increased limestone moisture.

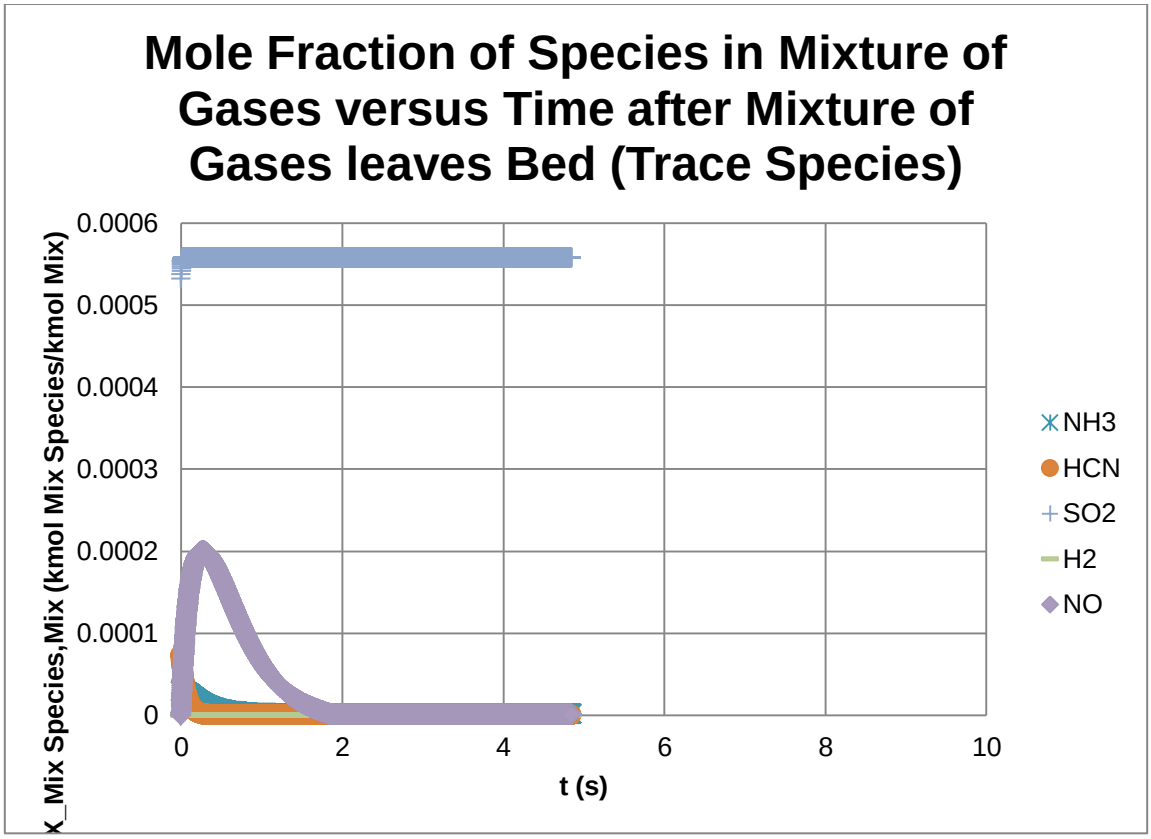

Fig. 71. Mole fraction of trace species versus time for anonymous CFB boiler firing tire fuel with increased limestone moisture.

The nearly identical trends are again greatly evident in the 'Output' tab of the Excel program as shown below in Table 38 where all species are basically unchanged except for H_2O. Continuing to increase $Y_{LS\ H_2O,LS}x100$ will end up flooding the combustor with water since more and more wetter and wetter limestone is needed to capture the same amount of SO_2. This will obviously greatly reduce heat output to the point of flame extinction. Also, the shorter and shorter time in the combustor continues to inhibit the complete burning of the SMD size tire fuel to higher and higher in the riser.

Table 38

Output tab for anonymous CFB boiler firing tire fuel with increased limestone moisture.

WET BASIS CONCENTRATION OF SPECIES IN MIXTURE OF GASES LEAVING CFB RISER										
	CO	H2O	O2	N2	NH3	HCN	SO2	CO2	H2	NO
ppm (Actual % O2)	1.00387E-20	82774.34726	14284.95941	752987.3999	1.300172572	8.38164E-20	557.9176716	149393.4868	2.51409E-05	0.588790138
Mole % (Actual % O2)	1.00387E-24	8.277434726	1.428495941	75.29873999	0.000130017	8.38164E-24	0.055791767	14.93934868	2.51409E-09	5.8879E-05
ppm (Standard % O2)	9.2326E-21	76127.93816	30000	755959.3458	1.195774541	7.70863E-20	513.1193831	137397.8594	2.31222E-05	0.541512929
Mole % (Standard % O2)	9.2326E-25	7.612793816	3	F7/10000	0.000119577	7.70863E-24	0.051311938	13.73978594	2.31222E-09	5.41513E-05
g/GJ	3.53024E-21	18722.72586	5739.101814	264893.182	0.2780562	2.84419E-20	448.7864975	82546.36864	6.36336E-07	0.340116499

DRY BASIS CONCENTRATION OF SPECIES IN MIXTURE OF GASES LEAVING CFB RISER										
	CO	H2O	O2	N2	NH3	HCN	SO2	CO2	H2	NO
ppm (Actual % O2)	1.09446E-20	0	15574.09495	820940.1881	1.417505679	9.13803E-20	608.2665372	162875.391	2.74097E-05	0.641925066
Mole % (Actual % O2)	1.09446E-24	0	1.557409495	82.09401881	0.000141751	9.13803E-24	0.060826654	16.2875391	2.74097E-09	6.41925E-05
ppm (Standard % O2)	1.01325E-20	0	30000	818644.5052	1.312330382	8.46002E-20	563.1347153	150790.4534	2.5376E-05	0.594295867
Mole % (Standard % O2)	1.01325E-24	0	3	F16/10000	0.000131233	8.46002E-24	0.056313472	15.07904534	2.5376E-09	5.94296E-05
g/GJ	3.53024E-21	0	5739.101814	264893.182	0.2780562	2.84419E-20	448.7864975	82546.36864	6.36336E-07	0.340116499

Decreasing $Y_{LS\ H_2O,LS}x100$ by 5%, decreases $Y_{LS,Fuel}\ x100$ which leads to less moisture immediately released during drying. The decrease in H_2O decreases $\dot{m}_{VL}$. Therefore, there is a decrease in $\dot{m}_{Bed\ Mix}$ in turn decreasing $V_{Bed\ Mix}$ which increases $t_{Res,Bed\ Mix}$ and Δt. The longer time in the combustor enhances the complete burning of the SMD size tire fuel only slightly lower in the riser. In fact, the changes are so small that other species are hardly affected by the decrease in $Y_{LS\ H_2O,LS}x100$. The almost identical trends are shown below in the graphs of the mole fraction of species in the mixture of gases versus time after the mixture of gases leaves the CFB bed until they reach the CFB riser exit for all species in Fig. 72 and trace species in Fig. 73.

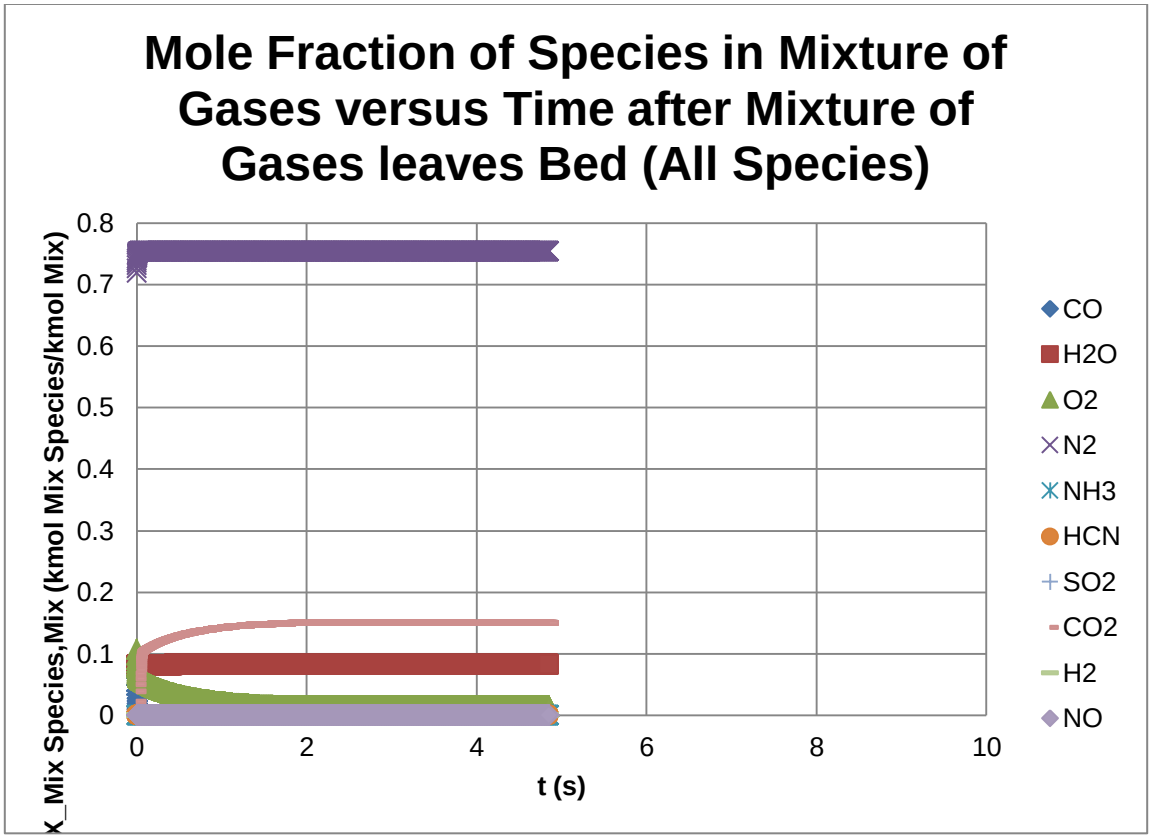

Fig. 72. Mole fraction of all species versus time for anonymous CFB boiler firing tire fuel with decreased limestone moisture.

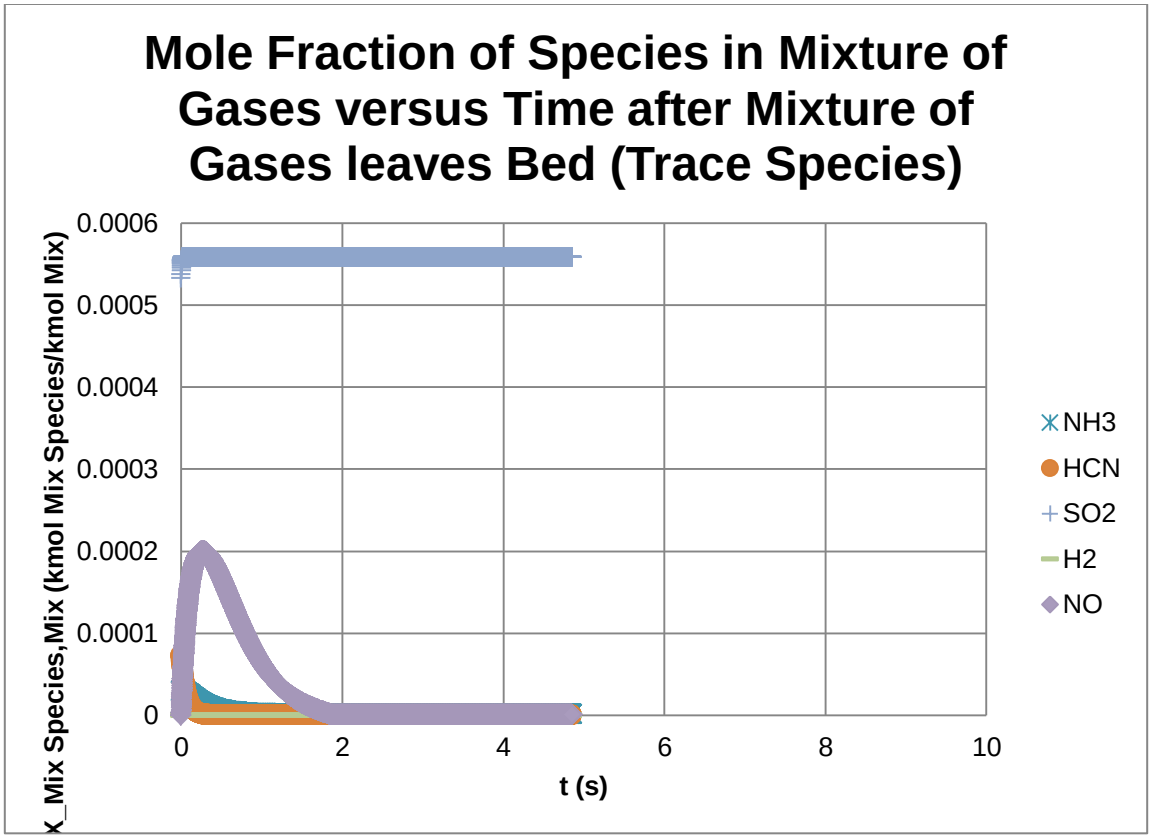

Fig. 73. Mole fraction of trace species versus time for anonymous CFB boiler firing tire fuel with decreased limestone moisture.

The nearly identical trends are again greatly evident in the 'Output' tab of the Excel program as shown below in Table 39 where all species are basically unchanged except for H_2O. Continuing to decrease $Y_{LS\ H_2O,LS}x100$ further to a negative percentage is unrealistic and meaningless since there is already no H_2O in the limestone.

Table 39

Output tab for anonymous CFB boiler firing tire fuel with decreased limestone moisture.

WET BASIS CONCENTRATION OF SPECIES IN MIXTURE OF GASES LEAVING CFB RISER										
	CO	H2O	O2	N2	NH3	HCN	SO2	CO2	H2	NO
ppm (Actual % O2)	9.25757E-21	81741.5078	14301.04475	753835.3005	1.301035303	7.66709E-20	558.5459138	149561.7111	2.51897E-05	0.588964793
Mole % (Actual % O2)	9.25757E-25	8.17415078	1.430104475	75.38353005	0.000130104	7.66709E-24	0.055854591	14.95617111	2.51897E-09	5.88965E-05
ppm (Standard % O2)	8.51493E-21	75184.21028	30000	756736.4299	1.19666635	7.05203E-20	513.7394032	137563.882	2.3169E-05	0.541718082
Mole % (Standard % O2)	8.51493E-25	7.518421028	3	F7/10000	0.000119667	7.05203E-24	0.05137394	13.7563882	2.3169E-09	5.41718E-05
g/GJ	3.25189E-21	18468.31174	5739.101731	264893.1822	0.277927744	2.59879E-20	448.7864975	82546.36864	6.36853E-07	0.339834719
DRY BASIS CONCENTRATION OF SPECIES IN MIXTURE OF GASES LEAVING CFB RISER										
	CO	H2O	O2	N2	NH3	HCN	SO2	CO2	H2	NO
ppm (Actual % O2)	1.00817E-20	0	15574.09474	820940.1893	1.416850825	8.34959E-20	608.2665377	162875.3911	2.7432E-05	0.641393244
Mole % (Actual % O2)	1.00817E-24	0	1.557409474	82.09401893	0.000141685	8.34959E-24	0.060826654	16.28753911	2.7432E-09	6.41393E-05
ppm (Standard % O2)	9.33363E-21	0	30000	818644.5064	1.311724115	7.73008E-20	563.1347152	150790.4534	2.53966E-05	0.593803504
Mole % (Standard % O2)	9.33363E-25	0	3	F16/10000	0.000131172	7.73008E-24	0.056313472	15.07904534	2.53966E-09	5.93804E-05
g/GJ	3.25189E-21	0	5739.101731	264893.1822	0.277927744	2.59879E-20	448.7864975	82546.36864	6.36853E-07	0.339834719

5.3.12 Average degree of sulfation

Returning $Y_{LS\ H_2O,LS}x100$ to its original value, $X_{LS\ CaSO_3,LS\ CaO}x100$ was then altered. Increasing $X_{LS\ CaSO_3,LS\ CaO}x100$ by 10%, increases the SO_2 captured by over 20% to an overall 56% captured. The SO_2 concentration is now just over 300 g SO_2/GJ, but this is still more than the US EPA regulation of 260 g SO_2/GJ (at least 70% SO_2 removal). The decrease in SO_2 decreases $\dot{m}_{VF}$ which decreases $\dot{m}_{Bed\ Mix}$ in turn decreasing $V_{Bed\ Mix}$ which increases $t_{Res,Bed\ Mix}$ and Δt. The longer time in the combustor enhances the complete burning of the SMD size tire fuel only slightly lower in the riser. In fact, the changes are so small that other species are hardly affected by the increase in $X_{LS\ CaSO_3,LS\ CaO}x100$. The almost identical trends are shown below in the graphs of the mole fraction of species in the mixture of gases versus time after the mixture of gases leaves the CFB bed until they reach the CFB riser exit for all species in Fig. 74 and trace species in Fig. 75.

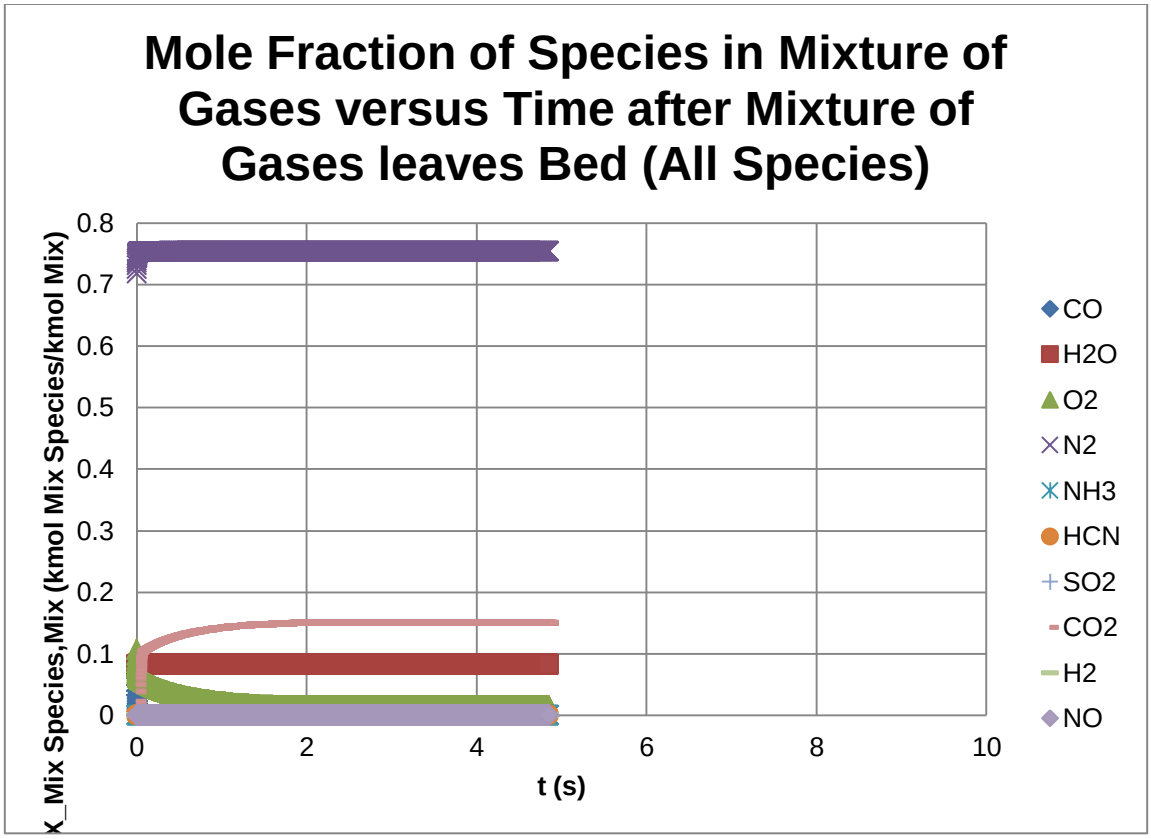

Fig. 74. Mole fraction of all species versus time for anonymous CFB boiler firing tire fuel with increased average degree of sulfation.

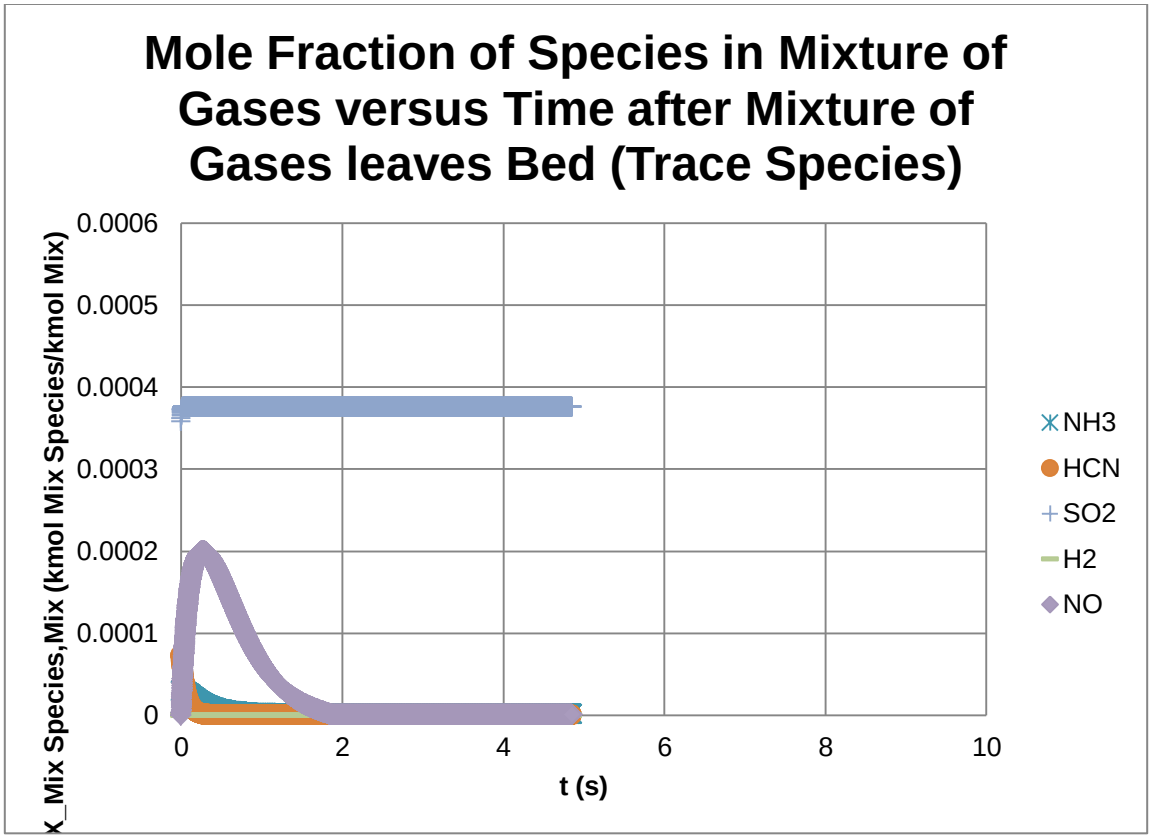

Fig. 75. Mole fraction of trace species versus time for anonymous CFB boiler firing tire fuel with increased average degree of sulfation.

The nearly identical trends are again greatly evident in the 'Output' tab of the Excel program as shown below in Table 40 where all species are basically unchanged except for SO_2. Continuing to increase $X_{LS\ CaSO_3,LS\ CaO} x100$ will allow 100% of SO_2 to be captured by the highly reactive limestone although 100% conversion is impossible due to the physical restraints described earlier in the limestone conversion process. Also, the longer and longer time in the combustor continues to enhance the complete burning of the SMD size tire fuel only slightly lower in the riser.

Table 40

Output tab for anonymous CFB boiler firing tire fuel with increased average degree of sulfation.

WET BASIS CONCENTRATION OF SPECIES IN MIXTURE OF GASES LEAVING CFB RISER										
	CO	H2O	O2	N2	NH3	HCN	SO2	CO2	H2	NO
ppm (Actual % O2)	9.49391E-21	82246.03255	14296.02711	753570.8167	1.300817584	7.89261E-20	375.9961546	149509.2373	2.51806E-05	0.589348128
Mole % (Actual % O2)	9.49391E-25	8.224603255	1.429602711	75.35708167	0.000130082	7.89261E-24	0.037599615	14.95092373	2.51806E-09	5.89348E-05
ppm (Standard % O2)	8.73209E-21	75646.32256	30000	756494.0221	1.196435421	7.25928E-20	345.8249049	137512.0919	2.316E-05	0.542056768
Mole % (Standard % O2)	8.73209E-25	7.564632256	3	F7/10000	0.000119644	7.25928E-24	0.03458249	13.75120919	2.316E-09	5.42057E-05
g/GJ	3.33608E-21	18588.8237	5739.101685	264893.1821	0.277978764	2.67617E-20	302.2154796	82546.36864	6.36847E-07	0.340175256
DRY BASIS CONCENTRATION OF SPECIES IN MIXTURE OF GASES LEAVING CFB RISER										
	CO	H2O	O2	N2	NH3	HCN	SO2	CO2	H2	NO
ppm (Actual % O2)	1.03447E-20	0	15577.18912	821103.3059	1.417392494	8.59992E-20	409.6916689	162907.7537	2.74372E-05	0.642163531
Mole % (Actual % O2)	1.03447E-24	0	1.557718912	82.11033059	0.000141739	8.59992E-24	0.040969167	16.29077537	2.74372E-09	6.42164E-05
ppm (Standard % O2)	9.57733E-21	0	30000	818795.9784	1.312246478	7.96196E-20	379.2996309	150822.8151	2.54018E-05	0.5945261
Mole % (Standard % O2)	9.57733E-25	0	3	F16/10000	0.000131225	7.96196E-24	0.037929963	15.08228151	2.54018E-09	5.94526E-05
g/GJ	3.33608E-21	0	5739.101685	264893.1821	0.277978764	2.67617E-20	302.2154796	82546.36864	6.36847E-07	0.340175256

Decreasing $X_{LS\ CaSO_3,LS\ CaO}x100$ by 10%, decreases the SO_2 captured by over 20% to an overall 14% captured. The SO_2 concentration is now just under 600 g SO_2/GJ which is still more than the US EPA regulation of 260 g SO_2/GJ (at least 70% SO_2 removal). The increase in SO_2 increases $\dot{m}_{VF}$ which increases $\dot{m}_{Bed\ Mix}$ in turn increasing $V_{Bed\ Mix}$ which decreases $t_{Res,Bed\ Mix}$ and Δt. The shorter time in the combustor enhances the complete burning of the SMD size tire fuel only slightly higher in the riser. In fact, the changes are so small that other species are hardly affected by the decrease in $X_{LS\ CaSO_3,LS\ CaO}x100$. The almost identical trends are shown below in the graphs of the mole fraction of species in the mixture of gases versus time after the mixture of gases leaves the CFB bed until they reach the CFB riser exit for all species in Fig. 76 and trace species in Fig. 77.

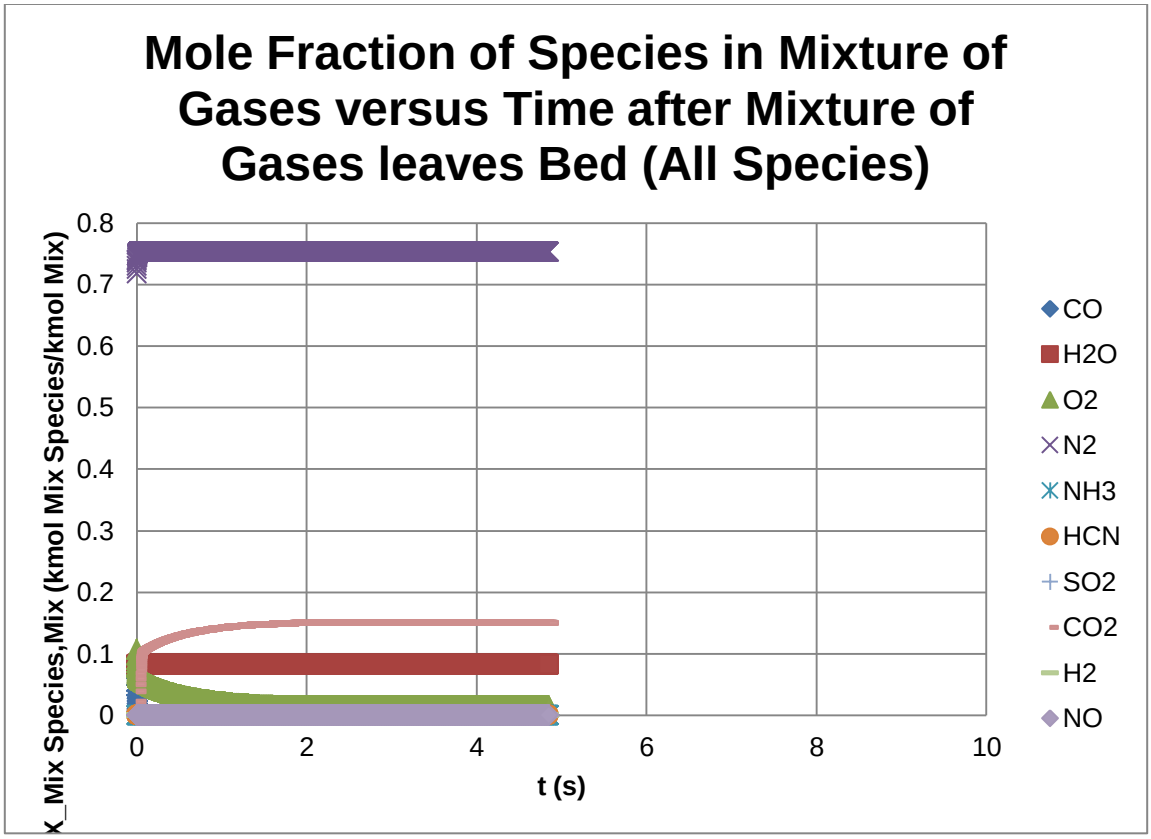

Fig. 76. Mole fraction of all species versus time for anonymous CFB boiler firing tire fuel with decreased average degree of sulfation.

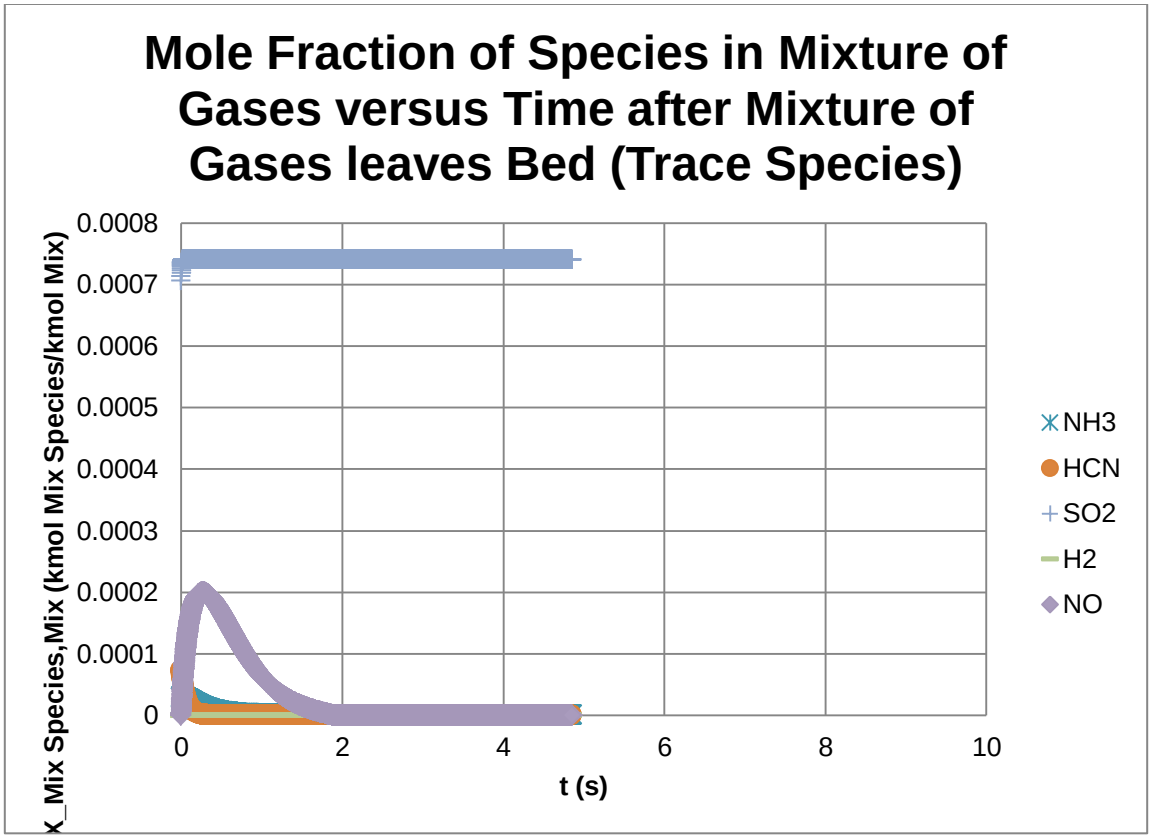

Fig. 77. Mole fraction of trace species versus time for anonymous CFB boiler firing tire fuel with decreased average degree of sulfation.

The nearly identical trends are again greatly evident in the 'Output' tab of the Excel program as shown below in Table 41 where all species are basically unchanged except for SO_2. Continuing to decrease $X_{LS\ CaSO_3,LS\ CaO}x100$ will end up with useless limestone in the combustor so that 0% of SO_2 is captured. This leads to a maximum SO_2 concentration of just under 700 g SO_2/GJ which is obviously more than the US EPA regulation of 260 g SO_2/GJ (at least 70% SO_2 removal). Also, the shorter and shorter

time in the combustor continues to inhibit the complete burning of the SMD size tire fuel only slightly higher in the riser.

Table 41

Output tab for anonymous CFB boiler firing tire fuel with decreased average degree of sulfation.

WET BASIS CONCENTRATION OF SPECIES IN MIXTURE OF GASES LEAVING CFB RISER										
	CO	H2O	O2	N2	NH3	HCN	SO2	CO2	H2	NO
ppm (Actual % O2)	9.74745E-21	82216.04781	14290.81453	753296.0833	1.300294825	8.10455E-20	740.4336992	149454.73	2.51718E-05	0.590291659
Mole % (Actual % O2)	9.74745E-25	8.221604781	1.429081453	75.32960833	0.000130029	8.10455E-24	0.07404337	14.945473	2.51718E-09	5.90292E-05
ppm (Standard % O2)	8.96504E-21	75616.72984	30000	756242.2334	1.195922757	7.45401E-20	681.0005648	137458.2973	2.31513E-05	0.542910126
Mole % (Standard % O2)	8.96504E-25	7.561672984	3	F7/10000	0.000119592	7.45401E-24	0.068100056	13.74582973	2.31513E-09	5.4291E-05
g/GJ	3.42642E-21	18588.82372	5739.101437	264893.1819	0.277968393	2.74903E-20	595.3575153	82546.36864	6.36857E-07	0.34084413

DRY BASIS CONCENTRATION OF SPECIES IN MIXTURE OF GASES LEAVING CFB RISER										
	CO	H2O	O2	N2	NH3	HCN	SO2	CO2	H2	NO
ppm (Actual % O2)	1.06206E-20	0	15571.00066	820777.1356	1.416776598	8.83056E-20	806.7625255	162843.0413	2.74267E-05	0.643170604
Mole % (Actual % O2)	1.06206E-24	0	1.557100066	82.07771356	0.000141678	8.83056E-24	0.080676253	16.28430413	2.74267E-09	6.43171E-05
ppm (Standard % O2)	9.83246E-21	0	30000	818493.0973	1.311634522	8.17523E-20	746.8909221	150758.1047	2.53913E-05	0.595439513
Mole % (Standard % O2)	9.83246E-25	0	3	F16/10000	0.000131163	8.17523E-24	0.074689092	15.07581047	2.53913E-09	5.9544E-05
g/GJ	3.42642E-21	0	5739.101437	264893.1819	0.277968393	2.74903E-20	595.3575153	82546.36864	6.36857E-07	0.34084413

5.3.13 Gas mixture pressure

Returning $X_{LS\ CaSO_3,LS\ CaO}x100$ to its original value, P_{Mix} was then altered. The pressure of the mixture of gases in the CFB riser realistically has an effect on the temperatures of the combustor such as T_{Mix} with higher pressure leading to higher temperatures while a lower pressure has the opposite effect. Therefore, changing of the pressure of the mixture of gases in the CFB riser without affecting temperatures such as T_{Mix} can only be achieved by increasing water flow through the tubes within the combustor walls to produce more steam which is assumed to be able to be handled by this combustor's tubes.

Adding 0.5 bars of pressure, increases $\rho_{Bed\ Mix}$ which increases $n'''_{Char,Bed\ Mix}$ and $n'''_{LS\ CaCO_3,Bed\ Mix}$ which in turn slightly decreases $a_{CS,Riser,Eff}$. These changes result in decreased $V_{Bed\ Mix}$ which increases the $t_{Res,Bed\ Mix}$ and Δt. This translates into the SMD size tire fuel completely burning lower in the riser at about a quarter of the way. Another change taking place from increased pressure is a decrease in $D_{O_2|Mix}$, but this is offset by the increase in $\rho_{Bed\ Mix}$ so that the overall mass transfer to the char is only slightly affected. Nevertheless, the trends according to the proposed model are almost exactly the same as before the increase in P_{Mix} except lengthened due to more time spent in the riser. These results are evident in the trends below in the graph of the mole fraction of species in the mixture of gases versus time after the mixture of gases leaves the CFB bed until they reach the CFB riser exit for all species in Fig. 78.

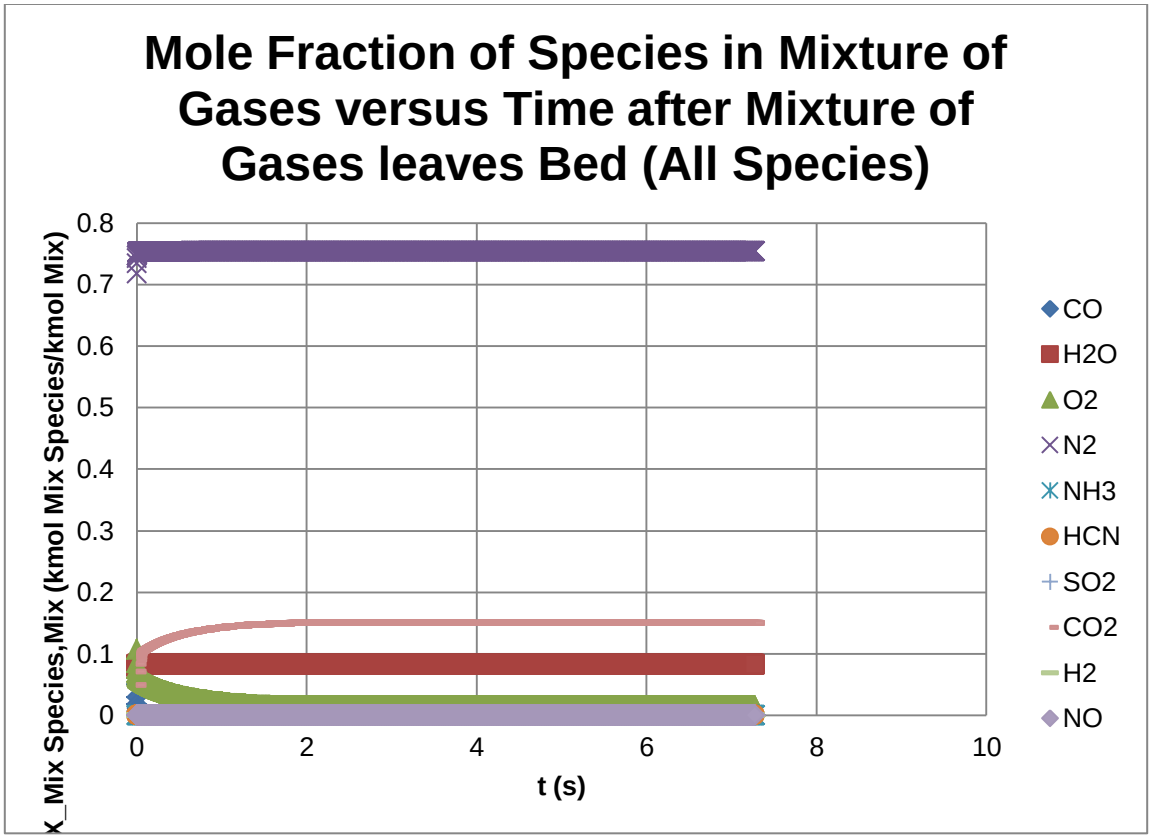

Fig. 78. Mole fraction of all species versus time for anonymous CFB boiler firing tire fuel with increased gas mixture pressure.

The NO concentration is most affected by the increased number of char particles to react with as seen by the smaller concentrations achieved at the peak and riser exit due to abundance of reducing surfaces. The CO is decreased and CO_2 increased due to the increased time to react after the char is completely burned. Also, HCN has decreased due to the increased time to be oxidized after the char is completely burned. However, NH_3 has increased due to both the lack of NO available to react with and HCN is more reactive with O_2 than NH_3. Also, there is an overall increase in the exit concentration of

H_2 as it is a product of NH_3 and HCN reactions. These trends are seen below in the graph of the mole fraction of species in the mixture of gases versus time after the mixture of gases leaves the CFB bed until they reach the CFB riser exit for trace species in Fig. 79.

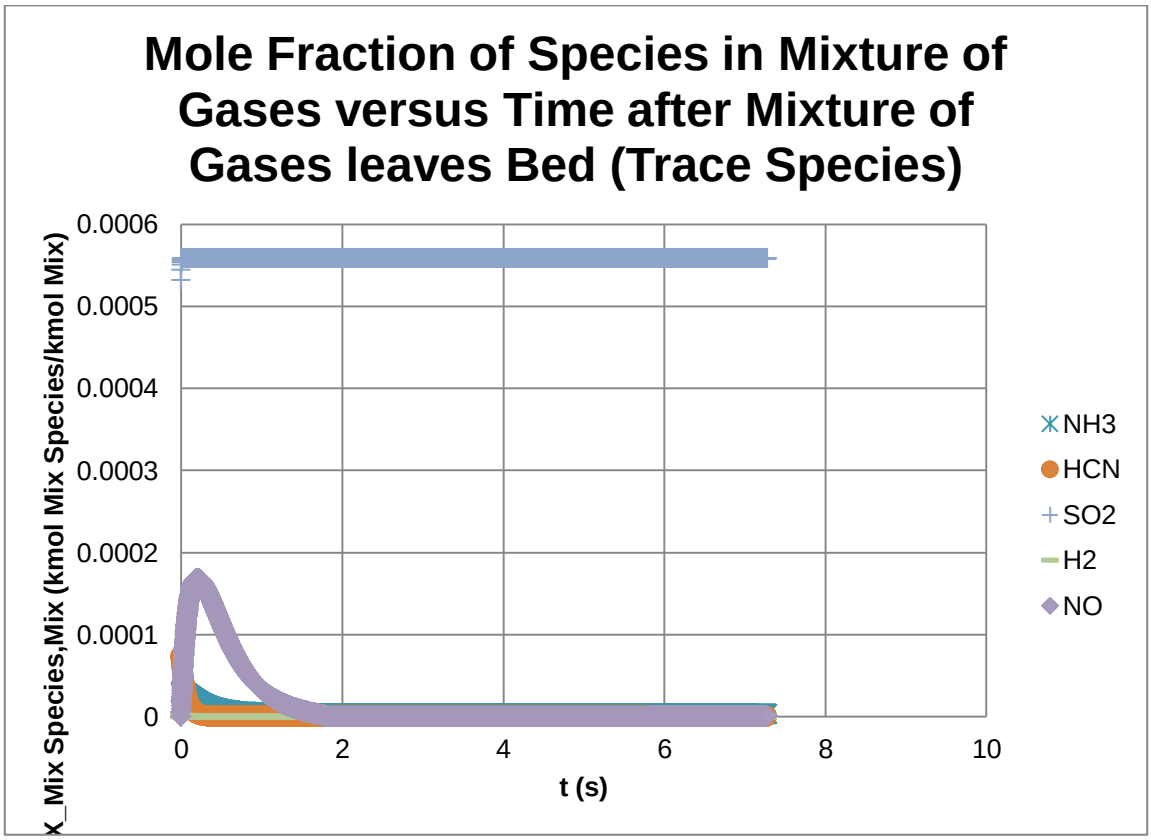

Fig. 79. Mole fraction of trace species versus time for anonymous CFB boiler firing tire fuel with increased gas mixture pressure.

The nearly matching trends are greatly evident in the 'Output' tab of the Excel program as shown below in Table 42 where all species are basically unchanged.

Continuing to increase P_{Mix} can begin to have drastic effects on the accuracy of the concentrations of the species predicted by the proposed model as more and more time is spent by the fuel particles in the bottom of the combustor so that eventually the combustor is not even fluidized anymore, but is a stationary combustor instead. Also, the ideal gas assumption of the proposed model may no longer be reasonable.

Table 42

Output tab for anonymous CFB boiler firing tire fuel with increased gas mixture pressure.

WET BASIS CONCENTRATION OF SPECIES IN MIXTURE OF GASES LEAVING CFB RISER										
	CO	H2O	O2	N2	NH3	HCN	SO2	CO2	H2	NO
ppm (Actual % O2)	5.98106E-30	82228.59111	14294.67864	753432.9219	2.954070217	7.75728E-29	558.2483798	149482.0405	8.47937E-05	0.565374617
Mole % (Actual % O2)	5.98106E-34	8.222859111	1.429467864	75.34329219	0.000295407	7.75728E-33	0.055824838	14.94820405	8.47937E-09	5.65375E-05
ppm (Standard % O2)	5.50108E-30	75629.75956	30000	756367.4242	2.717006545	7.13476E-29	513.4490349	137486.1302	7.7989E-05	0.520003393
Mole % (Standard % O2)	5.50108E-34	7.562975956	3	F7/10000	0.000271701	7.13476E-33	0.051344903	13.74861302	7.7989E-09	5.20003E-05
g/GJ	2.10208E-30	18588.26302	5739.60442	264892.8956	0.631386139	2.63076E-29	448.7864975	82546.36864	2.14492E-06	0.326396976

DRY BASIS CONCENTRATION OF SPECIES IN MIXTURE OF GASES LEAVING CFB RISER										
	CO	H2O	O2	N2	NH3	HCN	SO2	CO2	H2	NO
ppm (Actual % O2)	6.51694E-30	0	15575.4238	820937.4519	3.218742911	8.45231E-29	608.2651676	162875.0242	9.23909E-05	0.616029887
Mole % (Actual % O2)	6.51694E-34	0	1.55754238	82.09374519	0.000321874	8.45231E-33	0.060826517	16.28750242	9.23909E-09	6.1603E-05
ppm (Standard % O2)	6.03344E-30	0	30000	818642.1679	2.979940784	7.82522E-29	563.1372962	150791.1445	8.55363E-05	0.570325942
Mole % (Standard % O2)	6.03344E-34	0	3	F16/10000	0.000297994	7.82522E-33	0.05631373	15.07911445	8.55363E-09	5.70326E-05
g/GJ	2.10208E-30	0	5739.60442	264892.8956	0.631386139	2.63076E-29	448.7864975	82546.36864	2.14492E-06	0.326396976

A decrease in P_{Mix} without affecting temperatures such as T_{Mix} can only be achieved by decreasing water flows through the tubes within the combustor walls to produce less steam. Subtracting 0.5 bars of pressure, decreases $\rho_{Bed\ Mix}$ which decreases $n'''_{Char,Bed\ Mix}$ and $n'''_{LS\ CaCO_3,Bed\ Mix}$ which in turn slightly increases $a_{CS,Riser,Eff}$. These changes result in increased $V_{Bed\ Mix}$ which decreases the $t_{Res,Bed\ Mix}$ and Δt. This translates into the SMD size tire fuel completely burning higher in the riser at over three quarters of the way. Another change taking place from decreased pressure

is an increase in $D_{O_2|Mix}$, but this is offset by the decrease in $\rho_{Bed\ Mix}$ so that the overall mass transfer to the char is only slightly affected. Nevertheless, the trends according to the proposed model are almost exactly the same as before the decrease in P_{Mix} except shortened due to less time spent in the riser. These results are evident in the trends below in the graph of the mole fraction of species in the mixture of gases versus time after the mixture of gases leaves the CFB bed until they reach the CFB riser exit for all species.

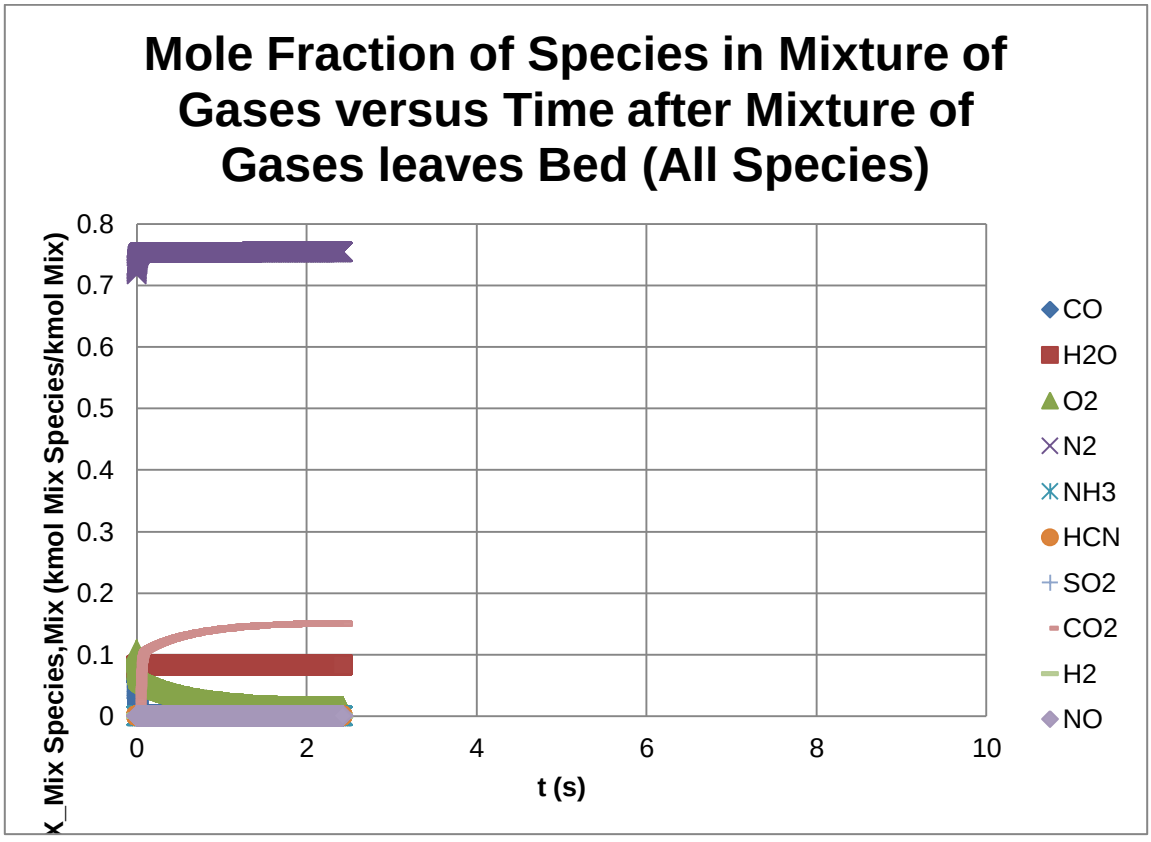

Fig. 80. Mole fraction of all species versus time for anonymous CFB boiler firing tire fuel with decreased gas mixture pressure.

The NO concentration is most affected by the decreased number of char particles to react with as seen by the larger concentrations achieved at the peak and riser exit due to lack of reducing surfaces. The CO is increased and CO_2 decreased due to the decreased time to react after the char is completely burned. Also, HCN has increased due to the decreased time to be oxidized after the char is completely burned. However, NH_3 has decreased due to both the abundance of NO available to react with and HCN is more reactive with O_2 than NH_3. Also, there is an overall decrease in the exit concentration of H_2 as it is a product of NH_3 and HCN reactions. These trends are seen below in the graph of the mole fraction of species in the mixture of gases versus time after the mixture of gases leaves the CFB bed until they reach the CFB riser exit for trace species in Fig. 81.

The nearly matching trends are greatly evident in the 'Output' tab of the Excel program as shown below in Table 43 where all species are basically unchanged. Continuing to decrease P_{Mix} can begin to have drastic effects on the concentration of the species as less and less time is given for reactions to take place in the combustor.

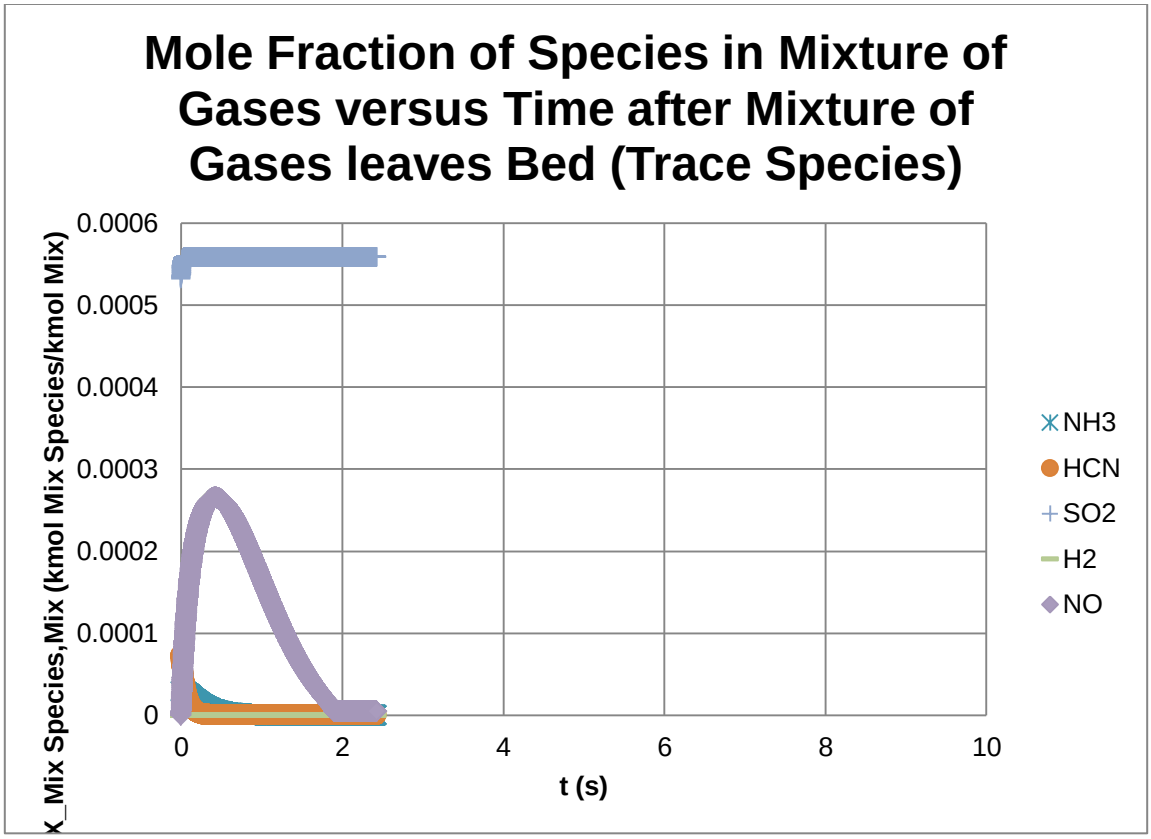

Fig. 81. Mole fraction of trace species versus time for anonymous CFB boiler firing tire fuel with decreased gas mixture pressure.

Table 43

Output tab for anonymous CFB boiler firing tire fuel with decreased gas mixture pressure.

WET BASIS CONCENTRATION OF SPECIES IN MIXTURE OF GASES LEAVING CFB RISER										
	CO	H2O	O2	N2	NH3	HCN	SO2	CO2	H2	NO
ppm (Actual % O2)	3.01825E-08	82232.75986	14290.28892	753431.5337	0.136337512	7.18231E-11	558.2479866	149481.9352	4.09537E-06	5.098007799
Mole % (Actual % O2)	3.01825E-12	8.223275986	1.429028892	75.34315337	1.36338E-05	7.18231E-15	0.055824799	14.94819352	4.09537E-10	0.000509801
ppm (Standard % O2)	2.77597E-08	75631.89733	30000	756366.9018	0.125393636	6.60578E-11	513.4371567	137482.9495	3.76663E-06	4.688788301
Mole % (Standard % O2)	2.77597E-12	7.563189733	3	F7/10000	1.25394E-05	6.60578E-15	0.051343716	13.74829495	3.76663E-10	0.000468879
g/GJ	1.06078E-08	18589.21848	5737.845898	264892.5941	0.029140024	2.43577E-11	448.7864975	82546.36864	1.03596E-07	2.943137968

DRY BASIS CONCENTRATION OF SPECIES IN MIXTURE OF GASES LEAVING CFB RISER										
	CO	H2O	O2	N2	NH3	HCN	SO2	CO2	H2	NO
ppm (Actual % O2)	3.28869E-08	0	15570.7115	820939.6683	0.148553475	7.82585E-11	608.267502	162875.6493	4.46232E-06	5.554793826
Mole % (Actual % O2)	3.28869E-12	0	1.55707115	82.09396683	1.48553E-05	7.82585E-15	0.06082675	16.28756493	4.46232E-10	0.000555479
ppm (Standard % O2)	3.04462E-08	0	30000	818643.5256	0.137528793	7.24506E-11	563.1258089	150788.0685	4.13116E-06	5.142552834
Mole % (Standard % O2)	3.04462E-12	0	3	F16/10000	1.37529E-05	7.24506E-15	0.056312581	15.07880685	4.13116E-10	0.000514255
g/GJ	1.06078E-08	0	5737.845898	264892.5941	0.029140024	2.43577E-11	448.7864975	82546.36864	1.03596E-07	2.943137968

5.3.14 Gas mixture temperature

Returning P_{Mix} to its original value, T_{Mix} was then altered. In order to only increase the temperatures within the CFB riser, the water flow through the tubes within the combustor walls needs to be decreased to produce less steam. The change in temperature also changes the volatile Nitrogen release amounts and limestone sulfation amount. The limestone sulfation amount change with temperature for the type of limestone used in the current combustor is unknown; and therefore, will not be varied. However, new $Y_{VN,N}x100$, $Y_{N_2,N}x100$, $Y_{NH_3,N}x100$, and $Y_{HCN,N}x100$ were all obtained by utilizing Kambara's coal data as described earlier with a new pyrolysis temperature near 1,200 K.

Adding 200 K, decreases $\rho_{Bed\ Mix}$ which decreases $n'''_{Char,Bed\ Mix}$ and $n'''_{LS\ CaCO_3,Bed\ Mix}$ which in turn slightly increases $a_{CS,Riser,Eff}$. These changes result in increased $V_{Bed\ Mix}$ which decreases the $t_{Res,Bed\ Mix}$ and Δt. This translates into the SMD size tire fuel completely burning higher in the riser getting closer to half of the way. Another change taking place from increased temperature is an increased $D_{O_2|Mix}$, but this is offset by the decrease in $\rho_{Bed\ Mix}$ and increase in μ_{Mix} so that the overall mass transfer to the char is only slightly affected. The increased T_{Mix} basically enhances all of the chemical reaction rates so that reactant species such as CO, O_2, NH_3, HCN, H_2, and NO all have lower concentrations at the riser, and product species such as H_2O, N_2, and CO_2 all have higher concentrations at the riser. The concentration of SO_2 is virtually the same. Nevertheless, the trends according to the proposed model are almost exactly the same as before the increase in T_{Mix} except shortened due to less time spent in the riser,

and only a decline in NO due to the greatly enhanced destruction on fixed Carbon even though there is a decreased number of char particles to react with. These results are evident in the trends below in the graphs of the mole fraction of species in the mixture of gases versus time after the mixture of gases leaves the CFB bed until they reach the CFB riser exit for all species in Fig. 82 and trace species in Fig. 83.

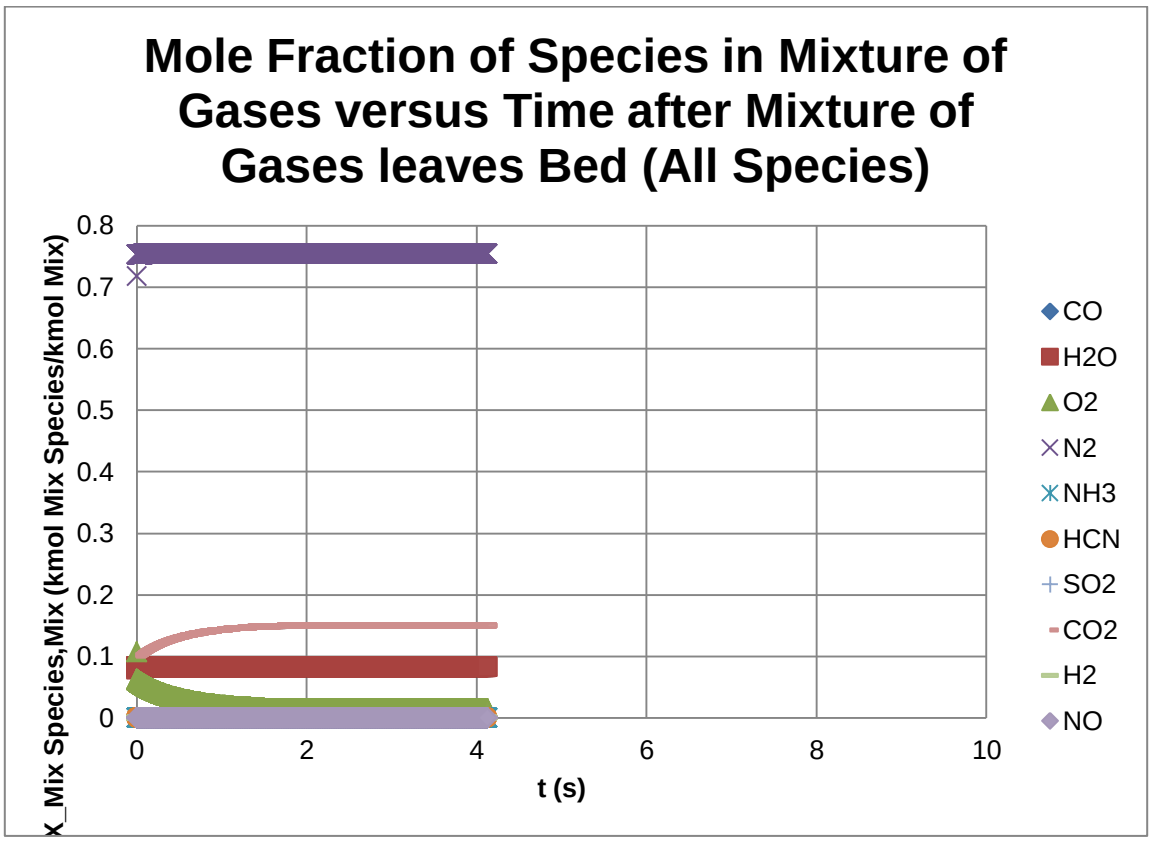

Fig. 82. Mole fraction of all species versus time for anonymous CFB boiler firing tire fuel with increased gas mixture temperature.

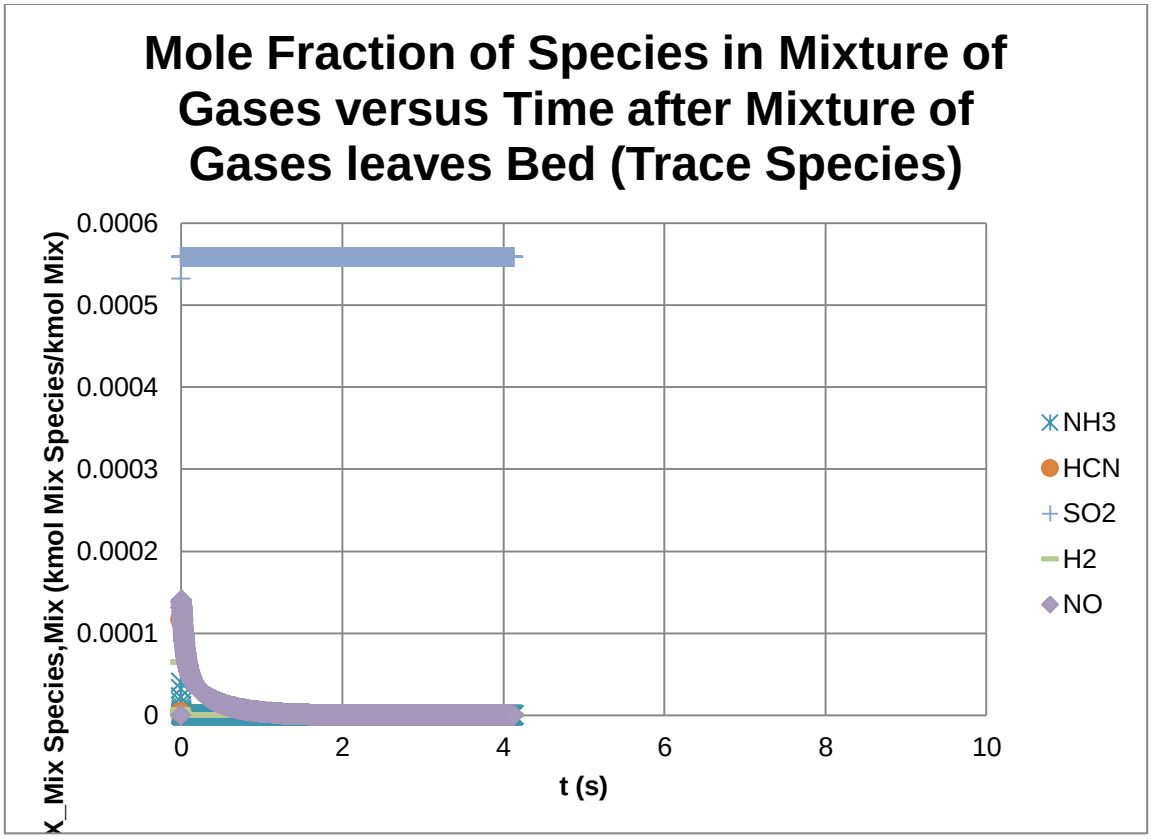

Fig. 83. Mole fraction of trace species versus time for anonymous CFB boiler firing tire fuel with increased gas mixture temperature.

The nearly matching trends are greatly evident in the 'Output' tab of the Excel program as shown below in Table 44 where all species are nearly unchanged. The HCN is a negative value because it was completely depleted so that when the concentration reaches a negative value in the proposed model it stops the reactions involving that species. Continuing to increase T_{Mix} can begin to have drastic effects on the accuracy of the concentrations of the species predicted by the proposed model as less and less time is given for reactions to take place in the combustor especially if the number of chemical

kinetics calculation rows is not properly increased to keep up with the greatly increased chemical kinetics.

Table 44

Output tab for anonymous CFB boiler firing tire fuel with increased gas mixture temperature.

WET BASIS CONCENTRATION OF SPECIES IN MIXTURE OF GASES LEAVING CFB RISER										
	CO	H2O	O2	N2	NH3	HCN	SO2	CO2	H2	NO
ppm (Actual % O2)	4.6186E-300	82232.99842	14292.64505	753434.172	2.0884E-299	-0.07078685	558.2479775	149482.0035	7.25091E-21	0.003795256
Mole % (Actual % O2)	4.6186E-304	8.223299842	1.429264505	75.3434172	2.0884E-303	-7.0787E-06	0.055824798	14.94820035	7.25091E-25	3.79526E-07
ppm (Standard % O2)	4.2479E-300	75633.02728	30000	756368.9235	1.9208E-299	-0.06510554	513.4433296	137484.6676	6.66896E-21	0.003490651
Mole % (Standard % O2)	4.2479E-304	7.563302728	3	F7/10000	1.9208E-303	-6.5106E-06	0.051344333	13.74846676	6.66896E-25	3.49065E-07
g/GJ	1.6232E-300	18589.26391	5738.789311	264893.4006	4.4636E-300	-0.02400624	448.786285	82546.36864	1.83418E-22	0.002191043
DRY BASIS CONCENTRATION OF SPECIES IN MIXTURE OF GASES LEAVING CFB RISER										
	CO	H2O	O2	N2	NH3	HCN	SO2	CO2	H2	NO
ppm (Actual % O2)	5.0324E-300	0	15573.28279	820942.7564	2.2755E-299	-0.07712944	608.2676502	162875.7661	7.9006E-21	0.004135315
Mole % (Actual % O2)	5.0324E-304	0	1.557328279	82.09427564	2.2755E-303	-7.7129E-06	0.060826765	16.28757661	7.9006E-25	4.13531E-07
ppm (Standard % O2)	4.659E-300	0	30000	818646.7633	2.1067E-299	-0.07140633	563.1333934	150790.1708	7.31437E-21	0.003828469
Mole % (Standard % O2)	4.659E-304	0	3	F16/10000	2.1067E-303	-7.1406E-06	0.056313339	15.07901708	7.31437E-25	3.82847E-07
g/GJ	1.6232E-300	0	5738.789311	264893.4006	4.4636E-300	-0.02400624	448.786285	82546.36864	1.83418E-22	0.002191043

In order to only decrease the temperatures within the CFB riser, the water flow through the tubes within the combustor walls needs to be increased to produce more steam which is assumed to be able to be handled by this combustor's tubes. The change in temperature also changes the volatile Nitrogen release amounts and limestone sulfation amount. The limestone sulfation amount change with temperature for the type of limestone used in the current combustor is unknown; and therefore, will not be varied. However, new $Y_{VN,N}x100$, $Y_{N_2,N}x100$, $Y_{NH_3,N}x100$, and $Y_{HCN,N}x100$ were all obtained by utilizing Kambara's coal data as described earlier with a new pyrolysis temperature near 800 K.

Subtracting 200 K, increases $\rho_{Bed\ Mix}$ which increases $n'''_{Char,Bed\ Mix}$ and $n'''_{LS\ CaCO_3,Bed\ Mix}$ which in turn slightly decreases $a_{CS,Riser,Eff}$. These changes result in decreased $V_{Bed\ Mix}$ which increases the $t_{Res,Bed\ Mix}$ and Δt. This translates into the SMD size tire fuel completely burning lower in the riser at less than a third of the way. Another change taking place from decreased temperature is a decreased $D_{O_2|Mix}$, but this is offset mostly by the increase in $\rho_{Bed\ Mix}$ and decrease in μ_{Mix} so that the overall mass transfer to the char is increased causing a lower O_2 concentration at the riser exit. The decreased T_{Mix} basically inhibits all of the chemical reaction rates so that reactant species such as CO, NH_3, HCN, H_2, and NO all have higher concentrations at the riser, and product species such as H_2O, N_2, and CO_2 all have lower concentrations at the riser. The concentration of SO_2 is virtually the same. Nevertheless, the trends according to the proposed model are very similar before the decrease in T_{Mix} except lengthened due to more time spent in the riser, and a much higher peak and riser exit NO due to the greatly inhibited destruction on fixed Carbon even though there is an increased number of char particles to react with. These results are evident in the trends below in the graphs of the mole fraction of species in the mixture of gases versus time after the mixture of gases leaves the CFB bed until they reach the CFB riser exit for all species in Fig. 84 and trace species in Fig. 85.

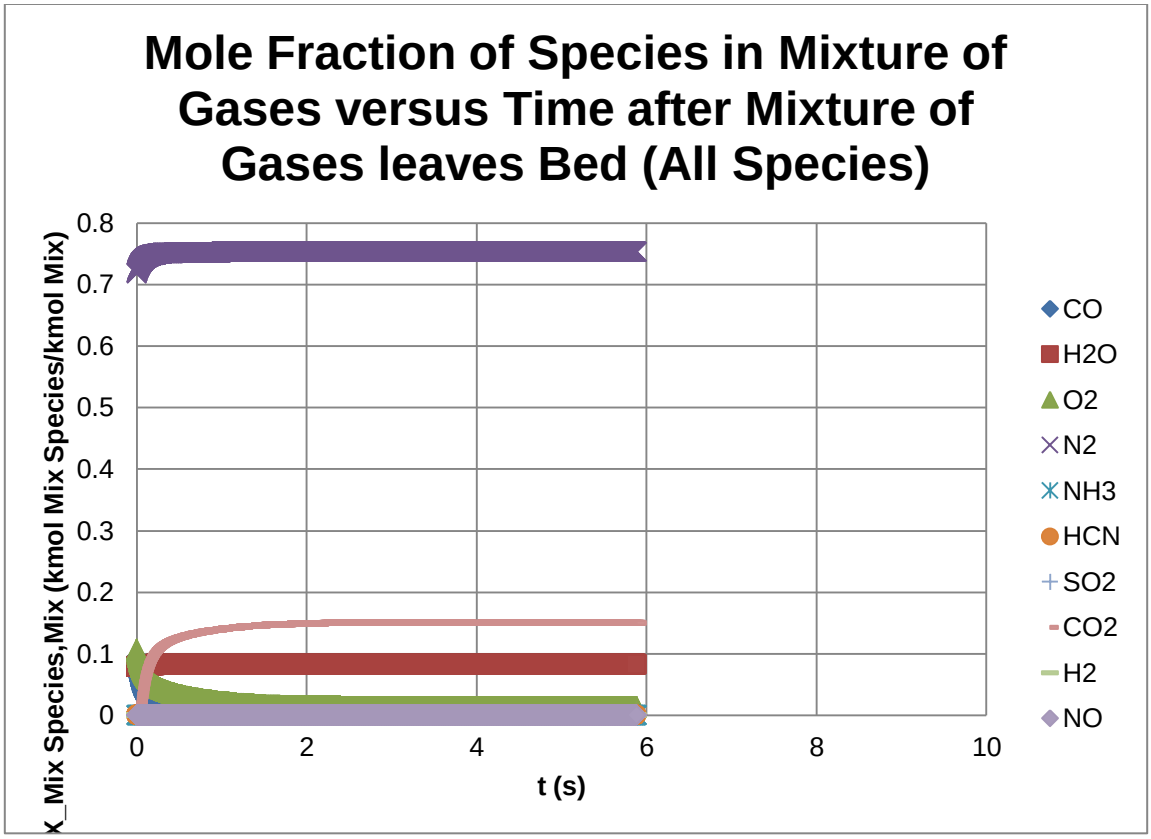

Fig. 84. Mole fraction of all species versus time for anonymous CFB boiler firing tire fuel with decreased gas mixture temperature.

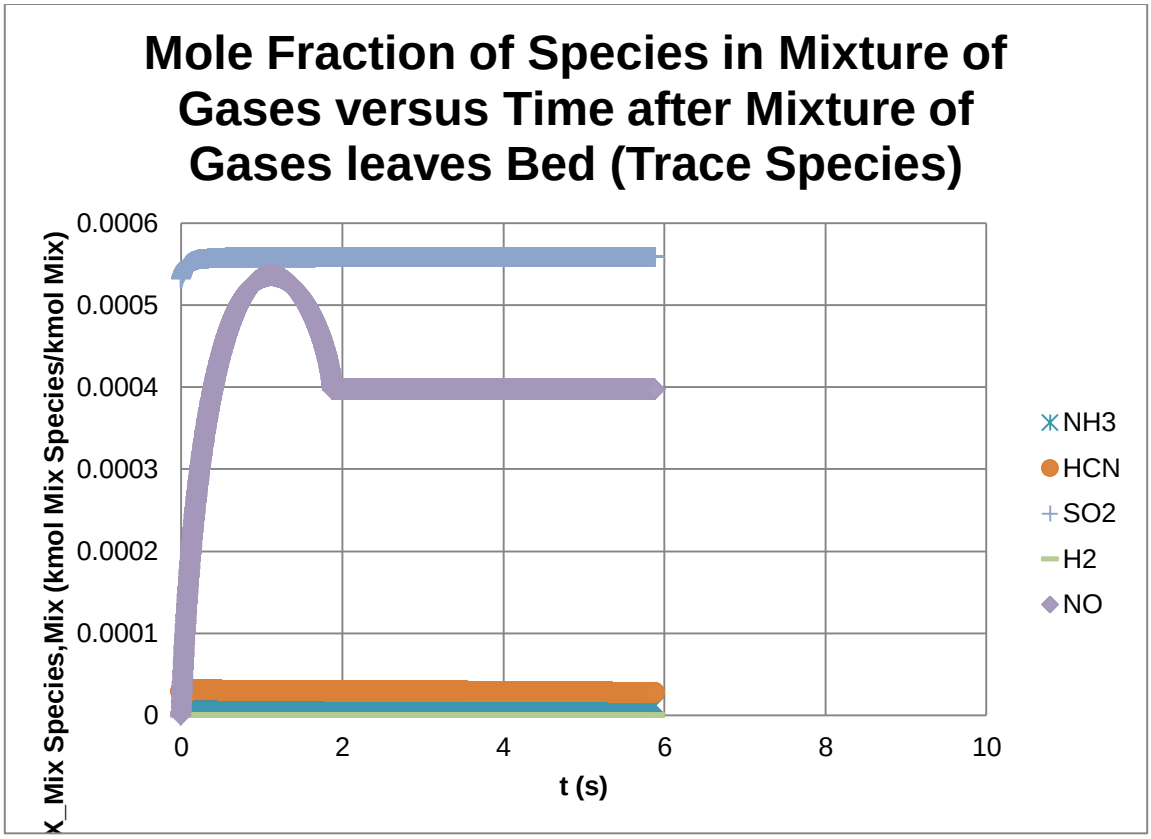

Fig. 85. Mole fraction of trace species versus time for anonymous CFB boiler firing tire fuel with decreased gas mixture temperature.

The nearly matching trends are greatly evident in the 'Output' tab of the Excel program as shown below in Table 45 where all species are barely changed. Continuing to decrease T_{Mix} can begin to have drastic effects on the accuracy of the concentrations of the species predicted by the proposed model as more and more time is spent by the fuel particles in the bottom of the combustor so that eventually the combustor is not even fluidized anymore, but is a stationary combustor instead. Also, the ideal gas assumption of the proposed model may no longer be reasonable. The trend of the O_2 concentration

is eventually reversed resulting in a higher concentration at the riser exit as chemical reaction rates are drastically reduced to possibly flame extinction. In addition, the NH_3 and HCN concentrations will be none since at lower temperatures the fuel will cease to release volatile Nitrogen in any form (will be all fixed Nitrogen) which in turn leads to no H_2 also.

Table 45

Output tab for anonymous CFB boiler firing tire fuel with decreased gas mixture temperature.

WET BASIS CONCENTRATION OF SPECIES IN MIXTURE OF GASES LEAVING CFB RISER										
	CO	H2O	O2	N2	NH3	HCN	SO2	CO2	H2	NO
ppm (Actual % O2)	0.075080424	82201.13966	14137.48609	753212.9496	11.81905666	27.53323257	558.2457534	149453.7289	0.000545047	397.0220875
Mole % (Actual % O2)	7.50804E-06	8.220113966	1.413748609	75.32129496	0.001181906	0.002753323	0.055824575	14.94537289	5.45047E-08	0.039702209
ppm (Standard % O2)	0.06899981	75543.83349	30000	756192.2594	10.86185486	25.30337104	513.0345445	137349.7698	0.000500905	364.8680614
Mole % (Standard % O2)	6.89998E-06	7.554383349	3	F7/10000	0.001086185	0.002530337	0.051303454	13.73497698	5.00905E-08	0.036486806
g/GJ	0.026392435	18585.56819	5677.560879	264865.5895	2.526615106	9.339222972	448.8691755	82546.32717	1.379E-05	229.2485157
DRY BASIS CONCENTRATION OF SPECIES IN MIXTURE OF GASES LEAVING CFB RISER										
	CO	H2O	O2	N2	NH3	HCN	SO2	CO2	H2	NO
ppm (Actual % O2)	0.081804878	0	15403.68669	820673.2239	12.87761096	29.99920109	608.2441126	162839.3054	0.000593863	432.5807153
Mole % (Actual % O2)	8.18049E-06	0	1.540368669	82.06732239	0.001287761	0.00299992	0.060824411	16.28393054	5.93863E-08	0.043258072
ppm (Standard % O2)	0.075668844	0	30000	818372.4815	11.91168493	27.74901592	562.6208349	150625.0271	0.000549319	400.1336275
Mole % (Standard % O2)	7.56688E-06	0	3	F16/10000	0.001191168	0.002774902	0.056262083	15.06250271	5.49319E-08	0.040013363
g/GJ	0.026392435	0	5677.560879	264865.5895	2.526615106	9.339222972	448.8691755	82546.32717	1.379E-05	229.2485157

5.3.15 Riser cross-sectional area

Returning T_{Mix} to its original value, $a_{CS,Riser}$ was then altered. Adding 50 m^2, merely decreases $V_{Bed\ Mix}$ which increases the $t_{Res,Bed\ Mix}$ and Δt. This translates into the SMD size tire fuel completely burning lower in the riser at just over a quarter of the way. The increased $a_{CS,Riser}$ basically allows more time for all of the chemical reactions so that reactant species such as CO, O_2, NH_3, and HCN have lower concentrations at the riser, and product species such as H_2O and N_2 have higher concentrations at the riser.

Therefore, the trends according to the proposed model are almost exactly the same as before the increase in $a_{CS,Riser}$ except lengthened due to more time spent in the riser. These results are evident in the trends below in the graphs of the mole fraction of species in the mixture of gases versus time after the mixture of gases leaves the CFB bed until they reach the CFB riser exit for all species in Fig. 86 and trace species in Fig. 87.

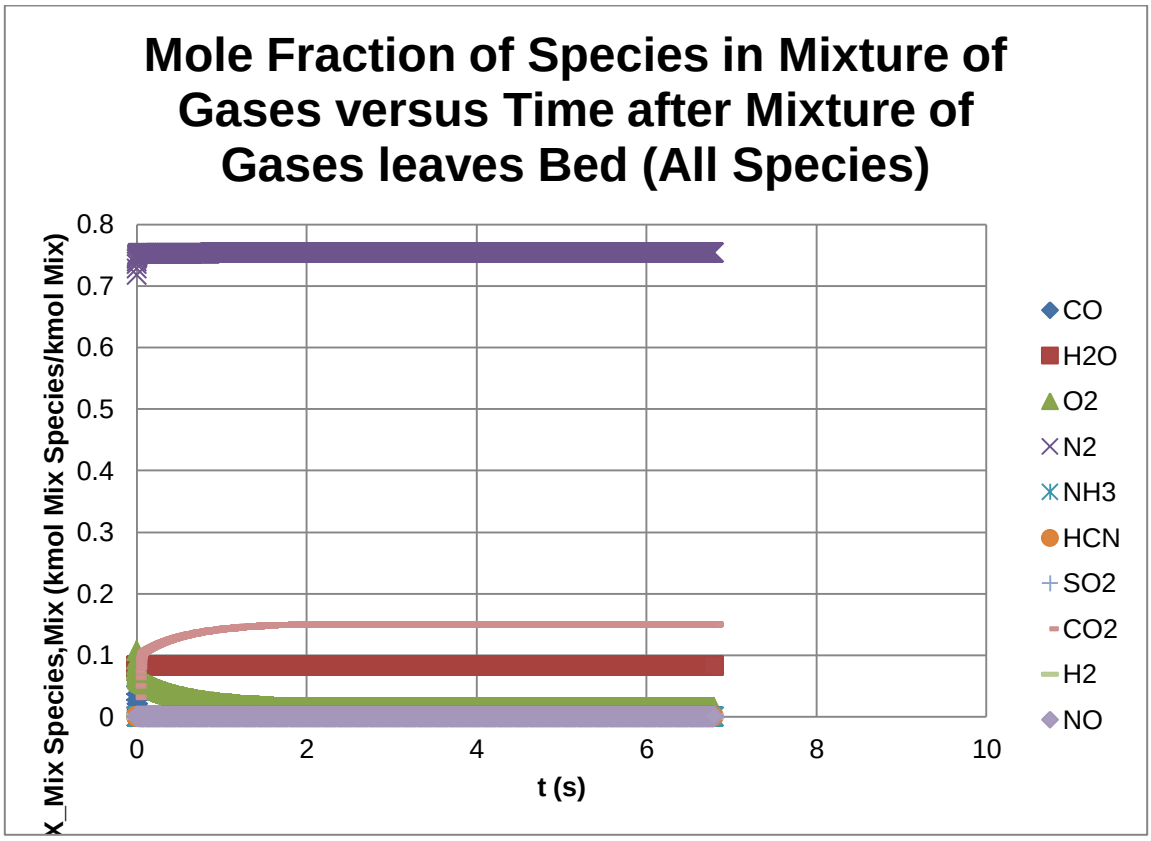

Fig. 86. Mole fraction of all species versus time for anonymous CFB boiler firing tire fuel with increased riser cross-sectional area.

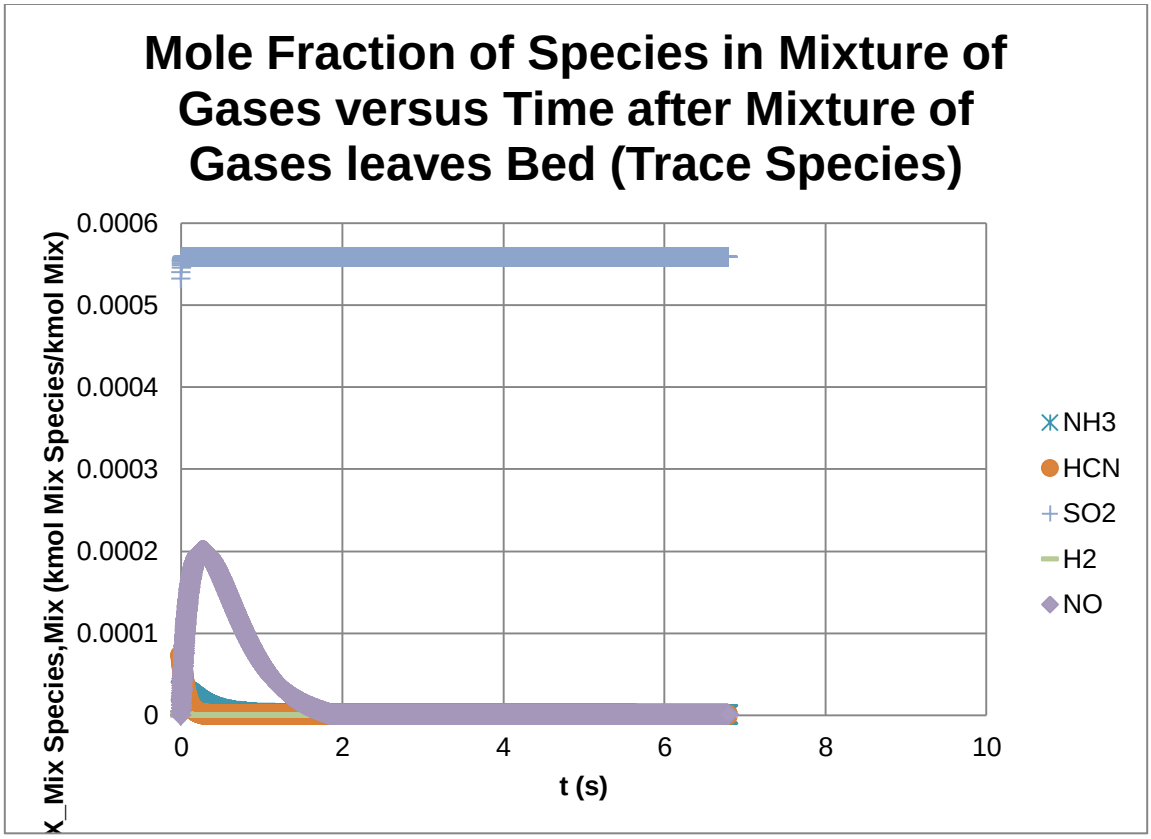

Fig. 87. Mole fraction of trace species versus time for anonymous CFB boiler firing tire fuel with increased riser cross-sectional area.

The nearly matching trends are greatly evident in the 'Output' tab of the Excel program as shown below in Table 46 where all species only have minor changes due to the lengthened time to react. Continuing to increase $a_{CS,Riser}$ can begin to have drastic effects on the accuracy of the concentrations of the species predicted by the proposed model as more and more time is spent by the fuel particles in the bottom of the combustor so that eventually the combustor is not even fluidized anymore, but is a stationary combustor instead.

Table 46

Output tab for anonymous CFB boiler firing tire fuel with increased riser cross-sectional area.

WET BASIS CONCENTRATION OF SPECIES IN MIXTURE OF GASES LEAVING CFB RISER										
	CO	H2O	O2	N2	NH3	HCN	SO2	CO2	H2	NO
ppm (Actual % O2)	5.20483E-28	82231.18824	14293.31406	753433.4273	1.198622754	4.32729E-27	558.2481349	149481.9749	3.33781E-05	0.648772144
Mole % (Actual % O2)	5.20483E-32	8.223118824	1.429331406	75.34334273	0.000119862	4.32729E-31	0.055824813	14.94819749	3.33781E-09	6.48772E-05
ppm (Standard % O2)	4.78711E-28	75631.62092	30000	756368.1235	1.102425779	3.98E-27	513.4452295	137485.1112	3.06993E-05	0.596704121
Mole % (Standard % O2)	4.78711E-32	7.563162092	3	F7/10000	0.000110243	3.98E-31	0.051344523	13.74851112	3.06993E-09	5.96704E-05
g/GJ	1.82927E-28	18588.85827	5739.059031	264893.1895	0.256186911	1.46753E-27	448.7864975	82546.36864	8.44324E-07	0.374543449
DRY BASIS CONCENTRATION OF SPECIES IN MIXTURE OF GASES LEAVING CFB RISER										
	CO	H2O	O2	N2	NH3	HCN	SO2	CO2	H2	NO
ppm (Actual % O2)	5.67118E-28	0	15573.98102	820940.3257	1.306018181	4.71501E-27	608.2666219	162875.4137	3.63687E-05	0.706901494
Mole % (Actual % O2)	5.67118E-32	0	1.557398102	82.09403257	0.000130602	4.71501E-31	0.060826662	16.28754137	3.63687E-09	7.06901E-05
ppm (Standard % O2)	5.25039E-28	0	30000	818644.6159	1.209114262	4.36517E-27	563.1344638	150790.3861	3.36702E-05	0.654450827
Mole % (Standard % O2)	5.25039E-32	0	3	F16/10000	0.000120911	4.36517E-31	0.056313446	15.07903861	3.36702E-09	6.54451E-05
g/GJ	1.82927E-28	0	5739.059031	264893.1895	0.256186911	1.46753E-27	448.7864975	82546.36864	8.44324E-07	0.374543449

Subtracting 50 m^2, merely increases $V_{Bed\ Mix}$ which decreases the $t_{Res,Bed\ Mix}$ and Δt. This translates into the SMD size tire fuel completely burning higher in the riser at almost two thirds of the way. The decreased $a_{CS,Riser}$ basically allows less time for all of the chemical reactions so that reactant species such as CO, O_2, NH_3, and HCN have higher concentrations at the riser, and product species such as H_2O have a lower concentration at the riser. Therefore, the trends according to the proposed model are almost exactly the same as before the decrease in $a_{CS,Riser}$ except shortened due to less time spent in the riser. These results are evident in the trends below in the graphs of the mole fraction of species in the mixture of gases versus time after the mixture of gases leaves the CFB bed until they reach the CFB riser exit for all species in Fig. 88 and trace species in Fig. 89.

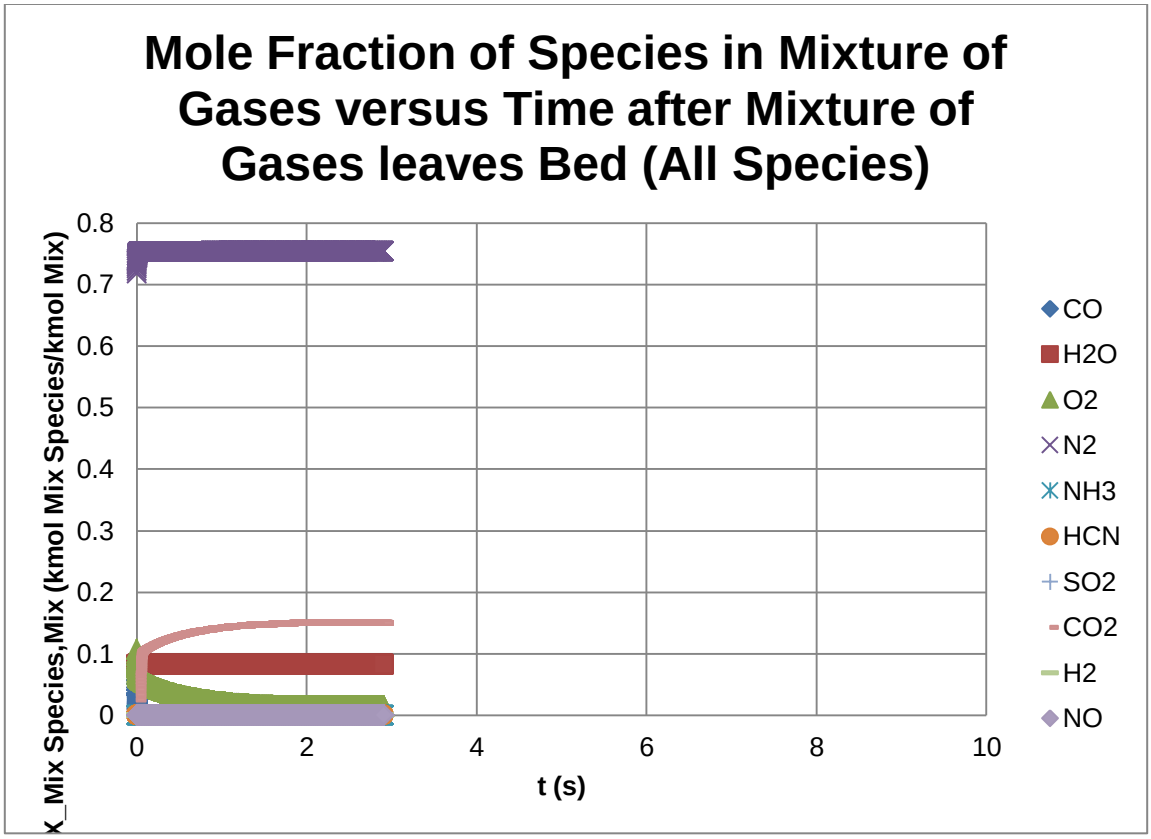

Fig. 88. Mole fraction of all species versus time for anonymous CFB boiler firing tire fuel with decreased riser cross-sectional area.

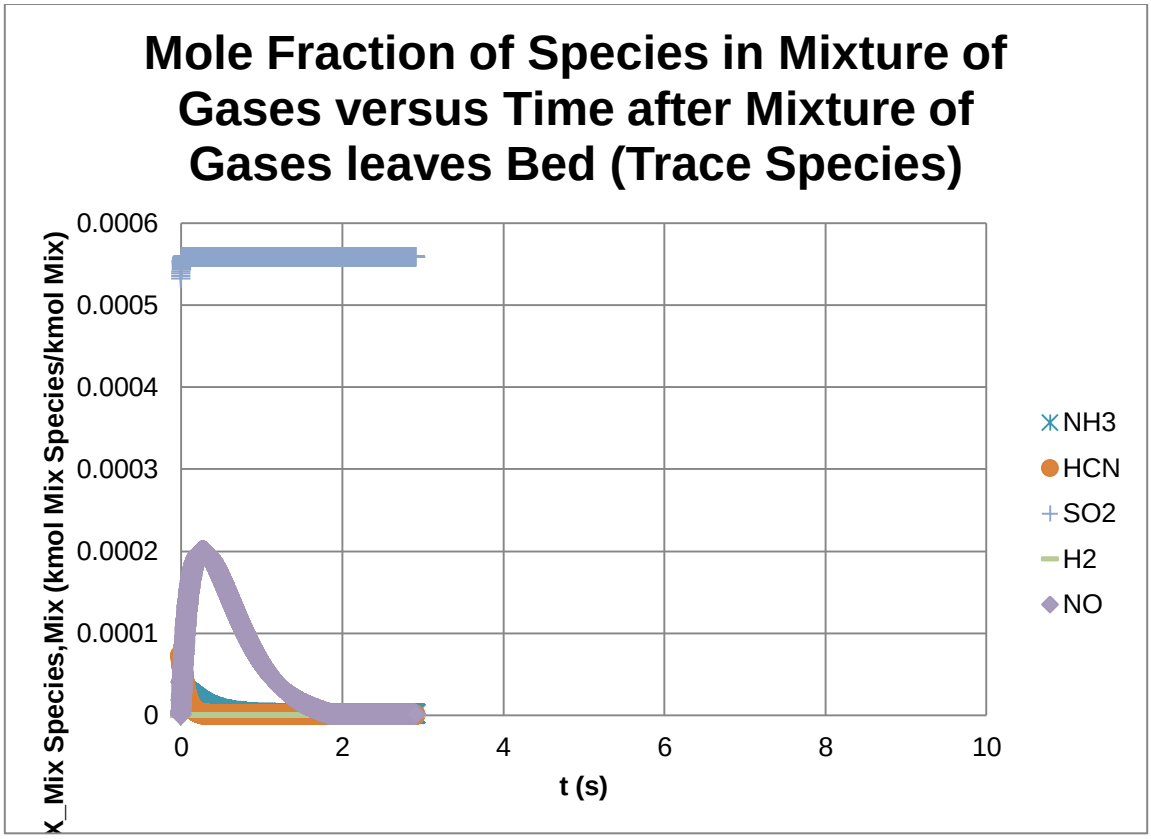

Fig. 89. Mole fraction of trace species versus time for anonymous CFB boiler firing tire fuel with decreased riser cross-sectional area.

The nearly matching trends are greatly evident in the 'Output' tab of the Excel program as shown below in Table 47 where all species only have minor changes due to the lengthened time to react. Continuing to decrease $a_{CS,Riser}$ can begin to have drastic effects on the accuracy of the concentrations of the species predicted by the proposed model as less and less time is given for reactions to take place in the combustor.

Table 47

Output tab for anonymous CFB boiler firing tire fuel with decreased riser cross-sectional area.

WET BASIS CONCENTRATION OF SPECIES IN MIXTURE OF GASES LEAVING CFB RISER										
	CO	H2O	O2	N2	NH3	HCN	SO2	CO2	H2	NO
ppm (Actual % O2)	1.68166E-13	82230.87976	14293.53502	753433.4261	1.40714497	1.39811E-12	558.248164	149481.9827	1.58196E-05	0.521107532
Mole % (Actual % O2)	1.68166E-17	8.223087976	1.429353502	75.34334261	0.000140714	1.39811E-16	0.055824816	14.94819827	1.58196E-09	5.21108E-05
ppm (Standard % O2)	1.5467E-13	75631.42259	30000	756368.0845	1.294214244	1.28591E-12	513.445836	137485.2736	1.455E-05	0.479285934
Mole % (Standard % O2)	1.5467E-17	7.563142259	3	F7/10000	0.000129421	1.28591E-16	0.051344584	13.74852736	1.455E-09	4.79286E-05
g/GJ	5.9103E-14	18588.78757	5739.147452	264893.1753	0.300755266	4.74148E-13	448.7864975	82546.36864	4.0017E-07	0.300841218
DRY BASIS CONCENTRATION OF SPECIES IN MIXTURE OF GASES LEAVING CFB RISER										
	CO	H2O	O2	N2	NH3	HCN	SO2	CO2	H2	NO
ppm (Actual % O2)	1.83234E-13	0	15574.21655	820940.0485	1.533223268	1.52338E-12	608.2664492	162875.3674	1.7237E-05	0.567798067
Mole % (Actual % O2)	1.83234E-17	0	1.557421655	82.09400485	0.000153322	1.52338E-16	0.060826645	16.28753674	1.7237E-09	5.67798E-05
ppm (Standard % O2)	1.69638E-13	0	30000	818644.394	1.419462909	1.41035E-12	563.1349861	150790.5259	1.59581E-05	0.525669231
Mole % (Standard % O2)	1.69638E-17	0	3	F16/10000	0.000141946	1.41035E-16	0.056313499	15.07905259	1.59581E-09	5.25669E-05
g/GJ	5.9103E-14	0	5739.147452	264893.1753	0.300755266	4.74148E-13	448.7864975	82546.36864	4.0017E-07	0.300841218

5.3.16 Riser height

Returning $a_{CS,Riser}$ to its original value, h_{Riser} was then altered. Adding 30 meters, simply increases the $t_{Res,Bed\ Mix}$ and Δt basically allowing more time for all of the chemical reactions. This also translates into the SMD size tire fuel completely burning lower in the riser at just over a fifth of the way. The increased h_{Riser} basically enables all of the chemical reactions to go on longer so that reactant species such as CO, O_2, NH_3, and HCN have lower concentrations at the riser, and product species such as H_2O and N_2 have higher concentrations at the riser. Therefore, the trends according to the proposed model are almost exactly the same as before the increase in h_{Riser} except lengthened due to more time spent in the riser. These results are evident in the trends below in the graphs of the mole fraction of species in the mixture of gases versus time after the mixture of gases leaves the CFB bed until they reach the CFB riser exit for all species in Fig. 90 and trace species in Fig. 91.

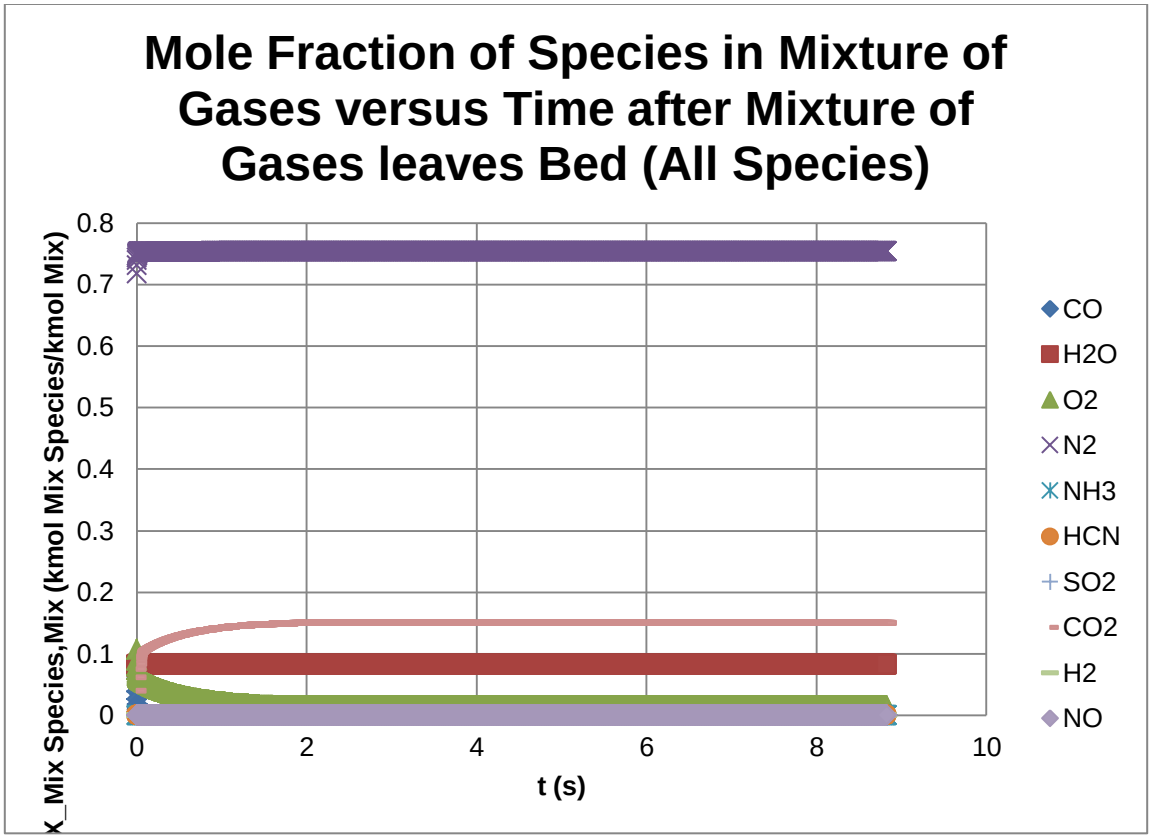

Fig. 90. Mole fraction of all species versus time for anonymous CFB boiler firing tire fuel with increased riser height.

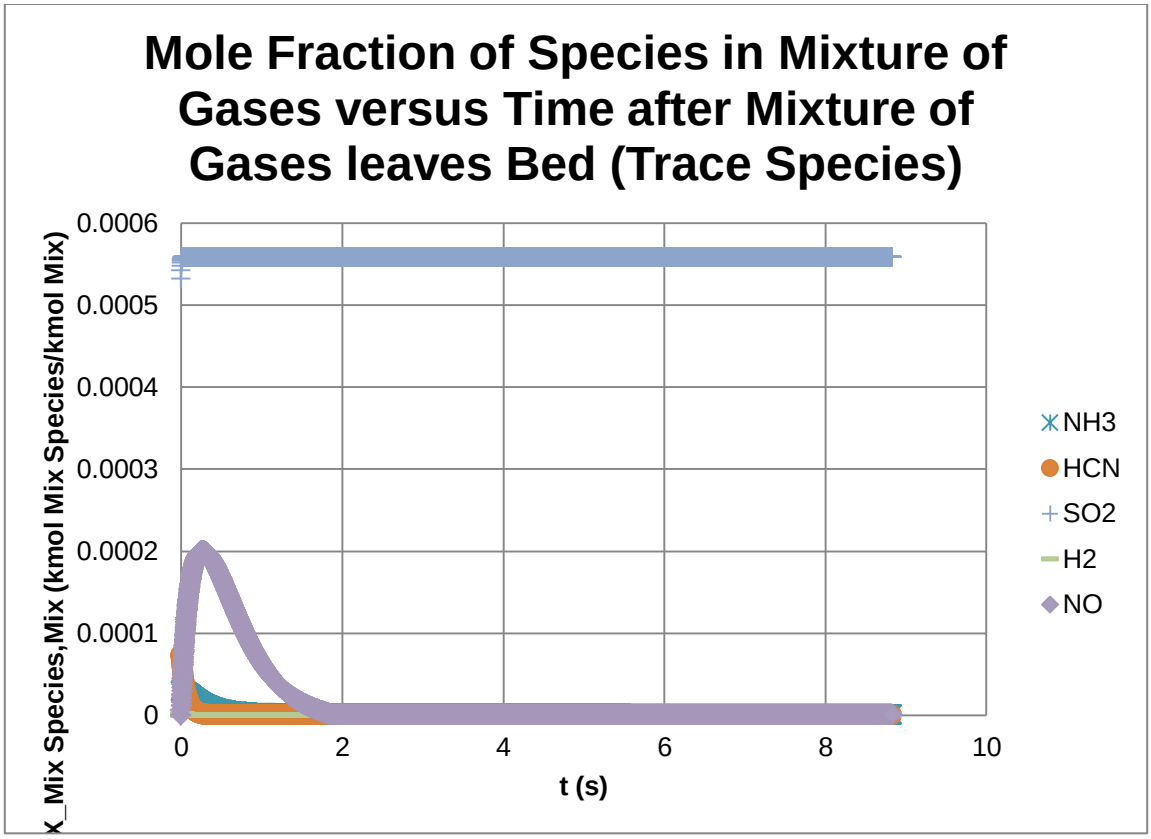

Fig. 91. Mole fraction of trace species versus time for anonymous CFB boiler firing tire fuel with increased riser height.

The nearly matching trends are greatly evident in the 'Output' tab of the Excel program as shown below in Table 48 where all species only have minor changes due to the lengthened time to react. Continuing to increase h_{Riser} continues the trends until all of the reactant species are converted to final product species.

Table 48

Output tab for anonymous CFB boiler firing tire fuel with increased riser height.

WET BASIS CONCENTRATION OF SPECIES IN MIXTURE OF GASES LEAVING CFB RISER										
	CO	H2O	O2	N2	NH3	HCN	SO2	CO2	H2	NO
ppm (Actual % O2)	1.16401E-35	82231.3375	14293.21237	753433.433	1.097727604	9.67766E-35	558.2481208	149481.9711	4.06585E-05	0.700102927
Mole % (Actual % O2)	1.16401E-39	8.22313375	1.429321237	75.3433433	0.000109773	9.67766E-39	0.055824812	14.94819711	4.06585E-09	7.00103E-05
ppm (Standard % O2)	1.07059E-35	75631.71891	30000	756368.1463	1.009627571	8.90097E-35	513.4449497	137485.0363	3.73954E-05	0.643914953
Mole % (Standard % O2)	1.07059E-39	7.563171891	3	F7/10000	0.000100963	8.90097E-39	0.051344495	13.74850363	3.73954E-09	6.43915E-05
g/GJ	4.09099E-36	18588.89248	5739.018344	264893.1982	0.234622153	3.28203E-35	448.7864975	82546.36864	1.02849E-06	0.404177297
DRY BASIS CONCENTRATION OF SPECIES IN MIXTURE OF GASES LEAVING CFB RISER										
	CO	H2O	O2	N2	NH3	HCN	SO2	CO2	H2	NO
ppm (Actual % O2)	1.26831E-35	0	15573.87275	820940.4655	1.196083119	1.05448E-34	608.2667055	162875.4361	4.43014E-05	0.762831589
Mole % (Actual % O2)	1.26831E-39	0	1.557387275	82.09404655	0.000119608	1.05448E-38	0.060826671	16.28754361	4.43014E-09	7.62832E-05
ppm (Standard % O2)	1.1742E-35	0	30000	818644.7294	1.107335544	9.76237E-35	563.1342276	150790.3228	4.10143E-05	0.706230629
Mole % (Standard % O2)	1.1742E-39	0	3	F16/10000	0.000110734	9.76237E-39	0.056313423	15.07903228	4.10143E-09	7.06231E-05
g/GJ	4.09099E-36	0	5739.018344	264893.1982	0.234622153	3.28203E-35	448.7864975	82546.36864	1.02849E-06	0.404177297

Subtracting 30 meters, simply decreases the $t_{Res,Bed\ Mix}$ and Δt basically allowing less time for all of the chemical reactions. This translates into the SMD size tire fuel not completely burning in the riser. In fact, almost 20% of the tire is still left unburned at the exit of the riser. The decreased h_{Riser} basically cuts short all of the chemical reactions so that reactant species such as CO, O_2, NH_3, HCN, H_2, and NO all have higher concentrations at the riser, and product species such as H_2O, N_2, and CO_2 all have lower concentrations at the riser. The concentration of SO_2 is virtually the same. Therefore, the trends according to the proposed model are almost exactly the same as before the decrease in h_{Riser} except shortened due to less time spent in the riser. These results are evident in the trends below in the graphs of the mole fraction of species in the mixture of gases versus time after the mixture of gases leaves the CFB bed until they reach the CFB riser exit for all species in Fig. 92 and trace species in Fig. 93.

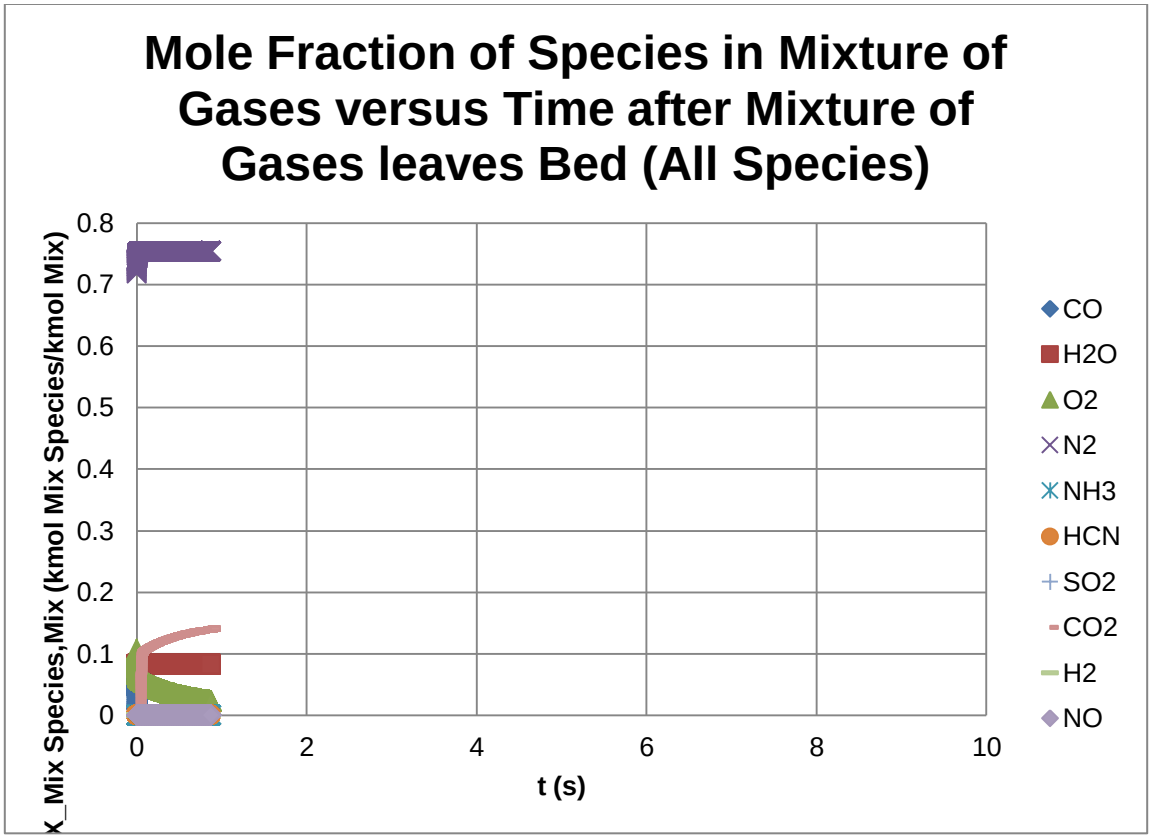

Fig. 92. Mole fraction of all species versus time for anonymous CFB boiler firing tire fuel with decreased riser height.

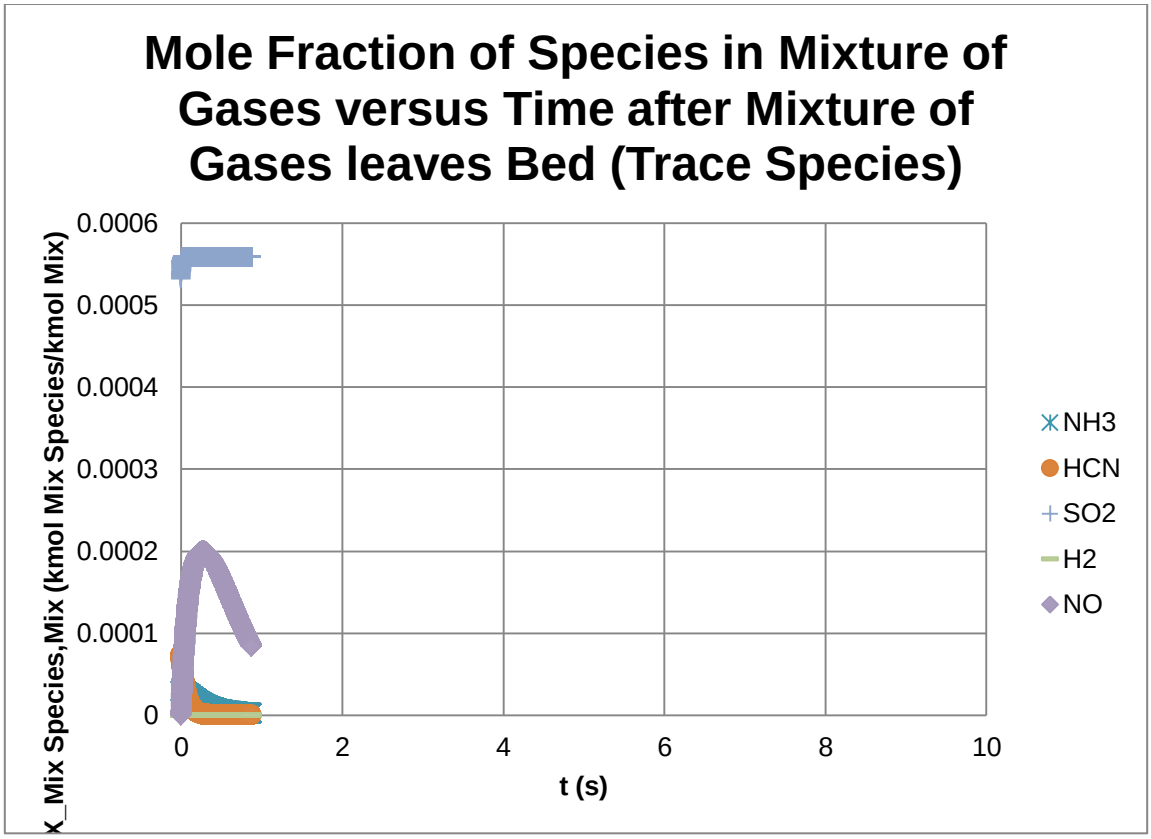

Fig. 93. Mole fraction of trace species versus time for anonymous CFB boiler firing tire fuel with decreased riser height.

The nearly matching trends are also reflected in the 'Output' tab of the Excel program as shown below in Table 49 where all species have changes due to the shortened time to react. Continuing to decrease h_{Riser} continues the trends until the concentrations are those of what leaves the bed due to the lack of time to react in the riser.

Table 49

Output tab for anonymous CFB boiler firing tire fuel with decreased riser height.

WET BASIS CONCENTRATION OF SPECIES IN MIXTURE OF GASES LEAVING CFB RISER										
	CO	H2O	O2	N2	NH3	HCN	SO2	CO2	H2	NO
ppm (Actual % O2)	183.8047408	82226.45946	23136.61665	753306.9921	2.623830668	0.000310497	558.2305491	140500.7366	0.000368643	84.53539835
Mole % (Actual % O2)	0.018380474	8.222645946	2.313661665	75.33069921	0.000262383	3.10497E-08	0.055823055	14.05007366	3.68643E-08	0.00845354
ppm (Standard % O2)	177.0536996	79206.32945	30000	754654.7049	2.527458894	0.000299093	537.7270658	135340.2263	0.000355103	81.43046235
Mole % (Standard % O2)	0.01770537	7.920632945	3	F7/10000	0.000252746	2.99093E-08	0.053772707	13.53402263	3.55103E-08	0.00814306
g/GJ	68.63885698	19750.14048	9870.747765	281410.5368	0.595871579	0.000111885	476.8354647	82438.52158	9.90824E-06	51.85505054
DRY BASIS CONCENTRATION OF SPECIES IN MIXTURE OF GASES LEAVING CFB RISER										
	CO	H2O	O2	N2	NH3	HCN	SO2	CO2	H2	NO
ppm (Actual % O2)	200.272434	0	25209.50499	820798.333	2.8589086	0.000338316	608.2443266	153088.6764	0.000401671	92.1092128
Mole % (Actual % O2)	0.020027243	0	2.520950499	82.0798333	0.000285891	3.38316E-08	0.060824433	15.30886764	4.01671E-08	0.009210921
ppm (Standard % O2)	195.0805863	0	30000	819999.9193	2.784794467	0.000329545	592.476246	149120.017	0.000391258	89.72138044
Mole % (Standard % O2)	0.019508059	0	3	F16/10000	0.000278479	3.29545E-08	0.059247625	14.9120017	3.91258E-08	0.008972138
g/GJ	68.63885698	0	9870.747765	281410.5368	0.595871579	0.000111885	476.8354647	82438.52158	9.90824E-06	51.85505054

5.3.17 Number of chemical kinetics calculation rows

Returning h_{Riser} to its original value, the number of chemical kinetics calculation rows was then altered. Adding 4,000 rows in the 'Input' tab as well as the 'Riser' tab and adjusting equations and graphs to include the new rows as required, simply decreases Δt refining the kinetics so that they are less finite than before with lower average concentrations in each time step since the species' concentrations have less time to react in each time step. This leads to slightly longer burning time (burns completely yet slightly higher in the riser) since less mass is consumed over each smaller time step since there is lower average O_2 concentration in each time step. Also, each chemical reaction has less time to react in each time step with higher average concentrations so that the reactant species such as CO, O_2, NH_3, and HCN have higher concentrations at the riser, and product species such as H_2O have lower concentration at the riser. Nevertheless, the trends according to the proposed model are almost exactly the same as before the increase in the rows. These results are evident in the trends below in the graphs of the mole fraction of species in the mixture of gases versus time after the

mixture of gases leaves the CFB bed until they reach the CFB riser exit for all species in Fig. 94 and trace species in Fig. 95.

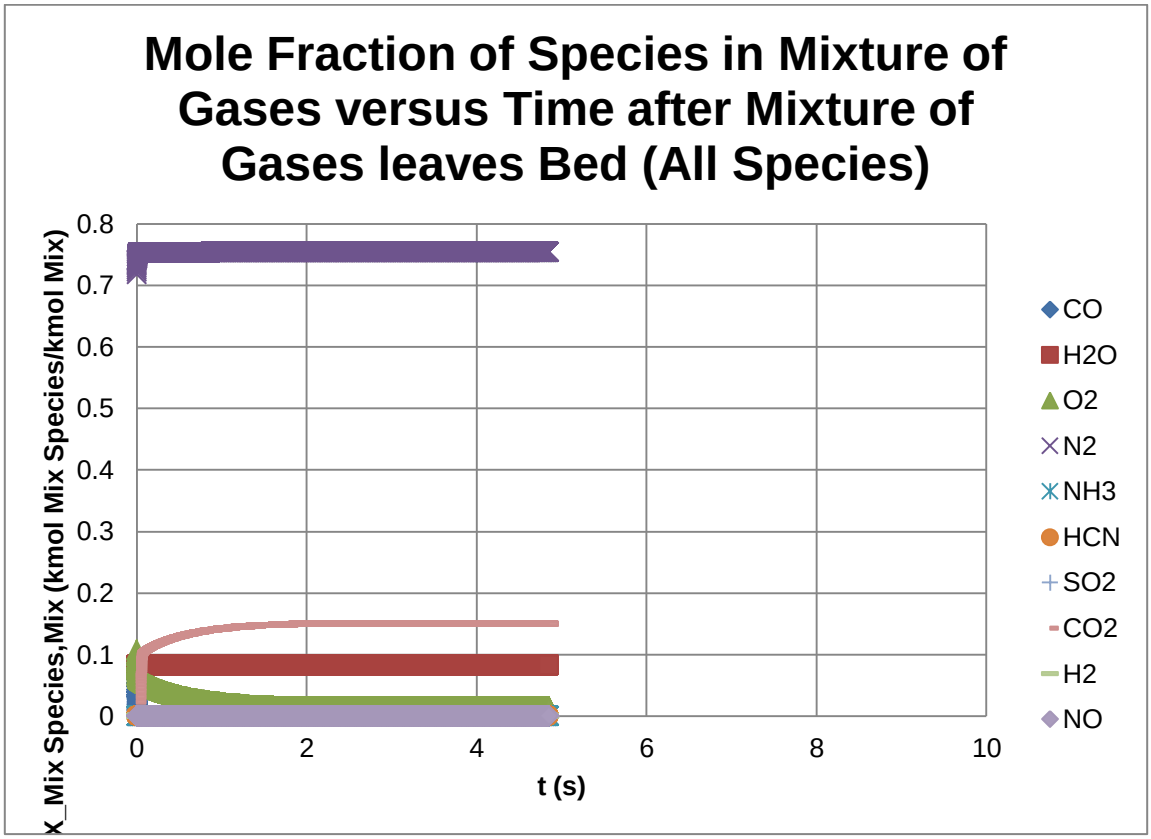

Fig. 94. Mole fraction of all species versus time for anonymous CFB boiler firing tire fuel with increased number of chemical kinetics calculation rows.

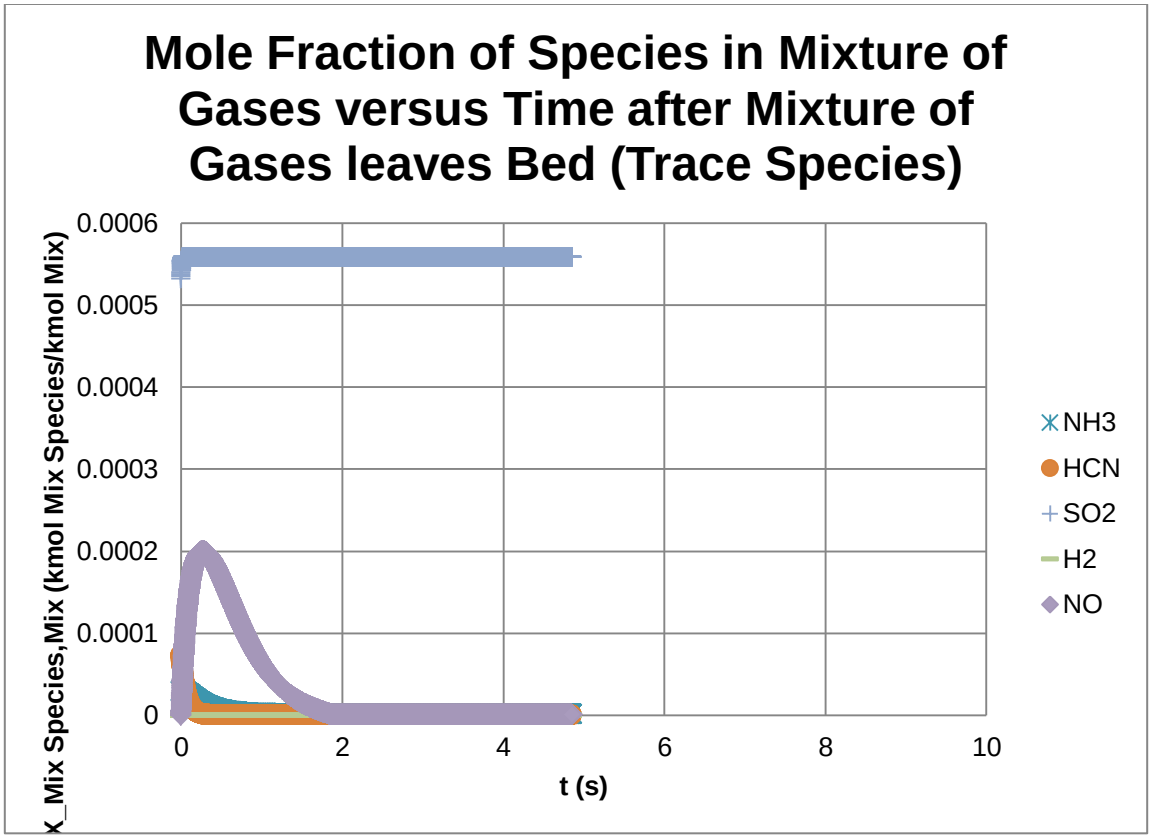

Fig. 95. Mole fraction of trace species versus time for anonymous CFB boiler firing tire fuel with increased number of chemical kinetics calculation rows.

The nearly matching trends are greatly evident in the 'Output' tab of the Excel program as shown below in Table 50 where all species only have minor changes due to the concentrations being updated more frequently similar to real time due to a shorter length of time between the reactions taking place. Continuing to increase the rows further refines the calculations to be more accurate because they are more continuous as reality where concentrations are constantly changing, but also increases the computational time when inputs are varied.

Table 50

Output tab for anonymous CFB boiler firing tire fuel with increased number of chemical kinetics calculation rows.

WET BASIS CONCENTRATION OF SPECIES IN MIXTURE OF GASES LEAVING CFB RISER										
	CO	H2O	O2	N2	NH3	HCN	SO2	CO2	H2	NO
ppm (Actual % O2)	1.07143E-20	82231.03177	14293.43155	753433.4321	1.304402858	8.90782E-20	558.2481496	149481.9788	1.39192E-05	0.573192147
Mole % (Actual % O2)	1.07143E-24	8.223103177	1.429343155	75.34334321	0.00013044	8.90782E-24	0.055824815	14.94819788	1.39192E-09	5.73192E-05
ppm (Standard % O2)	9.85445E-21	75631.52241	30000	756368.1078	1.199717088	8.19291E-20	513.4455513	137485.1974	1.28021E-05	0.527190208
Mole % (Standard % O2)	9.85445E-25	7.563152241	3	F7/10000	0.000119972	8.19291E-24	0.051344555	13.74851974	1.28021E-09	5.2719E-05
g/GJ	3.76562E-21	18588.82241	5739.106055	264893.1842	0.278795751	3.02095E-20	448.7864975	82546.36864	3.52096E-07	0.330910258
DRY BASIS CONCENTRATION OF SPECIES IN MIXTURE OF GASES LEAVING CFB RISER										
	CO	H2O	O2	N2	NH3	HCN	SO2	CO2	H2	NO
ppm (Actual % O2)	1.16743E-20	0	15574.10639	820940.191	1.421275836	9.70595E-20	608.2665343	162875.3902	1.51663E-05	0.624549497
Mole % (Actual % O2)	1.16743E-24	0	1.557410639	82.0940191	0.000142128	9.70595E-24	0.060826653	16.28753902	1.51663E-09	6.24549E-05
ppm (Standard % O2)	1.08081E-20	0	30000	818644.5096	1.315820881	8.98579E-20	563.1347458	150790.4616	1.4041E-05	0.578209555
Mole % (Standard % O2)	1.08081E-24	0	3	F16/10000	0.000131582	8.98579E-24	0.056313475	15.07904616	1.4041E-09	5.7821E-05
g/GJ	3.76562E-21	0	5739.106055	264893.1842	0.278795751	3.02095E-20	448.7864975	82546.36864	3.52096E-07	0.330910258

Subtracting 4,000 rows in the 'Input' tab as well as the 'Riser' tab and adjusting equations and graphs to exclude the rows as required, simply increases Δt causing the kinetics to be more coarse so that they are more finite than before with higher average concentrations in each time step since the species' concentrations have more time to react in each time step. This leads to slightly shorter burning time (burns completely yet slightly lower in the riser) since more mass is consumed over each larger time step since there is higher average O_2 concentration in each time step. Also, each chemical reaction has more time to react in each time step with higher average concentrations so that reactant species such as CO, O_2, NH_3, and HCN have lower concentrations at the riser, and product species such as H_2O have higher concentration at the riser. Nevertheless, the trends according to the proposed model are still almost exactly the same as before the decrease in the rows. These results are evident in the trends below in the graphs of the mole fraction of species in the mixture of gases versus time after the mixture of gases

leaves the CFB bed until they reach the CFB riser exit for all species in Fig. 96 and trace species in Fig. 97.

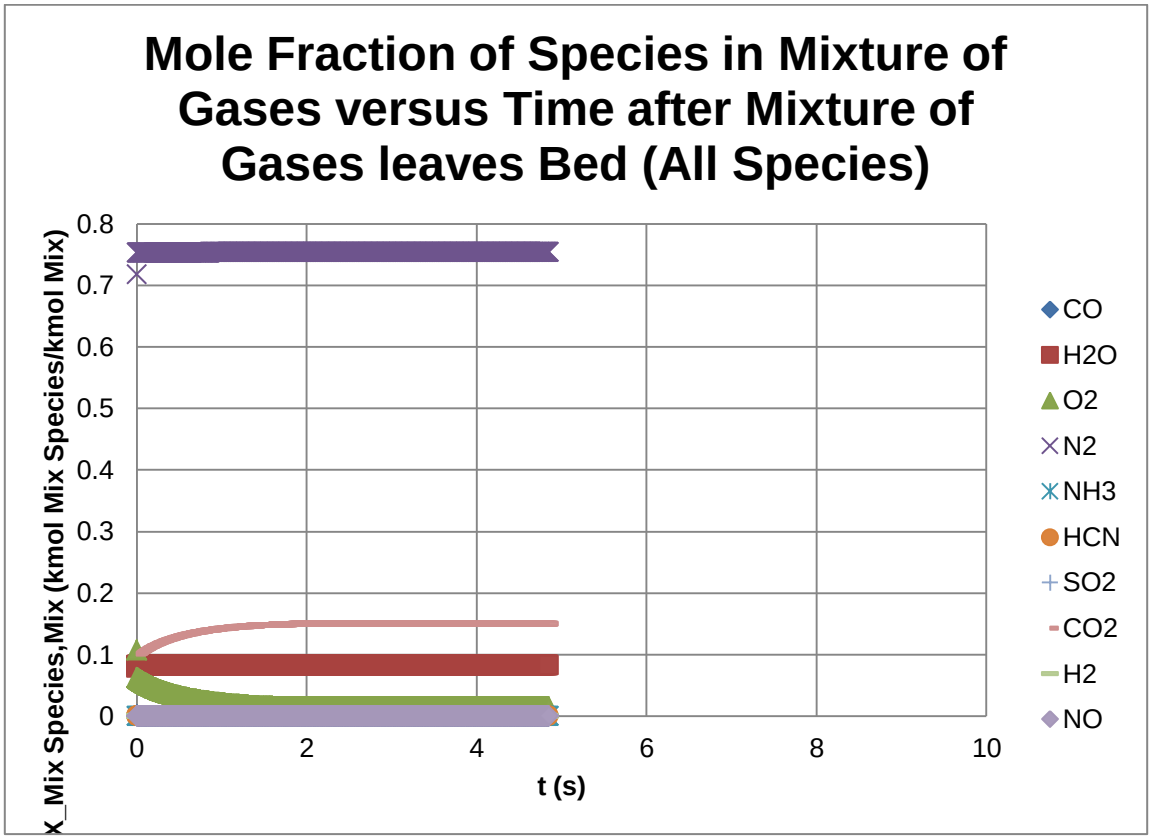

Fig. 96. Mole fraction of all species versus time for anonymous CFB boiler firing tire fuel with decreased number of chemical kinetics calculation rows.

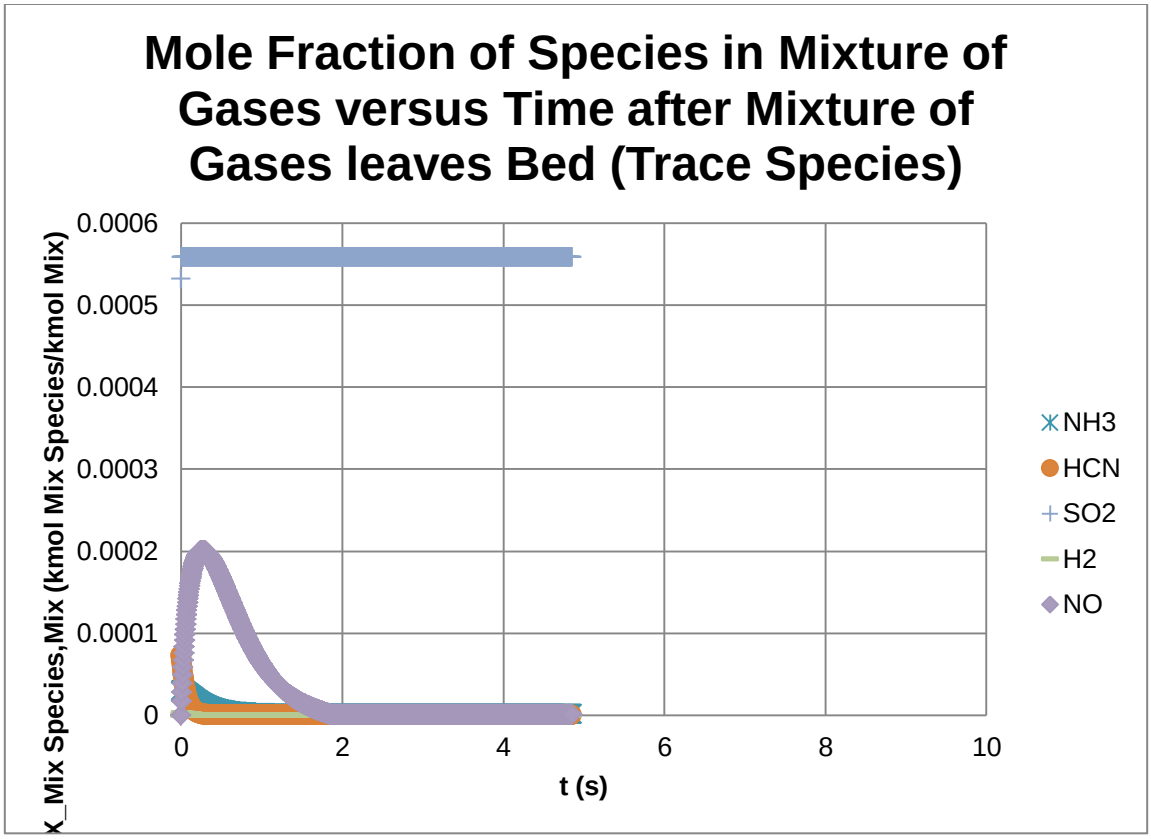

Fig. 97. Mole fraction of trace species versus time for anonymous CFB boiler firing tire fuel with decreased number of chemical kinetics calculation rows.

The nearly matching trends are greatly evident in the 'Output' tab of the Excel program as shown below in Table 51 where all species only have minor changes due to the concentrations being updated less frequently unlike real time due to a longer length of time between the reactions taking place. Continuing to decrease the rows further decreases the accuracy of the calculations to be less continuous unlike reality where concentrations are constantly changing, but also decreases the computational time when inputs are varied.

Table 51

Output tab for anonymous CFB boiler firing tire fuel with decreased number of chemical kinetics calculation rows.

WET BASIS CONCENTRATION OF SPECIES IN MIXTURE OF GASES LEAVING CFB RISER										
	CO	H2O	O2	N2	NH3	HCN	SO2	CO2	H2	NO
ppm (Actual % O2)	3.5331E-21	82231.08572	14293.33269	753433.3721	1.267853396	2.93742E-20	558.2481445	149481.9775	0.000129954	0.715949592
Mole % (Actual % O2)	3.5331E-25	8.223108572	1.429333269	75.34333721	0.000126785	2.93742E-24	0.055824814	14.94819775	1.29954E-08	7.1595E-05
ppm (Standard % O2)	3.24955E-21	75631.53383	30000	756368.0695	1.16610034	2.70167E-20	513.4452872	137485.1266	0.000119524	0.658490221
Mole % (Standard % O2)	3.24955E-25	7.563153383	3	F7/10000	0.00011661	2.70167E-24	0.051344529	13.74851266	1.19524E-08	6.5849E-05
g/GJ	1.24173E-21	18588.83478	5739.066412	264893.1656	0.270983876	9.96178E-21	448.7864975	82546.36864	3.28729E-06	0.413325737
DRY BASIS CONCENTRATION OF SPECIES IN MIXTURE OF GASES LEAVING CFB RISER										
	CO	H2O	O2	N2	NH3	HCN	SO2	CO2	H2	NO
ppm (Actual % O2)	3.84967E-21	0	15573.99958	820940.1739	1.381451667	3.2006E-20	608.2665645	162875.3983	0.000141598	0.780097889
Mole % (Actual % O2)	3.84967E-25	0	1.557399958	82.09401739	0.000138145	3.2006E-24	0.060826656	16.28753983	1.41598E-08	7.80098E-05
ppm (Standard % O2)	3.56403E-21	0	30000	818644.478	1.278950858	2.96313E-20	563.1344644	150790.3862	0.000131092	0.722216265
Mole % (Standard % O2)	3.56403E-25	0	3	F16/10000	0.000127895	2.96313E-24	0.056313446	15.07903862	1.31092E-08	7.22216E-05
g/GJ	1.24173E-21	0	5739.066412	264893.1656	0.270983876	9.96178E-21	448.7864975	82546.36864	3.28729E-06	0.413325737

5.3.18 Pre-exponential factor for $\boldsymbol{NO\ (g)\ +\ C\ (s)\ \rightarrow\ \frac{1}{2}\ N_2\ (g)\ +CO\ (g)}$

Returning the number of chemical kinetics calculation rows to its original value, the pre-exponential factor for $NO\ (g)\ +\ C\ (s)\ \rightarrow\ \frac{1}{2}\ N_2\ (g)\ +CO\ (g)$ was then altered. Multiplying the pre-exponential factor by ten, decreases CO due to a greater O_2 concentration from more fixed Carbon being reduced by NO instead of oxidized, but this increases CO_2. Also, H_2O and N_2 decrease from less NH_3 and HCN reduction reactions due to a lower concentration of NO. There is more NH_3 due to greatly reduced NO concentrations to react with while HCN is not as sensitive to NO reactions so that a greater amount of O_2 to react with causes more of an overall reduction in HCN. More H_2 is produced because more is created with greater NH_3 and HCN oxidation reactions than is destroyed by its own oxidation reactions. However, there is less of a peak of NO due to its greater reduction rate on the fixed Carbon surface, but there is more final NO due to a lower NO concentration causing slower reduction with NH_3 and HCN after the

fuel is completely burned. Even though the NO is helping to convert fixed Carbon more quickly along with having a higher surrounding O_2 concentration for burning the fuel, it takes slightly longer to burn due to the less burning favorable gas mixture created by more N_2 produced from the NO reduction of the fixed Carbon. These results are evident in the trends below in the graphs of the mole fraction of species in the mixture of gases versus time after the mixture of gases leaves the CFB bed until they reach the CFB riser exit for all species in Fig. 98 and trace species in Fig. 99.

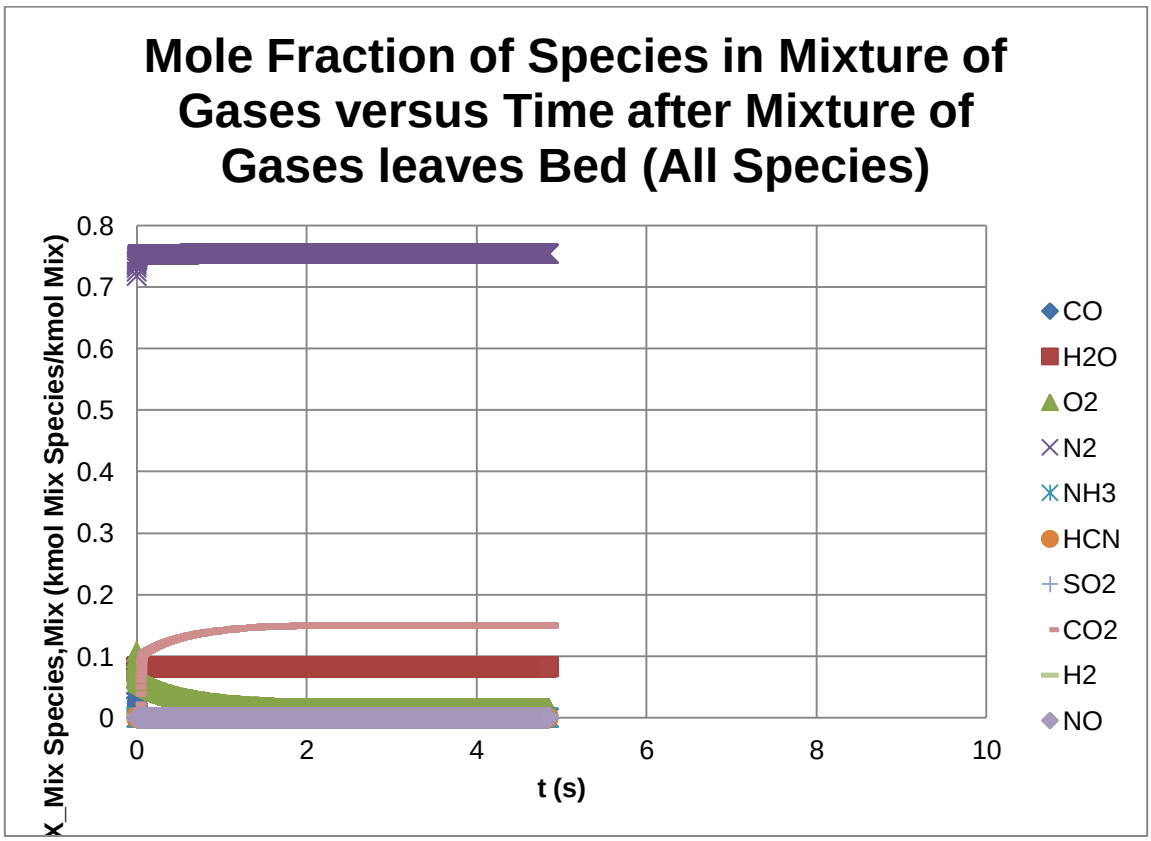

Fig. 98. Mole fraction of all species versus time for anonymous CFB boiler firing tire fuel with increased pre-exponential factor for $NO\ (g)\ +\ C\ (s)\ \rightarrow\ \frac{1}{2}\ N_2\ (g)\ +CO\ (g)$.

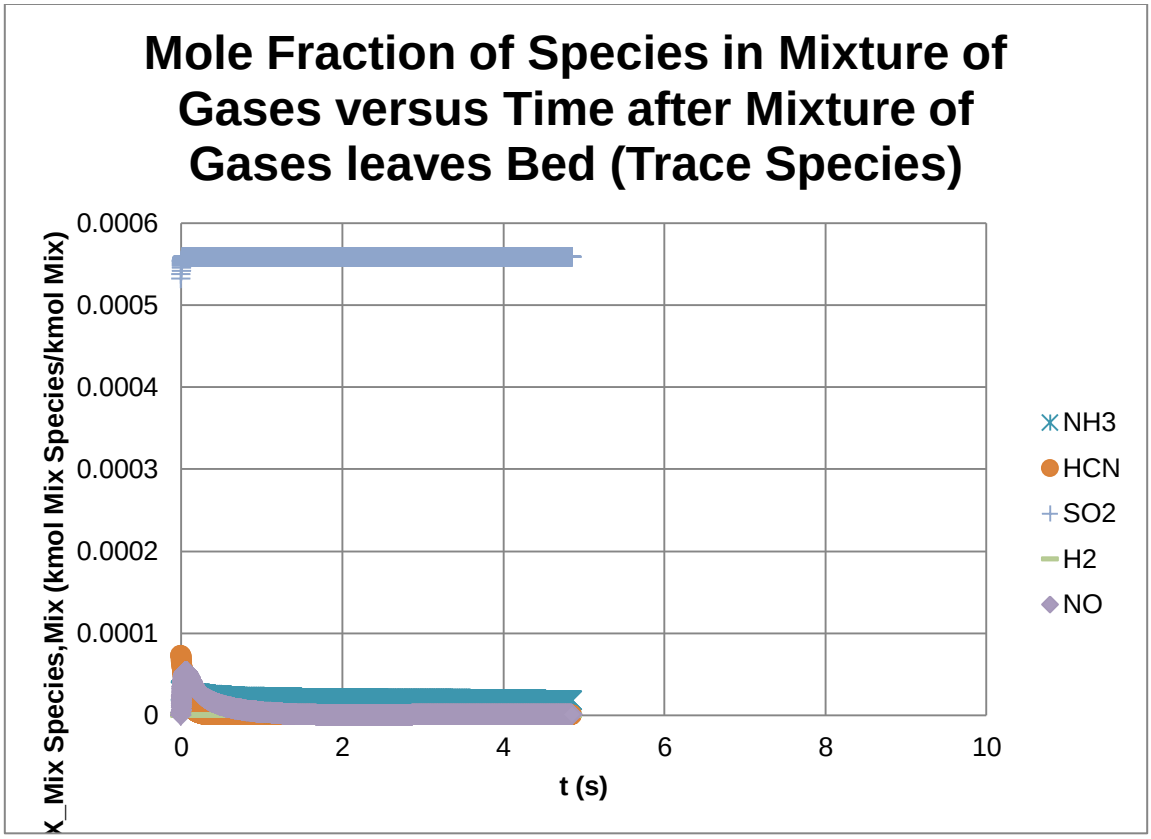

Fig. 99. Mole fraction of trace species versus time for anonymous CFB boiler firing tire fuel with increased pre-exponential factor for $NO\ (g)\ +\ C\ (s)\ \rightarrow\ \frac{1}{2}\ N_2\ (g)\ +CO\ (g)$.

The similar trends are evident in the 'Output' tab of the Excel program as shown below in Table 52 where most species only have minor changes. Continuing to increase the pre-exponential factor continues the trends only until the NO is being destroyed on the surface of the fixed Carbon as fast as it is being created.

Table 52

Output tab for anonymous CFB boiler firing tire fuel with increased pre-exponential factor for $NO\ (g)\ +\ C\ (s)\ \rightarrow\ \frac{1}{2}\ N_2\ (g)\ +CO\ (g)$.

WET BASIS CONCENTRATION OF SPECIES IN MIXTURE OF GASES LEAVING CFB RISER										
	CO	H2O	O2	N2	NH3	HCN	SO2	CO2	H2	NO
ppm (Actual % O2)	9.13822E-21	82206.26616	14305.82267	753427.9917	18.04394845	7.59052E-20	558.2504857	149482.6044	0.000419443	1.020295378
Mole % (Actual % O2)	9.13822E-25	8.220626616	1.430582267	75.34279917	0.001804395	7.59052E-24	0.055825049	14.94826044	4.19443E-08	0.00010203
ppm (Standard % O2)	8.40536E-21	75613.53184	30000	756360.9741	16.59686949	6.98178E-20	513.4802108	137494.4781	0.000385804	0.938470273
Mole % (Standard % O2)	8.40536E-25	7.561353184	3	F7/10000	0.001659687	6.98178E-24	0.051348021	13.74944781	3.85804E-08	9.3847E-05
g/GJ	3.21167E-21	18583.14623	5744.057308	264890.163	3.856596199	2.57419E-20	448.7864975	82546.36864	1.06101E-05	0.589025506
DRY BASIS CONCENTRATION OF SPECIES IN MIXTURE OF GASES LEAVING CFB RISER										
	CO	H2O	O2	N2	NH3	HCN	SO2	CO2	H2	NO
ppm (Actual % O2)	9.95672E-21	0	15587.18713	820912.1112	19.66013471	8.27039E-20	608.2526663	162871.6768	0.000457012	1.111682658
Mole % (Actual % O2)	9.95672E-25	0	1.558718713	82.09121112	0.001966013	8.27039E-24	0.060825267	16.28716768	4.57012E-08	0.000111168
ppm (Standard % O2)	9.21858E-21	0	30000	818620.4388	18.20262871	7.65727E-20	563.1597955	150797.1691	0.000423131	1.029267956
Mole % (Standard % O2)	9.21858E-25	0	3	F16/10000	0.001820263	7.65727E-24	0.05631598	15.07971691	4.23131E-08	0.000102927
g/GJ	3.21167E-21	0	5744.057308	264890.163	3.856596199	2.57419E-20	448.7864975	82546.36864	1.06101E-05	0.589025506

Dividing the pre-exponential factor by ten, increases CO due to a lesser O_2 concentration from less fixed Carbon being reduced by NO instead of oxidized, and this decreases CO_2. Also, H_2O increases from more NH_3 and HCN reduction reactions due to a higher concentration of NO. On the other hand, less N_2 is created due to less being formed from the slower NO reaction with fixed Carbon than is formed from the quicker NH_3 and HCN reduction reactions. There is less NH_3 due to greatly enlarged NO concentrations to react with while HCN is not as sensitive to NO reactions so that a lesser amount of O_2 to react with causes more of an overall enlargement in HCN. Less H_2 is produced because less is created with smaller NH_3 and HCN oxidation reactions than is destroyed by its own oxidation reactions. However, there is more of a peak of NO as well as final NO due to its lesser reduction rate on the fixed Carbon surface even though there is a higher NO concentration causing quicker reduction with NH_3 and HCN after the fuel is completely burned. Even though the NO is helping to convert fixed

Carbon more slowly along with having a lower surrounding O_2 concentration for burning the fuel, it takes slightly shorter to burn due to the more burning favorable gas mixture created by less N_2 produced from the NO reduction of the fixed Carbon. These results are evident in the trends below in the graphs of the mole fraction of species in the mixture of gases versus time after the mixture of gases leaves the CFB bed until they reach the CFB riser exit for all species in Fig. 100 and trace species in Fig. 101.

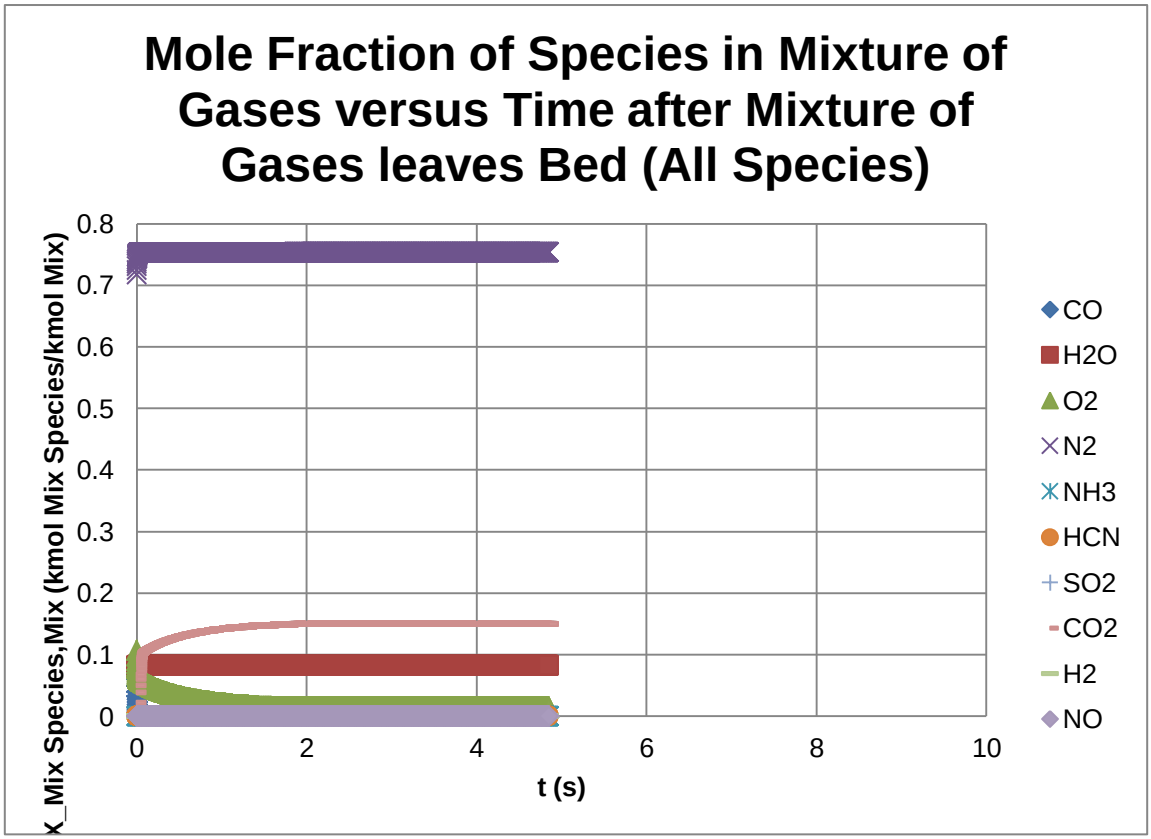

Fig. 100. Mole fraction of all species versus time for anonymous CFB boiler firing tire fuel with decreased pre-exponential factor for $NO\ (g)\ +\ C\ (s)\ \rightarrow\ \frac{1}{2}\ N_2\ (g)\ +CO\ (g)$.

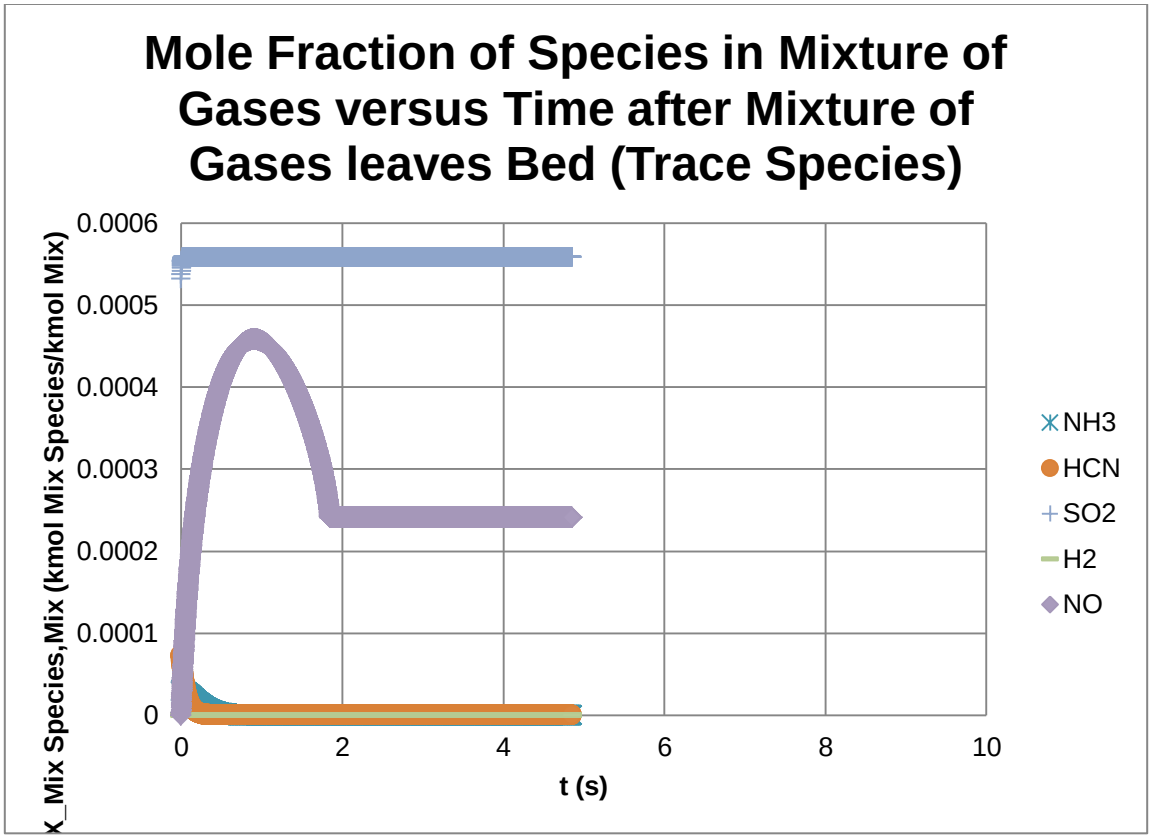

Fig. 101. Mole fraction of trace species versus time for anonymous CFB boiler firing tire fuel with decreased pre-exponential factor for $NO\ (g)\ +\ C\ (s)\ \rightarrow\ \frac{1}{2}\ N_2\ (g)\ +\ CO\ (g)$.

The similar trends are evident in the 'Output' tab of the Excel program as shown below in Table 53 where most species only have minor changes. Continuing to decrease the pre-exponential factor continues the trends except for the burning of the fuel does begin to slow down due to the continually decreasing reaction of NO with the fixed Carbon until the NO is no longer being destroyed on the surface of the fixed Carbon so that a maximum NO level is achieved.

Table 53

Output tab for anonymous CFB boiler firing tire fuel with decreased pre-exponential factor for $NO\ (g)\ +\ C\ (s)\ \rightarrow\ \frac{1}{2}\ N_2\ (g)\ +CO\ (g)$.

WET BASIS CONCENTRATION OF SPECIES IN MIXTURE OF GASES LEAVING CFB RISER										
	CO	H2O	O2	N2	NH3	HCN	SO2	CO2	H2	NO
ppm (Actual % O2)	1.27839E-20	82232.96157	14172.08516	753313.4752	9.95697E-11	1.07032E-19	558.2479676	149481.9301	2.19332E-13	241.3000393
Mole % (Actual % O2)	1.27839E-24	8.223296157	1.417208516	75.33134752	9.95697E-15	1.07032E-23	0.055824797	14.94819301	2.19332E-17	0.024130004
ppm (Standard % O2)	1.17506E-20	75586.43054	30000	756278.6867	9.15219E-11	9.83809E-20	513.1272232	137399.9587	2.01605E-13	221.7968113
Mole % (Standard % O2)	1.17506E-24	7.558643054	3	F7/10000	9.15219E-15	9.83809E-24	0.051312722	13.73999587	2.01605E-17	0.022179681
g/GJ	4.49298E-21	18589.26471	5690.384844	264851.096	2.12815E-11	3.62982E-20	448.7864975	82546.36864	5.54819E-15	139.3052658

DRY BASIS CONCENTRATION OF SPECIES IN MIXTURE OF GASES LEAVING CFB RISER										
	CO	H2O	O2	N2	NH3	HCN	SO2	CO2	H2	NO
ppm (Actual % O2)	1.39294E-20	0	15441.91997	820811.212	1.08491E-10	1.16622E-19	608.267615	162875.6796	2.38985E-13	262.920795
Mole % (Actual % O2)	1.39294E-24	0	1.544191997	82.0811212	1.08491E-14	1.16622E-23	0.060826761	16.28756796	2.38985E-17	0.026292079
ppm (Standard % O2)	1.28871E-20	0	30000	818505.7201	1.00373E-10	1.07896E-19	562.7531413	150688.2794	2.21102E-13	243.2473793
Mole % (Standard % O2)	1.28871E-24	0	3	F16/10000	1.00373E-14	1.07896E-23	0.056275314	15.06882794	2.21102E-17	0.024324738
g/GJ	4.49298E-21	0	5690.384844	264851.096	2.12815E-11	3.62982E-20	448.7864975	82546.36864	5.54819E-15	139.3052658

5.3.19 Pre-exponential factor for $\boldsymbol{CO\ (g)\ +\ \frac{1}{2}\ O_2\ (g)\ \rightarrow\ CO_2\ (g)}$

Returning the pre-exponential factor for $NO\ (g)\ +\ C\ (s)\ \rightarrow\ \frac{1}{2}\ N_2\ (g)\ +\ CO\ (g)$ to its original value, the pre-exponential factor for $CO\ (g)\ +\ \frac{1}{2}\ O_2\ (g)\ \rightarrow\ CO_2\ (g)$ was then altered. Multiplying the pre-exponential factor by ten, decreases CO and O_2 concentrations, but also decreases CO_2 merely due to the pseudo-deflation caused by other species changing. The decrease in O_2 also causes the fuel to take slightly longer to completely burn. These results are evident in the trends below in the graphs of the mole fraction of species in the mixture of gases versus time after the mixture of gases leaves the CFB bed until they reach the CFB riser exit for all species in Fig. 102 and trace species in Fig. 103.

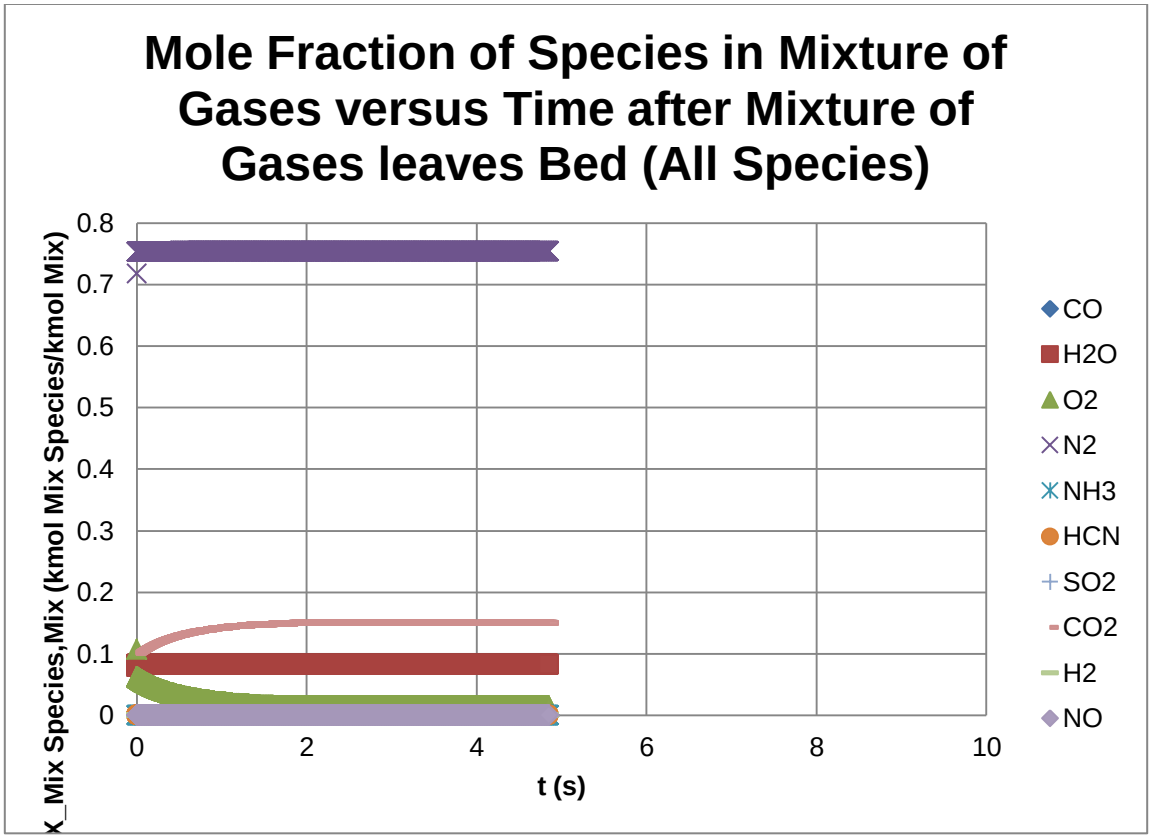

Fig. 102. Mole fraction of all species versus time for anonymous CFB boiler firing tire fuel with increased pre-exponential factor for $CO\ (g)\ +\ \frac{1}{2}\ O_2\ (g)\ \rightarrow\ CO_2\ (g)$.

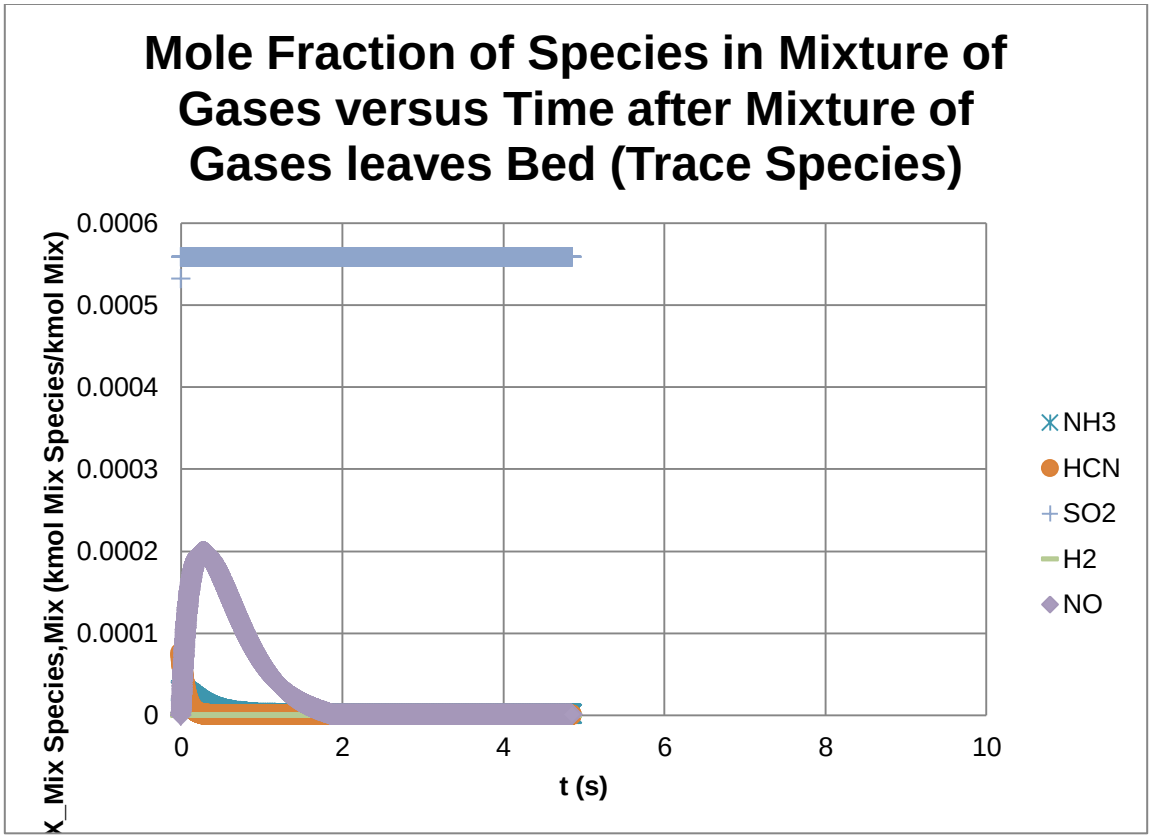

Fig. 103. Mole fraction of trace species versus time for anonymous CFB boiler firing tire fuel with increased pre-exponential factor for $CO\ (g)\ +\ \frac{1}{2}\ O_2\ (g)\ \rightarrow\ CO_2\ (g)$.

The nearly exact trends are evident in the 'Output' tab of the Excel program as shown below in Table 54 where all species only have minor changes. Continuing to increase the pre-exponential factor continues the trends only until the CO is oxidized as fast as it is created.

Table 54

Output tab for anonymous CFB boiler firing tire fuel with increased pre-exponential factor for $CO\ (g)\ +\ \frac{1}{2}\ O_2\ (g)\ \rightarrow\ CO_2\ (g)$.

WET BASIS CONCENTRATION OF SPECIES IN MIXTURE OF GASES LEAVING CFB RISER										
	CO	H2O	O2	N2	NH3	HCN	SO2	CO2	H2	NO
ppm (Actual % O2)	8.47552E-22	82231.04358	14293.41409	753433.4231	1.296407192	7.80929E-20	558.2481485	149481.9785	2.51692E-05	0.596082412
Mole % (Actual % O2)	8.47552E-26	8.223104358	1.429341409	75.34334231	0.000129641	7.80929E-24	0.055824815	14.94819785	2.51692E-09	5.96082E-05
ppm (Standard % O2)	7.79531E-22	75631.52653	30000	756368.1025	1.192363014	7.18255E-20	513.4455045	137485.1848	2.31492E-05	0.548243349
Mole % (Standard % O2)	7.79531E-26	7.563152653	3	F7/10000	0.000119236	7.18255E-24	0.05134455	13.74851848	2.31492E-09	5.48243E-05
g/GJ	2.97877E-22	18588.82512	5739.099054	264893.1816	0.277086803	2.6484E-20	448.7864975	82546.36864	6.36675E-07	0.344125066
DRY BASIS CONCENTRATION OF SPECIES IN MIXTURE OF GASES LEAVING CFB RISER										
	CO	H2O	O2	N2	NH3	HCN	SO2	CO2	H2	NO
ppm (Actual % O2)	9.23491E-22	0	15574.08756	820940.1918	1.412563787	8.50899E-20	608.2665409	162875.392	2.74244E-05	0.649490711
Mole % (Actual % O2)	9.23491E-26	0	1.557408756	82.09401918	0.000141256	8.50899E-24	0.060826654	16.2875392	2.74244E-09	6.49491E-05
ppm (Standard % O2)	8.5497E-22	0	30000	818644.5076	1.307755116	7.87764E-20	563.1346974	150790.4486	2.53895E-05	0.601300138
Mole % (Standard % O2)	8.5497E-26	0	3	F16/10000	0.000130776	7.87764E-24	0.05631347	15.07904486	2.53895E-09	6.013E-05
g/GJ	2.97877E-22	0	5739.099054	264893.1816	0.277086803	2.6484E-20	448.7864975	82546.36864	6.36675E-07	0.344125066

Dividing the pre-exponential factor by ten, increases CO and O_2 concentrations, but also increases CO_2 merely due to the pseudo-inflation caused by other species changing. The increase in O_2 also causes the fuel to take slightly shorter to completely burn. These results are evident in the trends below in the graphs of the mole fraction of species in the mixture of gases versus time after the mixture of gases leaves the CFB bed until they reach the CFB riser exit for all species in Fig. 104 and trace species in Fig. 105.

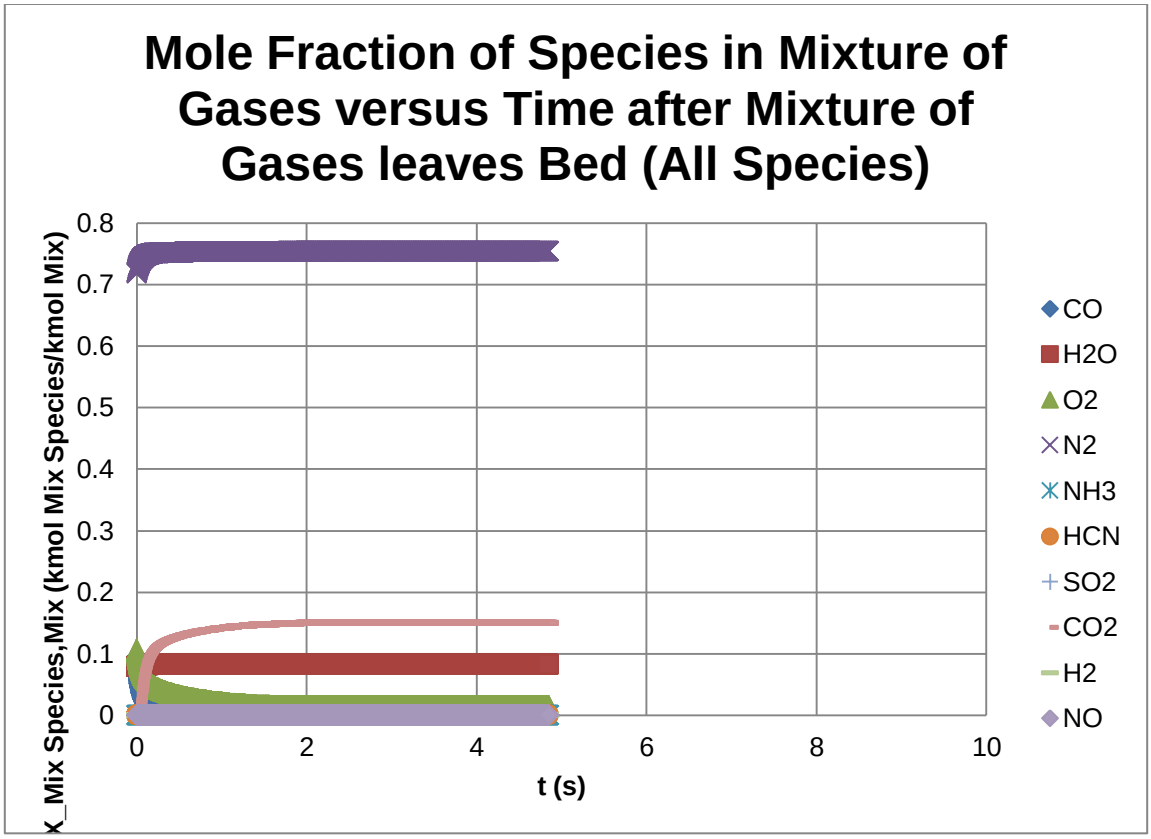

Fig. 104. Mole fraction of all species versus time for anonymous CFB boiler firing tire fuel with decreased pre-exponential factor for $CO\ (g) + \frac{1}{2}\ O_2\ (g) \rightarrow\ CO_2\ (g)$.

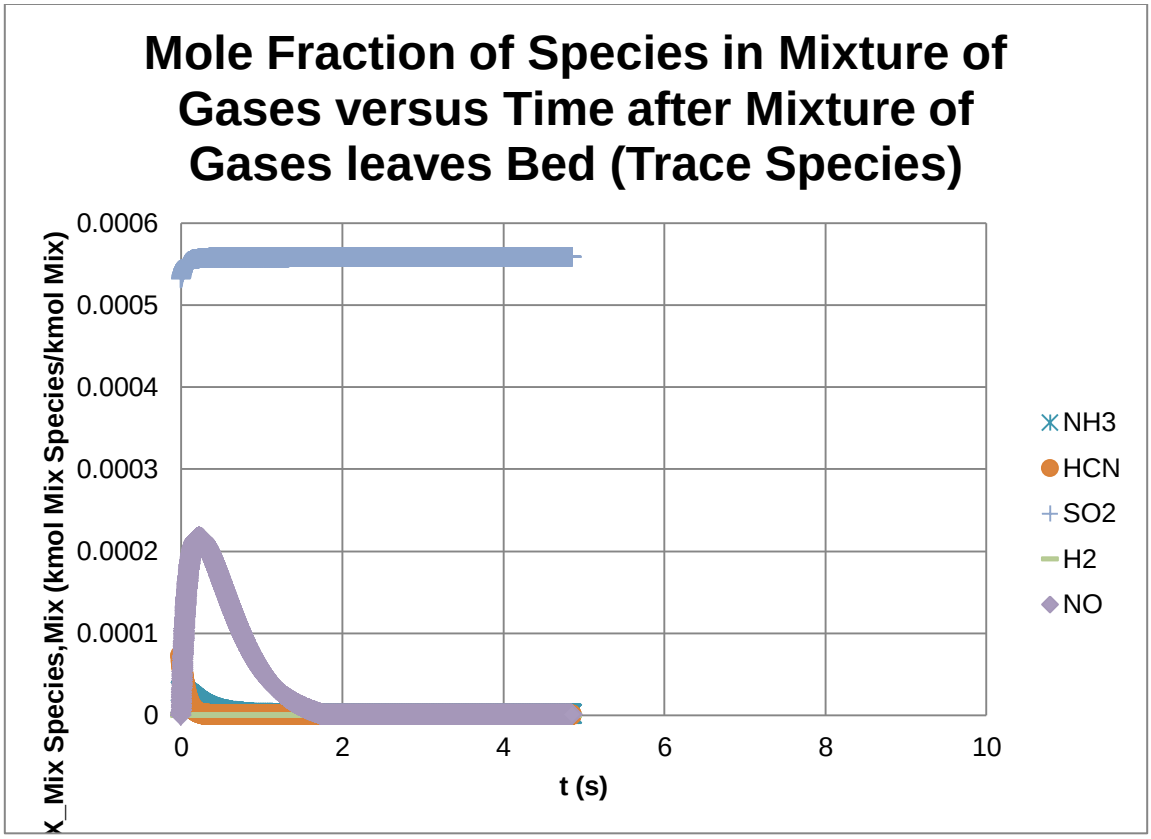

Fig. 105. Mole fraction of trace species versus time for anonymous CFB boiler firing tire fuel with decreased pre-exponential factor for $CO\ (g) + \frac{1}{2}\ O_2\ (g) \rightarrow\ CO_2\ (g)$.

The nearly exact trends are evident in the 'Output' tab of the Excel program as shown below in Table 55 where all species only have minor changes. Continuing to decrease the pre-exponential factor continues the trends except for the CO_2 does begin to decrease due to the continually decreasing CO oxidation until the CO is no longer being oxidized at all so that a maximum CO level is achieved.

Table 55

Output tab for anonymous CFB boiler firing tire fuel with decreased pre-exponential factor for $CO\ (g)\ +\ \frac{1}{2}\ O_2\ (g)\ \rightarrow\ CO_2\ (g)$.

WET BASIS CONCENTRATION OF SPECIES IN MIXTURE OF GASES LEAVING CFB RISER										
	CO	H2O	O2	N2	NH3	HCN	SO2	CO2	H2	NO
ppm (Actual % O2)	7.69007E-09	82230.95105	14293.44408	753433.3865	1.358955025	1.04052E-19	558.2481572	149481.9809	2.68043E-05	0.63036494
Mole % (Actual % O2)	7.69007E-13	8.223095105	1.429344408	75.34333865	0.000135896	1.04052E-23	0.055824816	14.94819809	2.68043E-09	6.30365E-05
ppm (Standard % O2)	7.0729E-09	75631.45301	30000	756368.0637	1.249891213	9.57009E-20	513.4455912	137485.208	2.46531E-05	0.579774595
Mole % (Standard % O2)	7.0729E-13	7.563145301	3	F7/10000	0.000124989	9.57009E-24	0.051344559	13.7485208	2.46531E-09	5.79775E-05
g/GJ	2.70272E-09	18588.80391	5739.111008	264893.1646	0.290455421	3.52875E-20	448.7864975	82546.36864	6.78037E-07	0.363916749
DRY BASIS CONCENTRATION OF SPECIES IN MIXTURE OF GASES LEAVING CFB RISER										
	CO	H2O	O2	N2	NH3	HCN	SO2	CO2	H2	NO
ppm (Actual % O2)	8.37909E-09	0	15574.11867	820940.0691	1.480715684	1.13375E-19	608.2664891	162875.3781	2.9206E-05	0.686844845
Mole % (Actual % O2)	8.37909E-13	0	1.557411867	82.09400691	0.000148072	1.13375E-23	0.060826649	16.28753781	2.9206E-09	6.86845E-05
ppm (Standard % O2)	7.75738E-09	0	30000	818644.3986	1.370850534	1.04962E-19	563.1347395	150790.4599	2.70389E-05	0.635882791
Mole % (Standard % O2)	7.75738E-13	0	3	F16/10000	0.000137085	1.04962E-23	0.056313474	15.07904599	2.70389E-09	6.35883E-05
g/GJ	2.70272E-09	0	5739.111008	264893.1646	0.290455421	3.52875E-20	448.7864975	82546.36864	6.78037E-07	0.363916749

5.3.20 Pre-exponential factor for $NH_3\ (g)\ +\ O_2\ (g)\ \rightarrow$ NO (g) $+\ H_2O$ (g) $+\ \frac{1}{2}\ H_2\ (g)$

Returning the pre-exponential factor for $CO\ (g)\ +\ \frac{1}{2}\ O_2\ (g)\ \rightarrow\ CO_2\ (g)$ to its original value, the first pre-exponential factor for $NH_3\ (g)\ +\ O_2\ (g)\ \rightarrow$ NO (g) $+\ H_2O$ (g) $+\ \frac{1}{2}\ H_2\ (g)$ was then altered. Multiplying the pre-exponential factor by ten, obviously decreases NH_3 and O_2 concentrations while increasing NO, H_2O, and H_2. Due to higher NO, there is also higher N_2 concentration from fixed Carbon, NH_3, and HCN reduction reactions. The concentration of HCN increases because HCN is more sensitive to oxidation than reduction so that a lower level of O_2 means less HCN converted even though NO increases. The CO level is higher from less O_2 available to destroy CO and more NO reacting with fixed Carbon and HCN to form CO even though less O_2 is available to react with fixed Carbon and HCN to form CO. However, the lesser amount of O_2 overrides the greater amount of CO to end up with less CO_2. These

results are evident in the trends below in the graphs of the mole fraction of species in the mixture of gases versus time after the mixture of gases leaves the CFB bed until they reach the CFB riser exit for all species in Fig. 106 and trace species in Fig. 107.

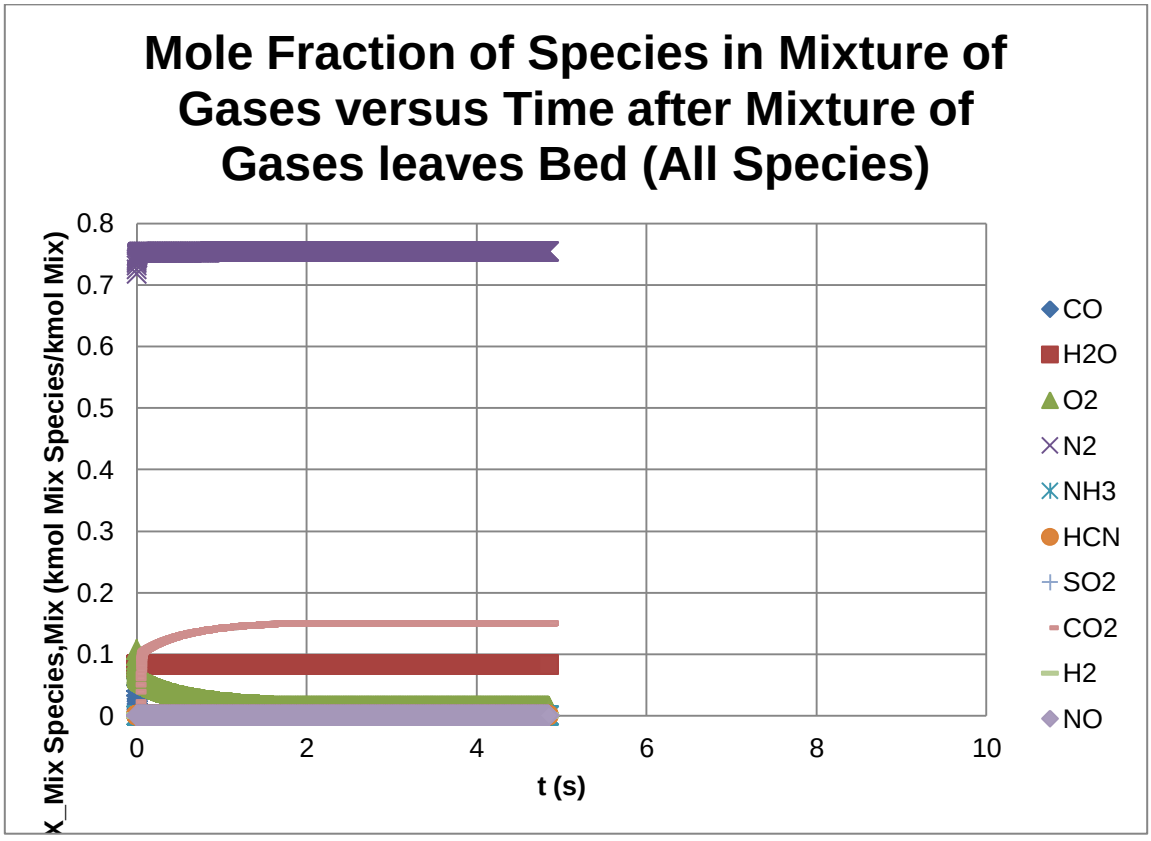

Fig. 106. Mole fraction of all species versus time for anonymous CFB boiler firing tire fuel with increased pre-exponential factor for $NH_3\ (g)\ +\ O_2\ (g)\ \rightarrow\ \mathrm{NO\ (g)}\ +\ H_2O\ \mathrm{(g)}\ +\ \frac{1}{2}\ H_2\ (g)$.

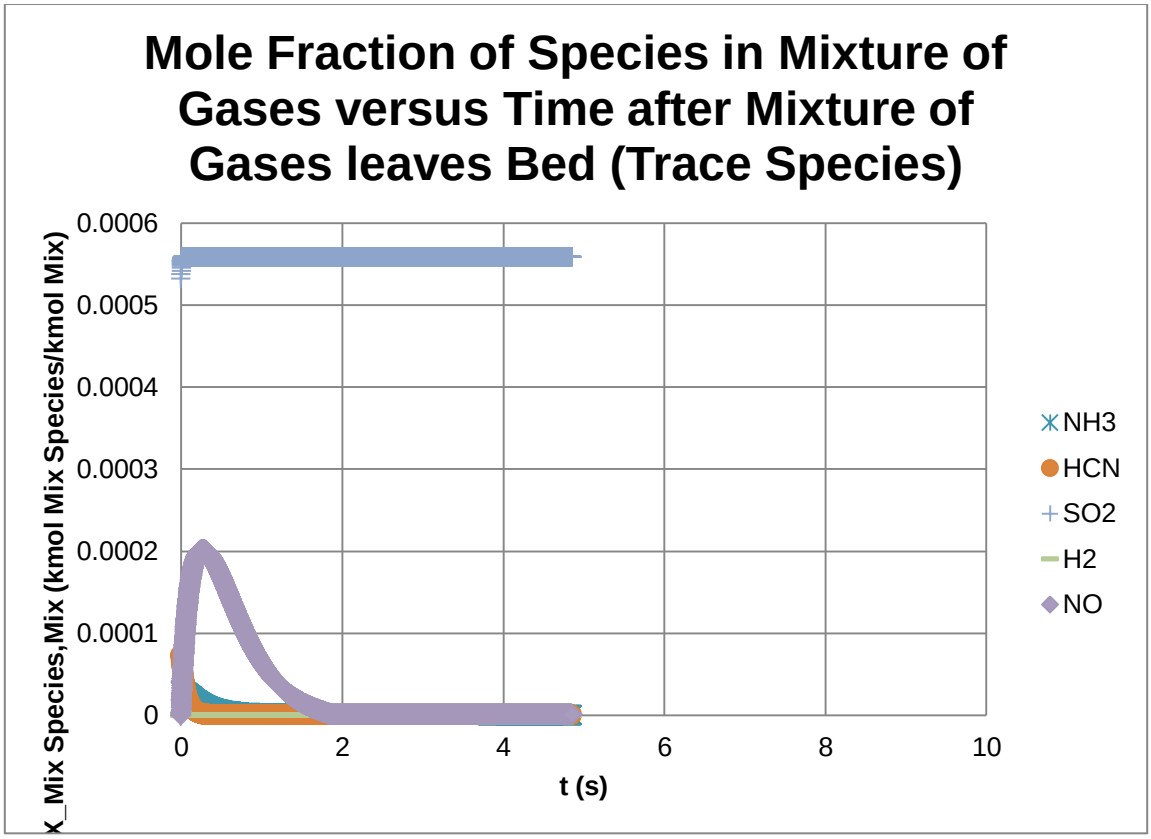

Fig. 107. Mole fraction of trace species versus time for anonymous CFB boiler firing tire fuel with increased pre-exponential factor for $NH_3\ (g)\ +\ O_2\ (g)\ \rightarrow\ \mathrm{NO\ (g)}\ +\ H_2O\ \mathrm{(g)}\ +\ \frac{1}{2}\ H_2\ (g)$.

The nearly exact trends are evident in the 'Output' tab of the Excel program as shown below in Table 56 where all species only have minor changes. Continuing to increase the pre-exponential factor continues the trends except for the H_2 and NO begin to decrease due to destructive reactions overtaking the increased creation from NH_3 oxidation only until the NH_3 or O_2 is depleted.

Table 56

Output tab for anonymous CFB boiler firing tire fuel with increased pre-exponential factor for $NH_3\ (g)\ +\ O_2\ (g)\ \rightarrow\ \mathrm{NO\ (g)}\ +\ H_2O\ \mathrm{(g)}\ +\ \frac{1}{2}\ H_2\ (g)$.

WET BASIS CONCENTRATION OF SPECIES IN MIXTURE OF GASES LEAVING CFB RISER										
	CO	H2O	O2	N2	NH3	HCN	SO2	CO2	H2	NO
ppm (Actual % O2)	9.64488E-21	82232.44448	14292.50033	753433.518	0.349477086	8.0192E-20	558.2480163	149481.9431	5.21949E-05	0.996467876
Mole % (Actual % O2)	9.64488E-25	8.223244448	1.429250033	75.3433518	3.49477E-05	8.0192E-24	0.055824802	14.94819431	5.21949E-09	9.96468E-05
ppm (Standard % O2)	8.87078E-21	75632.46187	30000	756368.3468	0.321428027	7.37558E-20	513.4429856	137484.5104	4.80058E-05	0.916491284
Mole % (Standard % O2)	8.87078E-25	7.563246187	3	F7/10000	3.21428E-05	7.37558E-24	0.051344299	13.74845104	4.80058E-09	9.16491E-05
g/GJ	3.38975E-21	18589.1462	5738.733519	264893.2777	0.07469529	2.71959E-20	448.7864975	82546.36864	1.32031E-06	0.575272223

DRY BASIS CONCENTRATION OF SPECIES IN MIXTURE OF GASES LEAVING CFB RISER										
	CO	H2O	O2	N2	NH3	HCN	SO2	CO2	H2	NO
ppm (Actual % O2)	1.05091E-20	0	15573.1157	820941.5483	0.380790412	8.73773E-20	608.2673254	162875.602	5.68716E-05	1.085751909
Mole % (Actual % O2)	1.05091E-24	0	1.55731157	82.09415483	3.8079E-05	8.73773E-24	0.060826733	16.2875602	5.68716E-09	0.000108575
ppm (Standard % O2)	9.72927E-21	0	30000	818645.6203	0.352534961	8.08937E-20	563.1326088	150789.8893	5.26516E-05	1.005186831
Mole % (Standard % O2)	9.72927E-25	0	3	F16/10000	3.52535E-05	8.08937E-24	0.056313261	15.07898893	5.26516E-09	0.000100519
g/GJ	3.38975E-21	0	5738.733519	264893.2777	0.07469529	2.71959E-20	448.7864975	82546.36864	1.32031E-06	0.575272223

Dividing the pre-exponential factor by ten, obviously increases NH_3 and O_2 concentrations while decreasing NO, H_2O, and H_2. Due to lower NO, there is also lower N_2 concentration from fixed Carbon, NH_3, and HCN reduction reactions. The concentration of HCN decreases because HCN is more sensitive to oxidation than reduction so that a higher level of O_2 means more HCN converted even though NO decreases. The CO level is lower from more O_2 available to destroy CO and less NO reacting with fixed Carbon and HCN to form CO even though more O_2 is available to react with fixed Carbon and HCN to form CO. However, the greater amount of O_2 overrides the lesser amount of CO to end up with more CO_2. These results are evident in the trends below in the graphs of the mole fraction of species in the mixture of gases versus time after the mixture of gases leaves the CFB bed until they reach the CFB riser exit for all species in Fig. 108 and trace species in Fig. 109.

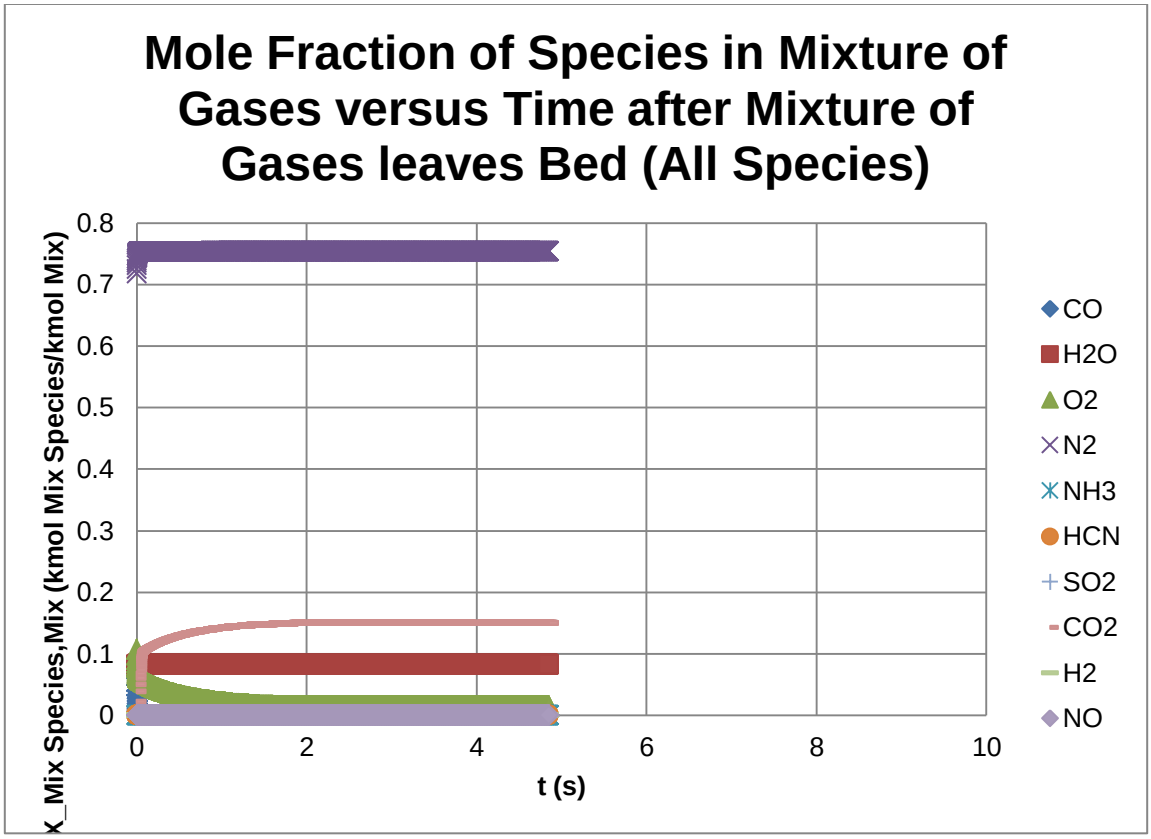

Fig. 108. Mole fraction of all species versus time for anonymous CFB boiler firing tire fuel with decreased pre-exponential factor for $NH_3\ (g)\ +\ O_2\ (g)\ \rightarrow\ \mathrm{NO\ (g)}\ +\ H_2O\ \mathrm{(g)}\ +\ \frac{1}{2}\ H_2\ (g)$.

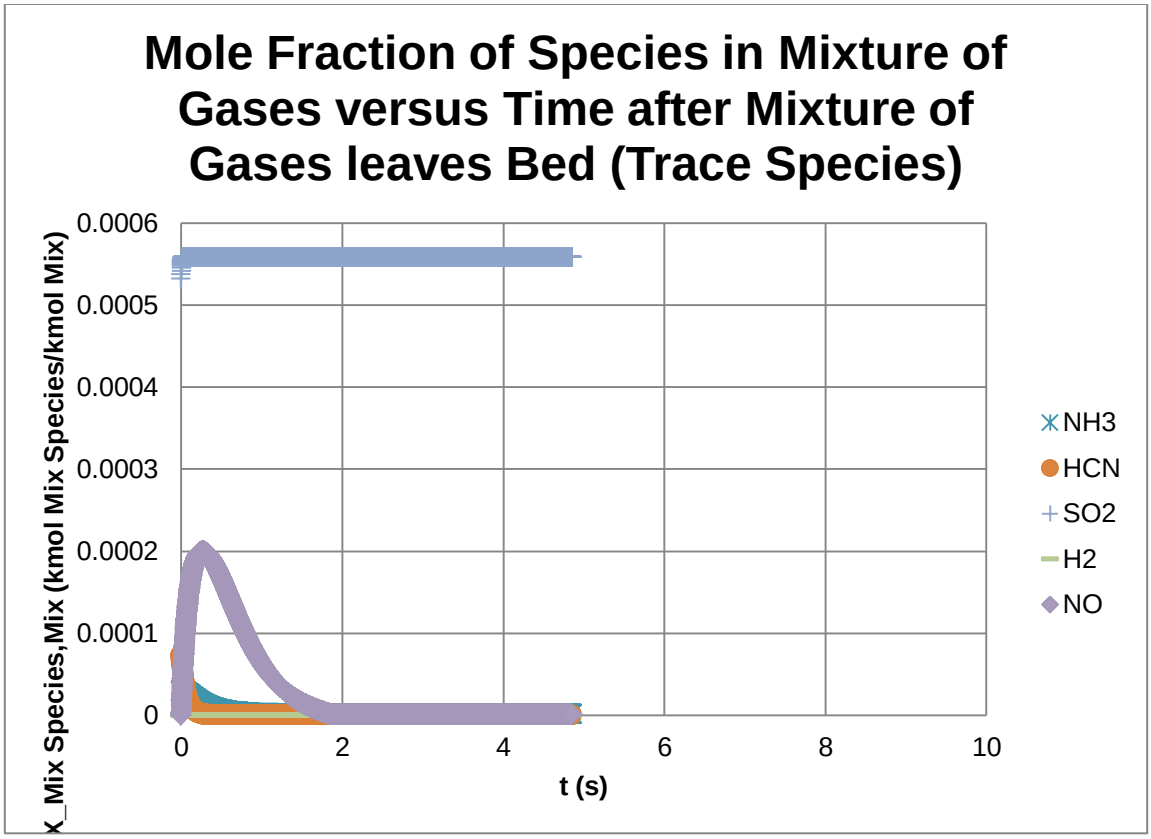

Fig. 109. Mole fraction of trace species versus time for anonymous CFB boiler firing tire fuel with decreased pre-exponential factor for $NH_3\ (g)\ +\ O_2\ (g)\ \rightarrow\ \mathrm{NO\ (g)}\ +\ H_2O\ \mathrm{(g)}\ +\ \frac{1}{2}\ H_2\ (g)$.

The nearly exact trends are evident in the 'Output' tab of the Excel program as shown below in Table 57 where all species only have minor changes. Continuing to decrease the pre-exponential factor continues the trends until the NH_3 is no longer being oxidized at all.

Table 57

Output tab for anonymous CFB boiler firing tire fuel with decreased pre-exponential factor for $NH_3\ (g)\ +\ O_2\ (g)\ \rightarrow\ \mathrm{NO\ (g)}\ +\ H_2O\ \mathrm{(g)}\ +\ \frac{1}{2}\ H_2\ (g)$.

WET BASIS CONCENTRATION OF SPECIES IN MIXTURE OF GASES LEAVING CFB RISER										
	CO	H2O	O2	N2	NH3	HCN	SO2	CO2	H2	NO
ppm (Actual % O2)	9.61613E-21	82230.76307	14293.61366	753433.4207	1.486025254	7.99468E-20	558.248175	149481.9856	8.56315E-06	0.482707171
Mole % (Actual % O2)	9.61613E-25	8.223076307	1.429361366	75.34334207	0.000148603	7.99468E-24	0.055824817	14.94819856	8.56315E-10	4.82707E-05
ppm (Standard % O2)	8.84439E-21	75631.34566	30000	756368.066	1.366764523	7.35307E-20	513.4460524	137485.3315	7.87592E-06	0.443967581
Mole % (Standard % O2)	8.84439E-25	7.563134566	3	F7/10000	0.000136676	7.35307E-24	0.051344605	13.74853315	7.87592E-10	4.43968E-05
g/GJ	3.37964E-21	18588.76083	5739.178914	264893.1682	0.317614689	2.71127E-20	448.7864975	82546.36864	2.16612E-07	0.278672254

DRY BASIS CONCENTRATION OF SPECIES IN MIXTURE OF GASES LEAVING CFB RISER										
	CO	H2O	O2	N2	NH3	HCN	SO2	CO2	H2	NO
ppm (Actual % O2)	1.04777E-20	0	15574.30025	820939.9383	1.619170914	8.71099E-20	608.2663839	162875.3499	9.3304E-06	0.525957018
Mole % (Actual % O2)	1.04777E-24	0	1.557430025	82.09399383	0.000161917	8.71099E-24	0.060826638	16.28753499	9.3304E-10	5.25957E-05
ppm (Standard % O2)	9.70031E-21	0	30000	818644.3042	1.499034155	8.06466E-20	563.135168	150790.5746	8.63811E-06	0.486932867
Mole % (Standard % O2)	9.70031E-25	0	3	F16/10000	0.000149903	8.06466E-24	0.056313517	15.07905746	8.63811E-10	4.86933E-05
g/GJ	3.37964E-21	0	5739.178914	264893.1682	0.317614689	2.71127E-20	448.7864975	82546.36864	2.16612E-07	0.278672254

5.3.21 Pre-exponential factor for $\boldsymbol{NH_3\ (g)\ +\ NO\ (g)\ \rightarrow\ N_2\ (g)\ +\ H_2O\ (g)\ +\ \frac{1}{2}\ H_2\ (g)}$

Returning the first pre-exponential factor for $NH_3\ (g)\ +\ O_2\ (g)\ \rightarrow\ \mathrm{NO\ (g)}\ +\ H_2O\ \mathrm{(g)}\ +\ \frac{1}{2}\ H_2\ (g)$ to its original value, the pre-exponential factor for $NH_3\ (g)\ +\ NO\ (g)\ \rightarrow\ N_2\ (g)\ +\ H_2O\ \mathrm{(g)}\ +\ \frac{1}{2}\ H_2\ (g)$ was then altered. Multiplying the pre-exponential factor by ten, obviously decreases NH_3 and NO concentrations while increasing N_2 and H_2O. However, H_2 actually decreases due to NO and O_2 concentrations being lower so that less H_2 is formed from NH_3 and HCN oxidation as well as HCN reduction reactions. The lower NO causes lower O_2 concentration mostly from more fixed Carbon being oxidized than reduced by NO. The concentration of HCN increases because there is less NO and O_2 for the HCN to react with. The CO level is higher from less O_2 available to destroy CO even though there is less NO reacting with fixed Carbon and HCN to form CO and less O_2 is available to react with fixed Carbon

and HCN to form CO. However, the lesser amount of O_2 overrides the greater amount of CO to end up with less CO_2. These results are evident in the trends below in the graphs of the mole fraction of species in the mixture of gases versus time after the mixture of gases leaves the CFB bed until they reach the CFB riser exit for all species in Fig. 110 and trace species in Fig. 111.

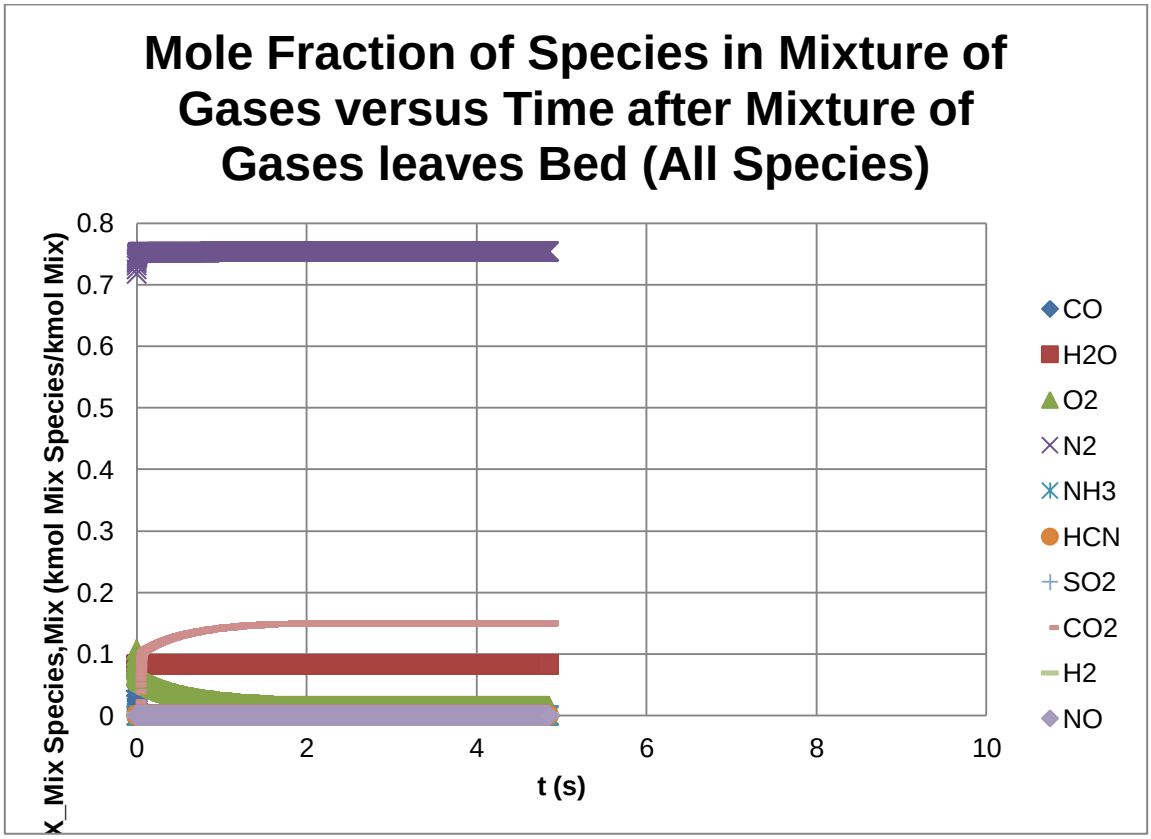

Fig. 110. Mole fraction of all species versus time for anonymous CFB boiler firing tire fuel with increased pre-exponential factor for $NH_3\ (g)\ +\ NO\ (g)\ \rightarrow\ N_2\ (\mathrm{g})\ +\ H_2O\ (\mathrm{g})\ +\ \frac{1}{2}\ H_2\ (g)$.

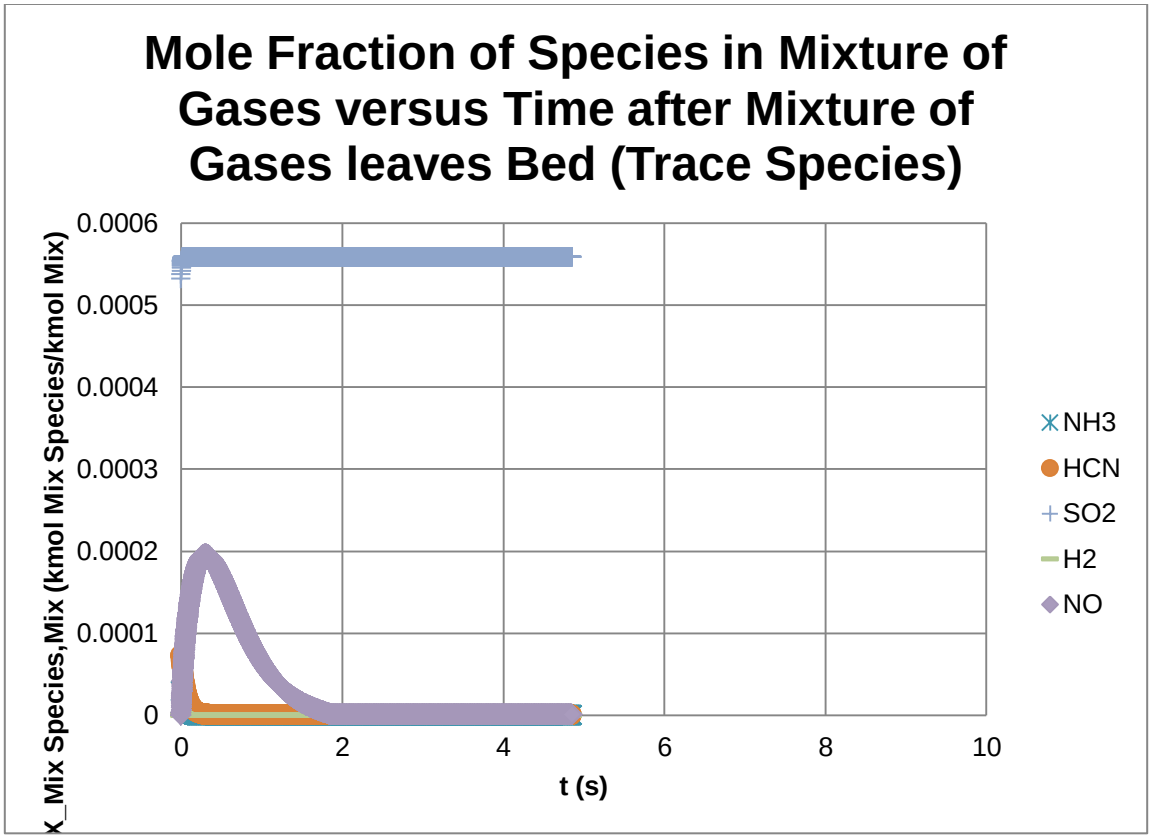

Fig. 111. Mole fraction of trace species versus time for anonymous CFB boiler firing tire fuel with increased pre-exponential factor for $NH_3\ (g)\ +\ NO\ (g)\ \rightarrow\ N_2\ (\mathrm{g})\ +\ H_2O\ (\mathrm{g})\ +\ \frac{1}{2}\ H_2\ (g)$.

The nearly exact trends are evident in the 'Output' tab of the Excel program as shown below in Table 58 where all species only have minor changes. Continuing to increase the pre-exponential factor continues the trends until NH_3 is depleted or NO is being consumed as quickly as it is being produced.

Table 58

Output tab for anonymous CFB boiler firing tire fuel with increased pre-exponential factor for $NH_3\ (g)\ +\ NO\ (g)\ \rightarrow\ N_2\ (\mathrm{g})\ +\ H_2O\ (\mathrm{g})\ +\ \frac{1}{2}\ H_2\ (g)$.

WET BASIS CONCENTRATION OF SPECIES IN MIXTURE OF GASES LEAVING CFB RISER										
	CO	H2O	O2	N2	NH3	HCN	SO2	CO2	H2	NO
ppm (Actual % O2)	9.65084E-21	82232.96157	14292.47622	753433.8663	2.04461E-12	8.02421E-20	558.2479676	149481.9301	1.26598E-15	0.517907834
Mole % (Actual % O2)	9.65084E-25	8.223296157	1.429247622	75.34338663	2.04461E-16	8.02421E-24	0.055824797	14.94819301	1.26598E-19	5.17908E-05
ppm (Standard % O2)	8.87627E-21	75632.92814	30000	756368.6712	1.88051E-12	7.38018E-20	513.4428775	137484.4814	1.16437E-15	0.476340451
Mole % (Standard % O2)	8.87627E-25	7.563292814	3	F7/10000	1.88051E-16	7.38018E-24	0.051344288	13.74844814	1.16437E-19	4.7634E-05
g/GJ	3.39185E-21	18589.26471	5738.724343	264893.4232	4.37004E-13	2.72128E-20	448.7864975	82546.36864	3.20239E-17	0.298994101
DRY BASIS CONCENTRATION OF SPECIES IN MIXTURE OF GASES LEAVING CFB RISER										
	CO	H2O	O2	N2	NH3	HCN	SO2	CO2	H2	NO
ppm (Actual % O2)	1.05156E-20	0	15573.09821	820942.3903	2.22781E-12	8.74319E-20	608.267615	162875.6796	1.37941E-15	0.56431296
Mole % (Actual % O2)	1.05156E-24	0	1.557309821	82.09423903	2.22781E-16	8.74319E-24	0.060826761	16.28756796	1.37941E-19	5.64313E-05
ppm (Standard % O2)	9.73529E-21	0	30000	818646.3972	2.0625E-12	8.09442E-20	563.1328262	150789.9476	1.27706E-15	0.522439702
Mole % (Standard % O2)	9.73529E-25	0	3	F16/10000	2.0625E-16	8.09442E-24	0.056313283	15.07899476	1.27706E-19	5.2244E-05
g/GJ	3.39185E-21	0	5738.724343	264893.4232	4.37004E-13	2.72128E-20	448.7864975	82546.36864	3.20239E-17	0.298994101

Dividing the pre-exponential factor by ten, obviously increases NH_3 and NO concentrations while decreasing N_2 and H_2O. However, H_2 actually increases due to NO and O_2 concentrations being higher so that more H_2 is formed from NH_3 and HCN oxidation as well as HCN reduction reactions. The higher NO causes higher O_2 concentration mostly from less fixed Carbon being oxidized than reduced by NO. The concentration of HCN decreases because there is more NO and O_2 for the HCN to react with. The CO level is lower from more O_2 available to destroy CO even though there is more NO reacting with fixed Carbon and HCN to form CO and more O_2 is available to react with fixed Carbon and HCN to form CO. However, the greater amount of O_2 overrides the lesser amount of CO to end up with more CO_2. These results are evident in the trends below in the graphs of the mole fraction of species in the mixture of gases versus time after the mixture of gases leaves the CFB bed until they reach the CFB riser exit for all species in Fig. 112 and trace species in Fig. 113.

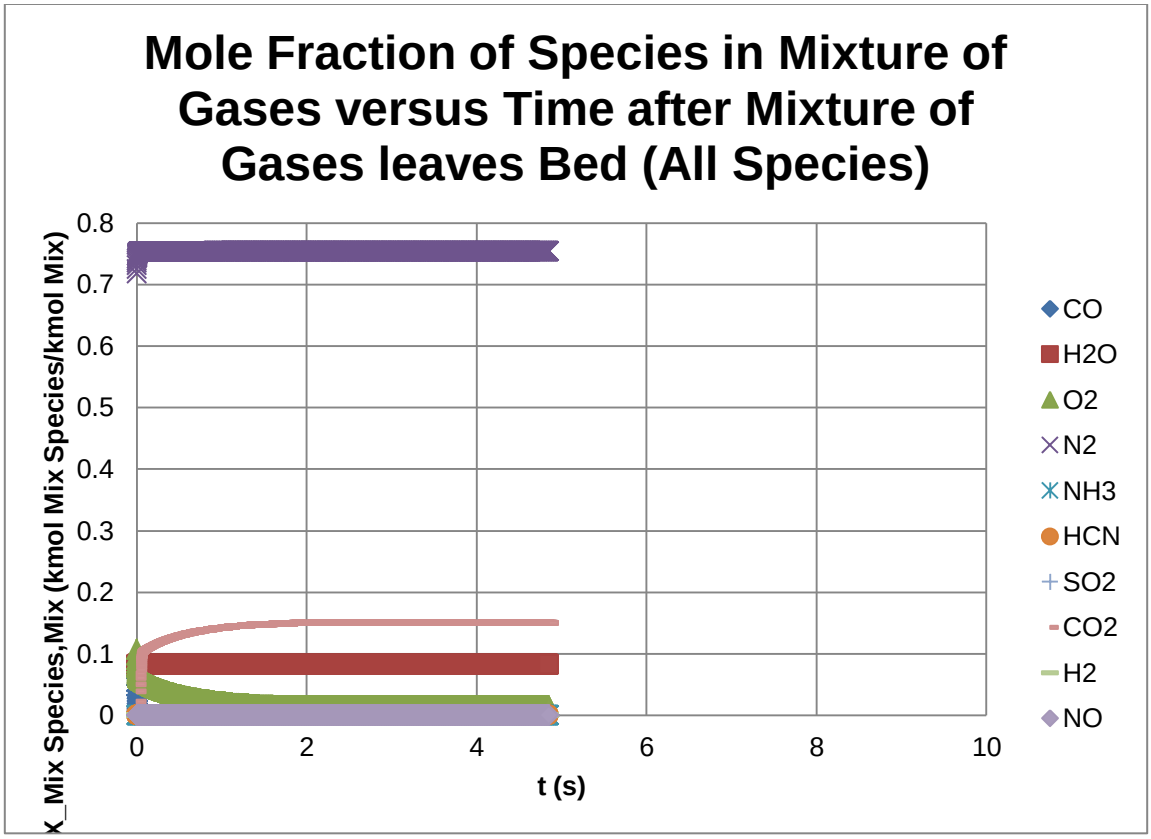

Fig. 112. Mole fraction of all species versus time for anonymous CFB boiler firing tire fuel with decreased pre-exponential factor for $NH_3\ (g)\ +\ NO\ (g)\ \rightarrow\ N_2\ (\mathrm{g})\ +\ H_2O\ (\mathrm{g})\ +\ \frac{1}{2}\ H_2\ (g)$.

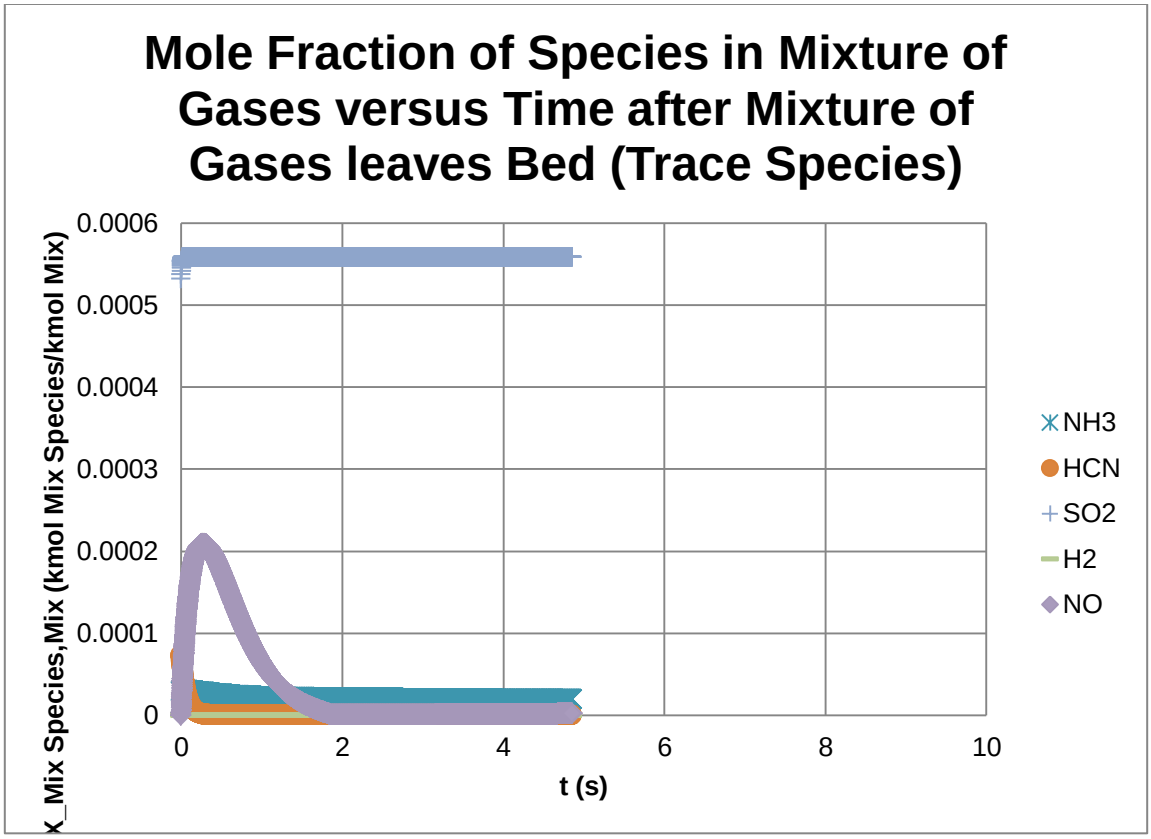

Fig. 113. Mole fraction of trace species versus time for anonymous CFB boiler firing tire fuel with decreased pre-exponential factor for $NH_3\ (g)\ +\ NO\ (g)\ \rightarrow\ N_2\ (\mathrm{g})\ +\ H_2O\ (\mathrm{g})\ +\ \frac{1}{2}\ H_2\ (g)$.

The nearly exact trends are evident in the 'Output' tab of the Excel program as shown below in Table 59 where all species only have minor changes. Continuing to decrease the pre-exponential factor continues the trends until the NH_3 is no longer being reduced by NO at all.

Table 59

Output tab for anonymous CFB boiler firing tire fuel with decreased pre-exponential factor for $NH_3\ (g)\ +\ NO\ (g)\ \rightarrow\ N_2\ (\mathrm{g})\ +\ H_2O\ (\mathrm{g})\ +\ \frac{1}{2}\ H_2\ (g)$.

WET BASIS CONCENTRATION OF SPECIES IN MIXTURE OF GASES LEAVING CFB RISER										
	CO	H2O	O2	N2	NH3	HCN	SO2	CO2	H2	NO
ppm (Actual % O2)	9.30272E-21	82204.34119	14306.24979	753427.0328	19.3451747	7.72685E-20	558.2506673	149482.653	0.000308615	2.12709136
Mole % (Actual % O2)	9.30272E-25	8.220434119	1.430624979	75.34270328	0.001934517	7.72685E-24	0.055825067	14.9482653	3.08615E-08	0.000212709
ppm (Standard % O2)	8.55669E-21	75611.92628	30000	756360.0187	17.79377953	7.10719E-20	513.4814986	137494.823	0.000283866	1.956508291
Mole % (Standard % O2)	8.55669E-25	7.561192628	3	F7/10000	0.001779378	7.10719E-24	0.05134815	13.7494823	2.83866E-08	0.000195651
g/GJ	3.26948E-21	18582.70503	5744.226934	264889.7397	4.134710491	2.62043E-20	448.7864975	82546.36864	7.80663E-06	1.227988172
DRY BASIS CONCENTRATION OF SPECIES IN MIXTURE OF GASES LEAVING CFB RISER										
	CO	H2O	O2	N2	NH3	HCN	SO2	CO2	H2	NO
ppm (Actual % O2)	1.01359E-20	0	15587.61981	820909.3446	21.07786686	8.41892E-20	608.2515885	162871.3882	0.000336257	2.31760887
Mole % (Actual % O2)	1.01359E-24	0	1.558761981	82.09093446	0.002107787	8.41892E-24	0.060825159	16.28713882	3.36257E-08	0.000231761
ppm (Standard % O2)	9.38453E-21	0	30000	818617.941	19.51530057	7.7948E-20	563.1600509	150797.2375	0.000311329	2.145797486
Mole % (Standard % O2)	9.38453E-25	0	3	F16/10000	0.00195153	7.7948E-24	0.056316005	15.07972375	3.11329E-08	0.00021458
g/GJ	3.26948E-21	0	5744.226934	264889.7397	4.134710491	2.62043E-20	448.7864975	82546.36864	7.80663E-06	1.227988172

5.3.22 Pre-exponential factor for $\boldsymbol{HCN\ (g)\ +\ O_2\ (g)\ \rightarrow\ \mathrm{NO}\ (\mathrm{g})\ +\ CO\ (\mathrm{g})\ +\ \frac{1}{2}\ H_2\ (g)}$

Returning the pre-exponential factor for $NH_3\ (g)\ +\ NO\ (g)\ \rightarrow\ N_2\ (\mathrm{g})\ +\ H_2O\ (\mathrm{g})\ +\ \frac{1}{2}\ H_2\ (g)$ to its original value, the pre-exponential factor for $HCN\ (g)\ +\ O_2\ (g)\ \rightarrow\ \mathrm{NO}\ (\mathrm{g})\ +\ CO\ (\mathrm{g})\ +\ \frac{1}{2}\ H_2\ (g)$ was then altered. Multiplying the pre-exponential factor by ten, obviously decreases HCN and O_2 concentrations. However, the NO also decreases because of increased rates of NO destruction on fixed Carbon since less fixed Carbon is oxidized due to lower O_2 concentration, increased initial rates of NO destruction with HCN and NH_3 from the higher NO formation from HCN oxidation, and a decreased rate of NO formation from NH_3 oxidation due to lower O_2 concentration. Also, the CO decreases mostly due to the greatly decreased overall HCN reduction reaction with NO due to both HCN and NO being lower overall even though the HCN oxidation reaction produces more CO and the CO oxidation reaction destroys

less from the decrease in O_2 concentration. The lesser amount of O_2 and CO end up with less CO_2. The H_2 also decreases mostly due to the greatly decreased overall HCN reduction reaction with NO as well as the decreased NH_3 oxidation reaction even though the HCN oxidation reaction and NH_3 reduction reaction with NO both create more and the H_2 oxidation reaction destroys less due to lower O_2 concentration. On the other hand, there is a higher N_2 concentration from increased fixed Carbon and NH_3 reduction reactions with NO even though the HCN reduction reaction with NO decreases. The concentration of NH_3 decreases because the increased initial rate of reduction with NO increases more than the decreased rate of oxidation. However, the H_2O level is higher because of the increased HCN oxidation and NH_3 reduction reaction with NO even though the HCN reduction reaction with NO and the NH_3 oxidation were decreased along with a decrease in H_2 oxidation due to lower O_2 concentration. These results are evident in the trends below in the graphs of the mole fraction of species in the mixture of gases versus time after the mixture of gases leaves the CFB bed until they reach the CFB riser exit for all species in Fig. 114 and trace species in Fig. 115.

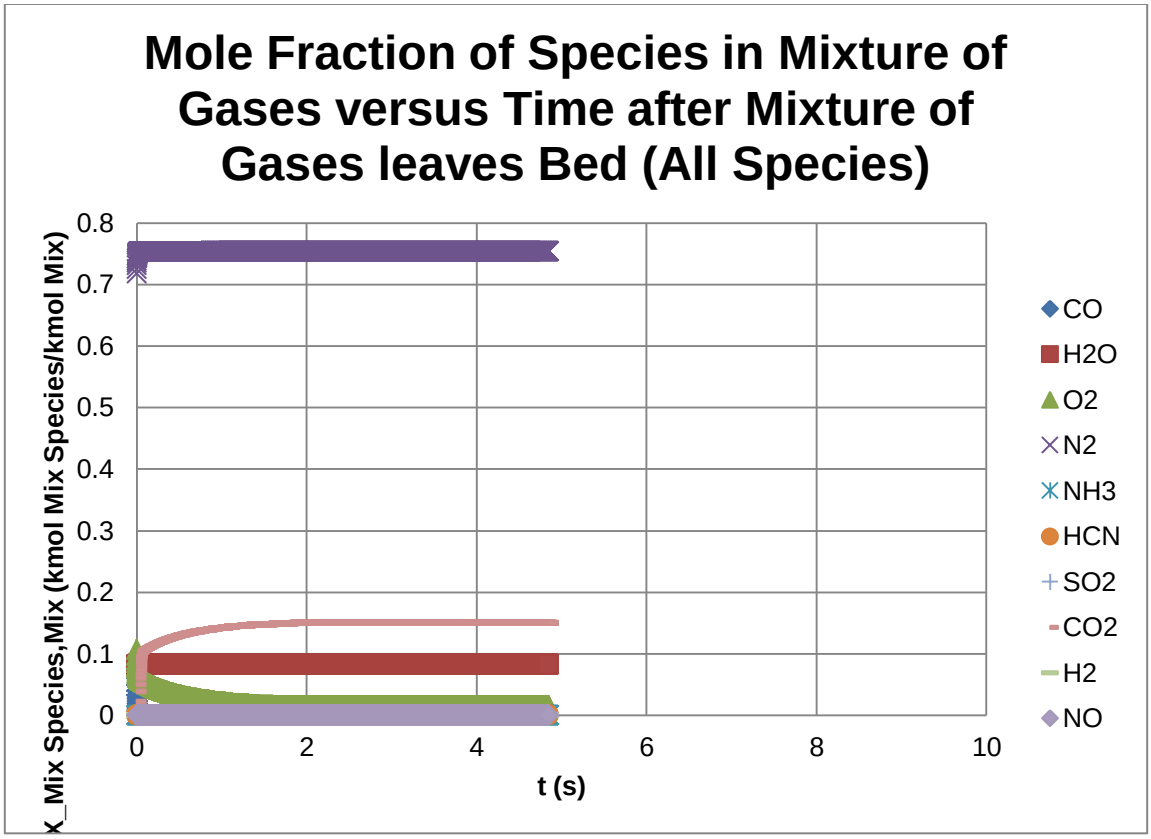

Fig. 114. Mole fraction of all species versus time for anonymous CFB boiler firing tire fuel with increased pre-exponential factor for $HCN\ (g)\ +\ O_2\ (g)\ \rightarrow\ \mathrm{NO\ (g)}\ +\ CO\ \mathrm{(g)}\ +\ \frac{1}{2}\ H_2\ (g)$.

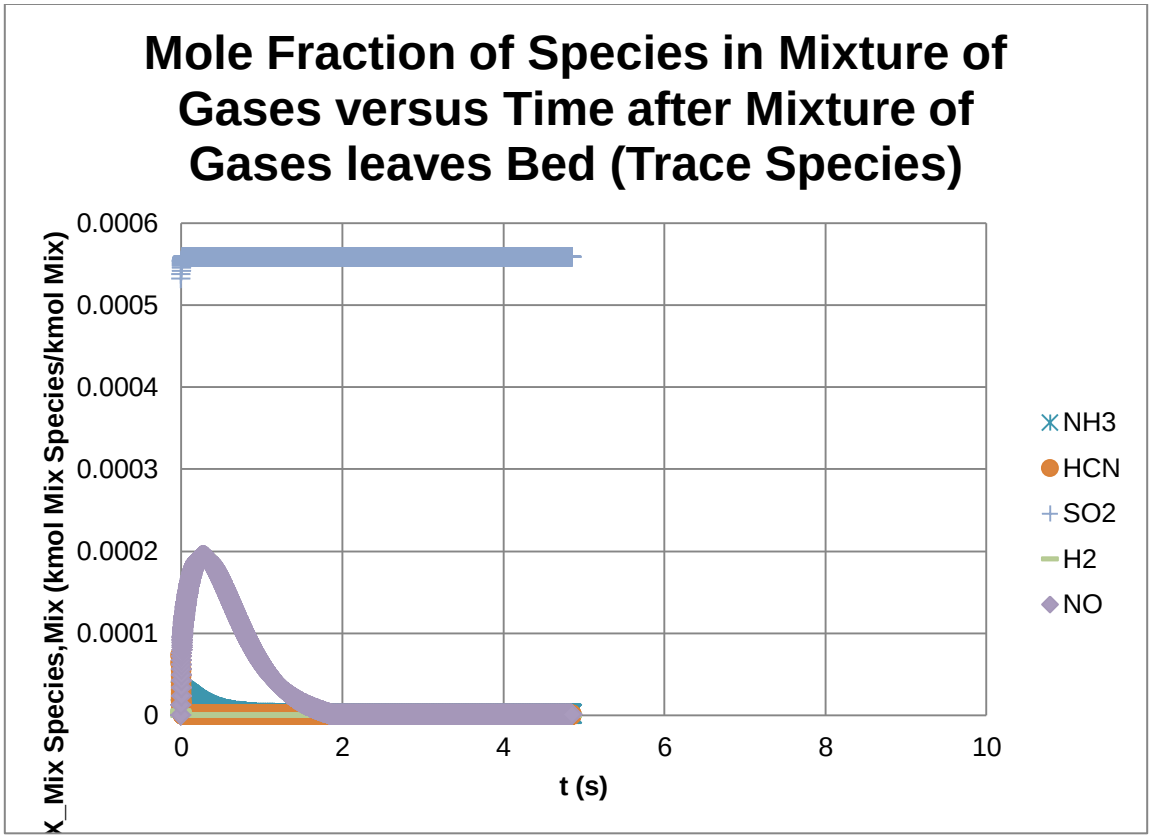

Fig. 115. Mole fraction of trace species versus time for anonymous CFB boiler firing tire fuel with increased pre-exponential factor for $HCN\ (g)\ +\ O_2\ (g)\ \rightarrow\ \mathrm{NO\ (g)}\ +\ CO\ \mathrm{(g)}\ +\ \frac{1}{2}\ H_2\ (g)$.

The nearly exact trends are evident in the 'Output' tab of the Excel program as shown below in Table 60 where all species only have minor changes. Continuing to increase the pre-exponential factor continues the trends only until the HCN or O_2 is depleted.

Table 60

Output tab for anonymous CFB boiler firing tire fuel with increased pre-exponential factor for $HCN\ (g)\ +\ O_2\ (g)\ \rightarrow\ \mathrm{NO\ (g)}\ +\ CO\ \mathrm{(g)}\ +\ \frac{1}{2}\ H_2\ (g)$.

WET BASIS CONCENTRATION OF SPECIES IN MIXTURE OF GASES LEAVING CFB RISER										
	CO	H2O	O2	N2	NH3	HCN	SO2	CO2	H2	NO
ppm (Actual % O2)	1.5863E-106	82231.06035	14293.40924	753433.4304	1.285075325	6.1351E-219	558.2481469	149481.9781	2.48636E-05	0.588701504
Mole % (Actual % O2)	1.5863E-110	8.223106035	1.429340924	75.34334304	0.000128508	6.1351E-223	0.055824815	14.94819781	2.48636E-09	5.88702E-05
ppm (Standard % O2)	1.459E-106	75631.54008	30000	756368.11	1.181940565	5.6427E-219	513.4454903	137485.181	2.28681E-05	0.541454788
Mole % (Standard % O2)	1.459E-110	7.563154008	3	F7/10000	0.000118194	5.6427E-223	0.051344549	13.7485181	2.28681E-09	5.41455E-05
g/GJ	5.5751E-107	18588.82896	5739.097124	264893.1849	0.274664794	2.0806E-219	448.7864975	82546.36864	6.28943E-07	0.339863986

DRY BASIS CONCENTRATION OF SPECIES IN MIXTURE OF GASES LEAVING CFB RISER										
	CO	H2O	O2	N2	NH3	HCN	SO2	CO2	H2	NO
ppm (Actual % O2)	1.7284E-106	0	15574.08256	820940.2147	1.400216622	6.6848E-219	608.2665503	162875.3945	2.70913E-05	0.641448493
Mole % (Actual % O2)	1.7284E-110	0	1.557408256	82.09402147	0.000140022	6.6848E-223	0.060826655	16.28753945	2.70913E-09	6.41448E-05
ppm (Standard % O2)	1.6002E-106	0	30000	818644.528	1.296324046	6.1888E-219	563.1346916	150790.4471	2.50812E-05	0.593854617
Mole % (Standard % O2)	1.6002E-110	0	3	F16/10000	0.000129632	6.1888E-223	0.056313469	15.07904471	2.50812E-09	5.93855E-05
g/GJ	5.5751E-107	0	5739.097124	264893.1849	0.274664794	2.0806E-219	448.7864975	82546.36864	6.28943E-07	0.339863986

Dividing the pre-exponential factor by ten, obviously increases the HCN concentration. However, the O_2 concentration decreases mostly from decreased rates of NO destruction on fixed Carbon since more fixed Carbon is oxidized due to higher initial O_2 concentration. The NO increases because of decreased rates of NO destruction on fixed Carbon, decreased initial rates of NO destruction with HCN and NH_3 from the lower NO formation from HCN oxidation, and an increased rate of NO formation from NH_3 oxidation due to higher initial O_2 concentration. Also, the CO increases mostly due to the greatly increased overall HCN reduction reaction with NO due to both HCN and NO being higher overall as well as the CO oxidation reaction destroys less from the decrease in overall O_2 concentration even though the HCN oxidation reaction produces less CO. The lesser amount of overall O_2 overrides the greater amount of CO to end up with less CO_2. The H_2 also increases mostly due to the greatly increased overall HCN

reduction reaction with NO, the increased NH_3 oxidation reaction, the increased NH_3 reduction reaction with NO, and the H_2 oxidation reaction destroys less due to lower overall O_2 concentration even though the HCN oxidation reaction creates less. On the other hand, there is a lower N_2 concentration from decreased fixed Carbon reduction reaction with NO even though the HCN and NH_3 reduction reactions with NO increase. The concentration of NH_3 decreases because the increased initial rate of oxidation as well as increased rate of reduction with NO. However, the H_2O level is lower because of the decreased HCN oxidation along with a decrease in H_2 oxidation due to lower overall O_2 concentration even though the HCN and NH_3 reduction reactions with NO and the NH_3 oxidation were increased. These results are evident in the trends below in the graphs of the mole fraction of species in the mixture of gases versus time after the mixture of gases leaves the CFB bed until they reach the CFB riser exit for all species in Fig. 116 and trace species in Fig. 117.

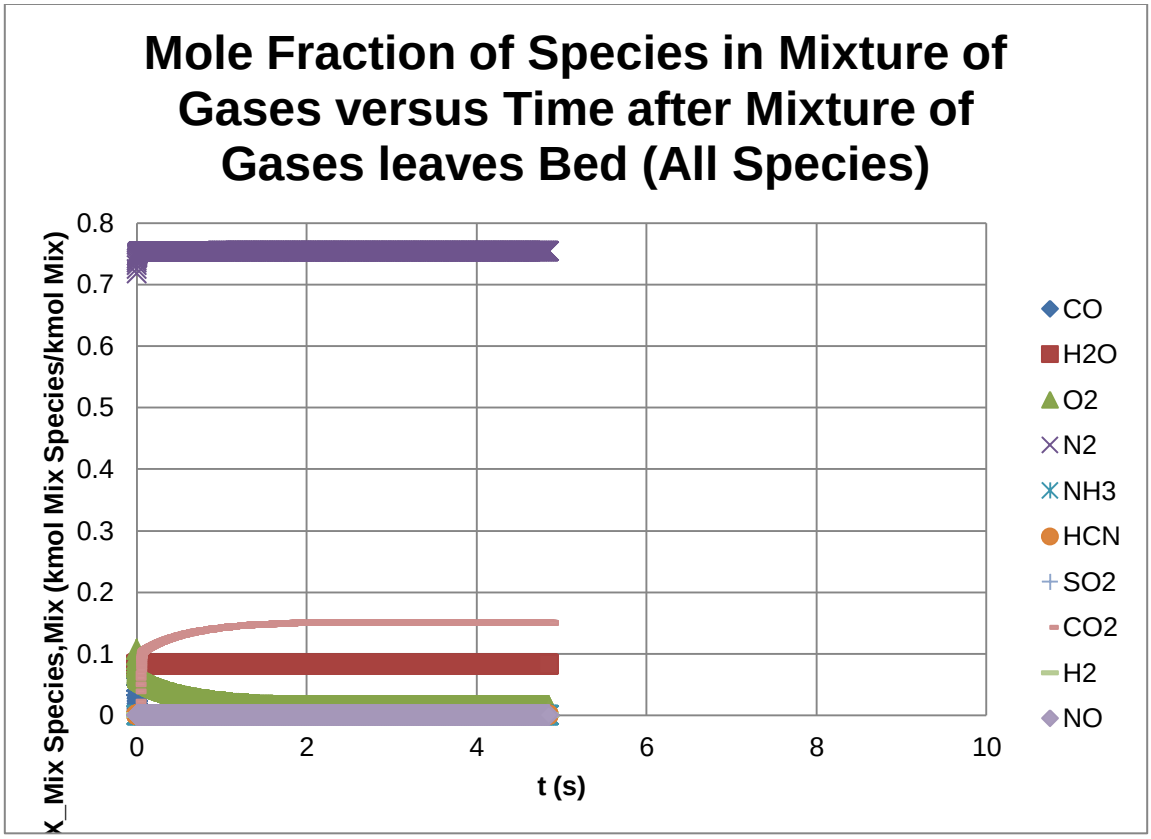

Fig. 116. Mole fraction of all species versus time for anonymous CFB boiler firing tire fuel with decreased pre-exponential factor for $HCN\ (g)\ +\ O_2\ (g)\ \rightarrow\ \mathrm{NO\ (g)}\ +\ CO\ \mathrm{(g)}\ +\ \frac{1}{2}\ H_2\ (g)$.

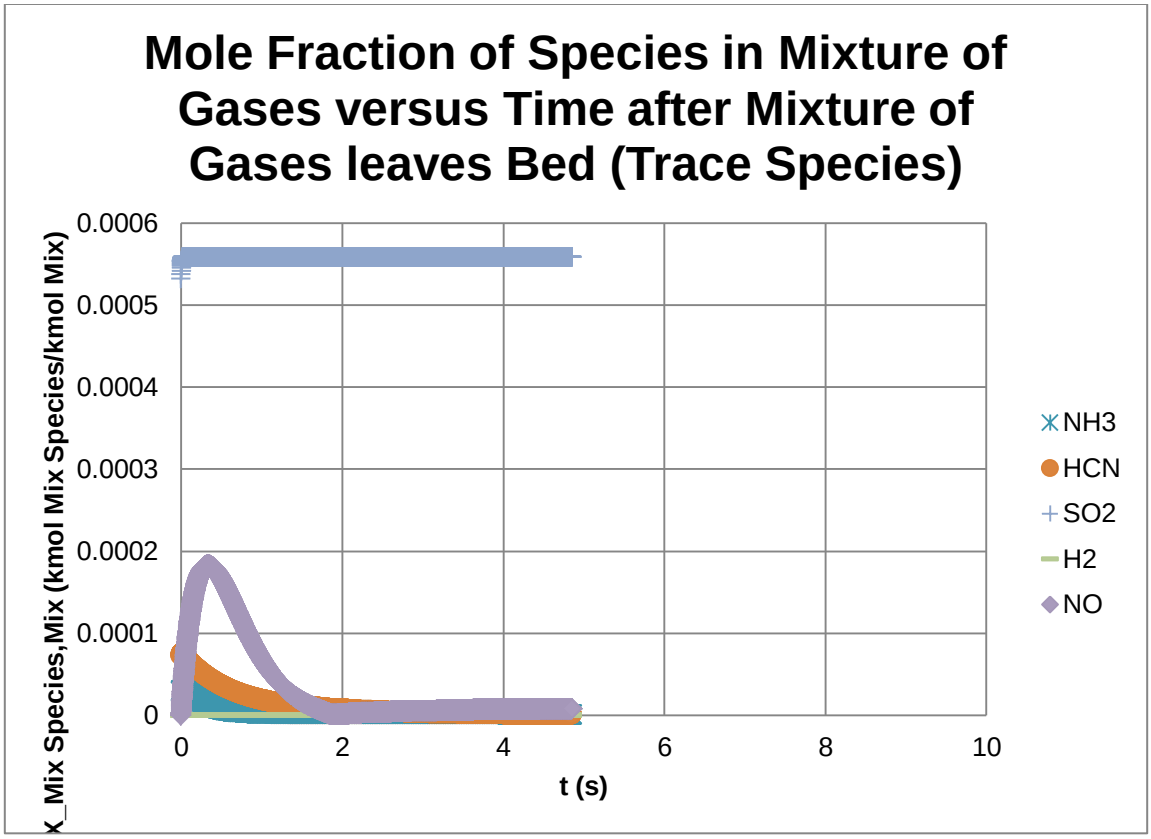

Fig. 117. Mole fraction of trace species versus time for anonymous CFB boiler firing tire fuel with decreased pre-exponential factor for $HCN\ (g)\ +\ O_2\ (g)\ \rightarrow\ \mathrm{NO}\ (\mathrm{g})\ +\ CO\ (\mathrm{g})\ +\ \frac{1}{2}\ H_2\ (g)$.

The nearly exact trends are evident in the 'Output' tab of the Excel program as shown below in Table 61 where all species only have minor changes. Continuing to decrease the pre-exponential factor begins to reverse many of the trends as more O_2 becomes available until the HCN is no longer being oxidized at all.

Table 61

Output tab for anonymous CFB boiler firing tire fuel with decreased pre-exponential factor for $HCN\ (g)\ +\ O_2\ (g)\ \rightarrow\ \mathrm{NO\ (g)}\ +\ CO\ \mathrm{(g)}\ +\ \frac{1}{2}\ H_2\ (g)$.

WET BASIS CONCENTRATION OF SPECIES IN MIXTURE OF GASES LEAVING CFB RISER										
	CO	H2O	O2	N2	NH3	HCN	SO2	CO2	H2	NO
ppm (Actual % O2)	0.006754207	82231.00539	14290.49411	753429.4991	1.102816991	0.622369536	558.2480327	149481.3184	0.000349692	7.702725426
Mole % (Actual % O2)	6.75421E-07	8.223100539	1.429049411	75.34294991	0.000110282	6.2237E-05	0.055824803	14.94813184	3.49692E-08	0.000770273
ppm (Standard % O2)	0.00621205	75630.36299	30000	756364.9952	1.014294413	0.572412239	513.4377373	137482.5264	0.000321623	7.084431441
Mole % (Standard % O2)	6.21205E-07	7.563036299	3	F7/10000	0.000101429	5.72412E-05	0.051343774	13.74825264	3.21623E-08	0.000708443
g/GJ	0.002373816	18588.89774	5737.951704	264892.9598	0.235710949	0.21106776	448.788366	82546.36491	8.84578E-06	4.446889269

DRY BASIS CONCENTRATION OF SPECIES IN MIXTURE OF GASES LEAVING CFB RISER										
	CO	H2O	O2	N2	NH3	HCN	SO2	CO2	H2	NO
ppm (Actual % O2)	0.007359376	0	15570.90531	820935.882	1.201628076	0.678133103	608.2663894	162874.6659	0.000381024	8.392880422
Mole % (Actual % O2)	7.35938E-07	0	1.557090531	82.0935882	0.000120163	6.78133E-05	0.060826639	16.28746659	3.81024E-08	0.000839288
ppm (Standard % O2)	0.006813217	0	30000	818640.0488	1.112452095	0.627807061	563.1253402	150787.3084	0.000352747	7.770022682
Mole % (Standard % O2)	6.81322E-07	0	3	F16/10000	0.000111245	6.27807E-05	0.056312534	15.07873084	3.52747E-08	0.000777002
g/GJ	0.002373816	0	5737.951704	264892.9598	0.235710949	0.21106776	448.788366	82546.36491	8.84578E-06	4.446889269

5.3.23 Pre-exponential factor for $\boldsymbol{HCN\ (g)\ +\ NO\ (g)\ \rightarrow\ N_2\ (g)\ +\ CO\ (g)\ +\ \frac{1}{2}\ H_2\ (g)}$

Returning the pre-exponential factor for $HCN\ (g)\ +\ O_2\ (g)\ \rightarrow\ \mathrm{NO\ (g)}\ +\ CO\ \mathrm{(g)}\ +\ \frac{1}{2}\ H_2\ (g)$ to its original value, the pre-exponential factor for $HCN\ (g)\ +\ NO\ (g)\ \rightarrow\ N_2\ \mathrm{(g)}\ +\ CO\ \mathrm{(g)}\ +\ \frac{1}{2}\ H_2\ (g)$ was then altered. Multiplying the pre-exponential factor by ten, obviously decreases HCN and NO concentrations. However, the N_2 also decreases from decreased fixed Carbon and NH_3 reduction reactions with NO due to the lower NO concentration even though the HCN reduction reaction with NO increases. Also, the CO decreases mostly due to the HCN oxidation reaction producing less CO due to lower HCN and the CO oxidation reaction destroying more CO from the increase in O_2 concentration even though the HCN reduction reaction with NO increases. The greater amount of O_2 which is mostly from the decrease in HCN

oxidation due to lower HCN cancels out the lesser amount of CO to end up with basically the same amount of CO_2. The H_2 increases mostly due to the greatly increased overall HCN reduction reaction with NO as well as the increased NH_3 oxidation reaction and the H_2 oxidation reaction destroying less even though the HCN oxidation reaction and NH_3 reduction reaction with NO both create less. The concentration of NH_3 increases because the increased rate of oxidation increases less than the decreased rate of reduction with NO. However, the H_2O level is lower because of the decreased HCN oxidation and NH_3 reduction reaction with NO along with a decrease in H_2 oxidation even though the HCN reduction reaction with NO and the NH_3 oxidation were increased. These results are evident in the trends below in the graphs of the mole fraction of species in the mixture of gases versus time after the mixture of gases leaves the CFB bed until they reach the CFB riser exit for all species in Fig. 118 and trace species in Fig. 119.

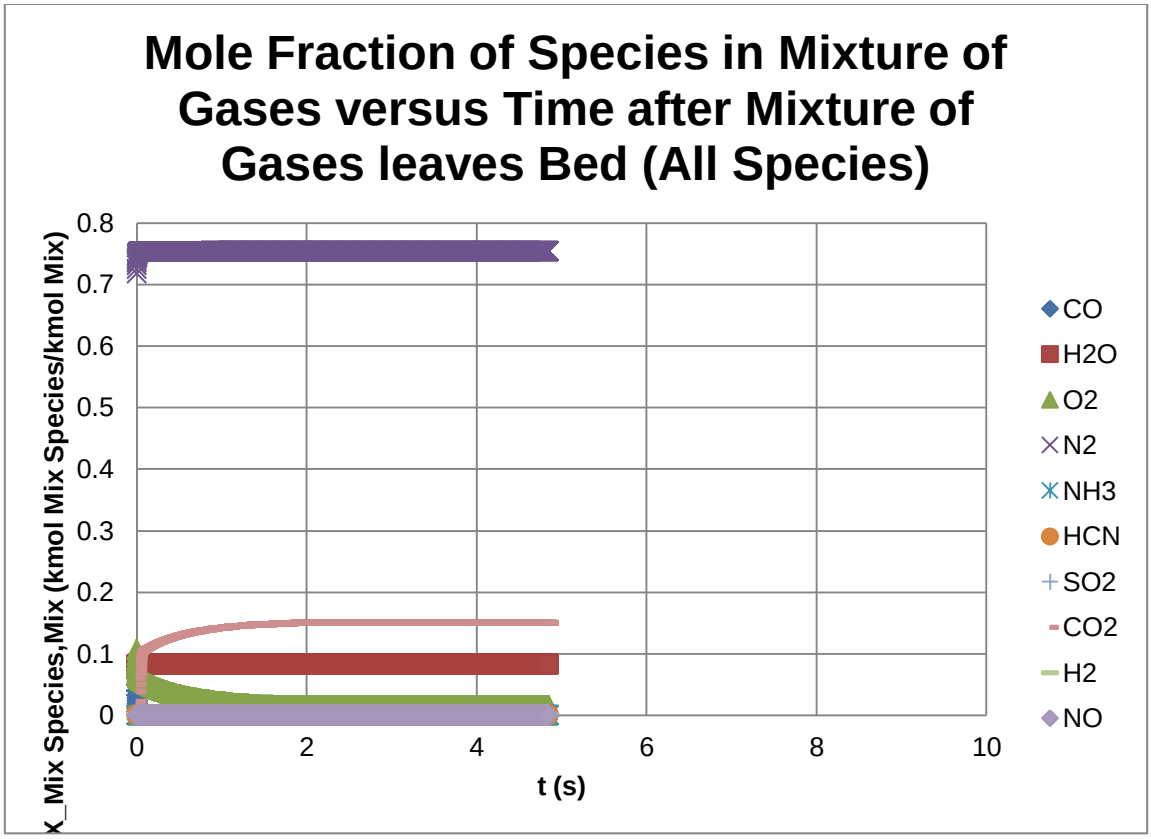

Fig. 118. Mole fraction of all species versus time for anonymous CFB boiler firing tire fuel with increased pre-exponential factor for $HCN\ (g)\ +\ NO\ (g)\ \rightarrow\ N_2\ (\mathrm{g})\ +\ CO\ (\mathrm{g})\ +\ \frac{1}{2}\ H_2\ (g)$.

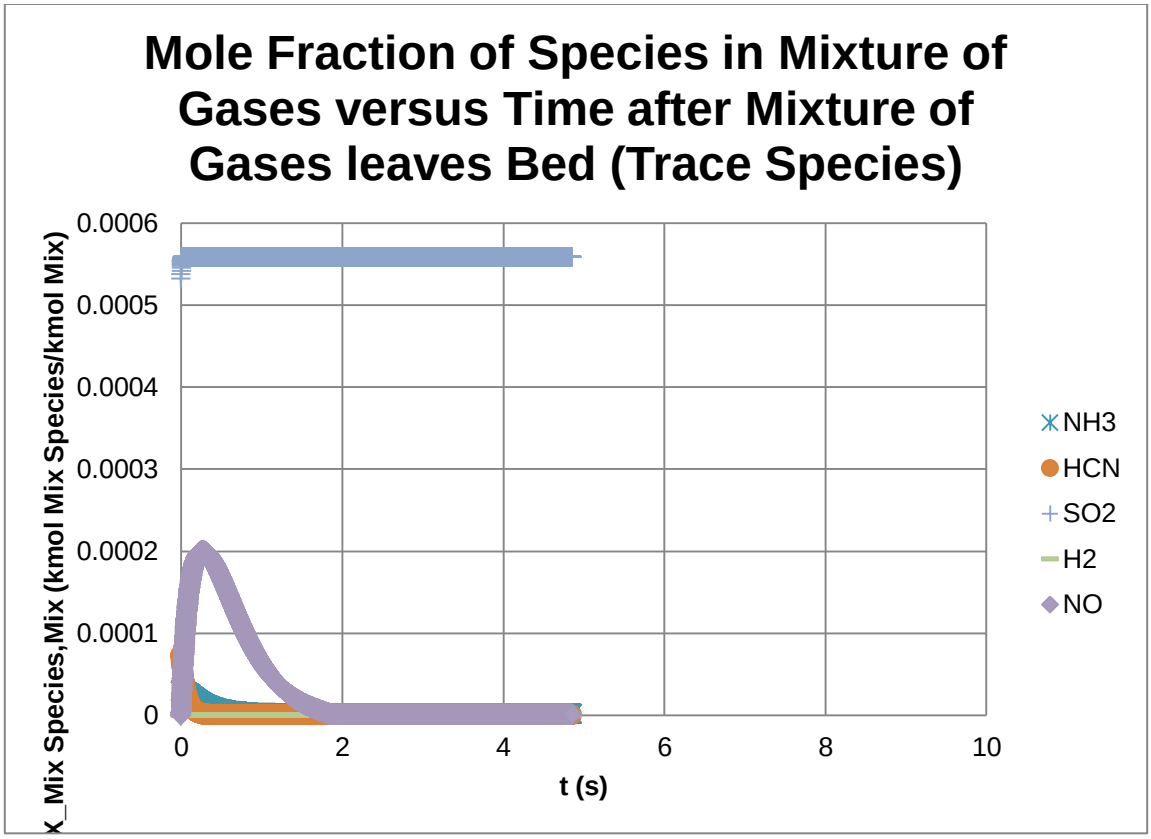

Fig. 119. Mole fraction of trace species versus time for anonymous CFB boiler firing tire fuel with increased pre-exponential factor for $HCN\ (g)\ +\ NO\ (g)\ \rightarrow\ N_2\ (\mathrm{g})\ +\ CO\ (\mathrm{g})\ +\ \frac{1}{2}\ H_2\ (g)$.

The nearly exact trends are evident in the 'Output' tab of the Excel program as shown below in Table 62 where all species only have minor changes. Continuing to increase the pre-exponential factor continues the trends except NO and CO_2 begin to increase mostly due to the continually increasing O_2 available until HCN is depleted or NO is being consumed as quickly as it is being produced.

Table 62

Output tab for anonymous CFB boiler firing tire fuel with increased pre-exponential factor for $HCN\ (g)\ +\ NO\ (g)\ \rightarrow\ N_2\ (\mathrm{g})\ +\ CO\ (\mathrm{g})\ +\ \frac{1}{2}\ H_2\ (g)$.

WET BASIS CONCENTRATION OF SPECIES IN MIXTURE OF GASES LEAVING CFB RISER										
	CO	H2O	O2	N2	NH3	HCN	SO2	CO2	H2	NO
ppm (Actual % O2)	9.48067E-21	82231.03659	14293.42089	753433.4249	1.301132867	7.88211E-20	558.2481492	149481.9787	2.51847E-05	0.589595176
Mole % (Actual % O2)	9.48067E-25	8.223103659	1.429342089	75.34334249	0.000130113	7.88211E-24	0.055824815	14.94819787	2.51847E-09	5.89595E-05
ppm (Standard % O2)	8.71979E-21	75631.52273	30000	756368.103	1.196709467	7.24952E-20	513.4455229	137485.1898	2.31635E-05	0.542276771
Mole % (Standard % O2)	8.71979E-25	7.563152273	3	F7/10000	0.000119671	7.24952E-24	0.051344552	13.74851898	2.31635E-09	5.42277E-05
g/GJ	3.33204E-21	18588.82352	5739.10178	264893.1819	0.278096841	2.67309E-20	448.7864975	82546.36864	6.37068E-07	0.340379911

DRY BASIS CONCENTRATION OF SPECIES IN MIXTURE OF GASES LEAVING CFB RISER										
	CO	H2O	O2	N2	NH3	HCN	SO2	CO2	H2	NO
ppm (Actual % O2)	1.03301E-20	0	15574.09486	820940.1875	1.417712865	8.58834E-20	608.266537	162875.3909	2.74413E-05	0.642422221
Mole % (Actual % O2)	1.03301E-24	0	1.557409486	82.09401875	0.000141771	8.58834E-24	0.060826654	16.28753909	2.74413E-09	6.42422E-05
ppm (Standard % O2)	9.56366E-21	0	30000	818644.5047	1.312522195	7.9511E-20	563.1347149	150790.4533	2.54052E-05	0.594756135
Mole % (Standard % O2)	9.56366E-25	0	3	F16/10000	0.000131252	7.9511E-24	0.056313471	15.07904533	2.54052E-09	5.94756E-05
g/GJ	3.33204E-21	0	5739.10178	264893.1819	0.278096841	2.67309E-20	448.7864975	82546.36864	6.37068E-07	0.340379911

Dividing the pre-exponential factor by ten, obviously increases HCN and NO concentrations. However, the N_2 is about the same from increased fixed Carbon and NH_3 reduction reactions with NO due to the higher NO concentration balancing out the decreased HCN reduction reaction with NO. Also, the CO increases mostly due to the HCN oxidation reaction producing more CO due to higher HCN and the CO oxidation reaction destroying less CO from the decrease in O_2 concentration even though the HCN reduction reaction with NO decreases. The lesser amount of O_2 which is mostly from the increase in HCN oxidation due to higher HCN cancels out the greater amount of CO to end up with basically the same amount of CO_2. The H_2 decreases mostly due to the greatly decreased overall HCN reduction reaction with NO as well as the decreased NH_3 oxidation reaction and the H_2 oxidation reaction destroying more even though the HCN oxidation reaction and NH_3 reduction reaction with NO both create more. The concentration of NH_3 decreases because the decreased rate of oxidation decreases less than the increased rate of reduction with NO. However, the H_2O level is higher because of the increased HCN oxidation and NH_3 reduction reaction with NO along with an increase in H_2 oxidation even though the HCN reduction reaction with NO and the NH_3 oxidation were decreased. These results are evident in the trends below in the graphs of the mole fraction of species in the mixture of gases versus time after the mixture of gases leaves the CFB bed until they reach the CFB riser exit for all species in Fig. 120 and trace species in Fig. 121.

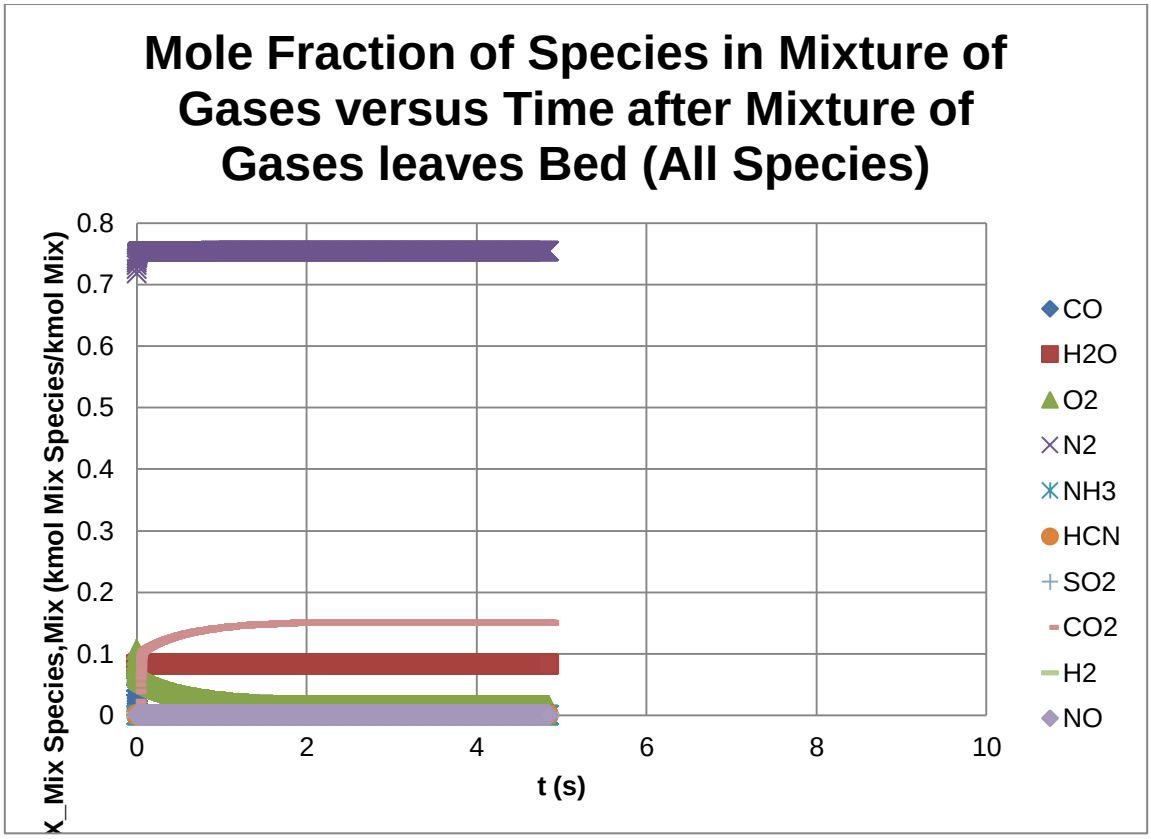

Fig. 120. Mole fraction of all species versus time for anonymous CFB boiler firing tire fuel with decreased pre-exponential factor for $HCN\ (g)\ +\ NO\ (g)\ \rightarrow\ N_2\ (\mathrm{g})\ +\ CO\ (\mathrm{g})\ +\ \frac{1}{2}\ H_2\ (g)$.

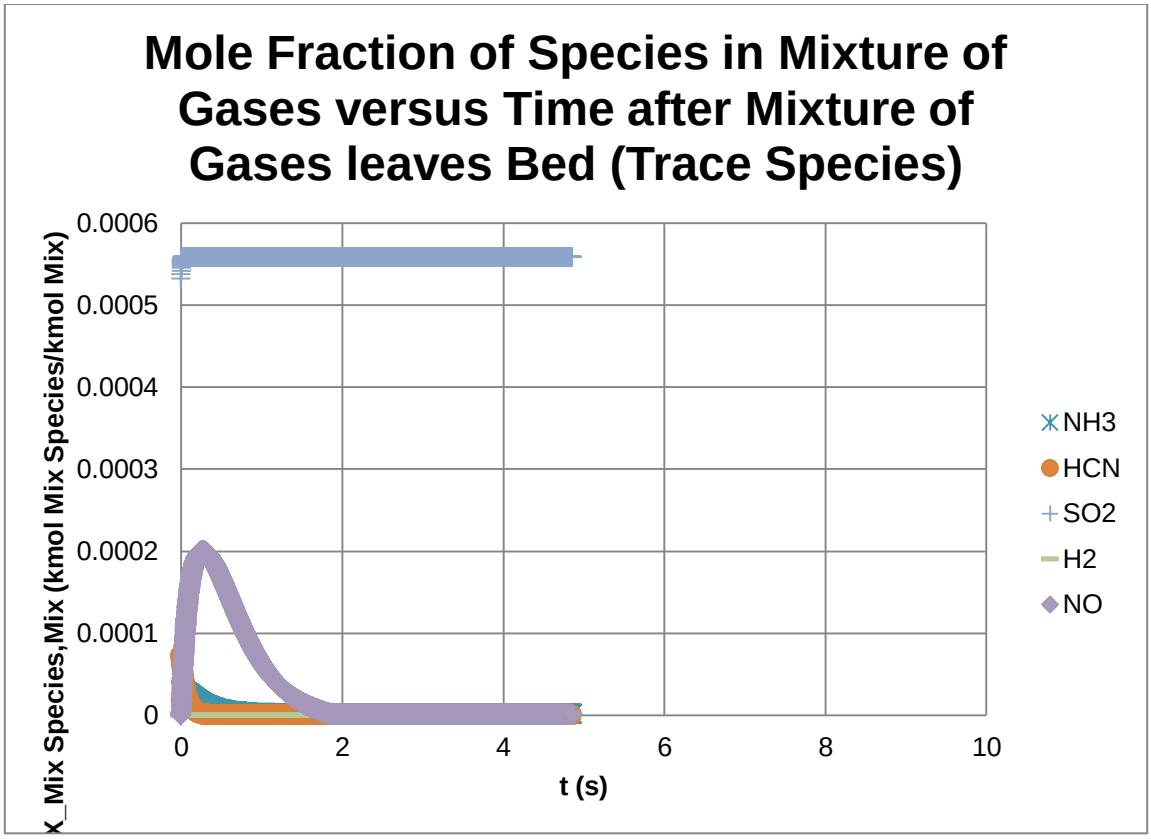

Fig. 121. Mole fraction of trace species versus time for anonymous CFB boiler firing tire fuel with decreased pre-exponential factor for $HCN\ (g)\ +\ NO\ (g)\ \rightarrow\ N_2\ (\mathrm{g})\ +\ CO\ (\mathrm{g})\ +\ \frac{1}{2}\ H_2\ (g)$.

The nearly exact trends are evident in the 'Output' tab of the Excel program as shown below in Table 63 where all species only have minor changes. Continuing to decrease the pre-exponential factor continues the trends until the HCN is no longer being reduced by NO at all.

Table 63

Output tab for anonymous CFB boiler firing tire fuel with decreased pre-exponential factor for $HCN\ (g)\ +\ NO\ (g)\ \rightarrow\ N_2\ (\mathrm{g})\ +\ CO\ (\mathrm{g})\ +\ \frac{1}{2}\ H_2\ (g)$.

WET BASIS CONCENTRATION OF SPECIES IN MIXTURE OF GASES LEAVING CFB RISER										
	CO	H2O	O2	N2	NH3	HCN	SO2	CO2	H2	NO
ppm (Actual % O2)	9.63392E-21	82231.03751	14293.42042	753433.4251	1.300515578	8.00958E-20	558.2481491	149481.9787	2.5173E-05	0.589613078
Mole % (Actual % O2)	9.63392E-25	8.223103751	1.429342042	75.34334251	0.000130052	8.00958E-24	0.055824815	14.94819787	2.5173E-09	5.89613E-05
ppm (Standard % O2)	8.86074E-21	75631.52339	30000	756368.1032	1.196141716	7.36676E-20	513.4455216	137485.1894	2.31527E-05	0.542293234
Mole % (Standard % O2)	8.86074E-25	7.563152339	3	F7/10000	0.000119614	7.36676E-24	0.051344552	13.74851894	2.31527E-09	5.42293E-05
g/GJ	3.3859E-21	18588.82373	5739.10159	264893.182	0.277964906	2.71632E-20	448.7864975	82546.36864	6.36771E-07	0.340390246
DRY BASIS CONCENTRATION OF SPECIES IN MIXTURE OF GASES LEAVING CFB RISER										
	CO	H2O	O2	N2	NH3	HCN	SO2	CO2	H2	NO
ppm (Actual % O2)	1.04971E-20	0	15574.09436	820940.1885	1.417040269	8.72723E-20	608.2665375	162875.3911	2.74285E-05	0.642441728
Mole % (Actual % O2)	1.04971E-24	0	1.557409436	82.09401885	0.000141704	8.72723E-24	0.060826654	16.28753911	2.74285E-09	6.42442E-05
ppm (Standard % O2)	9.71825E-21	0	30000	818644.5056	1.3118995	8.07969E-20	563.1347139	150790.453	2.53933E-05	0.594774192
Mole % (Standard % O2)	9.71825E-25	0	3	F16/10000	0.00013119	8.07969E-24	0.056313471	15.0790453	2.53933E-09	5.94774E-05
g/GJ	3.3859E-21	0	5739.10159	264893.182	0.277964906	2.71632E-20	448.7864975	82546.36864	6.36771E-07	0.340390246

5.3.24 Pre-exponential factor for $2\ H_2\ (g)\ +\ O_2\ (g) \rightarrow\ 2\ H_2O\ (g)$

Returning the pre-exponential factor for $HCN\ (g)\ +\ NO\ (g)\ \rightarrow\ N_2\ (\mathrm{g})\ +\ CO\ (\mathrm{g})\ +\ \frac{1}{2}\ H_2\ (g)$ to its original value, the pre-exponential factor for $2\ H_2\ (g)\ +\ O_2\ (g) \rightarrow\ 2\ H_2O\ (g)$ was then altered. Increasing the pre-exponential factor doesn't have any effect on the concentrations of any species because the H_2 is already oxidized as quickly as it is created. Also, it takes dividing the pre-exponential factor by 100,000,000 before any noticeable concentration trends take place. Obviously, the H_2 and O_2 increase while the H_2O decreases. The CO increases and the CO_2decreases mostly due to the CO oxidation reaction being inhibited by the decrease in H_2O concentration. The NO increases mainly due to less NO being reduced on the fixed Carbon surface since more fixed Carbon is oxidized with the greater O_2 concentration. Similarly, the N_2 decreases mainly due to less NO being reduced on the fixed Carbon. The concentration of NH_3 decreases while the HCN increases because the NH_3 is more

sensitive to the increased O_2 and NO concentrations. These results are evident in the trends below in the graphs of the mole fraction of species in the mixture of gases versus time after the mixture of gases leaves the CFB bed until they reach the CFB riser exit for all species in Fig. 122 and trace species in Fig. 123.

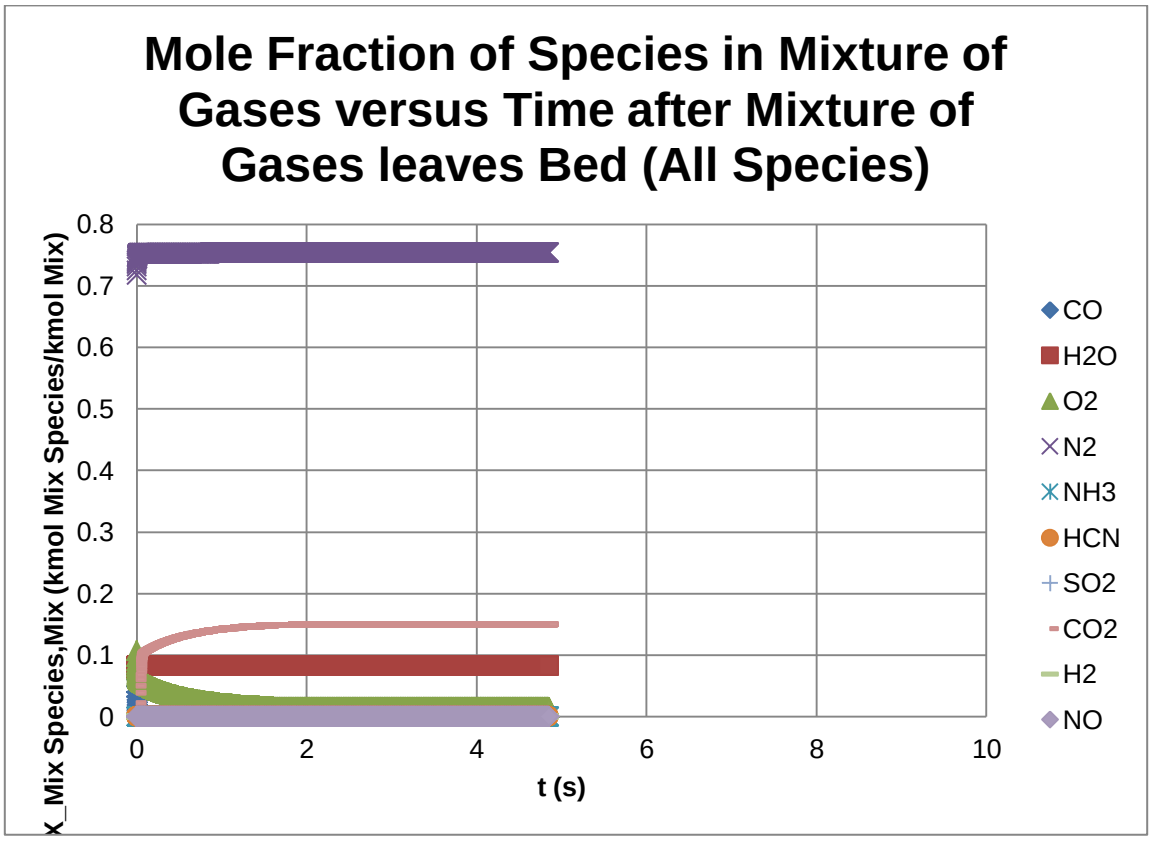

Fig. 122. Mole fraction of all species versus time for anonymous CFB boiler firing tire fuel with decreased pre-exponential factor for $2\ H_2\ (g)\ +\ O_2\ (g) \rightarrow\ 2\ H_2O\ (g)$.

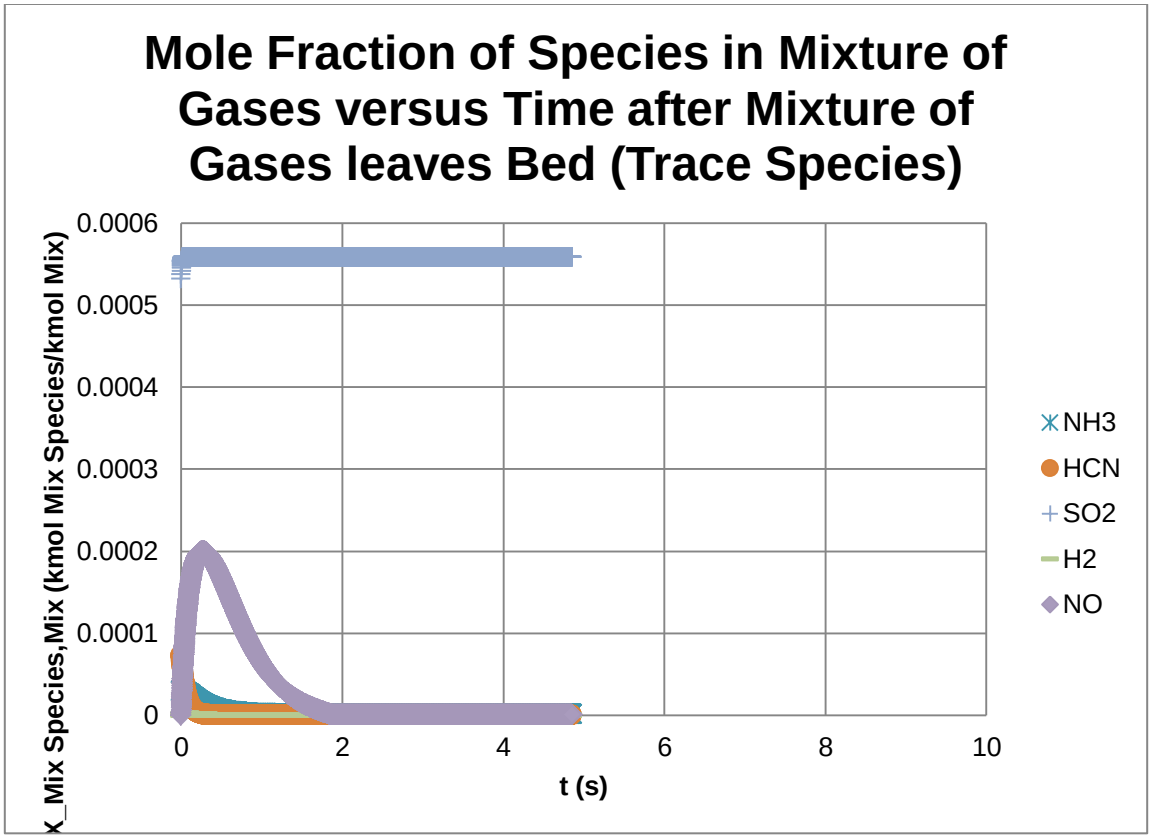

Fig. 123. Mole fraction of trace species versus time for anonymous CFB boiler firing tire fuel with decreased pre-exponential factor for $2\ H_2\ (g)\ +\ O_2\ (g) \rightarrow\ 2\ H_2O\ (g)$.

The nearly exact trends are evident in the 'Output' tab of the Excel program as shown below where all species only have minor changes. Continuing to decrease the pre-exponential factor continues the trends except for the CO and HCN begin to decrease as more O_2 becomes available to oxidize them until the H_2 is no longer being oxidized at all.

Table 64

Output tab for anonymous CFB boiler firing tire fuel with decreased pre-exponential factor for $2\,H_2\,(g)\,+\,O_2\,(g)\rightarrow\,2\,H_2O\,(g)$.

WET BASIS CONCENTRATION OF SPECIES IN MIXTURE OF GASES LEAVING CFB RISER										
	CO	H2O	O2	N2	NH3	HCN	SO2	CO2	H2	NO
ppm (Actual % O2)	9.61992E-21	82231.02763	14293.42501	753433.4214	1.300562724	7.99794E-20	558.2481465	149481.978	0.009443591	0.589782463
Mole % (Actual % O2)	9.61992E-25	8.223102763	1.429342501	75.34334214	0.000130056	7.99794E-24	0.055824815	14.9481978	9.44359E-07	5.89782E-05
ppm (Standard % O2)	8.84787E-21	75631.51608	30000	756368.0991	1.196185107	7.35606E-20	513.4455312	137485.192	0.008685689	0.542449038
Mole % (Standard % O2)	8.84787E-25	7.563151608	3	F7/10000	0.000119619	7.35606E-24	0.051344553	13.7485192	8.68569E-07	5.42449E-05
g/GJ	3.38098E-21	18588.82158	5739.103461	264893.182	0.277974984	2.71237E-20	448.7864975	82546.36864	0.000238883	0.340488036

DRY BASIS CONCENTRATION OF SPECIES IN MIXTURE OF GASES LEAVING CFB RISER										
	CO	H2O	O2	N2	NH3	HCN	SO2	CO2	H2	NO
ppm (Actual % O2)	1.04819E-20	0	15574.09919	820940.1757	1.417091625	8.71454E-20	608.2665281	162875.3886	0.010289726	0.642626283
Mole % (Actual % O2)	1.04819E-24	0	1.557409919	82.09401757	0.000141709	8.71454E-24	0.060826653	16.28753886	1.02897E-06	6.42626E-05
ppm (Standard % O2)	9.70413E-21	0	30000	818644.4944	1.311947078	8.06795E-20	563.1347192	150790.4545	0.009526255	0.594945069
Mole % (Standard % O2)	9.70413E-25	0	3	F16/10000	0.000131195	8.06795E-24	0.056313472	15.07904545	9.52625E-07	5.94945E-05
g/GJ	3.38098E-21	0	5739.103461	264893.182	0.277974984	2.71237E-20	448.7864975	82546.36864	0.000238883	0.340488036

6. SUMMARY AND CONCLUSIONS

The following is a summary of conclusions:

1. A CFB boiler combustion model was developed using current combustion theory via extensive literature review.
2. The model was incorporated into Microsoft Excel which enables approximately ten seconds computation time (independent of type of computer used so that the Microsoft Excel software may be the limiting factor on computation time, but this is still far faster than other software simulations found in the literature review) after parameters are changed with 5,000 chemical kinetics calculation rows. The result is accurate estimates of emission levels of various species that are considered important in combustion as well as significant with respect to government regulations produced by a CFB boiler when certain key appropriate and minimal inputs are varied. Where information was not readily available to provide adequate understanding, assumptions were made and documented for the model.
3. The model was validated by entering the required inputs acquired from both an anonymous company and documented data. The validation of the anonymous industrial CFB boiler firing lignite coal fuel resulted in emission concentrations being 22% different or less between the model predictions and the actual emissions when kinetics were slightly modified to better fit the specific boiler/fuel combination. The validation of the Babcock and Wilcox

pilot/laboratory scale BFB boiler firing subbituminous coal fuel resulted in emission concentrations being 10% different at most between the model predictions and the actual emissions without kinetics modification except for the O_2 concentration being off by about 74%. The large difference is likely attributed to the fact that the BFB has a greater portion of particles in the dense bed region of the combustor that don't become entrained due to the low $V_{Bed\ Mix}$ so that the O_2 has much more char to react with than is predicted by a CFB model that assumes that all of the particles immediately become entrained moving continually upwards.

4. Once sufficiently validated for the base case of lignite coal fuel in the anonymous CFB boiler, the program was modified to using tire as the fuel in the anonymous CFB boiler assuming similar combustion characteristics to coal. The switch in fuel required changing the inputs of higher heating value, density, proximate and ultimate analyses, and volatile Nitrogen release amounts and types for the new tire fuel. The increase in higher heating value from lignite coal to tire fuel necessitated a decrease in the tire fuel mass flow rate in order to have a similar total heat generated by combustion of almost 750 MW. The resulting outputs associated with the modified inputs are an increase in concentration of N_2, NH_3, and H_2, a decrease in concentration of CO, H_2O, HCN, SO_2, and NO, and a decrease in riser height where the average sized tire fuel particle was completely burned.

5. The fuel mass flow rate was increased by ten kilograms per second for the anonymous CFB boiler firing tire fuel resulting in increased concentration of CO and HCN as well as increased burn height.
6. The fuel mass flow rate was decreased by ten kilograms per second for the anonymous CFB boiler firing tire fuel resulting in decreased concentration of CO and HCN as well as decreased burn height.
7. The fuel density was increased by 400 kilograms per cubic meter for the anonymous CFB boiler firing tire fuel resulting in increased burn height.
8. The fuel density was decreased by 400 kilograms per cubic meter for the anonymous CFB boiler firing tire fuel resulting in increased concentration of CO, NH_3, HCN, and NO as well as decreased burn height.
9. The fuel SMD was increased by ten times for the anonymous CFB boiler firing tire fuel resulting in increased concentration of CO, O_2, and NO, decreased concentration of NH_3, HCN, and CO_2, and increased burn height.
10. The fuel SMD was decreased by ten times for the anonymous CFB boiler firing tire fuel resulting in increased concentration of NO as well as decreased burn height.
11. The volatile Nitrogen to N_2 was increased by 4% and then 4% more for the anonymous CFB boiler firing tire fuel resulting each time in increased concentration of O_2 and NH_3, decreased concentration of CO and N_2, and increased burn height.

12. The volatile Nitrogen to NH_3 was increased by 4% for the anonymous CFB boiler firing tire fuel resulting in increased concentration of O_2, NH_3, and NO, decreased concentration of CO and H_2O, and increased burn height.
13. The volatile Nitrogen to NH_3 was decreased by 4% for the anonymous CFB boiler firing tire fuel resulting in increased concentration of CO and H_2O, decreased concentration of O_2, NH_3, and NO, and decreased burn height.
14. The volatile Nitrogen to HCN was increased by 4% for the anonymous CFB boiler firing tire fuel resulting in increased concentration of CO, H_2O, N_2, and HCN, decreased concentration of O_2, NH_3, and NO, and increased burn height.
15. The volatile Nitrogen to HCN was decreased by 4% for the anonymous CFB boiler firing tire fuel resulting in increased concentration of O_2, NH_3, and NO, decreased concentration of CO, H_2O, N_2, and HCN, and decreased burn height.
16. The excess air was increased by 20% for the anonymous CFB boiler firing tire fuel resulting in increased concentration of O_2, N_2, H_2, and NO, decreased concentration of CO, H_2O, NH_3, HCN, SO_2 and CO_2, and decreased burn height.
17. The excess air was decreased by 20% for the anonymous CFB boiler firing tire fuel resulting in increased concentration of CO, H_2O, NH_3, HCN, SO_2 and CO_2, decreased concentration of O_2, N_2, H_2, and NO, and increased burn height.
18. The air O_2 was increased by 10% for the anonymous CFB boiler firing tire fuel resulting in increased concentration of H_2O, O_2, NH_3, SO_2, CO_2, H_2, and NO, decreased concentration of CO, N_2, and HCN, and decreased burn height.

19. The air O_2 was decreased by 10% for the anonymous CFB boiler firing tire fuel resulting in increased concentration of CO, N_2, HCN, and NO, decreased concentration of H_2O, O_2, NH_3, SO_2, and CO_2, and increased burn height.
20. The Calcium-Sulfur Ratio was increased by one for the anonymous CFB boiler firing tire fuel resulting in increased concentration of H_2O and CO_2, decreased concentration of SO_2, and increased burn height.
21. The Calcium-Sulfur Ratio was decreased by one for the anonymous CFB boiler firing tire fuel resulting in increased concentration of SO_2, decreased concentration of H_2O and CO_2, and decreased burn height.
22. The dry limestone density was increased by 2,000 kilograms per cubic meter for the anonymous CFB boiler firing tire fuel resulting in decreased burn height.
23. The dry limestone density was decreased by 2,000 kilograms per cubic meter for the anonymous CFB boiler firing tire fuel resulting in increased burn height.
24. The limestone moisture was increased by 5% for the anonymous CFB boiler firing tire fuel resulting in increased concentration of H_2O as well as increased burn height.
25. The limestone moisture was decreased by 5% for the anonymous CFB boiler firing tire fuel resulting in decreased concentration of H_2O as well as decreased burn height.
26. The average degree of sulfation was increased by 10% for the anonymous CFB boiler firing tire fuel resulting in decreased concentration of SO_2 as well as decreased burn height.

27. The average degree of sulfation was decreased by 10% for the anonymous CFB boiler firing tire fuel resulting in increased concentration of SO_2 as well as increased burn height.
28. The gas mixture pressure was increased by 0.5 bars for the anonymous CFB boiler firing tire fuel resulting in increased concentration of NH_3, CO_2, and H_2, decreased concentration of CO, HCN, and NO, and decreased burn height.
29. The gas mixture pressure was decreased by 0.5 bars for the anonymous CFB boiler firing tire fuel resulting in increased concentration of CO and HCN, decreased concentration of NH_3, CO_2, H_2, and NO, and increased burn height.
30. The gas mixture temperature was increased by 200 K for the anonymous CFB boiler firing tire fuel resulting in increased concentration of H_2O, N_2, and CO_2, decreased concentration of CO, O_2, NH_3, HCN, H_2, and NO, and increased burn height.
31. The gas mixture temperature was decreased by 200 K for the anonymous CFB boiler firing tire fuel resulting in increased concentration of CO, NH_3, HCN, H_2, and NO, decreased concentration of H_2O, O_2, N_2, and CO_2, and decreased burn height.
32. The riser cross-sectional area was increased by 50 m^2 for the anonymous CFB boiler firing tire fuel resulting in increased concentration of H_2O and N_2, decreased concentration of CO, O_2, NH_3, and HCN, and decreased burn height.

33. The riser cross-sectional area was decreased by 50 m^2 for the anonymous CFB boiler firing tire fuel resulting in increased concentration of CO, O_2, NH_3, and HCN, decreased concentration of H_2O, and increased burn height.
34. The riser height was increased by 30 meters for the anonymous CFB boiler firing tire fuel resulting in increased concentration of H_2O and N_2, decreased concentration of CO, O_2, NH_3, and HCN, and decreased burn height.
35. The riser height was decreased by 30 meters for the anonymous CFB boiler firing tire fuel resulting in increased concentration of CO, O_2, NH_3, HCN, H_2, and NO, decreased concentration of H_2O, N_2 and CO_2, and increased burn height.
36. The number of chemical kinetics calculation rows was increased by 4,000 rows for the anonymous CFB boiler firing tire fuel resulting in increased concentration of CO, O_2, NH_3, and HCN, decreased concentration of H_2O, and increased burn height and computation time.
37. The number of chemical kinetics calculation rows was decreased by 4,000 rows for the anonymous CFB boiler firing tire fuel resulting in increased concentration of H_2O, decreased concentration of CO, O_2, NH_3, and HCN, and decreased burn height and computation time.
38. The pre-exponential factor for $NO\ (g)\ +\ C\ (s)\ \rightarrow\ \frac{1}{2}\ N_2\ (g)\ + CO\ (g)$ was increased by ten times for the anonymous CFB boiler firing tire fuel resulting in increased concentration of O_2, NH_3, CO_2, H_2, and NO, decreased concentration of CO, H_2O, N_2, and HCN, and increased burn height.

39. The pre-exponential factor for $NO\ (g)\ +\ C\ (s)\ \rightarrow\ \frac{1}{2}\ N_2\ (g)\ +CO\ (g)$ was decreased by ten times for the anonymous CFB boiler firing tire fuel resulting in increased concentration of CO, H_2O, HCN, and NO, decreased concentration of O_2, N_2, NH_3, CO_2, and H_2, and decreased burn height.
40. The pre-exponential factor for $CO\ (g)\ +\ \frac{1}{2}\ O_2\ (g)\ \rightarrow\ CO_2\ (g)$ was increased by ten times for the anonymous CFB boiler firing tire fuel resulting in decreased concentration of CO, O_2, and CO_2 as well as increased burn height.
41. The pre-exponential factor for $CO\ (g)\ +\ \frac{1}{2}\ O_2\ (g)\ \rightarrow\ CO_2\ (g)$ was decreased by ten times for the anonymous CFB boiler firing tire fuel resulting in increased concentration of CO, O_2, and CO_2 as well as decreased burn height.
42. The pre-exponential factor for $NH_3\ (g)\ +\ O_2\ (g)\ \rightarrow$ NO (g) $+\ H_2O$ (g) $+\ \frac{1}{2}\ H_2\ (g)$ was increased by ten times for the anonymous CFB boiler firing tire fuel resulting in increased concentration of CO, H_2O, N_2, HCN, H_2, and NO as well as decreased concentration of O_2, NH_3, and CO_2.
43. The pre-exponential factor for $NH_3\ (g)\ +\ O_2\ (g)\ \rightarrow$ NO (g) $+\ H_2O$ (g) $+\ \frac{1}{2}\ H_2\ (g)$ was decreased by ten times for the anonymous CFB boiler firing tire fuel resulting in increased concentration of O_2, NH_3, and CO_2 as well as decreased concentration of CO, H_2O, N_2, HCN, H_2, and NO.
44. The pre-exponential factor for $NH_3\ (g)\ +\ NO\ (g)\ \rightarrow\ N_2$ (g) $+\ H_2O$ (g) $+\ \frac{1}{2}\ H_2\ (g)$ was increased by ten times for the anonymous CFB boiler firing tire

fuel resulting in increased concentration of CO, H_2O, N_2, and HCN as well as decreased concentration of O_2, NH_3, CO_2, H_2, and NO.

45. The pre-exponential factor for $NH_3\ (g)\ +\ NO\ (g)\ \rightarrow\ N_2$ (g) $+\ H_2O$ (g) $+\ \frac{1}{2}\ H_2\ (g)$ was decreased by ten times for the anonymous CFB boiler firing tire fuel resulting in increased concentration of O_2, NH_3, CO_2, H_2, and NO as well as decreased concentration of CO, H_2O, N_2, and HCN.
46. The pre-exponential factor for $HCN\ (g)\ +\ O_2\ (g)\ \rightarrow$ NO (g) $+\ CO$ (g) $+\ \frac{1}{2}\ H_2\ (g)$ was increased by ten times for the anonymous CFB boiler firing tire fuel resulting in increased concentration of H_2O and N_2 as well as decreased concentration of CO, O_2, NH_3, HCN, CO_2, H_2, and NO.
47. The pre-exponential factor for $HCN\ (g)\ +\ O_2\ (g)\ \rightarrow$ NO (g) $+\ CO$ (g) $+\ \frac{1}{2}\ H_2\ (g)$ was decreased by ten times for the anonymous CFB boiler firing tire fuel resulting in increased concentration of CO, HCN, H_2, and NO as well as decreased concentration of H_2O, O_2, N_2, NH_3, and CO_2.
48. The pre-exponential factor for $HCN\ (g)\ +\ NO\ (g)\ \rightarrow\ N_2$ (g) $+\ CO$ (g) $+\ \frac{1}{2}\ H_2\ (g)$ was increased by ten times for the anonymous CFB boiler firing tire fuel resulting in increased concentration of O_2, NH_3, and H_2 as well as decreased concentration of CO, H_2O, N_2, HCN, and NO.
49. The pre-exponential factor for $HCN\ (g)\ +\ NO\ (g)\ \rightarrow\ N_2$ (g) $+\ CO$ (g) $+\ \frac{1}{2}\ H_2\ (g)$ was decreased by ten times for the anonymous CFB boiler firing tire

fuel resulting in increased concentration of CO, H_2O, HCN, and NO as well as decreased concentration of O_2, NH_3, and H_2.

50. Increasing the pre-exponential factor for $2\ H_2\ (g)\ +\ O_2\ (g) \rightarrow\ 2\ H_2O\ (g)$ doesn't have any effect because the H_2 is already oxidized as quickly as it is created.
51. It takes decreasing the pre-exponential factor for $2\ H_2\ (g)\ +\ O_2\ (g) \rightarrow\ 2\ H_2O\ (g)$ by 100,000,000 times for the anonymous CFB boiler firing tire fuel before any noticeable concentration trends take place resulting in increased concentration of CO, O_2, HCN, H_2, and NO as well as decreased concentration of H_2O, NH_3, and CO_2.

In Table 65 below, the conclusions from the parametric analysis of the anonymous CFB boiler firing tire fuel including the changes that took place when the fuel was switched from lignite coal to tire fuel can be viewed graphically. A 'D' represents a decrease in the output value, an 'I' represents an increase in the output value of the table, and an '*' represents a more important/sensitive parameter that caused a more significant variance in certain emissions with the given variation.

Table 65

Parametric analysis summary.

Parameter Change	CO	H2O	O2	N2	NH3	HCN	SO2	CO2	H2	NO	Burned Height	Sensitive
Fuel switched from lignite coal to tire	D	D		I	I	D	D		I	D	D	*
Fuel mass flow rate increased by 10 kg/s	I					I					I	
Fuel mass flow rate decreased by 10 kg/s	D					D					D	
Fuel density increased by 400 kg/m^3											I	
Fuel density decreased by 400 kg/m^3	I				I	I				I	D	
Fuel SMD increased by ten times	I		I		D	D		D		I	I	*
Fuel SMD decreased by ten times										I	D	
Volatile Nitrogen to N2 increased by 4%	D		I	D	I						I	
Volatile Nitrogen to N2 increased by 8%	D		I	D	I						I	
Volatile Nitrogen to NH3 increased by 4%	D	D	I		I					I	I	
Volatile Nitrogen to NH3 decreased by 4%	I	I	D		D					D	D	
Volatile Nitrogen to HCN increased by 4%	I	I	D	I	D	I				D	I	
Volatile Nitrogen to HCN decreased by 4%	D	D	I	D	I	D				I	D	
Excess air increased by 20%	D	D	I	I	D	D	D	D	I	I	D	
Excess air decreased by 20%	I	I	D	D	I	I	I	I	D	D	I	*
Air O2 increased by 10%	D	I	I	D	I	D	I	I	I	I	D	
Air O2 decreased by 10%	I	D	D	I	D	I	D	D		I	I	
Calcium-Sulfur Ratio increased by one		I					D	I			I	*
Calcium-Sulfur Ratio decreased by one		D					I	D			D	*
Dry limestone density increased by 2,000 kg/m^3											D	
Dry limestone density decreased by 2,000 kg/m^3											I	
Limestone moisture increased by 5%		I									I	
Limestone moisture decreased by 5%		D									D	
Average degree of sulfation increased by 10%							D				D	*
Average degree of sulfation decreased by 10%							I				I	*
Gas mixture pressure increased by 0.5 bars	D				I	D		I	I	D	D	
Gas mixture pressure decreased by 0.5 bars	I				D	I		D	D	D	I	
Gas mixture temperature increased by 200 K	D	I	D	I	D	D		I	D	D	I	
Gas mixture temperature decreased by 200 K	I	D	D	D	I	I		D	I	I	D	*
Riser cross-sectional area increased by 50 m^2	D	I	D	I	D	D					D	
Riser cross-sectional area decreased by 50 m^2	I	D	I		I	I					I	
Riser height increased by 30 m	D	I	D	I	D	D					D	
Riser height decreased by 30 m	I	D	I	D	I	I		D	I	I	I	*
Number of chemical kinetics calculation rows increased by 4,000 rows	I	D	I		I	I					I	
Number of chemical kinetics calculation rows decreased by 4,000 rows	D	I	D		D	D					D	
Pre-exponential factor for NO + C -> 1/2 N2 + CO increased by ten times	D	D	I	D	I	D		I	I	I	I	
Pre-exponential factor for NO + C -> 1/2 N2 + CO decreased by ten times	I	I	D	D	D	I		D	D	I	D	*
Pre-exponential factor for CO + 1/2 O2 -> CO2 increased by ten times	D		D					D			I	
Pre-exponential factor for CO + 1/2 O2 -> CO2 decreased by ten times	I		I					I			D	
Pre-exponential factor for NH3 + O2 -> NO + H2O + 1/2 H2 increased by ten times	I	I	D	I	D	I		D	I	I		
Pre-exponential factor for NH3 + O2 -> NO + H2O + 1/2 H2 decreased by ten times	D	D	I	D	I	D		I	D	D		
Pre-exponential factor for NH3 + NO -> N2 + H2O + 1/2 H2 increased by ten times	I	I	D	I	D	I		D	D	D		
Pre-exponential factor for NH3 + NO -> N2 + H2O + 1/2 H2 decreased by ten times	D	D	I	D	I	D		I	I	I		*
Pre-exponential factor for HCN + O2 -> NO + CO + 1/2 H2 increased by ten times	D	I	D	I	D	D		D	D	D		
Pre-exponential factor for HCN + O2 -> NO + CO + 1/2 H2 decreased by ten times	I	D	D	D	D	I		D	I	I		*
Pre-exponential factor for HCN + NO -> N2 + CO + 1/2 H2 increased by ten times	D	D	I	D	I	D			I	D		
Pre-exponential factor for HCN + NO -> N2 + CO + 1/2 H2 decreased by ten times	I	I	D		D	I			D	I		
Pre-exponential factor for 2 H2 + O2 -> 2 H2O increased												
Pre-exponential factor for 2 H2 + O2 -> 2 H2O decreased by 100,000,000 times	I	D	I		D	I		D	I	I		

7. FUTURE WORK

The following is a list of further work that can be performed in the field of study:

1. Experiments can be conducted on both industrial and pilot/laboratory scale CFB boilers firing tire fuel to further validate the proposed model.
2. The program could be expanded to allow for time dependent reactions in the CFB bed to enable the model to be used for gasification, BFB, or possibly even stationary purposes.
3. Co-firing of multiple fuels should be considered rather than just one fuel used at a time such as is currently in the proposed model. This may be accomplished through the averaging of different fuel properties and chemical kinetics reaction rates of multiple fuels based on the mass fraction of each fuel.
4. The effects of the recirculated particles being assumed negligible in the proposed model is likely to only cause small changes in the average/SMD char particle (or char particle size distribution) and the number of char particles per cubic meter of the mixture of gases (and therefore the effective cross-sectional area of the CFB riser leading to a slight decrease in the residence time of the gas mixture in the riser), but may have a greater effect on the chemical kinetics that are based on the amount of char particles (such as fixed Carbon and Nitrogen oxidizing) especially the reduction of gaseous NO on the solid fixed Carbon as well as the additional reduction effects of ash and sorbent particles [10,63]. Therefore,

effects of the recirculated particles could be incorporated into future improvements in the model for greater accuracy of the CFB combustion process.

5. The proposed model could potentially be used for the prediction of temperature and pressure of the gas mixture in the CFB riser based on the fuel, limestone, and air rates and properties.
6. The addition of secondary air ports in the model should especially improve NO results even though Desroches-Ducarne et al. show little change in emission concentrations at the riser exit with air staging/secondary air [31].
7. Injection of NH_3 (or Selective Non-Catalytic Reduction/SNCR) is also common just before or in the cyclone, or downstream of the cyclone, to have a beneficial effect on NO emission [6] which is not currently included in the proposed model.
8. Other trace species could also be considered to expand the number of species developed by the model to include such species as HCl, CH_4, N_2O, NO_2, SO_3, and H_2S [6,8,10,23,27,31,36,42,54,55,61-63,66].
9. Thermal and prompt NO [5,10,16,23,33,54,55] could be included to further enhance emission accuracy especially outside of normal operating temperatures.
10. The program could be improved to keep certain inputs from being entered and outputs from being calculated to help ensure more novice users don't abuse the program.

REFERENCES

[1] Atal A, Levendis YA. Comparison of the combustion behaviour of pulverized waste tyres and coal. Fuel 1995; 74(11):1570-81.

[2] The US Environmental Protection Agency. Combustion Emissions from Hazardous Waste Incinerators, Boilers and Industrial Furnaces, and Municipal Solid Waste Incinerators – Results from Five STAR Grants and Research Needs. December 2006: <http://epa.gov/ncer/publications/research_results_needs/combustionEmmissionsReport.pdf> [accessed July 2015].

[3] Dai X, Yin X, Wu C, Zhang W, Chen Y. Pyrolysis of waste tires in a circulating fluidized-bed reactor. Energy 2001; 26(4):385-99.

[4] Kim JR, Lee JS, Kim SD. Combustion characteristics of shredded waste tires in a fluidized bed combustor. Energy 1994; 19(8):845-54.

[5] Anthony EJ. Fluidized bed combustion of alternative solid fuels; status, successes and problems of the technology. Prog Energy Combust Sci 1995; 21:239-68.

[6] Johnsson JE. Formation and reduction of nitrogen oxides in fluidized-bed combustion. Fuel 1994; 73(9):1398-415.

[7] Koornneef J, Junginger M, Faaij A. Development of fluidized bed combustion—An overview of trends, performance and cost. Prog Energy Combust Sci 2007; 33:19-55.

[8] Adanez J, Gayan P, de Diego LF, Garcia-Labiano F, Abad A. Combustion of wood chips in a CFBC. Modeling and validation. Ind Eng Chem Res 2003; 42(5):987-99.

[9] Lee JM, Kim DW, Kim JS, Park K, Lee TH. Evaluation of the performance of a commercial circulating fluidized bed boiler by using IEA-CFBC model: Effect of primary to secondary air ratio. Korean J Chem Eng 2013; 30(5):1058-66.

[10] Sotudeh-Gharebaagh R, Legros R, Chaouki J, Paris J. Simulation of circulating fluidized bed reactors using ASPEN PLUS. Fuel 1998; 77(4):327-37.

[11] Arena U, Chirone R, D'Amore M, Miccio M, Salatino P. Some issues in modelling bubbling and circulating fluidized-bed coal combustors. Powder Technology 1995; 82:301-16.

[12] Huilin L, Guangbo Z, Rushan B, Yongjin C, Gidaspow D. A coal combustion model for circulating fluidized bed boilers. Fuel 2000; 79:165-72.

[13] Huilin L, Rushan B, Wenti L, Binxi L, Lidan Y. Computations of a circulating fluidized-bed boiler with wide particle size distributions. Ind Eng Chem Res 2000; 39(9):3212-20.

[14] Wang Q, Luo Z, Li X, Fang M, Ni M, Cen K. A mathematical model for a circulating fluidized bed (CFB) boiler. Energy 1999; 24:633-53.

[15] de Souza-Santos ML. Comprehensive simulator (CSFMB) applied to circulating fluidized bed boilers and gasifiers. The Open Chemical Engineering Journal 2008; 2:106-18.

[16] Gungor A. Prediction of SO_2 and NO_x emissions for low-grade Turkish lignites in CFB combustors. Chemical Engineering Journal 2009; 146:388-400.

[17] Leckner B. Fluidized bed combustion: mixing and pollutant limitation. Prog Energy Combust Sci 1998; 24:31-61.

[18] Lee JM, Kim JS. Simulation of the 200 MWe Tonghae thermal power plant circulating fluidized bed combustor by using IEA-CFBC model. Korean J Chem Eng 1999; 16(5):640-5.

[19] Saxena SC, Jotshi CK. Fluidized-bed incineration of waste materials. Prog Energy Combust Sci 1994; 20:281-324.

[20] Mattisson T, Lyngfelt A. A sulphur capture model for circulating fluidized-bed boilers. Chemical Engineering Science 1998; 53(6):1163-73.

[21] Huilin L, Rushan B, Lidan Y, Guangbo Z, Xiu T. Numerical computation of a circulating fluidized bed combustor. Int J Energy Res 1998; 22:1351-64.

[22] Das A, Bhattacharya SC. Circulating fluidised-bed combustion. Applied Energy 1990; 37:227-46.

[23] Caneghem JV, Brems A, Lievens P, Block C, Billen P, Vermeulen I, Dewil R, Baeyens J, Vandecasteele C. Fluidized bed waste incinerators: Design, operational and environmental issues. Prog Energy Combust Sci 2012; 38:551-82.

[24] Basu P. Combustion of coal in circulating fluidized-bed boilers: a review. Chemical Engineering Science 1999; 54:5547-57.

[25] Chang YM, Lo YF, Ho CC. Application of fluidized bed combustion to industrial waste treatment. Environmental Pollution 1991; 71:31-42.

[26] Fox EC, Krishnan RP, Daw CS, Jones JE. A review of fluidized-bed combustion technology in the United States. Energy 1986; 11(11/12):1183-200.

[27] Gayan P, Adanez J, de Diego LF, Garcia-Labiano F, Cabanillas A, Bahillo A, Aho M, Veijonen K. Circulating fluidized bed co-combustion of coal and biomass. Fuel 2004; 83:277-86.

[28] Tillman D, Conn R, Duong D. Biomass fuel selection for cofiring in circulating fluidized bed boilers. Foster Wheeler North America Corp. 2009: < http://www.industrycortex.com/datasheets/profile/503501307/biomass-fuel-selection-for-cofiring-in-circulating-fluidized-bed-boilers> [accessed July 2015].

[29] Westby TS, Dangtran K, Edgar TF. Fluidized-bed combustion of Texas lignite. Fuel 1990; 69:590-9.

[30] Alagoz DE, Gorkem K, Selcuk N. A comprehensive fluidized bed combustion model coupled with a radiation model. Combust Sci and Tech 2008; 180:910-26.

[31] Desroches-Ducarne E, Dolignier JC, Marty E, Martin G, Delfosse L. Modelling of gaseous pollutants emissions in circulating fluidized bed combustion of municipal refuse. Fuel 1998; 77(13):1399-410.

[32] Gungor A, Eskin N. Analysis of environmental benefits of CFB combustors via one-dimensional model. Chemical Engineering Journal 2007; 131:301-17.

[33] Shimizu T, Inagaki M. Decomposition of N_2O over limestone under fluidized bed combustion conditions. Energy & Fuels 1993; 7(5):648-54.

[34] Singh S, Nimmo W, Javed MT, Williams PT. Cocombustion of pulverized coal with waste plastic and tire rubber powders. Energy & Fuels 2011; 25:108-18.

[35] Wang XS, Gibbs BM, Rhodes MJ. Modelling of circulating fluidized bed combustion of coal. Fuel 1994; 73(7):1120-7.

[36] de Souza-Santos ML. A new version of CSFB, comprehensive simulator for fluidised bed equipment. Fuel 2007; 86:1684-709.

[37] Selcuk N, Ozkan U. Testing of a model for fluidized bed coal combustors. The Combustion Institute 1984; Twentieth Symposium (International) on Combustion:1471-8.

[38] Knoebig T, Luecke K, Werther J. Mixing and reaction in the circulating fluidized bed - A three-dimensional combustor model. Chemical Engineering Science 1999; 54:2151-60.

[39] Overturf BW, Reklaitis GV. Part II: Coal combustion application. AIChE Journal 1983; 29(5):820-9.

[40] de Souza-Santos ML. Comprehensive modelling and simulation of fluidized bed boilers and gasifiers. Fuel 1989; 68:1507-21.

[41] Oymak O, Selcuk N, Onal I. Testing of a mathematical model for the combustion of lignites in an AFBC. Fuel 1993; 72:261-6.

[42] Goel S, Sarofim A, Kilpinen P, Hupa M. Emissions of nitrogen oxides from circulating fluidized-bed combustors: modeling results using detailed chemistry. The Combustion Institute 1996; Twenty-Sixth Symposium (International) on Combustion:3317-24.

[43] Lee JM, Kim JS, Kim JJ. Evaluation of the 200 MWe Tonghae CFB boiler performance with cyclone modification. Energy 2003; 28:575-89.

[44] Gungor A. Two-dimensional biomass combustion modeling of CFB. Fuel 2008; 87:1453-68.

[45] Gungor A, Eskin N. Two-dimensional coal combustion modeling of CFB. International Journal of Thermal Sciences 2008; 47:157-74.

[46] Gungor A. Simulation of emission performance and combustion efficiency in biomass fired circulating fluidized bed combustors. Biomass and Bioenergy 2010; 34:506-14.

[47] Pereira FJ, Beer JM, Gibbs B, Hedley AB. NO_x emissions from fluidized-bed coal combustors. Symposium (International) on Combustion 1975; 15(1):1149-56.

[48] Dam-Johansen K, Ostergaard K. High-temperature reaction between sulphur dioxide and limestone-I. Comparison of limestones in two laboratory reactors and a pilot plant. Chemical Engineering Science 1991; 46(3):827-37.

[49] Ogada T, Werther J. Combustion characteristics of wet sludge in a fluidized bed. Fuel 1996; 75(5):617-26.

[50] Knobig T, Werther J, Amand L-E, Leckner B. Comparison of large- and small-scale circulating fluidized bed combustors with respect to pollutant formation and reduction for different fuels. Fuel 1998; 77(14):1635-42.

[51] Lyngfelt A, Leckner B. Combustion of wood-chips in circulating fluidized bed boilers – NO and CO emissions as functions of temperature and air-staging. Fuel 1999; 78:1065-72.

[52] Topal H, Atimtay AT, Durmaz A. Olive cake combustion in a circulating fluidized bed. Fuel 2003; 82:1049-56.

[53] Fang M, Yang L, Chen G, Shi Z, Luo Z, Cen K. Experimental study on rice husk combustion in a circulating fluidized bed. Fuel Processing Technology 2004; 85:1273-82.

[54] Annamalai K, Puri IK. Combustion Science and Engineering. Boca Raton, FL. CRC Press (Taylor & Francis Group) 2007.

[55] Backreedy RI, Fletcher LM, Ma L, Pourkashanian M, Williams A. Modelling pulverised coal combustion using a detailed coal combustion model. Combust Sci and Tech 2006; 178:763-87.

[56] Carey VP. Statistical Thermodynamics and Microscale Thermophysics. New York, NY. Cambridge University Press 1999.

[57] Kambara S, Takarada T, Yamamoto Y, Kato K. Relation between functional forms of coal nitrogen and formation of NO_x precursors during rapid pyrolysis. Energy & Fuels 1993; 7(6):1013-20.

[58] Leppalahti J, Koljonen T. Nitrogen evolution from coal, peat and wood during gasification: Literature review. Fuel Processing Technology 1995; 43:1-45.

[59] Glarborg P, Jensen AD, Johnsson JE. Fuel nitrogen conversion in solid fuel fired systems. Prog Energy Combust Sci 2003; 29:89-113.

[60] Visona SP, Stanmore BR. Modeling NO_x release from a single coal particle. Part II. Formation of NO from char-nitrogen. Combustion and Flame 1996; 106:207-18.

[61] Johnsson JE, Glarborg P. Sulphur chemistry in combustion I. Pollutants from Combustion (NATO Science Series) 2000; 547:263-82.

[62] Thomas KM. The release of nitrogen oxides during char combustion. Fuel 1997; 76(6):457-73.

[63] Jones JM, Patterson PM, Pourkashanian M, Williams A. Approaches to modelling heterogeneous char NO formation/destruction during pulverised coal combustion. Carbon 1999; 37:1545-52.

[64] Wendt JOL. Fundamental coal combustion mechanisms and pollutant formation in furnaces. Prog Energy Combust Sci 1980; 6:201-22.

[65] Mitchell JW, Tarbell JM. A kinetic model of nitric oxide formation during pulverized coal combustion. AIChE Journal 1982; 28(2):302-11.

[66] Hansen PFB, Dam-Johansen K, Ostergaard K. High-temperature reaction between sulphur dioxide and limestone-V. The effect of periodically changing oxidizing and reducing conditions. Chemical Engineering Science 1993; 48(7):1325-41.

[67] Dam-Johansen K, Ostergaard K. High-temperature reaction between sulphur dioxide and limestone-II. An improved experimental basis for a mathematical model. Chemical Engineering Science 1991; 46(3):839-45.

[68] Hartman M, Coughlin RW. Reaction of sulfur dioxide with limestone and the influence of pore structure. Ind Eng Chem (Process Des Develop) 1974; 13(3):248-53.

[69] Li X, Luo Z, Ni M, Cen K. Modeling sulfur retention in circulating fluidized bed combustors. Chemical Engineering Science 1995; 50(14):2235-42.

[70] Anthony EJ, Granatstein DL. Sulfation phenomena in fluidized bed combustion systems. Prog Energy Combust Sci 2001; 27:215-36.

[71] Annamalai K, Ryan W. Interactive processes in gasification and combustion-II. Isolated carbon, coal and porous char particles. Prog Energy Combust Sci 1993; 19:383-446.

[72] Rajan RR, Wen CY. A comprehensive model for fluidized bed coal combustors. AIChE Journal 1980; 26(4):642-55.

[73] Selcuk N, Pekyilmaz A. Testing of a model for fluidized bed coal combustors-Effect of char combustion model. The Combustion Institute 1986; Twenty-first Symposium (International) on Combustion:585-92.

[74] Kobayashi H, Howard JB, Sarofim AF. Coal devolatilization at high temperatures. Symposium (International) on Combustion 1977; 16(1):411-25.

[75] Weinell CE, Dam-Johansen K, Johnsson JE. Single-particle behaviour in circulating fluidized beds. Powder Technology 1997; 92:241-52.

[76] Cooper CD, Alley FC. Air Pollution Control: A Design Approach (3rd ed.). Long Grove, IL. Waveland Press, Inc 2002.

[77] Selcuk N, Ozkan M. Simulation of circulating fluidized bed combustors firing indigenous lignite. International Journal of Thermal Sciences 2011; 50:1109-15.

[78] Cengel YA, Boles MA. Thermodynamics: An Engineering Approach (5^{th} ed.). New York, NY. McGraw-Hill (The McGraw-Hill Companies, Inc) 2006.

[79] Howard JB, Williams GC, Fine DH. Kinetics of carbon monoxide oxidation in postflame gases. Symposium (International) on Combustion 1973; 14(1):975-86.

[80] He R, Suda T, Takafuji M, Hirata T, Sato J. Analysis of low NO emission in high temperature air combustion for pulverized coal. Fuel 2004; 83:1133-41.

[81] Russell NV, Gibbins JR, Man CK, Williamson J. Coal char thermal deactivation under pulverized fuel combustion conditions. Energy & Fuels 2000; 14(4):883-8.

[82] Solomon PR, Colket MB. Coal devolatilization. Symposium (International) on Combustion 1979; 17(1):131-43.

[83] Carlin NT, Annamalai K, Oh H, Ariza GG, Lawrence B, V UA, Sweeten JM, Heflin K, Harman WL. Co-combustion and gasification of coal and cattle biomass: a review of research and experimentation. Green Energy (Progress in Green Energy) 2011; 1:123-79.

[84] Li C-Z, Tan LL. Formation of NO_x and SO_x precursors during the pyrolysis of coal and biomass. Part III. Further discussion on the formation of HCN and NH_3 during pyrolysis. Fuel 2000; 79:1899-906.

[85] Chang R. Chemistry (8^{th} ed.). New York, NY. McGraw-Hill (The McGraw-Hill Companies, Inc) 2005.

[86] White FM. Fluid Mechanics (6th ed.). New York, NY. McGraw-Hill (The McGraw-Hill Companies, Inc) 2008.

[87] Beer FP, Johnston ER, Clausen WE. Vector Mechanics for Engineers: Dynamics (8th ed.). New York, NY. McGraw-Hill (The McGraw-Hill Companies, Inc) 2007.

[88] Helland E, Occelli R, Tadrist L. Numerical study of cluster formation in a gas–particle circulating fluidized bed. Powder Technology 2000; 110:210-21.

[89] Aarna I, Suuberg EM. A review of the kinetics of the nitric oxide-carbon reaction. Fuel 1997; 76(6):475-91.

[90] Incropera FP, DeWitt DP, Bergman TL, Lavine AS. Fundamentals of Heat and Mass Transfer (6th ed.). Hoboken, NJ. John Wiley & Sons, Inc 2007.

[91] Reh L. Development potentials and research needs in circulating fluidized bed combustion. China Particuology 2003; 1(5):185-200.

APPENDIX

The Microsoft Excel spreadsheet of the proposed model described in the thesis text has been included as a separate supplemental file.